Exploring the Reciprocal Relationship Between the Immune System and the Tumour Microenvironment

Ana Cláudia da Costa Pires

Institute of Infection and Immunity,

School of Medicine,

Cardiff University

Thesis submitted for the degree of Doctor of Philosophy

May 2020

Acknowledgements

I am incredibly grateful to have been given the opportunity to complete my PhD within such supportive and encouraging research group. I would firstly like to thank my supervisors, Professor Awen Gallimore and Professor Andrew Godkin. This thesis would not have been possible without their guidance and extraordinary scientific knowledge. I want to especially thank Awen for being extremely supportive throughout the course of this PhD. Your encouragement, motivation and optimism were crucial during these years. I would also like to thank Andy for the extremely helpful insights and advice across the project. I consider myself very lucky to have had the opportunity to be your student, and to learn from you both and grow as a scientist.

I would also like to thank Dr Stephen Paisey and Dr Rhodri Smith at the Wales Research and Diagnostic PET Imaging Centre for their help with the PET-CT scans and image analysis; Howard Kendrick and Professor Matthew Smalley at the ECSCRI for their help with the TNC knockdown experiments; Pryia Subramanian and Professor Arne Akbar at UCL for their guidance with the senescence experiments; and Dr Rhiannon French at the ECSCRI for her help with the tumourspheres experiment.

Thank you to all of the Gallimore/Godkin lab members for their help and support during these years, and for making it a very enjoyable place to work. I would especially like to thank Emma Jones for her support and guidance during my first year while I was still trying to find my way around the lab; Kath and Sarah for their incredible help with pretty much everything related to mice; Michelle for her help and guidance through endless immunohistochemistry optimisations; and Alex for his bioinformatic knowledge, and for always encouraging me to think outside the box.

To all the members of office 3F02, both past and present, a huge thank you for all the good times, and especially for the friendship and support during the worse times! Also, a special thanks to Laud for always having an encouraging word, and for being the best party planner!

Leaving home for the first time to move to a different country was frightening, but I am truly thankful to have found such a supportive group of friends here in Cardiff. To Diana for making my transition to a new country and a different language so much easier; to Emma Campbell for being such an incredible friend during these years, in and outside work, and for always having the right words; to Amanda, for always being there; to my little Portuguese troop in Cardiff, especially to Ana Silva, for making it so much easier to be away from home - a massive thanks to you all! To Sara, I don't have enough words

to express my gratitude. A friendship that started way back in Portugal, that grew through the years; you are the sister I got to choose! Thank you so much for everything!

To all my friends back in Portugal, a huge thank you for always being there for me. Special thanks to Neves, Rodrigo, Micro, Joana and Helena for all of the traveling and for always having a place for me to stay! Xana; thank you for your lifelong friendship and for all of the support and encouragement over the years!

And finally, my family. You are my biggest supporters in everything I do, and I miss you all every day, especially grandma. A special thanks to my mum and my sister – you are everything to me, and I couldn't have done this without your constant support and motivation! These past few years haven't been easy for any of us, but you always find a way to be present. Thank you for always being a call away!

Abstract

The nature of the tumour microenvironment (TME) is thought to influence the ability of tumour-specific T cells, induced naturally or by immunotherapy, to control tumour growth.

This study tested the hypothesis that the composition of the TME prior to immunotherapy influences treatment success. To address this, the carcinogen 3-methylcholantrene was used to induce fibrosarcomas in $Foxp3^{DTR}$ mice, where $Foxp3^{+}$ cells can be depleted by administering diphtheria toxin. Depletion of $Foxp3^{+}$ regulatory T cells (Tregs) broadly resulted in two groups; responders, characterised by large numbers of tumour infiltrating lymphocytes (TILs) and control of tumour growth and non-responders, characterised by fewer TILs and a reduced capacity to control tumour growth.

To further identify features distinguishing responders and non-responders, an unbiased comparison of the transcriptomes of responders and non-responders revealed an inverse relationship between extracellular matrix (ECM) and T cell infiltrate. Responding tumours were T cell rich and ECM poor, whilst the inverse was observed in non-responders. Further experiments revealed that the ECM does not prevent induction of a successful response, but that loss of ECM is a consequence of an effective response. This may be due to transcriptional changes in tumour cells as a result of immune-driven tumour cell senescence.

Other changes to the TME comprised development of an organised lymphatic network in responder but not non-responder tumours and tumour cell intrinsic changes. Non-responder tumour cells exhibited a stem cell-like gene expression profile and superior sphere-formation capacity, while such features were significantly reduced in responder tumours. Metastatic capacity of non-responder tumours was also suggested by the presence of fibroblast-like cells in draining and non-draining lymph nodes in all non-responder mice.

These findings define an extended role for an effective immune response in widescale remodelling of the TME to favour loss of ECM, elimination of cancer stem cells and propagation of adaptive immunity.

Table of Contents

Acknowledgements ..... **iii**

Abstract ..... **v**

Table of Contents ..... **vii**

List of Figures ..... **x**

List of Tables ..... **xii**

List of Abbreviations ..... **xiii**

CHAPTER 1 *INTRODUCTION* **1**

1.1. Cancer Biology **3**

1.2. Tumour microenvironment **8**

1.2.1. Cancer stem cells 9

1.2.2. Tumour vasculature 10

1.2.3. Stromal cells 15

1.2.4. Extracellular matrix 18

1.2.5. Targeting the TME 20

1.3. Immune system in the TME **22**

1.3.1. Innate Immune Cells 23

1.3.2. T cells 25

1.3.2.1. Cytotoxic T Cells 25

1.3.2.2. T helper cells 27

1.3.2.3. Regulatory T cells 29

1.3.2.3.1. Foxp3 discovery 30

1.3.2.3.2. Treg subsets 31

1.3.2.3.3. Mechanisms of Treg suppression 31

1.3.2.3.4. Role of Tregs in the TME 33

1.3.3. Cancer immunosurveillance and Immunoediting 34

1.3.4. Cancer immunotherapy 39

1.4. Relationship between the TME and anti-tumour immune response **43**

1.5. Hypothesis and Aims **49**

CHAPTER 2 *METHODS* **51**

2.1. Mouse work **53**

2.1.1. Mice 53

2.1.2. Tumour induction, diphtheria toxin administration and monitoring 53

2.1.4. Dissection of Tissues 53

2.2. Histology **54**
2.2.1. Immunofluorescence 54
2.2.1.1. Frozen sections 54
2.2.1.2. Formalin fixed paraffin embedded sections 54
2.2.2. Immunohistochemistry 58
2.2.3. Quantification of immune cell infiltration 60

2.3. Positron Emission Tomography-Computed Tomography (PET-CT) scans **60**
2.3.1. Scanning 62
2.3.2. Analysis of PET-CT scans 62

2.4. TNC knockdown cell line **63**
2.4.1. Cell line establishment 65
2.4.2. Tumour induction 65
2.4.3. shRNA knockdown 65
2.4.4. Quantitative Real-Time Polymerase Chain Reaction (qRT-PCR) validation 66

2.5. RNAscope **67**

2.6. Senescence-associated β-galactosidase staining **69**

2.7. Telomere associated foci staining **69**

2.8. Tumoursphere assay **70**

2.9. Metastasis analysis **71**

2.10. Gene Expression Analysis **71**

2.11. Statistical analysis **71**

CHAPTER 3 ***EXAMINING THE RECIPROCAL RELATIONSHIP BETWEEN THE TUMOUR MICROENVIRONMENT AND AN EFFECTIVE ANTI-TUMOUR T CELL RESPONSE*** **73**

3.1. Introduction **75**

3.2. Results **78**
3.2.1. Expression patterns of ECM proteins in mouse fibrosarcomas 78
3.2.2. TNC in the tumour microenvironment 87
3.2.3. Distribution of TNC and T cells in tumours 93
3.2.4. T cell activity 96
3.2.5. Effect of TNC in response to immunotherapy 98
3.2.5.1. Exploring alterations in TNC expression during Treg depletion of tumour-bearing mice 98
3.2.5.2. Effect of knocking down TNC in a cell line inducing tumour model 106
3.2.6. Mechanism of TNC clearance from the TME 112

3.3. Discussion **114**

CHAPTER 4 *EXPLORING THE PROPERTIES OF THE TME IN TREG-DEPLETED RESPONDER AND NON-RESPONDER TUMOURS*.....125

4.1. Introduction.....127

4.2. Results.....128

4.2.1. The Lymphatic Network in ECM-Rich and ECM-Poor Tumours.....128

4.2.2. Properties of Cancer Cells In ECM-Rich and ECM-Poor Tumours.....130

4.2.2.1. Cell proliferation.....130

4.2.2.2. Cell death.....132

4.2.2.3. CSCs.....134

4.2.3. Cell Invasion in Untreated, Non-Responder and Responder Mice.....144

4.2.4. Cellular Senescence in Untreated, Non-Responder and Responder Tumours.....146

4.3. Discussion.....150

CHAPTER 5 *DISCUSSION*.....161

APPENDIX.....171

Methods.....173

Radiosynthesis of ^{89}Zr Oxalate.....173

Antibody Modification with p-SCN-Bn-DFO.....173

Preparation of ^{89}Zr-labeled TNC antibody.....174

Radio-TLC.....174

Radio-HPLC.....174

Bioinformatic analyses – Human data.....174

Analysis of RNAseq datasets from primary tumours in TCGA.....176

TNC Gene Expression Significantly Impacts Patient Survival in the Presence of a CTL Gene Signature.....176

Supplementary Figures.....177

REFERENCES.....183

List of Figures

Figure 1.1|Models of cancer propagation. 5
Figure 1.2|The hallmarks of cancer. 7
Figure 1.3|Routes for distant organ metastases formation..... 14
Figure 1.4|Origins of tumour stromal cells. 16
Figure 1.5| The cancer immunoediting model. 37
Figure 1.6|Immune-based classification of tumours. 46

Figure 2.1|Experimental timeline used to assess TNC expression over the course of Treg depletion. 61
Figure 2.2|TNC knockdown of primary cell lines by shRNA and tumour induction in mice. 64

Figure 3.1| Schematic representation of the response to Treg depletion in fibrosarcoma-bearing mice. 77
Figure 3.2| Bioinformatic transcriptome analysis of untreated, non-responder and responder tumours. 80
Figure 3.3| Tumour-infiltrating T cells are more abundant in responding tumours after Treg depletion. 82
Figure 3.4| Differential expression of extracellular matrix genes after Treg depletion. 84
Figure 3.5|Immunofluorescent staining of ECM proteins validates gene expression data. 86
Figure 3.6|Structure and active domains of Tenascin-C. 88
Figure 3.7| TNC presents different expression patterns within the same tumour. 90
Figure 3.8|Blood vessel pattern does not correlate with TNC expression. 92
Figure 3.9| Definition of TNC high and low areas. 94
Figure 3.10|TNC expression does not exclude T cells from tumours. 95
Figure 3.11|Granzyme-B is located in the cytoplasm of T cells in tumours with poor response to Treg depletion. 97
Figure 3.12|No difference in radioactivity uptake was observed between negative controls, untreated tumours and Treg depleted tumours. 101
Figure 3.13|Features of tumours scanned by PET-CT. 103
Figure 3.14|Signal obtained in PET-CT scans correspond to TNC staining in *ex-vivo* tumours. 105
Figure 3.15|Primary cell lines derived from MCA-induced tumours grow at a similar rate *in vivo*, even when Treg depleted. 107
Figure 3.16|Silencing of TNC expression through shRNAs was successful both *in vitro* and *in vivo*. 109
Figure 3.17| Cell line derived tumours respond to Treg depletion regardless of initial TNC expression. 111
Figure 3.18|Responding tumours to therapy express less TNC mRNA transcripts than other groups. 113
Figure 3.19| TNC is expressed mainly in tumour cells. 113
Figure 3.20|T cell infiltration in spontaneous mammary tumours. 117
Figure 3.21| Proposed mechanism for ECM clearance in responders TME. 122
Figure 3.22|Schematic representation of response to Treg depletion in murine fibrosarcomas. 124

Figure 4.1|Responder tumours exhibit improved lymphatic vessels, with expression of CCL21. ..129
Figure 4.2| Ki67 and TNC expression in the TME. 131
Figure 4.3| Cell death in untreated, non-responder and responder tumours. 133
Figure 4.4| Non-responder tumours exhibited enhanced gene expression associated with cancer stem cells. 135
Figure 4.5|EMT markers associated with CSC phenotype are differentially expressed between tumour groups. 137
Figure 4.6| Zeb1 expression in untreated, non-responder and responder tumours. 139
Figure 4.7| Fibrosarcoma associated CSC markers are differentially expressed between groups. 141
Figure 4.8|Cancer stem cells are affected by an effective response to Treg depletion. 143
Figure 4.9|Fibroblast-like cells can be found in draining and non-draining lymph nodes of all non-responder mice. 145
Figure 4.10|Cells derived from responding tumours to Treg depletion have high SA-β-Gal activity *in vitro*. 147
Figure 4.11| TAF^{+} cells in untreated, non-responder and responder tumours. 149
Figure 4.12| Events occurring in the TME of a non-responding tumour to Treg depletion. 155
Figure 4.13|Proposed mechanism for anti-tumour response regulated by ECM clearance. 157
Figure 4.14|Final representation of response to Treg depletion in murine fibrosarcomas. 159

List of Tables

Table 1.1|Examples of proteins secreted by CAFs and their function in tumour progression. 17

Table 2.1|Antibodies used in Immunofluorescent staining. 56
Table 2.2|Antibodies used in Immunohistochemical staining. 59
Table 2.3|Oligonucleotide sequences for TNC shRNAs. 66
Table 2.4|TaqMan® qRT-PCR probes. 67
Table 2.5|RNAscope amplification step conditions. 68

Table 3.1|Top 30 genes with opposing expressing patterns to *Tnc*. 81
Table 3.2|Breakdown of mice used in PET-CT scans. 99

List of Abbreviations

α-SMA	α-smooth muscle actin
γH2AX	Phosphorylated histone H2AX
ABC	ATP-binding cassette
ADAMTS	A disintegrin and metalloproteinase with thrombospondin motifs
ADCC	Antibody-dependent cell-mediated cytotoxicity
AF	Alexa Fluor
ALDH	Aldehyde dehydrogenase
APC	Antigen-presenting cell
BCR	B cell receptor
Bq	Becquerel
BSA	Bovine serum albumin
BTLA	B- and T-lymphocyte attenuator
CAA	Cancer associated adipocyte
CAEC	Cancer associated endothelial cell
CAF	Cancer associated fibroblast
CAR	Chimeric antigen receptor
Casp3	Caspase-3
CCL	Chemokine (C-C motif) ligand
CCR	C-C chemokine receptor
CD	Cluster of differentiation
Col3a1	Collagen type III alpha 1
CSC	Cancer stem cell
CSF1R	Colony stimulating factor 1 receptor
CTGF	Connective tissue growth factor
CTL	Cytotoxic T-lymphocyte
CTLA-4	Cytotoxic T-lymphocyte-associated protein 4
CXCL	Chemokine (C-X-C motif) ligand
DAMP	Danger associated molecular pattern
DC	Dendritic cell
DDR	DNA damage response
dH_2O	Distilled water
dLN	Tumour draining lymph node
DPX	Distryne, plasticizer and xylene
DT	Diphtheria toxin
ECM	Extracellular matrix
EGF	Epidermal growth factor

EMT	Epithelial-mesenchymal transition
EndMT	Endothelial-mesenchymal transition
EPR	Enhanced permeability and retention
Exo	Exosomes
EZH2	Enhancer of zeste homolog 2
FADD	FAS-associated death domain protein
FAP	Fibroblast activation protein
Fas	First apoptosis receptor
FasL	First apoptosis receptor ligand
FCS	Foetal Calf Serum
FDG	Fluorodeoxyglucose
FITC	Fluorescein isothiocyanate
FN	Fibronectin
FOS	Fos Proto-Oncogene, AP-1 Transcription Factor Subunit
Foxp3	Forkhead box P3
FSP1	Fibroblast specific protein 1
G3BP2	GTPase activating protein (SH3 domain) binding protein 2
GFP	Green fluorescent protein
GZMA	Granzyme-A
GZMB	Granzyme-B
HA	Haemagglutinin
HEV	High endothelial venule
HGF	Hepatocyte growth factor
HIER	Heat induced epitope retrieval
HIF	Hypoxia-inducible factor
HLA	Human leukocyte antigen
HRP	Horseradish peroxidase
I.p.	Intra-peritoneal
ICB	Immune checkpoint blockade
IDO	Indoleamine-pyrrole 2,3-dioxygenase
IFN-γ	Interferon-gamma
IL	Interleukin
IPEX	Dysregulation polyendocrinopathy X-linked syndrome
JAK	Janus kinase
LAG-3	Lymphocyte activation gene 3
LFA-1	Leukocyte function-associated antigen-1
LOX	Lysyl oxidase
Lum	Lumican

MAPK	Mitogen activated protein kinase
MCA	Methylcholantrene
MDSC	Myeloid derived suppressor cell
MeOH	Methanol
MHC	Major histocompatibility complex
miR	Micro RNA
MMP	Matrix metalloproteinase
NBFS	Neutral-buffered formalin solution
ndLN	Non-tumour draining lymph node
NF-κB	Nuclear factor κB
NFAT	Nuclear factor of activated T cells
NK	Natural killer
OCT	Optimal cutting temperature
OV	Oncolytic virus
PAMP	Pathogen-associated molecular pattern
PBS	Phosphate buffered saline
PD-1	Programmed cell death protein-1
PD-L1	Programmed death-ligand 1
PDGF	Platelet derived growth factor
PET-CT	Positron Emission Tomography-Computed Tomography
PNAd	Peripheral node addressin
PRR	Pattern recognition receptor
pTreg	peripheral-Treg
RGD	Arginine-glycine-aspartic acid
ROI	Region of interest
ROS	Reactive oxygen species
RT	Room temperature
SA-β-Gal	Senescence-Associated β-Galactosidase
SASP	Senescence associated secretory phenotype
SF	Soluble factors
SLO	Secondary lymphoid organ
STAT	Signal transducer and activator of transcription
SUV	Standardised uptake value
TAF	Telomere associated foci
TAM	Tumour associated macrophage
TAZ	Transcriptional coactivator with PDZ-binding motif
TCGA	The Cancer Genome Atlas
TCR	T cell receptor

Tfh	T follicular helper
TGF-β	Transforming growth factor β
Th	T helper
TIL	Tumour infiltrating lymphocyte
TIM-3	T-cell immunoglobulin and mucin-domain containing-3
TIMP	Tissue inhibitor of MMPs
TLR4	Toll-like receptor 4
TLS	Tertiary lymphoid structures
TME	Tumour microenvironment
TNC	Tenascin-C
TNF	Tumour necrosis factor
TRACERx	*TRA*cking non-small cell lung *C*ancer *E*volution through therapy (*Rx*)
TRAIL	TNF-related apoptosis-inducing ligand
Treg	Regulatory T cell
tTreg	thymic Treg
VEGF	Vascular endothelial growth factor
VEGFR2	VEGF-A receptor
WT	Wild type
XCR1	XC-chemokine receptor 1
YAP	Yes-associated protein

Chapter 1

Introduction

1.1. Cancer Biology

The term cancer incorporates a large group of diseases, all characterised by the abnormal growth of transformed cells, that can affect almost any part of the body. Cancer is a leading cause of mortality and morbidity worldwide, being responsible for at least 9.6 million deaths in 2018 only (World Health Organisation). There are more than 990 cancer diagnoses per day in the United Kingdom alone, and it is estimated that 1 in 2 people will be diagnosed with cancer at some point during their lifetime (Cancer Research UK).

A higher frequency of errors in DNA repair processes is observed in ageing cells and when normal cells are exposed to genotoxic agents, such as carcinogens or ultra-violet radiation. These alterations induce accumulation of somatic mutations in the progeny of dividing cells, allowing them to acquire a selective growth advantage, which culminates in proliferation of malignant cells (Greaves and Maley, 2012, Blanpain, 2013). During its progression, a cancer remains dynamic and continues to evolve, culminating in a molecularly heterogenous bulk of cells. This heterogeneity can be the consequence of genetic, transcriptomic, epigenetic, and/or phenotypic changes (Dagogo-Jack and Shaw, 2018). Phenotypic and functional heterogeneity can be present in the same organ and/or between patients. Inter-tumour heterogeneity is the basis of tumour subtype classification, which is characterised by their molecular profile, morphology and the expression of certain markers. Intra-tumour heterogeneity is defined by the variation within individual tumours, since distinct tumour cells can exhibit different properties and markers (Visvader, 2011). It is therefore important to understand how tumours evolve in order to select the most appropriate therapeutic approach. Several theories have been proposed to explain tumour initiation and progression; these include the Knudson two-hit hypothesis (Knudson, 1971), the clonal evolution model (Nowell, 1976), multistep mutation model (Fearon and Vogelstein, 1990), and the cancer stem cell (CSC) theory (Bonnet and Dick, 1997). From these, three main models can explain tumour progression in most cancer types: the CSC model, the clonal evolution model, and the interconversion model (Figure 1.1).

The clonal evolution model is centred on the genetic instability of cancer cells. This model is based on the premise that tumours initiate with a single somatic mutation forming a neoplastic cell, and continuous mutagenesis gives rise to a neoplasm with cellular diversity. The dominant cells in these tumours are those best fitted for survival and proliferation (Cross *et al.*, 2016). Studies performed to assess the mutational spectrum of tumours have demonstrated that their genomic landscape is complex and heterogenous, presenting alterations that range from point mutations to large structural variants (Weir *et al.*, 2007, Kan *et al.*, 2010, Imielinski *et al.*, 2012). TRACERx (*TRA*cking

non-small cell lung *C*ancer *E*volution through therapy (*Rx*)) is a prospective study in primary non-small cell lung cancer that aims to define the genomic landscape of these tumours and understand the impact of clonal heterogeneity in therapeutic and survival outcome (Jamal-Hanjani *et al.*, 2014). For this, the TRACERx consortium established methods to investigate the dynamics of genetic intra-tumour heterogeneity within individual tumours overtime, by multiregional and longitudinal tumour sampling and sequencing (Jamal-Hanjani et al., 2014). The results from the first 100 patients showed that chromosomal instability is a significant driver of parallel evolution and is associated with poor outcome (Jamal-Hanjani *et al.*, 2017). In the same study, Jamal-Hanjani and colleagues also demonstrated that there is an early clonal genome doubling, followed by widespread subclonal diversification. Months later, McGranahan and colleagues showed that 40% of the cancers analysed presented human leukocyte antigen (HLA) loss of heterozygosity, which was associated with high subclonal neoantigen burden (McGranahan *et al.*, 2017). When immune infiltration was analysed, it was shown that the immune microenvironment exerts a strong selection pressure in early stages of disease, promoting multiple routes to immune evasion (Rosenthal *et al.*, 2019).

The CSC model suggests that tumours are organised in a hierarchical manner, in which only a small subset of cells, the CSCs, have the potential for tumour initiation and maintenance. The irreversible loss of tumorigenicity, which gives origin to transient, terminally differentiated non-stem cancer cells, is determined by hierarchical mechanisms, such as asymmetrical cell division. This model can also explain tumour heterogeneity, as well as therapy resistance, minimal residual disease, and tumour recurrence (Vermeulen *et al.*, 2012, Kreso and Dick, 2014). Despite the fact that the model has been best studied in the context of haematological cancers, (Fearon *et al.*, 1986), there is evidence of a CSC hierarchy in many solid tumours, such as neuroblastoma (Shimada *et al.*, 1984), breast (Al-Hajj *et al.*, 2003), brain (Singh *et al.*, 2004), colon (Dalerba *et al.*, 2007), pancreatic (Li *et al.*, 2007) and ovarian (Zhang *et al.*, 2008) cancers.

Finally, the interconversion model combines elements of both models, and relies on the ability of tumorigenic cells to interconvert between proliferative and quiescent states. This has already been observed in leukaemia, a typical CSC model where some tumorigenic cells undergo clonal evolution and/or interconvert between different states of malignancy, and in melanoma, which has high levels of tumorigenic cells which can either propagate by clonal evolution or interconvert between highly proliferative and quiescent states (Shackleton, 2010, van Neerven *et al.*, 2016). This model also includes the role of stromal cells in maintaining a pool of stem-like cells (Vermeulen et al., 2012).

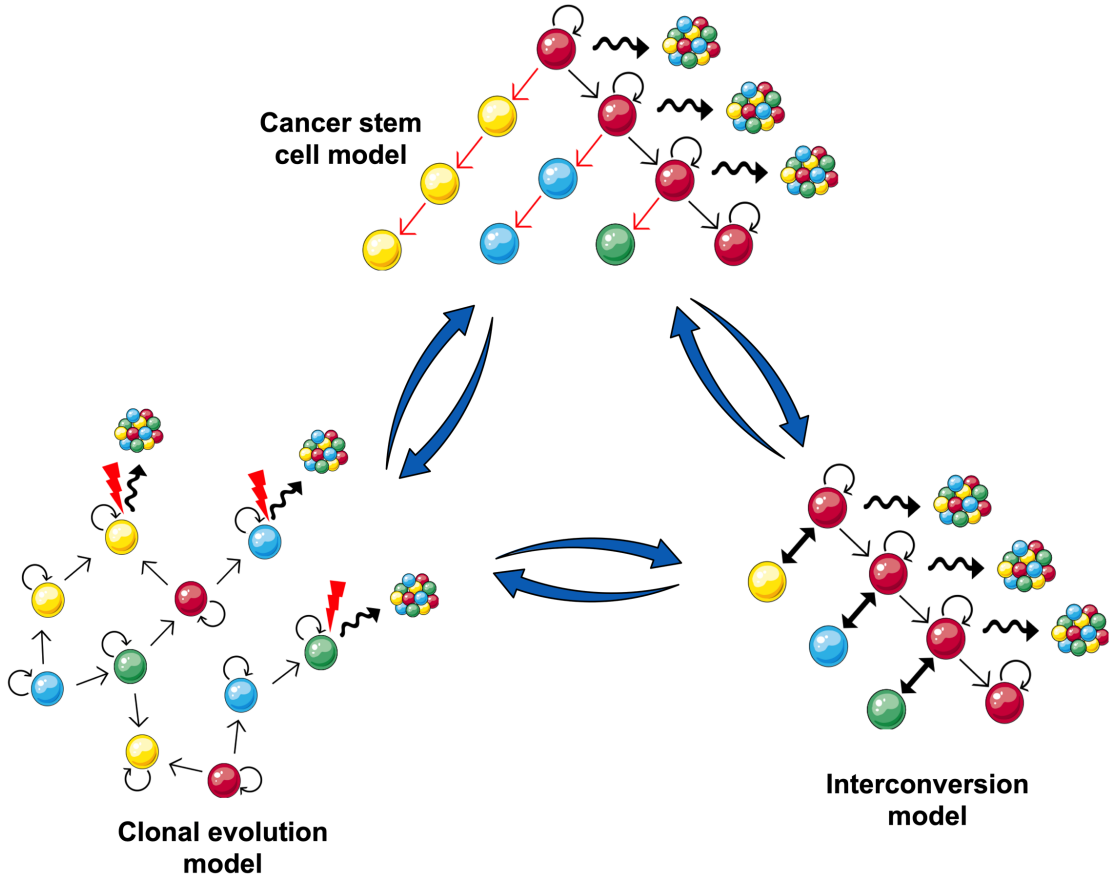

Figure 1.1|Models of cancer propagation.
In the CSC model, tumorigenic cells (red) give rise to more cells with tumorigenic potential and non-tumorigenic cells (yellow, blue and green) in an irreversible (red arrows) hierarchical manner. Circular arrows represent the self-renewal capacity of cells. In the clonal evolution model, different cells have tumorigenic potential but only some acquire extra genetic mutations (red flash) gaining advantage in disease-propagating potential. In the interconversion model, cells can interconvert (two-way arrows) between actively malignant and quiescent states. These models are not mutually exclusive, which results in the lack of a predominant model of cancer propagation (large central arrows). Adapted from Shackleton, 2010.

In a seminal review article published in 2000, Hanahan and Weinberg proposed six hallmarks of cancer which are essential to allow cells to progress to a neoplastic state and to enable tumour growth and metastatic dissemination (Hanahan and Weinberg, 2000). In 2011, the authors published an updated review to include two emerging hallmarks and two enabling characteristics of the process of cancer development (Hanahan and Weinberg, 2011). The final model includes eight different hallmarks of cancer and two enabling characteristics, as represented in Figure 1.2. Some of the hallmarks represent characteristics that are intrinsic to the cancer cell, such as sustained proliferation, cell death resistance, deregulation of cellular metabolism and replicative immortality, and others represent traits that are associated with the environment around cancer cells, known as tumour microenvironment (TME); these include tumour angiogenesis and formation of distant metastasis. One of the two enabling characteristics is the genomic instability in cancer cells, which drives random mutations allowing other hallmarks to arise. The other one is the tumour promoting inflammation that is driven by cells of the immune system, which aids in tumour progression (Hanahan and Weinberg, 2000, Hanahan and Weinberg, 2011).

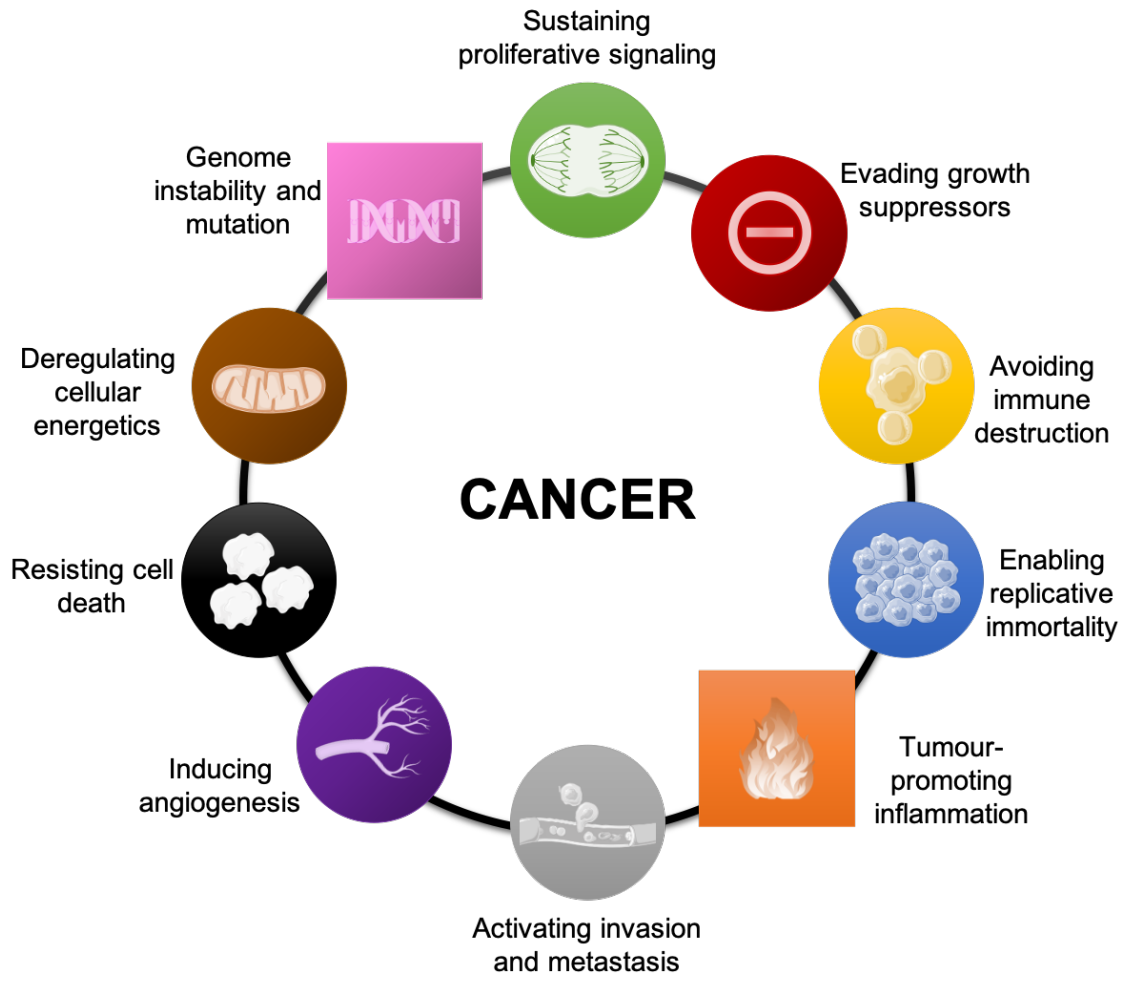

Figure 1.2|The hallmarks of cancer.
The diagram incorporates the ten hallmarks of cancer proposed by Hanahan and Weinberg. These are traits that either cancer cells acquire as they progress to malignancy, or tumours require in order to form a TME supportive of tumour progression. Characteristics inside a circle represent hallmarks, characteristics inside a square represent enabling features of cancer. Adapted from Hanahan and Weinberg, 2000 and Hanahan and Weinberg, 2011.

1.2. Tumour microenvironment

As discussed by Hanahan and Weinberg, cancers should be considered as complex organs and not just masses of tumour cells as was initially thought (Hanahan and Weinberg, 2011). Neighbouring cells can be recruited and transformed by malignant cells throughout tumorigenesis, and it is the interaction between transformed and non-transformed cells that creates the TME (Balkwill *et al.*, 2012). The idea that tumour cells interact with a specific organ microenvironment dates back to 1889, when Stephen Paget proposed the "seed and soil" hypothesis to explain the non-random pattern of metastasis. After analysing several autopsy records, Paget hypothesised that metastases formation was not due to chance, but that certain tumour cells, which he named the "seed", exhibit specific affinity for the environment of certain organs, which form the "soil" (Paget, 1889). Almost 40 years later, James Ewing proposed that the lymphatic and circulatory systems direct cancer cells to the metastatic site (Ewing, 1928). A key refinement of Paget's hypothesis was described in 2003, when Fidler proposed that the metastatic process is selective for cells that successfully survive migration to the distal organ, and that the interaction of these cells with the new microenvironment determines the success of metastatic cell proliferation (Fidler, 2003).

The TME is crucial in tumour initiation and progression, since alterations in tissue organisation and homeostasis often precede tumour formation, and the altered microenvironment favours proliferation of malignant cells over normal cells due to selective pressure. Changes in the TME also affects the way tumours respond to therapies, especially those targeting extracellular signalling pathways, such as growth factor receptor pathways (Polyak *et al.*, 2009).

Studying the individual components of the TME will be critical for understanding tumour biology and hence for devising effective interventions. Component parts include malignant cells (both cancer cells and CSCs), cells of the immune system, tumour vasculature and lymphatics, stromal cells, such as cancer associated fibroblasts (CAFs), and extracellular matrix (ECM). Each of these components will be described in the following subsections. The role of the immune system in cancer progression will be described in more detail later.

1.2.1. Cancer stem cells

CSCs are defined by their ability to efficiently initiate new tumours when inoculated into tissue, and by sharing the expression of markers with normal tissue-specific stem cells (Hanahan and Weinberg, 2011, van Niekerk *et al.*, 2017). The discovery of this phenotype allowed for the identification of CSCs in most cancers. The tumorigenicity associated with their tumour-initiating capacity also indicates that CSCs are involved in crucial processes of tumour development, cell proliferation and metastatic dissemination (Chang, 2016).

CSCs are usually resistant to chemotherapy and radiotherapy, which, due to their self-renewal capacity and consequent immortality, accounts for lack of complete response to these treatments (Chang, 2016). This self-renewal is regulated by symmetric and asymmetric divisions during cell proliferation; a feature shared by normal stem cells. If a symmetric division occurs, two daughter cells are formed which are identical to the parent cell, however, an asymmetric division will originate one cell with stem cell potential, and a second cell destined for terminal differentiation. In tumorigenesis there is often a dysregulation in the asymmetric divisions, favouring an increased formation of cells with stem potential (van Neerven et al., 2016).

CSCs can also arise from normal cancer cells via the process of epithelial-mesenchymal transition (EMT). EMT is the process by which epithelial cells undergo changes such as loss of polarity, transitioning the cells into a mesenchymal phenotype. This is associated with an increased capacity for migration and invasion, as well as resistance to apoptosis (Kalluri and Weinberg, 2009). There are three different subtypes of EMT which are associated with their biological context: type 1 is related to embryo formation and early development, type 2 is associated with tissue regeneration and wound healing, and type 3 occurs in tumour cells that have already suffered genetic or epigenetic alterations (Chang, 2016). EMT can be induced by either endogenous expression of transcription factors associated with EMT (e.g. Twist and Snail) or by exposure to particular cytokines (e.g. transforming growth factor beta, TGF-β). Signalling pathways often associated with stemness are also linked to EMT induction; these include Notch, Hedgehog, TGF-β and Wnt (Singh and Settleman, 2010).

Immune escape, described in detail later, is critical for tumour progression, and the immunosuppressive capacity of CSCs plays a fundamental role in this process. They can evade the immune system through different mechanisms, such as downregulation of major histocompatibility complex (MHC) class I molecules, (Di Tomaso *et al.*, 2010, Schatton *et al.*, 2010, Morrison *et al.*, 2018), downregulation of genes involved in antigen

processing and presentation (Di Tomaso et al., 2010, Sultan *et al.*, 2018), and low expression of Toll-like receptor 4 (TLR4) (Alvarado *et al.*, 2017). CSCs can also remodel the surrounding TME by secreting immunosuppressive molecules such as TGF-β, which inhibits immune cell proliferation and interleukin (IL)-4, which attenuates anti-tumour response. These cytokines promote the recruitment of other immunosuppressive cells (e.g. tumour associated macrophages (TAMs)) to the TME, creating a positive feedback loop (Yamashina *et al.*, 2014, Zhou *et al.*, 2015).

Even though CSCs are very plastic and highly resistant to conventional chemotherapy and radiotherapy, there are therapies available which are directed at these cells. An observation made in leukemic cells where the use of all-*trans* retinoic acid blocked the differentiation of CSCs, inspired the emergence of new therapies (Nowak *et al.*, 2009). These vary from inhibition of key stem cell signalling pathways, to ablation using antibody-drug conjugates, epigenetic therapy and targeting of CSCs in quiescence (Batlle and Clevers, 2017). However, since the microenvironment involving CSCs is so important for their development, as long as they have a permissive environment, CSCs will proliferate and thrive (Cabarcas *et al.*, 2011, Aponte and Caicedo, 2017, Lau *et al.*, 2017). It has been suggested therefore that CSC targeting should include CSC-niche interactions, such as targeting specific ECM proteins that are needed for CSC dissemination (Batlle and Clevers, 2017).

1.2.2. Tumour vasculature

Tumours need their own blood supply in order to receive sufficient oxygen and nutrients to fuel their metabolic requirements. In 1971, Judah Folkman established the link between tumour size and tumour angiogenesis, showing that tumours cannot grow larger than 2-3 mm without inducing angiogenesis (Folkman, 1971). Angiogenesis can occur through different mechanisms in normal tissues and tumours. Vessel formation can be achieved by sprouting, which is formation of new blood vessels from pre-existing ones mainly through growth factor stimulation (e.g. vascular endothelial growth factor, VEGF); by recruitment of bone marrow derived or vascular wall resident endothelial progenitor cells that differentiate into endothelial cells; or by intussusception, which happens when one existing blood vessel splits into two by formation of transvascular pillars (Carmeliet and Jain, 2011, Krishna Priya *et al.*, 2016). Other tumour-specific mechanisms include vessel co-option, when tumours take over the existing vasculature; vascular mimicry, when tumour cells mimic endothelial cells and form vascular channels;

and the ability of CSC to form non-endothelium lined blood vessels (Carmeliet and Jain, 2011, Krishna Priya et al., 2016).

There are several growth factors that can stimulate angiogenesis, VEGF being the most important. Chronic overproduction of these factors by tumours leads to uncontrolled development of new blood vessels. These tumour blood vessels usually present with an aberrant morphology, with excessive branching, abundant and aberrant protuberances, blind ends, discontinuous endothelial cell lining, and defective basement membrane and pericyte coverage (Krishna Priya et al., 2016, De Palma *et al.*, 2017). The basement membrane is a specialised ECM produced by endothelial cells that separates the epithelium from the stroma of any tissue (Kalluri, 2003). This membrane also prevents blood vessel infiltration of premalignant lesions, and is lost during tumour progression when tumour cells acquire an invasive phenotype and disseminate (De Palma et al., 2017).

With tumour development and progression, especially in solid tumours, poor blood supply due to aberrant vascularisation restricts cancer and stromal cell access to nutrients and oxygen, giving rise to hypoxic areas (Petrova *et al.*, 2018). Hypoxia is another modulator of angiogenesis, since it induces tumour and stromal cell production of hypoxia-inducible factors (HIF). Activation of HIF signalling promote, for example, secretion of VEGF-A by tumour cells, and expression of VEGFR2 (VEGF-A receptor) by endothelial cells of neighbouring blood vessels, inducing angiogenesis (De Palma et al., 2017, Petrova et al., 2018).

In normal tissues, the lymphatic vasculature is essential for immune function and tissue fluid homeostasis. Lymphatic vessels are necessary routes of antigen delivery to lymph nodes for induction of adaptive immune responses. The regulation of interstitial fluid pressure is very important for maintaining tissue fluid homeostasis, and when there is an increase of the fluid pressure, this stretches the ECM, opening the surrounding lymphatic vessels enabling draining of the interstitial fluid. However, in tumours, the accumulation of stromal components in the TME, causes ECM stiffness and contributes to lymphatic vessel compression, decreasing the ability of interstitial fluid removal by these vessels (Sabine *et al.*, 2016). Tumour-derived growth factors can influence lymphatic remodelling, by contributing to the sprouting of new vessels or lymphatic enlargement. VEGF-C and VEGF-D are key factors which promote intra- and peritumoral lymphangiogenesis, facilitating tumour dissemination (Mandriota *et al.*, 2001, Skobe *et al.*, 2001, Stacker *et al.*, 2001) to lymph nodes, and posteriorly, to distant organs (Stacker *et al.*, 2014). The phenotype of lymphatic endothelial cells is often altered in the TME. The most notable changes are in expression of chemokines,

immunoregulatory proteins and adhesion molecules; all of which affect leukocyte trafficking and behaviour (Vigl *et al.*, 2011). Such alterations may impact the ability of lymphatic vessels to transport antigen presenting cells to draining lymph nodes, and, ultimately, to lack of anti-tumour immunity (Lund, 2016).

High endothelial venules (HEVs) are specialised post capillary venules that can be found in all secondary lymphoid organs (SLOs), except the spleen. These venules are characterised by endothelial cells with plump and cuboidal morphology, that not only share common pan-endothelial cell markers, such as cluster of differentiation (CD)31 and VE-cadherin (Pfeiffer *et al.*, 2008), but also express genes that are important in the regulation of lymphocyte recruitment and immunological defence. These include enzymes involved in the synthesis of mucin-like glycoproteins, termed peripheral node addressins (PNAd), which act as adhesion molecules for L-selectin (CD62L) expressing lymphocytes (Lee *et al.*, 2014). These structures allow the migration of naïve and central memory T lymphocytes, naïve B cells and dendritic cells (DC) from the circulation into the lymphoid organ (Girard *et al.*, 2012, Ager and May, 2015).

HEVs can also be found outside SLOs, since they have been detected at sites of chronic inflammatory diseases (Aloisi and Pujol-Borrell, 2006) and infection (Neyt *et al.*, 2012). In 2011, HEVs were also found in the TME (Martinet *et al.*, 2011), mainly as part of lymphoid-like tissues named tertiary lymphoid structure (TLS) (Colbeck *et al.*, 2017a). Intratumoural HEVs have similar phenotypic characteristics as lymph node HEVs, including PNAd expression which facilitates their identification (Jones *et al.*, 2018). Whilst HEV were found initially in breast, melanoma, ovary, lung and colon cancers (Martinet et al., 2011), further research has identified the presence of HEVs in the microenvironment of most solid cancers, and HEVs alone can be a strong prognostic marker for a favourable clinical outcome (Colbeck et al., 2017a). HEV neogenesis may help lymphocyte infiltration in the tumour, specifically naïve and helper T cells (cytotoxic and helpers) that can specifically target tumour antigens and destroy tumour cells (Martinet et al., 2011).

Although the blood circulation has a pivotal role in metastatic dissemination, this is not the only route available to tumour cells (Figure 1.3-A). There is evidence supporting the involvement of lymph nodes as a gateway (Figure 1.3-B) for further tumour cell dissemination in mice (Chen *et al.*, 2005, Roberts *et al.*, 2006, Burton *et al.*, 2008) and humans (Jatoi *et al.*, 1999, Early Breast Cancer Trialists' Collaborative Group, 2005, Mohammed *et al.*, 2007). The latter studies revealed that lymphovascular invasion and nodal metastasis are associated with poor outcomes. HEVs were also suggested as a portal for tumour dissemination to distant organs, by giving tumour cells a direct access

to the blood circulation (Figure 1.3-C) (Qian *et al.*, 2007). This mechanism was recently confirmed by two independent studies. Brown and colleagues showed that 4T1 mammary carcinoma tumour cells accumulated within the subcapsular sinus of the draining lymph node. HEV involvement was demonstrated using intra-vital imaging which identified 4T1 cells closely associated with HEVs and intravasating their lumen (Brown *et al.*, 2018). Pereira and colleagues used different cancer cell lines, including 4T1 mammary carcinoma, B16F10 melanoma and SCCV2 squamous cell carcinoma, and engineered them to express a photoconvertible protein, Dendra2 (a green-light emitting protein, that is converted to a red-light emitting protein after excitation). After orthotopic implantation of these cells and tumour establishment, they photoconverted cells within the metastatic draining lymph node and detected red-light emitting cells in the systemic blood circulation and in the lungs (Pereira *et al.*, 2018).

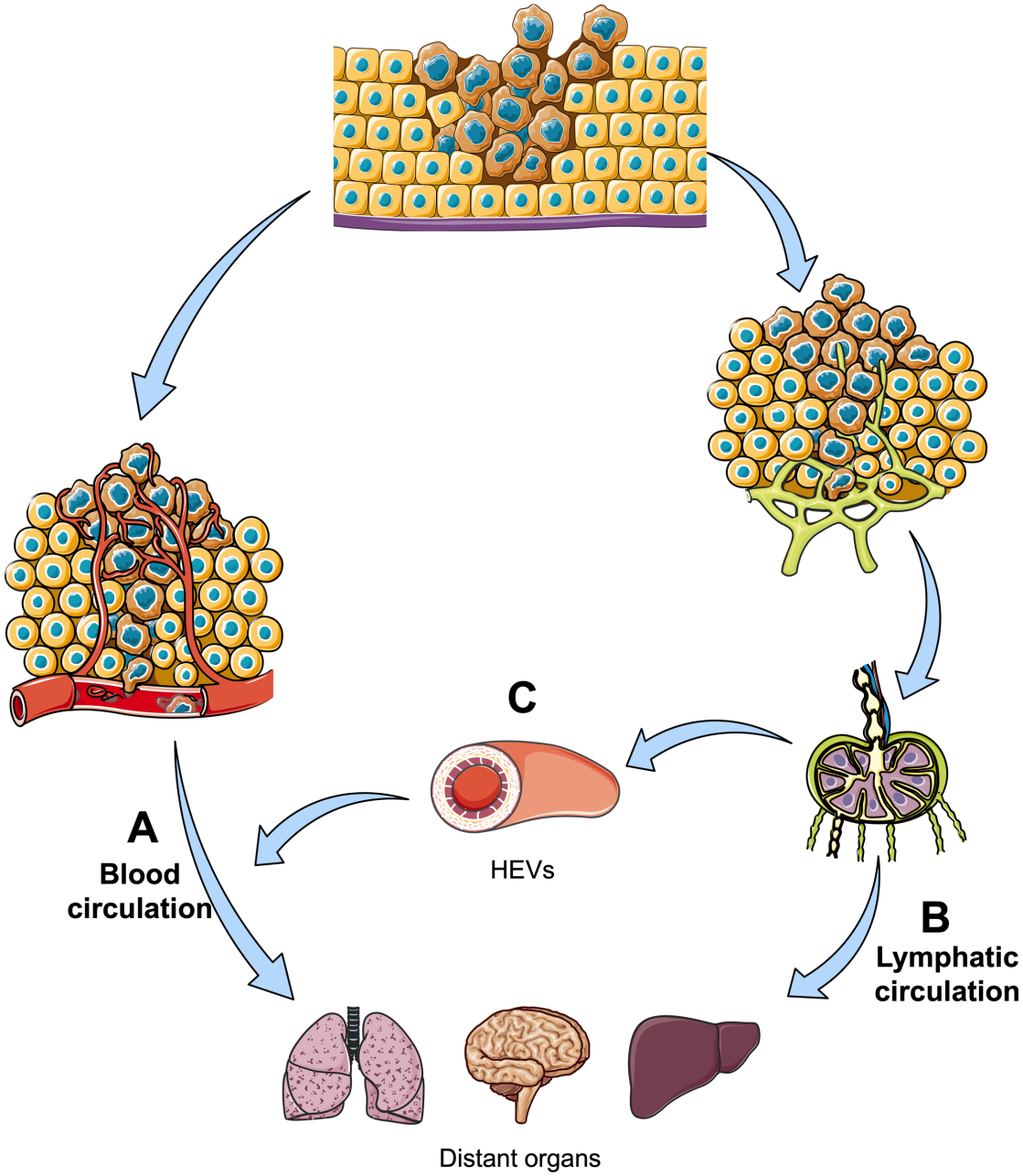

Figure 1.3|Routes for distant organ metastases formation.
After the acquisition of an invasive phenotype, tumour cells can infiltrate tumour blood vessels and get transported to distant organs where they may form micrometastases and colonise new tissue (**A**). However, if a tumour has lymphatic vessels, tumour cells can intravasate these and be transported to regional lymph nodes. Here, tumour cells can either follow the lymphatic stream (**B**) or have access the blood stream through HEVs (**C**). Either path gives access to distant organs, extravasating and forming metastases in the new tissue.

1.2.3. Stromal cells

As previously mentioned, tumour cells do not evolve into cancer alone. There are tissue resident cells that are recruited and reprogrammed by tumour cells, in order to provide a niche that is optimal for tumour progression (Hanahan and Weinberg, 2011). A role of these cells in promoting tumour angiogenesis and matrix remodelling has long since been described (Folkman, 1974, Bissell *et al.*, 1982, Dvorak, 1986). Their role in promoting tumour growth and tumour progression, as well as their contribution to therapeutic resistance, has however only recently been unveiled (Hanahan and Coussens, 2012). Indeed it has become clear that cancer stromal cells can contribute to each hallmark of cancer and, beyond the essential hallmarks, they also help create specialised vascular niches which serve to nurture CSC survival (Hanahan and Coussens, 2012).

Cells of different origins, such as fibroblasts (Kojima *et al.*, 2010), pericytes (Spaeth *et al.*, 2009), bone marrow mesenchymal stromal cells (Spaeth et al., 2009) and adipocytes (Nieman *et al.*, 2011), can be recruited by tumour cells to be part of the TME. These are then activated and transformed through different processes (secreted factors, microRNAs, exosomes, endothelial-mesenchymal transition) into three distinct subtypes: CAFs, cancer associated adipocytes (CAAs) or cancer associated endothelial cells (CAECs). Tumour cells can also be recruited as tumour stromal cells to support tumour development (Figure 1.4) (Scully *et al.*, 2012, Chen *et al.*, 2014).

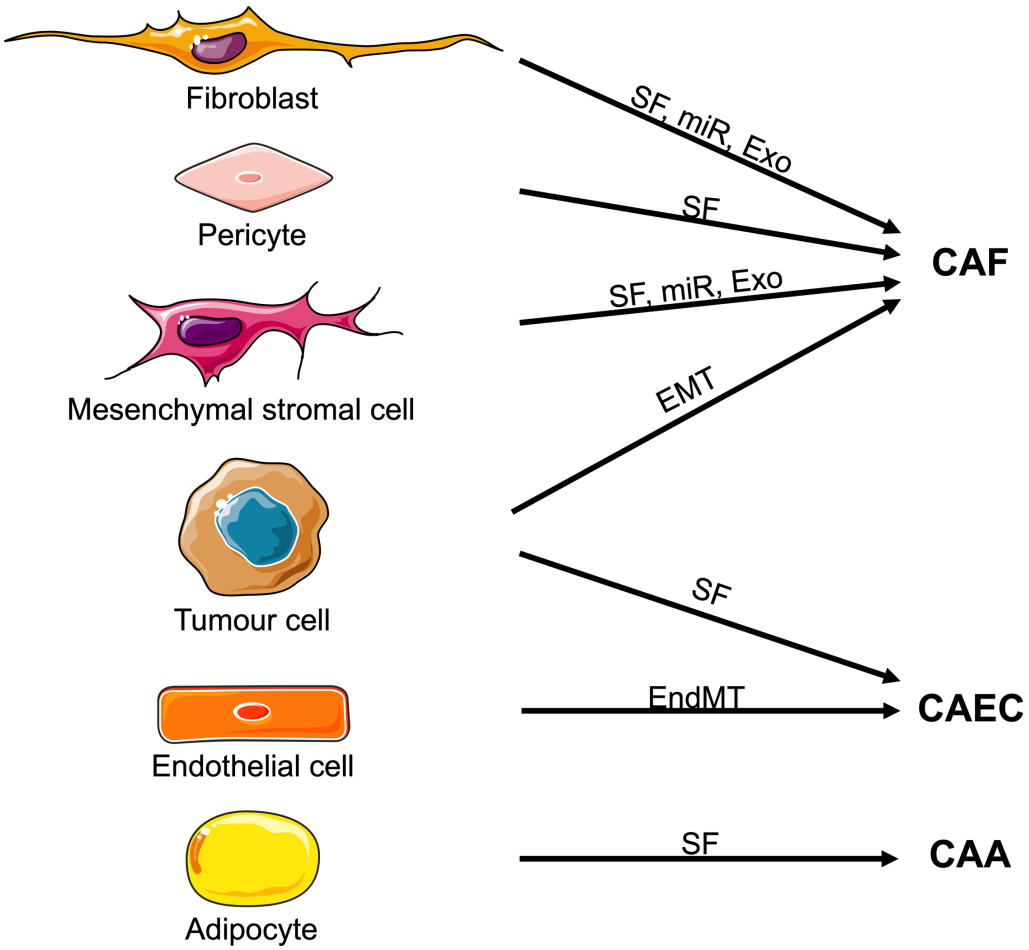

Figure 1.4|Origins of tumour stromal cells.

Tumour stromal cells can originate from different types of cells. Fibroblasts, pericytes, mesenchymal stromal cells and tumour cells give rise to CAFs, adipocytes give rise to CAAs and endothelial cells give rise to CAEC. These transformations may happen due to the presence of soluble factors (SF), specific miRNAs (miR) or exosomes (Exo) in the TME, or after EMT or endothelial-mesenchymal transition (EndMT) has taken place. Adapted from Bussard *et al.* (2016).

Fibroblasts in normal tissues are resting mesenchymal cells in the ECM, that can be activated during wound-healing, tissue inflammation or organ fibrosis. In cancer, CAFs are activated to promote tumour development, inflammation and fibrosis (Erez *et al.*, 2010, Cirri and Chiarugi, 2011, Öhlund *et al.*, 2014). CAFs constitute the majority of stromal cells in the TME and have the capacity to co-evolve with tumour cells, in order to acquire a pro-tumour phenotype. As a result of this, CAFs have the ability to survive and populate the TME. Morphologically, CAFs are larger than normal fibroblasts, presenting multiple cytoplasmic branches and indented nuclei. They have high proliferative rates, enhanced migratory properties and high capacity for ECM synthesis and remodelling. By creating a stiffer matrix, CAFs create a physical barrier to immune infiltration and a structural scaffold for tumour intercellular interactions (Chen and Song, 2019). By remodelling the ECM through release of matrix metalloproteinases (MMPs), CAFs promote the release of ligands that are sequestered in the matrix, allowing them to be free to interact with specific receptors. CAFs themselves can also synthesize specific molecules that contribute to cancer progression (Table 1.1).

Table 1.1|Examples of proteins secreted by CAFs and their function in tumour progression.

Function	Secreted proteins	Reference
Tumour cell proliferation	Chemokine (C-X-C motif) ligand (CXCL) 12	Orimo *et al.* (2005)
Cancer stemness maintenance	Hepatocyte growth factor (HGF)	Vermeulen *et al.* (2010)
Angiogenesis	CXCL12	Orimo et al. (2005)
	Connective tissue growth factor (CTGF)	Yang *et al.* (2005)
Invasion and Metastasis	Lysyl oxidase (LOX)	Levental *et al.* (2009)
	miR105	Zhou *et al.* (2014)
Resistance to therapy	Hyaluronan	Provenzano *et al.* (2012)
Inflammation	CXCL1, CXCL2, IL-1β, IL-6	Erez et al. (2010)

Only recently have CAAs been given more attention. Since adipocytes are the predominant cells in breast tissue, CAAs have been best studied in the context of breast cancer. CAAs can be found at the invasive tumour front where they are thought to play important roles in matrix remodelling and invasion and survival of tumour cells (Dirat *et al.*, 2011). Adipokines secreted by CAAs have a crucial role in these processes. *In vitro* studies demonstrated that leptin can enhance tumour proliferation and promote EMT in tumour cells. Another adipokine, adiponectin, is able to selectively induce apoptosis in tumour cells, and its cleaved form stimulates migration and invasion (Hoy *et al.*, 2017). Co-culture of ovarian cancer cells and adipocytes revealed a stimulation in lipolysis in adipocytes and β-oxidation in cancer cells, suggesting that the CAAs may be an energy source for cancer cells (Nieman et al., 2011).

CAECs derive mainly from bone marrow endothelial cells that have undergone endothelial-mesenchymal transition (EndMT), acquiring a fibroblast-like morphology. These cells exhibit reduced expression of endothelial cell markers, such as CD31, upregulation of CAF markers (fibroblast specific protein 1 (FSP1), α-smooth muscle actin (α-SMA)), and an abnormal responsiveness to growth factors, such as epidermal growth factor (EGF) and VEGF. This last factor stimulates migration and enhances the survival of CAEC by increasing their antiapoptotic potential. Observations that some tumour endothelial cells present the same chromosomal aberrations as the tumour cells indicate that CAECs might also develop from dedifferentiated tumour cells, retaining some of their properties (Streubel *et al.*, 2004). Cytogenetic analysis revealed that CAECs are karyotypically aneuploid, as opposed to normal endothelial cells which are diploid, and that CAECs associated with high metastatic tumours have a more complex abnormal karyotype than the ones associated with low metastatic tumours (Hida *et al.*, 2004, Akino *et al.*, 2009, Ohga *et al.*, 2012). These karyotypes are often associated with cancer cells containing multidrug resistance genes, and they can be the basis of resistance of these cells to chemotherapeutic drugs (Bussolati *et al.*, 2003, Xiong *et al.*, 2009)

1.2.4. Extracellular matrix

Although it was once thought that the ECM was just the filling of the extracellular interstitial space, it is known now that it represents a non-cellular component present in every tissue, and it not only provides biochemical and structural support, but it is also biologically active, enabling cell-cell communication, cell adhesion and proliferation. The ECM is composed of water, minerals, proteoglycans and fibrous proteins secreted by resident cells, and its composition varies from tissue to tissue depending on the individual

needs of each tissue. It is a highly dynamic structure that is continuously being remodelled. In order to maintain tissue homeostasis, this remodelling requires a balance between degradation and secretion (Frantz *et al.*, 2010, Lu *et al.*, 2011, Walker *et al.*, 2018).

Proteoglycans fill the majority of the ECM space and these play an essential role in the maintenance of a normal ECM since without proteoglycans, it has been shown that the ECM is dysfunctional and undergoes collapse (Costell *et al.*, 1999, Arikawa-Hirasawa *et al.*, 1999). Collagens, elastins, fibronectins (FNs) and laminins are all included in the group of fibrous proteins which form components of the ECM. Collagen is the most abundant protein in the ECM, forming the basis of its architecture. The collagen family, comprising 28 known subtypes of proteins, provides tensile strength, regulates cell adhesion, supports chemotaxis and migration and directs tissue development (Rozario and DeSimone, 2010). Elastin provides recoil to tissues that suffer repeated stretch. Elastin molecules are assembled into fibres and these are crosslinked by LOX, contributing to ECM stiffness (Wise and Weiss, 2009). The 20 different FN isoforms are encoded by one single gene. These proteins direct organisation of the ECM and mediate cell attachment and function. FN can be stretched by cells, exposing integrin-binding sites (Smith *et al.*, 2007). Other proteins with similar functions are also found in the ECM. One example is tenascin-C (TNC), which plays an important role in promoting fibroblast migration during wound healing (Frantz et al., 2010, Walker et al., 2018).

The arrangement and orientation of ECM constituents are critical for tumour progression. Tumours are stiffer than normal surrounding tissues due to ECM deposition and remodelling by CAFs. As previously mentioned, CAFs can deposit large quantities of ECM proteins and secrete growth factors. They can also apply strong contraction forces on the ECM, and, as consequence, the freshly deposited proteins are reoriented and crosslinked by LOX, giving rise to larger and more rigid fibrils that further stiffen the tissue. The increased deposition of matrix proteins drives tumour progression by interfering with cell-cell adhesion, cell polarity and amplifying growth factor signalling (Frantz et al., 2010, Walker et al., 2018).

The dynamic interplay between proliferating tumour cells and the microenvironment is facilitated by matrix remodelling enzymes in the TME. These can be either MMPs, adamalysin-related membrane proteinases, bone morphogenic protein-1, or tissue secreted proteinases (Liotta and Kohn, 2001). MMPs, the most abundant proteins in the ECM, are secreted mainly by tumour cells and CAFs, and they help to remodel the basal membrane of tissues, aiding tumour invasion. By degrading and

loosening the surrounding matrix, these enzymes can also release active growth factors and expose hidden integrin-binding sites, allowing integrins at tumour cell surface to contact directly with the matrix. This is the mechanism used by cells to sense matrix stiffness, modulating the cytoskeleton to adapt to new conditions. If the ECM gets to a critical-stiffness point, cell-cell adhesions are disrupted and tumour cells undergo EMT (Conlon and Murray, 2019).

1.2.5. Targeting the TME

The current conventional cancer therapy options available are surgery, radiation or chemotherapy, however, neither of these, alone or in combination, have proven to be completely effective. There is a need to reduce toxicity and improve treatment efficacy, and the recent recognition of the tumour as a complex organ, as opposed to a bulk of malignant cells, has uncovered possibilities for development of different methods to target cancer. As stated above, the TME has a crucial role in supporting tumour growth, invasion and metastasis, making the components of this compartment interesting targets for new therapies. Also, combining therapies targeting multiple compartments, including the immune system (see Section 1.3.4), may represent an effective way of preventing compensatory escape mechanisms which may occur in response to targeting individual compartments (Hanna *et al.*, 2009).

Although conventional chemotherapy will cause death of most cells in the tumour, CSCs are resistant to the great majority of these agents, due to the intrinsic mechanisms that permit resistance to radio- and chemotherapy. Normal stem cells are valuable for the organism since they maintain the pool of cells in the organism. To protect themselves, normal stem cells avoid death by apoptosis or senescence, by expressing high levels of anti-apoptotic molecules and maintaining high telomerase activity and a superior DNA damage response (DDR), when compared to non-stem cells. CSCs appear to exploit these mechanisms to resist anti-cancer therapies. Furthermore, high levels of expression and activity of ATP-binding cassette (ABC) transporters allow them to export any drug that might cross the cell membrane. These cells also have high activation of EMT and stemness pathways, making them more resistant to drugs by entering a state of quiescence that most drugs, designed to target proliferating cells, cannot reach (Prieto-Vila *et al.*, 2017). CSCs also express high levels of aldehyde dehydrogenase (ALDH) which protects them against reactive oxygen species (ROS), and ROS-inducing drugs (Yoshida and Saya, 2016, Prieto-Vila et al., 2017).

There are three classes of stemness-modulating drugs: stem cell targeting drugs, designed to selectively kill CSCs (Buommino *et al.*, 2011, Tang *et al.*, 2011, Wang *et al.*, 2011); stemness inhibiting drugs, designed to reduce stemness properties (Hyun *et al.*, 2011, Yang *et al.*, 2012b); and stemness promoting drugs, designed to increase stemness properties (Oliveras-Ferraros, 2010). They all can be used in combination with standard chemotherapeutic drugs, however, the advantages in specificity are not enough to deplete all cancer cells. The use of monoclonal antibodies to target either CSC cell surface markers or stemness signalling pathways have also been used in combination with standard chemotherapeutic drugs, albeit with little success (Yakisich, 2012).

After formulating the hypothesis that tumour growth is dependent on angiogenesis, Folkman pioneered the field of angiogenic inhibitors by reporting the first angiogenesis inhibitors in the 80's (Taylor and Folkman, 1982, Crum *et al.*, 1985). After this, new strategies were developed with two main methods involved; the first involves the disruption of pathways underpinning tumour angiogenesis, and the second involves direct anti-vascular effects. Both methods are more effective when used in combination with other agents e.g. targeting blood vessels with endostatin, a broad-spectrum angiogenesis inhibitor, is more effective when combined with conventional chemotherapy. A second example is the use of RGD (arginine-glycine-aspartic acid) peptide motifs in combination with oncolytic viruses; following expression at the tumour site, RGD binds to receptors in endothelial cells of cancer-associated vasculature, reducing tumour vascular permeability and enhancing anti-tumour efficiency of oncolytic viruses (Kurozumi *et al.*, 2007). The use of metronomic chemotherapy also has some anti-angiogenic effects, with the advantage of less associated toxicity. Bevacizumab, a monoclonal antibody against VEGF, is already approved by the FDA for use in lung and colorectal cancer, in combination regimens (Hanna et al., 2009). Another possibility is to target the platelet derived growth factor (PDGF)/PDGF receptor axis, however, this approach is context dependent and success rates were only observed in specific types of tumours, and in combination with other chemotherapeutic agents (Papadopoulos and Lennartsson, 2018). The Tie2-angiopoietin pathway is also being explored, with some inhibitors being tested in phase-I and II in clinical trials (Gillen *et al.*, 2019).

Given the important role of CAFs in supporting tumour growth, consideration has been given to their potential as a target for cancer therapy. Blockade of PDGF receptor signalling has been shown to result in a decrease in angiogenesis and α-SMA expression, and less migration and invasion of activated fibroblasts (Hanna et al., 2009, Togo *et al.*, 2013). Since fibroblast activation protein (FAP) is the best cell surface marker for CAFs, it has been tested as a target in several therapeutic approaches. In breast

carcinoma cells, a DNA vaccine targeting FAP resulted in suppression of neoangiogenesis, as well as decreased tumour growth and reduced metastasis (Loeffler *et al.*, 2006). The use of a monoclonal anti-FAP antibody covalently linked to DM1 (protein with antimitotic activity) in mice has also been assessed and shown to result in attenuated growth of tumour xenografts without toxicity for normal tissues (Ostermann *et al.*, 2008). However, the previous use of the same antibody in a clinical trial showed no efficacy in colorectal cancer patients (Hofheinz *et al.*, 2003). Pro-drugs which are proteolytically activated by FAP-expressing CAFs have been designed in order to enable specific tumour targeting. Some studies suggest that this is an effective approach to successful increase the therapeutic window of cytotoxic drugs (Togo et al., 2013, Deng *et al.*, 2017).

The approach of targeting the ECM proteins produced by CAFs has also been tested. By enzymatically destroying proteins such as collagen, decorin and hyaluronan, the resulting reduction in interstitial pressure leads to an increase in the microvasculature, facilitating delivery of macromolecules to tumours thereby increasing the cytotoxic effect of anti-cancer drugs (Hanna et al., 2009, Togo et al., 2013). TNC is a protein expressed in the ECM of several tumours, but it is absent in normal ECM. This characteristic makes TNC a specific tumour marker that has been used by several groups to deliver drugs to the TME. A non-internalizing antibody-drug compound against TNC was used in epidermoid carcinoma *in vivo*. As soon as the antibody bound to TNC, the drug was released, inhibiting tumour growth significantly (Dal Corso *et al.*, 2017). TNC has also been used as a target for functionalised liposomes with a TNC binding peptide. These liposomes were loaded with a CAF-specific drug, navitoclax, which was previously shown to trigger CAF apoptosis, diminish TNC expression, suppress tumour outgrowth and improve host survival in rats (Mertens *et al.*, 2013). When the drug was released from the liposomes in tumour tissues *in vivo* it had the same effect (Chen *et al.*, 2016). As well as TNC, other ECM molecules have been used for tumour-specific targeting; these include FN, galectin-1, aggrecan, heparan sulphate and chondroitin sulphate (Raavé *et al.*, 2018).

1.3. Immune system in the TME

Upon exposure to pathogens, the innate immune system is the first to react by controlling and eliminating antigens in a non-specific manner. The innate response involves various cell populations, such as DCs, natural killer (NK) cells, macrophages, neutrophils, eosinophils and basophils. These are sentinel cells that can be found in

tissues where they function to monitor their microenvironment through their pattern recognition receptors (PRRs). PRRs can recognise pathogen-associated molecular patterns (PAMPs) that are not usually present in the human body, as well as danger associated molecular patterns (DAMPs), which are molecules released by stressed or necrotic cells (Parham, 2015).

Activation of the innate immunity serves to promote activation of antigen-specific adaptive immune responses. This function is served by B and T cells which express highly variable antigen-specific receptors. B lymphocytes are activated through binding of antigens to B cell receptors (BCR), promoting proliferation, antibody production and generation of long-lived plasma cells. B cells can also act as antigen-presenting cells (APCs) by processing and presenting the antigens through the MHC. The expression of highly variable T cell receptors (TCRs) that recognise peptides presented by MHCs distinguishes T cells from other lymphocytes. Following peptide presentation to the TCR, a response is mounted depending on the T cell subpopulation that is participating (Parham, 2015).

The combination of innate and adaptive immune activation results, for the most part, in the removal of the invading pathogens as well as damaged cells and associated ECM. As well as pathogen clearance, immune cells at the site of infection help to maintain the balance between clearance of damaged tissue and tissue repair, thereby playing a fundamental role in maintaining tissue homeostasis. Immune cells can help in tissue clearance by either inducing senescence in damaged cells, mostly through release of interferon-gamma (IFN-γ) or tumour necrosis factor (TNF)-α, or by directly eliminating them, through the activity of innate and adaptive immune effectors (Senovilla *et al.*, 2013). On the other hand, macrophages and neutrophils play a key role in tissue repair, and the functional plasticity and reprogramming of these cells are essential for the process (Laurent *et al.*, 2017). When tissue homeostasis is chronically disturbed, there is an increased risk of cancer development (Rybinski *et al.*, 2014).

1.3.1. Innate Immune Cells

As previously mentioned, innate immune cells are involved in the initial response to tissue perturbation, having the ability not only to control or prevent tumour initiation and progression, but also to facilitate malignant development.

Tumour associated macrophages (TAMs) have been extensively studied in the past decades, since they have been shown to play an important role in tumour growth,

metastatic dissemination and resistance to therapy (Ojalvo *et al.*, 2010, Tang and Tsai, 2012, Hughes *et al.*, 2015). Macrophages were initially described as arising exclusively from circulating monocyte precursors, however, it was shown later that several organs contain self-renewing embryonic-derived populations of resident macrophages (Ginhoux *et al.*, 2010, Schulz *et al.*, 2012, Gomez Perdiguero *et al.*, 2015). Although TAM proliferation has been observed in different mouse models, this does not seem to sustain the numbers of TAMs in growing tumours. Studies have suggested that to maintain TAM population, recruitment of circulating cells is required, which may be conventional inflammatory monocytes and monocyte-related MDSCs (Franklin *et al.*, 2014). High TAM infiltration is usually associated with poor outcomes in different types of cancer, such as breast (Schnellhardt *et al.*, 2020), ovarian (Yuan *et al.*, 2017), and lung cancer (Zheng *et al.*, 2020), although some studies have reported that some phenotypes can be associated with enhanced anti-tumour immunity (Honkanen *et al.*, 2019, Zhao *et al.*, 2019, Macciò *et al.*, 2020). TAMs can shift between an immunosuppressive, tumour-promoting phenotype and a pro-inflammatory, tumour-suppressive phenotype. The latter were shown to be able to kill tumour cells through extracellular mechanisms, contributing to elimination of nascent tumours (Diefenbach *et al.*, 2000, Biswas and Mantovani, 2010). As tumours progress, a shift towards a tumour-promoting phenotype occurs, mainly promoted by other immune cells and stromal cells in the TME (Mantovani and Allavena, 2015). These TAMs have been shown to promote stimulation of angiogenesis (Yeo *et al.*, 2014), suppression of adaptive immunity (Kren *et al.*, 2010) and promote cancer growth and metastasis (Qian *et al.*, 2009).

There are two large groups of cells that constitute myeloid derived suppressor cells (MDSCs), the granulocytic or polymorphonuclear MDSCs, and the monocytic MDSCs. The first group is similar to neutrophils in phenotype and morphology, and the second group is similar to monocytes (Bronte *et al.*, 2016). MDSCs are attracted to the TME in response to different cytokines, such as the chemokine (C-C motif) ligand (CCL)2, CCL5, CXCL5 and CXCL6 (Kumar *et al.*, 2016), acquiring a potent suppressive phenotype once there (Movahedi *et al.*, 2008). It has been demonstrated that tumoral MDSCs can differentiate into TAMs (Corzo *et al.*, 2010) and DCs (Guilliams *et al.*, 2009).

Despite DCs being present in the TME in a small percentage, they play a crucial role in the initiation of antigen-specific immunity and tolerance, by sampling and presenting antigens to T cells, as well as providing immunomodulatory signals through cell-cell contacts and cytokines (Collin and Bigley, 2018). After maturation, DCs express certain chemokine receptors, such as CCR7, which is essential for migration of these cells from the TME into tumour draining lymph nodes (Roberts *et al.*, 2016); and co-

stimulatory molecules, such as CD86, which controls T cell suppression through binding to cytotoxic T-lymphocyte-associated protein 4 (CTLA-4) (Rowshanravan *et al.*, 2018). Immunosuppressive components of the TME can inhibit DC infiltration and function. Activation of β-catenin in tumours was shown to reduce CCL4 expression, leading to lower DC infiltration and tumour growth (Spranger *et al.*, 2015). On the other hand, IL-10 produced by macrophages can abolish IL-12 production by DCs, limiting their function (Ruffell *et al.*, 2014).

1.3.2. T cells

T cells are lymphocytes that are produced in the bone marrow and matured in the thymus. During development, a random TCR is generated via VDJ recombination, and at this point, T cells commit to becoming an αβ or γδ T cell. Both types can be found in vertebrates but with important differences between them. γδ T cells are primarily located at epithelial surfaces and are able to recognise and respond to a broad range of antigens, including non-classical MHC molecules, heat shock proteins and lipids (Fahl *et al.*, 2014). αβ T cells are found in lymphoid tissues and recognise antigens via classical MHC/peptide complexes. These cells can be further divided into $CD4^+$ and $CD8^+$ T cells, depending on the co-receptor that they express after a process of positive selection in the thymus (Takada and Takahama, 2015). The two key types of effector T cells, T helper (Th) cells and cytotoxic T-lymphocytes (CTLs), can be distinguished by the expression of the co-receptors CD4 and CD8, respectively. Th cells recognise antigens presented by MHC class II molecules, whilst CTLs recognise antigens presented by MHC class I molecules (Parham, 2015).

1.3.2.1. Cytotoxic T Cells

Once naïve $CD8^+$ T cells recognise antigenic peptides presented via MHC class I through their TCR, they are activated, go through clonal expansion, and differentiate into potent effectors. Usually, this presentation is done by professional APCs, particularly DCs, in a process called cross-priming. This was first described in the 1970s after intravenously MHC-mismatched cells were shown to induce CTL restricted responses by host MHC (Bevan, 1976). Since then, cross-priming has been demonstrated in the context of viral infections and tumours (Huang *et al.*, 1994, Sigal *et al.*, 1999), as well as vaccination with protein antigens (Yewdell and Haeryfar, 2005). Mutations in tumours

can give rise to thousands of potentially immunogenic neo-antigens, and studies have shown that cross-presentation of these neo-antigens can occur efficiently in the tumour draining lymph nodes (Marzo *et al.*, 1999).

Effector $CD8^+$ T cells, or CTLs, release effector cytokines, such as IFN-γ and TNF-α, and express chemokines and homing receptors that are essential for migration into peripheral tissues. The main function of CTLs is to kill target cells and secrete cytokines to contain the spread of pathogens and cancer, playing an important role in immunosurveillance, as it will be discussed in section 1.3.2. There is an extensive literature reporting the correlation between high CTL infiltration in tumours and good prognosis in different types of cancer (Vesalainen *et al.*, 1994, Lee *et al.*, 2008, Hwang *et al.*, 2012, Mei *et al.*, 2014, Geng *et al.*, 2015, Salgado *et al.*, 2015). The degree and location of CTL infiltration is one of the components of the Immunoscore, a powerful tumour staging classification system that includes the immune contexture (discussed in detail in section 1.4) (Galon *et al.*, 2012).

Induction of apoptosis in tumour cells by CTLs can be achieved by two different mechanisms: release of lytic granules containing perforin and granzymes upon antigen recognition; and binding of first apoptosis receptor (Fas) ligand (FasL) expressed on CTLs to Fas on the surface of the tumour cell (Parham, 2015). Although controversial, some studies indicate that after antigen clearance, 5-10% of CTLs survive and differentiate into memory $CD8^+$ T cells, which are maintained long term in the absence of antigens, and exert rapid effector functions in response to previously encountered antigens (Wherry and Ahmed, 2004). Youngblood and colleagues have recently shown that long-lived memory $CD8^+$ T cells derive from a small subset of effector T cells through dedifferentiation (Youngblood *et al.*, 2017). By using a model of lymphocytic choriomeningitis virus infection, the authors observed that there is a repression of the naïve transcriptional program associated with *de novo* methylation, which is lost as these cells re-acquire specific aspects of the naïve-like gene expression program. These results are supported by the enhanced kinetics for development of memory cells acquired after the conditional deletion of the *de novo* DNA methyltransferase responsible for the process at the effector stage.

CTLs can also become exhausted if the host immune response fails and the antigen persists, a state that can occur in chronic infections and cancer (Day *et al.*, 2006, Mueller and Ahmed, 2009). T cell ‘exhaustion” was first described in the 1990s, using a mouse model of chronic lymphocytic choriomeningitis virus infection (Moskophidis *et al.*, 1993, Gallimore *et al.*, 1998, Zajac *et al.*, 1998). These studies revealed that virus specific $CD8^+$ T cells have a reduced effector function and proliferative capacity when

exposed to continuous antigen stimulation. Exhausted T cells are distinct from naïve, effector or memory T cells, since they have a unique transcriptional and epigenetic signature that includes overexpression of several inhibitory receptors, dysregulated cytokine signalling pathways, and altered metabolic fitness (Barber *et al.*, 2006, Wherry and Kurachi, 2015, Sen *et al.*, 2016, Bengsch *et al.*, 2016).

The first inhibitory receptor discovered was CTLA-4, in the 1990s. Although it was initially thought to be another costimulatory molecule (Linsley *et al.*, 1992), two different groups showed that CTLA-4 downregulated T cell responses. Once T cells are activated, CTLA-4 accumulates at the T cell-APC interface. Through competition for the ligands B7.1 and B7.2, it blocks co-stimulation via CD28, abolishing activated T cell responses and impeding activation of naïve T cells (Walunas *et al.*, 1994, Krummel and Allison, 1995). Allison's group found that blocking CTLA-4 resulted in release of endogenous immune responses to undefined antigens and different types of cancer (Leach *et al.*, 1996, Hurwitz *et al.*, 1998, Waitz *et al.*, 2012). Data resultant from these investigations led to the development of an antibody against CTLA-4, ipilimumab, which was FDA approved in 2011 (Hodi *et al.*, 2010).

This discovery opened a new field of research on immune checkpoint therapy, which led to the discovery of many additional immune checkpoints. The discovery of programmed cell death-1 (PD-1) ligand, PD-L1, in 2000 by Freeman and colleagues, revealed an immune checkpoint that limits the responses of activated CTLs (Freeman *et al.*, 2000). PD-1 does not interfere with co-stimulation, as opposed to what was described for CTLA-4, but it interferes with signalling mediated by the T cell antigen receptor. One of its two ligands, PD-L1, can be expressed on many cell types, such as T cells and tumour cells, after exposure to IFN-γ released by activated T cells, suggesting that the PD-1/PD-L1 pathway acts to protect cells from T cell attack (Dong *et al.*, 2002).

1.3.2.2. T helper cells

Depending on the nature of the antigen signal they receive, and cytokines secreted by APCs, naïve $CD4^+$ T cells differentiate into functionally distinct effector Th cells (Th1, Th2, Th9, Th17 and Th22), T follicular helper (Tfh) cell or Treg subsets. $CD4^+$ T cells coordinate immune responses by secreting distinct sets of cytokines. Hence, they adapt their response to the threat encountered, supporting CTL responses (Bevan, 2004), aiding B cells in antibody production (Crotty, 2015), and regulating the size and duration

of immune responses. Cytotoxic $CD4^+$ T cells have also been described in infection (van Leeuwen *et al.*, 2004, Zaunders *et al.*, 2004) and cancer (Quezada *et al.*, 2010).

Th1 immune responses are usually induced by intracellular pathogens, promoting IL-2, IFN-γ, lymphotoxin and TNF-α production by Th1 cells (T R Mosmann and Coffman, 1989). IL-12 production by DCs and macrophages promotes Th1 activation and expansion through the master transcription factor T-bet. This transcription factor controls the unique gene expression pattern present in Th1 cells (Szabo *et al.*, 2000, Szabo *et al.*, 2003). The presence of these cells in the TME, or cytokines derived from these cells, has been associated with improved patient prognosis in gastric cancer (Hennequin *et al.*, 2016), colorectal cancer (Tosolini *et al.*, 2011), hepatocellular carcinoma (Gao *et al.*, 2011) and ovarian carcinoma (Kusuda *et al.*, 2005).

Parasites such as helminth and nematodes usually induce Th2 responses. Th2 cells, initially described in 1978 (Tada *et al.*, 1978), are now known to produce IL-4, IL-5, IL-6 and IL-13, and GATA-3 is the transcription factor necessary for Th2 differentiation (Zheng and Flavell, 1997, Zhu and Paul, 2010). IL-4 is also required for Th2 differentiation to be initiated (Noben-Trauth *et al.*, 2000). Preclinical and human studies revealed that Th2 cells predominantly regulate tumour promotional mechanisms, driving activation of tumour infiltrating myeloid cells (Sheu *et al.*, 2001, Kusuda et al., 2005, DeNardo *et al.*, 2009, Nevala *et al.*, 2009, Shiao *et al.*, 2015).

Th17 responses are induced by yeast, fungi and extracellular bacteria. Th17 cells are induced by IL-6, IL-23 and TGF-β (Chen *et al.*, 2007), and the transcription factor RORγt has been described as the master regulator of transcription in this lineage, inducing the production of IL-17, IL-22 and IL-23 (Ivanov *et al.*, 2006, Zhu and Paul, 2010). The impact of Th17 cells on cancer progression is far from clear as high numbers of Th17 cells has been correlated with improved outcomes in prostate carcinoma (Sfanos *et al.*, 2008), non-small cell lung carcinoma (Ye *et al.*, 2010), breast cancer (Yang *et al.*, 2012a), and ovarian cancer (Kryczek *et al.*, 2009), but poor outcomes in preclinical models of melanoma and bladder carcinoma (Wang *et al.*, 2009), lung adenocarcinoma (Chang *et al.*, 2014) and hepatocellular carcinoma (Kuang *et al.*, 2009), and in human hepatocellular carcinoma (Zhang *et al.*, 2009), and colorectal cancer (Tosolini et al., 2011)

Th9 cell development is dependent on the transcription factors PU.1 and IRF4, and differentiation is initiated by IL-4 and TGF-β (Tripathi and Lahesmaa, 2014). These cells can have dual roles, since they can either promote immunity against parasites and participate in anti-tumour activity, or they can aggravate the immune response in asthma

and contribute to inflammatory bowel disease (Kaplan *et al.*, 2015). Beneficial anti-tumour effects have been reported for Th9 cells. Suppressed tumour growth was observed in a B16-F10 melanoma mouse model (Purwar *et al.*, 2012) and in a pulmonary metastatic melanoma mouse model (Lu *et al.*, 2012).

IL-6 and TNF initiate Th22 cell differentiation which is controlled by the AhR transcription factor. Like Th17 and NK cells, Th22 cells produce large amounts of IL-22 but are uniquely distinct from these other cell types through lack of IL-17 and IFN-γ production (Duhen *et al.*, 2009). Th22 cells are believed to have an important role in tissue repair, as well as protective effects in models of inflammatory bowel disease, pancreatitis and hepatitis (Trifari *et al.*, 2009, Sabat *et al.*, 2014). In solid tumours, Th22 cells are positively associated with tumour stage in hepatocellular carcinoma (Kuang *et al.*, 2014), and IL-22 production by T cells was reported to promote stemness in colon carcinoma cells (Kryczek *et al.*, 2014).

Tfh cells are regulated by the transcription factor Bcl-6, and their differentiation depends on IL-6 and IL-21. They participate in generation of B cell responses in germinal centres by secreting IL-21 (Tripathi and Lahesmaa, 2014). Although Tfh cells are thought to promote haematological neoplasias (Ueno *et al.*, 2015), they were correlated with improved patient prognosis in breast cancer (Gu-Trantien *et al.*, 2013), colorectal cancer (Bindea *et al.*, 2013) and non-small cell lung carcinoma (Ma *et al.*, 2016).

The Treg lineage is defined by the expression of the transcription factor Forkhead box 3 (Foxp3), and these cells, through, for example, production of the immunosuppressive cytokines IL-10, IL-35 and TGF-β play a key role in controlling excessive immune responses and immune homeostasis (Corthay, 2009).

1.3.2.3. Regulatory T cells

Tregs are a subset of T cells that control and limit immune responses to both foreign and self-antigens, protecting the body against excessive immune responses and autoimmunity. The existence of this subset was first proposed by Gershon and colleagues, and later on supported by studies by Powrie and colleagues (Gershon *et al.*, 1972, Powrie and Mason, 1990), However, it was only in 1995 that these cells were identified as a distinct thymically-derived subset marked by expression of CD4 and CD25, since depletion of these cells in mice led to breakdown of peripheral tolerance and activation of self-reactive T cells. Tolerance was restored by adoptive transfer of purified $CD4^+CD25^+$ T cells (Sakaguchi *et al.*, 1995, Asano *et al.*, 1996). Subsequent

studies have defined other markers of Tregs, most notably GITR, CTLA-4, lymphocyte activation gene 3 (LAG-3) and CD127 (Corthay, 2009), but transient expression on each of these on other T cell subsets precludes use of either marker as a specific and unique determinant of a Treg. Identification of Tregs was aided by identification of the transcription factor Foxp3, which was found to be highly expressed on $CD4^+CD25^+$ but not on $CD4^+CD25^-$ cells (Fontenot *et al.*, 2003). Currently, Tregs are generally identified using the panel of markers $CD3^+$, $CD4^+$, $CD25^+$, $Foxp3^+$ and $CD127^{lo/-}$ (Santegoets *et al.*, 2015). Since Foxp3 is an intracellular marker, the use of cell surface markers is essential for cell isolation experiments. Expression of CD127, the receptor for IL-7, is low on $CD4^+CD25^+Foxp3^+$ cells compared to other $CD4^+$ T cells and therefore serve as a convenient marker to enable isolation of Tregs (Liu *et al.*, 2006).

1.3.2.3.1. Foxp3 discovery

Observations of patients with "immune dysfunction, polyendocrinopathy, enteropathy X-linked" (IPEX) syndrome revealed that the disease is caused by mutations of *Foxp3* which results in uncontrolled T cell proliferation and activation (Bennett *et al.*, 2001). In parallel, Brunkow and colleagues showed that *Foxp3* was defective in scurfy mice due to a frameshift mutation. These mice exhibited an autoimmune phenotype similar to the one presented by IPEX patients. This mutation results in hyper-responsiveness of $CD4^+$ T cells and the onset of autoimmune disease (Brunkow *et al.*, 2001). Fontenot and colleagues not only discovered that Foxp3 is highly expressed in $CD4^+CD25^+$ cells, but also that Foxp3 is required for Treg development, since they observed that Foxp3 deficient mice lack a Treg population. In the same study, the authors injected $CD4^+CD25^-$ T cells transduced with a retrovirus expressing Foxp3-green fluorescent protein (GFP) or GFP alone into RAG deficient mice, and observed that mice without Foxp3 developed autoimmunity whilst animals with Foxp3 showed no signs of disease (Fontenot et al., 2003). The same group developed a new mouse strain, which was engineered to express the diphtheria toxin receptor under the Foxp3 gene promoter. Use of this transgenic mouse enabled selective and complete depletion of $Foxp3^+$ cells after injection of diphtheria toxin, The study confirmed the key role $Foxp3^+$ T cells play in maintaining immune homeostasis, as their depletion resulted in lymphoproliferative disease as observed in scurfy mice (Kim *et al.*, 2007).

1.3.2.3.2. Treg subsets

There are two main subsets of Foxp3^{+} Tregs: thymic Tregs (tTreg) and peripheral-Tregs (pTregs). As the name implies, tTregs are developed in the thymus, and pTregs arise from the thymus as conventional T cells but convert to Foxp3 expressing Tregs in peripheral tissues.

Like conventional T cells, tTregs develop in the thymus where they are subjected to positive and negative selection processes. The importance of specificity for self-peptide in directing the selection of tTregs was first demonstrated by Jordan and colleagues where they used transgenic mice with T cells bearing a high avidity TCR specific for haemagglutinin (HA) and crossed them with animals expressing HA. The authors found that in mice expressing both TCR and antigen the CD4^{+} thymocytes specific for HA were not clonally deleted, but 30% of the population were CD25^{+}. Conversely, only 13% of peripheral T cells were CD25^{+} within HA transgenic animals. This study indicates that specificity for self-peptide is important for directing the selection of tTregs (Jordan *et al.*, 2001). A more recent study demonstrated that tTregs can arise from two different progenitor cells, CD25^{+}Foxp3^{-} Treg and CD25^{-}Foxp3^{lo} Treg, following two distinct developmental programs in the thymus. The authors showed that both progenitor Tregs express distinct TCRs, contributing to the unique TCR clones observed in mature Treg cell repertoire. Both progenitor Tregs were also shown to protect against immune responses to self-antigens, limit immune responses to commensal organisms and resolve immune responses against foreign pathogens (Owen *et al.*, 2019).

pTregs can be converted into Tregs in peripheral organs upon TCR stimulation in the presence of TGF-β. A key experiment performed by Haribhai and colleagues demonstrated that the autoimmune phenotype derived from Foxp3 deficiency cannot be completely rescued by transferring tTregs alone; co-transfer of CD4^{+}Foxp3^{-} T cells, which were shown to convert into Foxp3^{+} pTregs was also necessary, thereby providing strong evidence for an essential role of pTregs in maintaining peripheral tolerance (Haribhai *et al.*, 2011).

1.3.2.3.3. Mechanisms of Treg suppression

Tregs can suppress immune responses either directly, by targeting effector T cells, or indirectly, by targeting DCs and preventing activation of naïve T cells.

One of the direct mechanisms used by Tregs is through competition for IL-2. Since Tregs have a higher affinity for IL-2 compared to conventional T cells, there is evidence that they can promote local cytokine deprivation by consuming the available IL-2, thereby reducing the capacity of conventional T cells to proliferate and survive (Thornton and Shevach, 1998). A second mechanism involves the ectoenzymes, CD39 and CD73, which are expressed by a large proportion of Tregs, and which promote immunosuppression through catabolism of ATP and production of adenosine (Deaglio *et al.*, 2007).

Tregs can also suppress immune cells by releasing immunosuppressive cytokines, such as TGF-β, IL-10 and IL-35. Studies have shown that mice that are either TGF-β deficient or TGF-β-unresponsive, develop T cell mediated autoimmunity shortly after birth (Li *et al.*, 2006, Marie *et al.*, 2006). IL-10 secretion by Tregs *in vivo* was shown to be important for control of gut inflammation, infection and experimental autoimmune encephalomyelitis, but dispensable for regulation of other autoimmune diseases and control of allergic responses (Schmidt *et al.*, 2012). Sojka and Fowell have also demonstrated that Treg-derived IL-10 is required to regulate levels of IFN-γ secreted by effector T cells in the skin (Sojka and Fowell, 2011). Treg secreted IL-35 was demonstrated to inhibit proliferation of conventional T cells by Collison and colleagues (Collison *et al.*, 2007), and later, Wei *et al*. demonstrated that IL-10 and IL-35 producing Tregs work in a cooperative manner to maintain immune tolerance (Wei *et al.*, 2017).

Tregs can also directly kill autologous immune cells, through production of perforin and secretion of granzymes-A (GZMA) and -B (GZMB), and in a perforin dependent manner they are able to eliminate several autologous immune cells (Grossman *et al.*, 2004, Gondek *et al.*, 2005). It has also been demonstrated *in vitro* that Tregs expressing Fas can engage with antigen presenting B cells expressing FasL, driving target cell apoptosis (Janssens *et al.*, 2003).

Tregs can also suppress through interactions with APCs. An *in vitro* study conducted by Onishi and colleagues showed that Tregs exert suppression in a two-step manner, where there is an initial leukocyte function-associated antigen-1 (LFA-1)-dependent formation of Treg aggregates on immature DCs, followed by a LFA-1- and CTLA-4-dependent downregulation of CD80/86 on DCs. This process prevents antigen-reactive naïve T cells from being activated by antigen-presenting DCs, culminating in specific immune suppression and tolerance (Onishi *et al.*, 2008) Tregs can also suppress DC activation through LAG-3 expression and binding to MHC class II on DCs (Liang *et al.*, 2008).

1.3.2.3.4. Role of Tregs in the TME

Early studies conducted by North and Bursuker using a methylcholanthrene-induced fibrosarcoma cell line, MethA, showed that even though an effective anti-tumour T cell response could be mounted, the immune response was unable to completely control tumour growth due to the progressive development of tumour-induced suppressor T cell activity (North and Bursuker, 1984). These experiments, which provided several indirect lines of evidence for a role of suppressor T cells in cancer immunity, are reviewed in detail in Gallimore and Godkin (2008) and Hughes *et al.* (2018). This suppressor T cell subset was later identified as $CD4^+$, since specific depletion of $CD4^+$ T cells resulted in efficient tumour rejection (Awwad and North, 1988). The identification of CD25 as a Treg marker allowed the use of depleting anti-CD25 monoclonal antibodies to assess the impact of Tregs in tumours. Studies with these antibodies revealed that Treg depletion induced an effective anti-tumour $CD8^+$ T cell response with control of tumour growth, in different tumour cell line models (Onizuka *et al.*, 1999, Shimizu *et al.*, 1999). These findings were validated by other groups, which have demonstrated that tumour rejection and long term T cell mediated immunity against tumour cells could be established after depletion of $CD25^+$ Tregs (Sutmuller *et al.*, 2001, Jones *et al.*, 2002). Experiments where adoptive transfer of $CD4^+CD25^+$ T cells into tumour bearing mice provided a direct link between presence of Tregs in the TME and anti-tumour immunity (Turk *et al.*, 2004, Antony *et al.*, 2005). Similar findings were made in later experiments where, following injection of mice with the chemical carcinogen, methylcholanthrene (MCA), depletion of $CD25^+$ cells resulted in a lower rate of tumour development compared to unmanipulated mice (Tawara *et al.*, 2002, Betts *et al.*, 2007).

The identification of Foxp3 as a specific marker for Tregs preceded many independent studies demonstrating that selective $Foxp3^+$ Treg depletion could prevent tumour development or contribute to regression of established tumours (Klages *et al.*, 2010, Li *et al.*, 2010, Teng *et al.*, 2010, Hindley *et al.*, 2012). These studies support the idea that Tregs prevent development of effective anti-tumour immunity. In preclinical models and in humans, the homeostatic ratio of conventional T cells to Tregs is significantly disturbed in cancers. Several mouse models have shown a preferential accumulation of Tregs within the tumour mass (Betts et al., 2007, Hindley *et al.*, 2011), and many studies in humans revealed selective enrichment of Tregs in peripheral blood, or in the TME of different tumour types (Nishikawa and Sakaguchi, 2010, Whiteside, 2012, Quezada *et al.*, 2011, Scurr *et al.*, 2012). These studies not only show that this enrichment is often associated with poor clinical outcomes (Curiel *et al.*, 2004, Bates *et*

al., 2006, Perrone *et al.*, 2008), but also that an elevated CTL to Treg ratio is associated with an improved clinical prognosis (Sato *et al.*, 2005, Gao *et al.*, 2007, Sinicrope *et al.*, 2009).

1.3.3. Cancer immunosurveillance and Immunoediting

In the early 1900s, Paul Ehrlich proposed for the first time the idea that the immune system can protect the organism against nascent pre-malignant cells. This idea led other researchers to investigate the role of the immune system in controlling carcinogenesis. Fifty years later, Foley showed that tumours induced in mice by MCA were antigenic within the host (Foley, 1953). This observation led Burnet and Thomas to develop the theory of cancer immunosurveillance, proposing that specific tumour antigens were capable of activating immune responses. This theory stated that lymphocytes act as sentinels of host tissues, recognising and eliminating newly transformed cells (Burnet, 1957).

This theory was abandoned for nearly 50 years, especially after Stutman's experiments revealed that the cancer susceptibility of immunocompetent mice was similar to that of immunodeficient mice (Stutman, 1974). After considerable advances in genetics, the generation of RAG knockout mice was possible in the 1990s. With this model it was possible to deplete NK, B and T cells, whilst the non-lymphocytic lineages remained. Shankaran and colleagues observed that after MCA injection, RAG-2$^{-/-}$ mice developed tumours faster and had a higher tumour burden compared to wild type (WT) mice pointing to a role of the adaptive immune system in controlling tumours (Shankaran *et al.*, 2001). The same group analysed development of spontaneous tumours by monitoring unmanipulated WT and RAG-2$^{-/-}$ mice for 15 to 21 months. All RAG-2$^{-/-}$ developed neoplastic lesions in the intestine and elsewhere, whilst no WT mice developed cancer. The possibility of the immune system affecting the immunogenic phenotype of tumours during chemical carcinogenesis was also assessed. They observed that tumour cells derived from WT and RAG-2$^{-/-}$ mice inoculated in RAG-2$^{-/-}$ mice induced tumour growth with equivalent kinetics in both groups, and WT mice-derived tumours transplanted into WT immunocompetent hosts resulted in formation of tumours in all recipients. However, tumour cells derived from RAG-2$^{-/-}$ mice inoculated in WT mice had a 40% rejection rate. These studies led the authors to conclude that tumours that develop in lymphocyte deficient animals are more immunogenic than those developing in immunocompetent hosts, thus, the immune system favours outgrowth of tumours that are more capable of escaping immune detection. These findings led to use

of the term “immunoediting” instead of “immunosurveillance”, to describe the actions of the immune system in both eliminating and sculpting developing tumours (Shankaran et al., 2001).

In 2002, the Schreiber group presented the cancer immunoediting model (Figure 1.5). This model describes three sequential processes: elimination, equilibrium and escape (Dunn *et al.*, 2002). Elimination is an updated version of cancer immunosurveillance and explains how the innate and adaptive immune system work together to recognise and destroy malignant cells before they form a clinically detectable tumour. IFN-γ was found to play a key role. Dighe and colleagues used a model whereby MCA induced tumours were rendered genetically unresponsive to IFN-γ. They observed that these tumours had an increased growth rate when compared to WT MCA tumours following transplantation into syngeneic recipients. On the other hand, when WT and IFN-γ insensitive tumours grew in SCID mice, which lack B and T lymphocytes, their growth characteristics were similar, thereby showing the importance of IFN-γ production by lymphocytes (Dighe *et al.*, 1994). Later, the same group assessed the role of IFN-γ in the development of spontaneous tumours. Mice lacking the tumour suppressor gene, p53, were crossed with IFN-γ insensitive mice to generate a double KO. Tumour growth rates were significantly faster in the double knockout mice (Kaplan *et al.*, 1998). Perforins were also identified as key mediators of tumour surveillance, since mice lacking this molecule develop significantly more tumours compared to perforin sufficient mice (van den Broek *et al.*, 1996).

The role of the innate arm of the immune system in immunosurveillance was demonstrated by Mark Smyth’s group and their studies on NK cells. By inoculating two different cell lines in C57BL/6 mice, perforin deficient or WT, they could observe that cells were cleared less efficiently in perforin deficient mice and in WT mice treated with an NK depleting antibody (anti-NK1.1) than in WT mice without treatment. This rejection was IL-12 independent and did not require T cells (Smyth *et al.*, 2000). Later on, using an antibody that was shown to specifically deplete NK cells (anti-asialo-GM_1) in MCA-induced tumours, they observed that depletion of NK cells alone was sufficient to significantly increase the incidence of sarcomas in mice (Smyth *et al.*, 2001).

Tumour cells which escape elimination proceed to the next phase, where the immune system and the tumour cells enter into a dynamic equilibrium. This phase is often termed immune mediated tumour dormancy, and its characterised by simultaneous prevention of tumour outgrowth and sculpting of tumour cell immunogenicity by antigen-specific T cells. Koebel and colleagues assessed whether the equilibrium phase

occurred during primary tumorigenesis, using mice injected with a low dose MCA, which resulted in developed of progressively growing tumours in only a minority of mice. Whilst these mice were removed from the study, remaining mice presenting with small masses at the injection site were treated with monoclonal antibodies against specific immunological components. Almost half of mice developed progressively growing sarcomas following depletion of $CD4^+/CD8^+$ cells, IFN-γ and/or IL-12; all components of the adaptive immunity. No tumour outgrowth was observed after NK cell depletion (Koebel *et al.*, 2007). During this phase, there is evidence that a balance between anti-tumour effector cells, such as CTLs, and immunosuppressive cells, such as Tregs and myeloid derived suppressor cells (MDSCs) are important, since a balance in favour of suppressive cells is associated with immune escape (Wu *et al.*, 2013).

Lastly, the escape phase occurs when tumour cells, uncontrollable by the immune system form a clinically detectable mass. Progression to this phase can occur due to changes in the tumour cell population in response to editing by the immune system, leading to reduced immune recognition. This may happen through emergence of tumour cells that lack expression of rejection antigens, loss of MHC class I proteins, or antigen processing function, and consequent lack of antigen presentation to tumour-specific T cells. Tumour cells can also induce anti-apoptotic mechanisms involving persistent activation of transcription factors (e.g. signal transducer and activator of transcription (STAT) 3), or expression of anti-apoptotic effector molecules (e.g. BCL-2) in order to promote tumour outgrowth. Surviving tumour cells may also establish an immunosuppressive microenvironment, by either expressing immunosuppressive cytokines (VEGF, TGF-β and Indoleamine-pyrrole 2,3-dioxygenase (IDO)) or by recruiting regulatory immune cells (Tregs and MDSCs) (Dunn et al., 2002, Schreiber *et al.*, 2011).

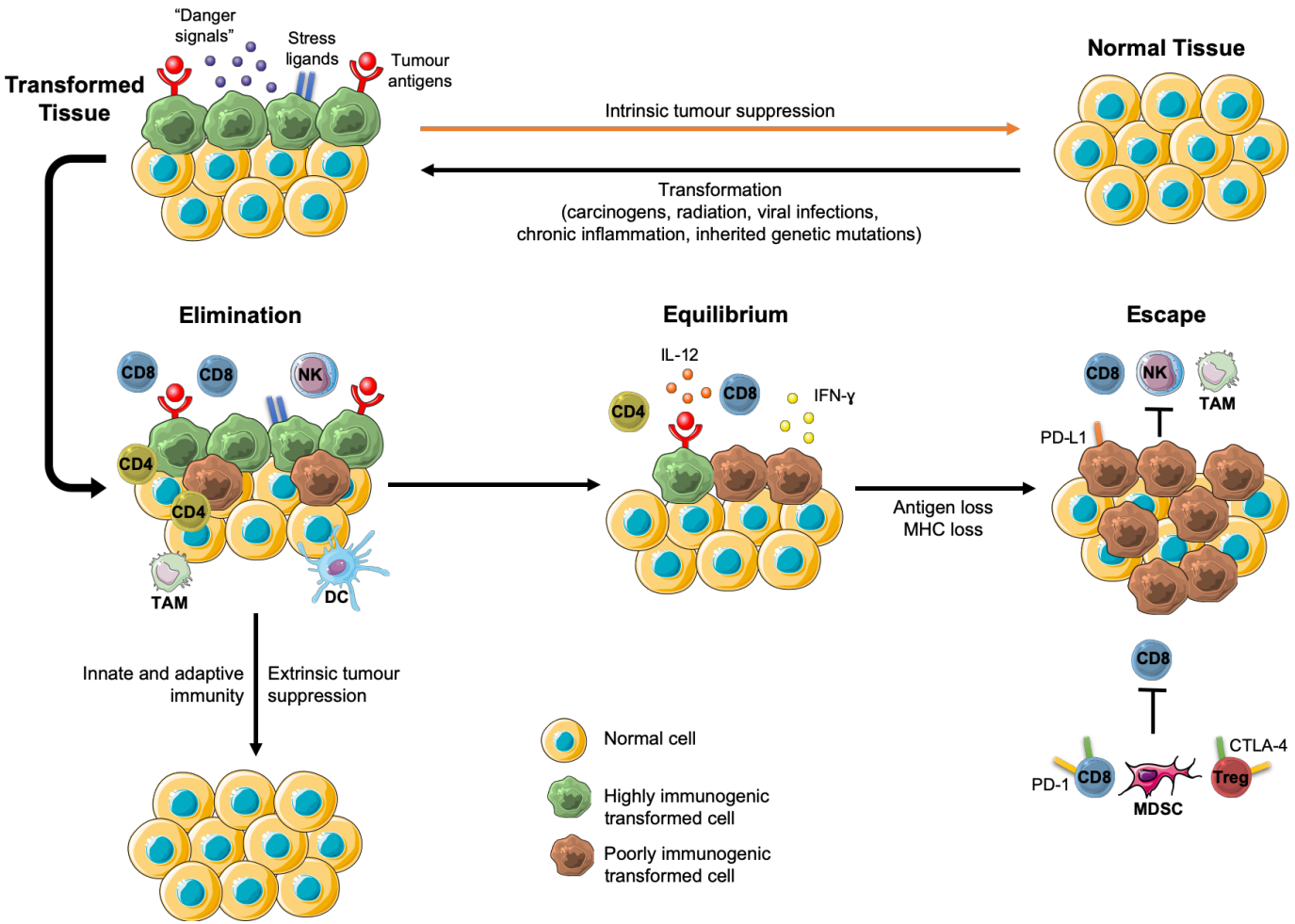

Figure 1.5| The cancer immunoediting model.
Cancer immunoediting is a tumour suppressor mechanism that involves three phases: elimination, equilibrium and escape. The elimination phase results in the destruction of developing tumours due to the collaboration of the innate and adaptive arms of the immune system, before it becomes clinically detectable. If the immune

system is capable of completely eliminating transformed cells, then the host remains free of cancer. If some cell variants become resistant to the actions of the immune system, it enters in the equilibrium phase. In this phase, tumour outgrowth is controlled by immune mechanisms, specifically by the adaptive immune arm. Editing of tumour immunogenicity takes place in this phase, since the immune system applies a constant immune selection pressure on unstable tumour cells. This can result in the emergence of tumour cell variants that are no longer recognised by adaptive immunity, become insensitive to immune effector mechanisms, or induce an immunosuppressive microenvironment. These tumour cells enter the escape phase, and their outgrowth can no longer be blocked by the immune system, creating clinically detectable tumours. PD-1, programmed cell death protein-1; PD-L1, programmed death-ligand 1; CTLA-4, cytotoxic T-lymphocyte-associated protein 4; TAM, tumour associated macrophage. Adapted from Schreiber et al., 2011.

1.3.4. Cancer immunotherapy

For an anti-tumour immune response to result in effective killing of cancer cells, a series of stepwise events must occur – described as the cancer-immunity cycle (Chen and Mellman, 2013). The process is initiated with the release of neoantigens generated as a result of oncogenesis. These are then captured by DCs, which migrate to the lymph node to prime and activate effector $CD8^+$ cells against cancer-specific antigens. In order to achieve an anticancer T cell response, signals to induce peripheral tolerance must be present. These can be proinflammatory cytokines and factors released by dying tumour cells. At this stage, the nature of the immune response is defined, where the final outcome is dependent on the CTLs/Tregs ratio. Activated effector T cells traffic to the tumour and infiltrate the TME, where they specifically recognise and bind to cancer cells through the interaction between their TCR and the cognate antigen bound to MHC class I, and finally kill their target cancer cells. Killing of these cells completes the cycle, by releasing additional tumour-associated antigens in order to potentiate the immune response (Chen and Mellman, 2013). However, at each step of the cycle, several factors can contribute to suppress or drive anticancer immunity (Gajewski *et al.*, 2006, Rabinovich *et al.*, 2007, Chen and Mellman, 2013). These include a lack of tumour antigens, antigens which induce Treg responses, inefficient T cell homing to tumours, barriers to T cell infiltration in the TME, or presence of immunosuppressive components in the TME. Examples of these components are the expression of PD-L1 by tumour cells and TILs which impairs CTL activity (Kim and Chen, 2016).

Advances in the understanding of the interplay between developing tumours and the immune system has enabled immunological manipulation to treat human cancers, through promoting effective anti-tumour immunity and reducing tumour-mediated immunosuppression. This area of research has grown exponentially in recent years, mainly focusing on approaches to overcome breaks and kick-start the cancer-immunity cycle, which has demonstrated impressive therapeutic benefit and increased survival in some patients.

Adoptive cell therapy is a form of immunotherapy that involves the *ex vivo* expansion of patient tumour infiltrating lymphocytes (TILs) that are subsequently re-infused. The isolated TILs can be engineered to express TCRs or chimeric antigen receptors (CARs) specific to tumour associated antigens (Rosenberg and Restifo, 2015). CARs are synthetic molecules engineered into T cells, constituted by an extracellular binding domain, a transmembrane domain and an intracellular signalling/activation

domain. The extracellular domain consists of a single chain variable fragment derived from an antibody, which recognises and binds specific tumour associated antigens in an MHC-independent manner. The intracellular domain is made by a CD3ζ segment and one or two costimulatory domains, which are responsible for triggering T cell activation (Eshhar *et al.*, 1993, Zhong *et al.*, 2010). CAR-T cell therapy has been shown to be successful in haematological cancers. The first CAR-T cell therapy was approved for acute lymphoblastic leukaemia treatment in 2017, after a phase II trial demonstrated that the use of anti-CD19 CAR-T cells induced 60% complete remission rate and 81% overall response rate (Maude *et al.*, 2018). However, in solid tumours the efficacy of this therapy is not as good due to the multiple difficulties that CAR T cells can encounter, such as efficient trafficking to the tumour, the presence of an abnormal vasculature, matrix barriers and an immunosuppressive environment (Yong *et al.*, 2017). Many strategies are underway to improve CAR T cell performance in these tumours, such as modifying them to secrete PD-1-blocking single-chain variable fragments (Rafiq *et al.*, 2018), or through deleting genes expressing inhibitory receptors, such as PD-1 (Ren *et al.*, 2017).

TCR therapy has the advantage that TCRs can recognise more antigens than CARs, since MHC molecules can present peptide chains obtained from the cell surface or from the metabolism of intracellular proteins (Zhao and Cao, 2019). TCR therapy has proven successful in solid tumours, particularly in melanoma and sarcoma (Robbins *et al.*, 2011, Robbins *et al.*, 2015). A large effort is being made to improve this type of therapy through, for example, genetic deletion of the PD-1 gene (Gao *et al.*, 2019). Another option is to increase TCR affinity to optimal levels whilst avoiding off-target activities; this approach has been successfully demonstrated with the affinity-enhanced anti-NY-ESO-1 TCR (Rapoport *et al.*, 2015, D'Angelo *et al.*, 2018, Nowicki *et al.*, 2019). Nonetheless, both CAR T cell and TCR-based therapies are associated with side effects, such as off-tumour toxicities (Johnson *et al.*, 2009, Linette *et al.*, 2013), cytokine release syndrome (Norelli *et al.*, 2018) and neurotoxicity (Wang and Han, 2018).

The development of immune checkpoint blockade (ICB) therapies using monoclonal antibodies targeting CTLA4 and the PD-1/PD-L1 axis, has represented a fundamental step forward for cancer immunotherapy. The combination of anti-CTLA-4 and anti-PD-1 therapies has demonstrated better outcome than single therapy in preclinical studies (Curran *et al.*, 2010). In a five-year follow-up study, Larkin and colleagues recently demonstrated that the overall survival of patients with advanced melanoma at 5 years was 52% for the group receiving nivolumab plus ipilimumab, compared to 44% receiving nivolumab only, and 26% receiving ipilimumab only. (Larkin *et al.*, 2019). It was initially thought that anti-CTLA4 antibodies directly targeted mainly

$CD4^+$ and $CD8^+$ effector cells. However, pre-clinical mouse studies revealed that the anti-CTLA4 antibodies (in this case IgG2a) induced antibody-dependent cell-mediated cytotoxicity (ADCC) of tumour infiltrating $Foxp3^+$ Tregs. ADCC is a process whereby antibody-coated cells are recognised and lysed predominantly by NK cells or macrophages. This process was shown to be more important for promoting anti-tumour effects than the direct activation of $CD4^+$ and $CD8^+$ cells by the same antibodies (Selby *et al.*, 2013, Simpson *et al.*, 2013). Following these studies, reduced Treg numbers and an increased CTL/Treg ratio was observed in cancer patients treated with the human IgG1 antibody, ipilimumab, which in humans, induces higher ADCC activity than the IgG2a antibodies (Liakou *et al.*, 2008, Romano *et al.*, 2015). Since PD-L1 and PD-L2 are also upregulated on Tregs in the TME of human tumours (De Simone *et al.*, 2016), it is possible that PD-1 blockade also targets Tregs. However, recent studies have shown that the way PD-1 blockade affects Tregs is context dependent. Whilst PD-1 blockade inhibited PD-L1-induced Treg expansion in glioblastoma (DiDomenico *et al.*, 2018) and melanoma (Gambichler *et al.*, 2020), it was shown to facilitate the proliferation of highly suppressive Tregs in hyperprogressive disease in the context of gastric cancer (Kamada *et al.*, 2019). It has recently become clear that tumours can induce upregulation of many co-inhibitory receptors on T cells therefore new targets are currently under investigation. These include LAG-3, T-cell immunoglobulin and mucin-domain containing-3 (TIM-3) and B- and T-lymphocyte attenuator (BTLA) (Smyth *et al.*, 2016, Ribas and Wolchok, 2018, Dougan *et al.*, 2019).

As previously mentioned, Treg enrichment in tumours represents a major obstacle to successful immunotherapy, therefore, depletion of Tregs has been investigated as a way to promote tumour regression. Onizuka and colleagues demonstrated that administration of an anti-CD25 antibody to deplete $CD4^+CD25^+$ Tregs in mice resulted in tumour rejection or delay of tumour growth (Onizuka et al., 1999). The use of anti-CD25 antibodies has also been evaluated in clinical studies, in combination with vaccination programs. In breast cancer patients, Treg depletion with the anti-CD25 antibody daclizumab following vaccination with tumour associated peptides was associated with prolonged stable disease (Rech *et al.*, 2012). However, systemic Treg depletion might increase the risk of autoimmunity-related toxicities (Sakaguchi et al., 1995, Kim et al., 2007), so targeting Tregs that are abundant in the TME rather than the entire population would have increased benefits by improving anti-tumour effects and minimising autoimmunity. In 2017, the Quezada group re-evaluated CD25 as a target for Treg depletion and showed that the commonly used anti-CD25 antibody PC-61 failed to effectively deplete intra-tumoural Tregs in established mouse tumours (Arce Vargas *et al.*, 2017). By using an antibody isotype optimised for engagement of activating Fc

gamma receptors to induce ADCC, the authors of the study observed a superior intra-tumoural Treg depletion and a strong synergy when combined with PD-1 blockade. They have also demonstrated that CD25 expression in the effector compartment is minimal *in vivo*, emphasizing the potential of this marker as a therapeutic target in combination with immunotherapies. A study of melanoma patients showed that an intra-tumoural Tregs subset enriched for CCR4, exhibited strong immunosuppressive activity. The use of an anti-CCR4 antibody (mogamulizumab) could selectively deplete tumour Tregs and induce tumour-antigen-specific $CD4^+$ and $CD8^+$ T cells in these patients (Sugiyama *et al.*, 2013). An alternative approach for targeting Tregs is by activating immune-checkpoint molecules on the TNF receptor superfamily. Targeting OX40, ICOS or GITR have all been shown to reduce the immunosuppressive activity of Tregs whilst stimulating effector T cells (Shimizu *et al.*, 2002, Griseri *et al.*, 2010, Nagase *et al.*, 2017). It is also possible to target molecules that are crucial for Treg survival and function. Maintenance and function are dependent on PI3Kδ signalling (Ahmad *et al.*, 2017), and selective inactivation of this subunit in Tregs results in increased activity of $CD8^+$ T cells, controlling tumour development, progression and metastasis (Ali *et al.*, 2014). High doses of cyclophosphamide, an alkylating agent, are used as chemotherapy for human cancers (Sistigu *et al.*, 2011). However, low doses of cyclophosphamide have been shown to result in an effective anti-tumour immune response in mice and humans, by modulation of Treg cells (Le and Jaffee, 2012, Scurr *et al.*, 2017a, Scurr *et al.*, 2017b). Since the balance between effector T cells and Tregs is essential in dictating an effective anti-tumour immune response, another alternative to improve response to therapy is to shift that balance away from Tregs (Quezada *et al.*, 2006, Quezada et al., 2011), which can be achieved with ICB therapies.

Finding a way to prime naïve T cells has been in the centre of several studies, and cancer vaccines seem to be the elected method for this. The use of these vaccines was firstly demonstrated in 1991 following identification of the melanoma antigen, MAGE-A1 by T cells (van der Bruggen *et al.*, 1991). Since then, many tumour antigens have been identified. Some vaccines show limited efficacy due to the difficulty in overcoming self-tolerance, however, the addition of some immune adjuvants, such as IL-2, has improved this aspect (Makkouk and Weiner, 2015). The use of DCs pulsed with tumour associated antigens as a cancer vaccine has also been explored, and in 2010, the FDA approved Provenge, an antigen-pulsed DC cancer vaccine for the treatment of metastatic prostate cancer. This vaccine demonstrated increased survival in the three separate phase III clinical trials (Small *et al.*, 2006, Higano *et al.*, 2009, Kantoff *et al.*, 2010). Chronic antigen exposure can cause T cell exhaustion in response to a cancer vaccine, decreasing its

efficacy. Therefore, the combination of cancer vaccines with therapies to bypass T cell exhaustion is being explored (Kissick and Sanda, 2015).

The potential of oncolytic viruses (OVs) has also been explored, especially in patients and tumour types that have poor responses to ICB. As well as promoting direct tumour lysis, the immunogenic cell death induced by OVs can lead to innate immune activation leading to the recruitment and maturation of effector T cells (van Vloten *et al.*, 2018) and reviewed in (Harrington *et al.*, 2019). Combination therapies using OVs with PD-1 and PD-L1 or CTLA4-trageting therapies are currently being tested in clinical studies (Chesney *et al.*, 2018, LaRocca and Warner, 2018). In pre-clinical models, OVs have also been used to deliver immunological payloads to tumours where the advantage is that the payload, e.g. anti-CTLA4 antibodies, are selectively delivered to the tumour, thereby reducing the risk of the toxic side-effects associated with systemic delivery of such antibodies (Dias *et al.*, 2012, Du *et al.*, 2014).

Research has also been focusing on altering the TME to a less immunosuppressive phenotype. There are several possible approaches which involve manipulation of immune cells. Myeloid cells can be inhibited, depleted or reprogrammed into anti-tumour macrophages or DCs with increased potential to present antigens (Cubillos-Ruiz *et al.*, 2015, Akalu *et al.*, 2017, Dougan *et al.*, 2018). Colony stimulating factor 1 receptor (CSF1R) is expressed on macrophages, and its blocking resulted in loss of TAMs and improved anti-tumour response in early phase trials of pancreatic cancer (Pyonteck *et al.*, 2013, Zhu *et al.*, 2014).The systemic administration of specific cytokines, and the Treg approaches described in the previous section can also contribute to TME remodelling (Smyth et al., 2016, Dougan et al., 2019).

1.4. Relationship between the TME and anti-tumour immune response

Since the concept that tumour progression describes a balance between invasive tumour cells and the actions of the host immune system has become more widely accepted, more attention has been focussed on immune cells in the TME. The most common system for tumour progression classification has been in place for about 80 years with recurrent improvements. This system, the TNM classification, is focussed only on the tumour cells, evaluating the tumour burden (T), the presence of tumour cells in regional lymph nodes (N), and evidence of metastases (M), and fails to incorporate the effects of the host immune response (Galon et al., 2012, Angell and Galon, 2013). More

recently, classification systems are being refined to take into account the presence of non-neoplastic cells in the tumour, such as immune cells which are often more than 50% of the total cell population in a tumour; the precise characterisation of tumour infiltrating cells, including their phenotype and location, i.e., which type of cells can be found in the tumour core or in the invasive margin (Galon *et al.*, 2014).

The analysis of the type, functional orientation, density and location of immune tumour infiltrating cells within different tumour regions is called the immune contexture of a tumour (Galon *et al.*, 2006). From this, the Immunoscore was born, and several international pathology expert centres are currently working together to implement this as a part of a new TNM classification. The Immunoscore is based on the standardised enumeration of two lymphocyte populations (CD3 and CD8) in the core and the invasive margin of the tumour, giving a stronger prognostic factor than the TNM classification alone (Galon et al., 2014). The Immunoscore classification ranges from Immunoscore 0 (I0), for tumours with low densities and even absence of both cell types in both regions, to I4, for tumours with high immune cell densities in both locations, introducing the notion of “hot” (highly infiltrated, I4) and “cold” (non-infiltrated, I0) tumours (Galon and Bruni, 2019).

Hot tumours are considered the most immunogenic, since there is a high infiltration of CTLs, expression of PD-L1 on tumour associated immune cells, genomic instability and indications of pre-existing anti-tumour immune responses (Hegde *et al.*, 2016). These tumours have higher response rates to ICB, one example being the subset of colorectal cancers with high microsatellite instability (Binnewies *et al.*, 2018). Cold tumours are poorly infiltrated with T cells and are immunologically ignorant, as implied by lack of PD-L1 expression. In general, they are also characterised by high tumour cell proliferation rates, low expression of neoantigens and antigen presentation components, such as MHC class I (Hegde et al., 2016) These tumours are frequently of epithelial origin, such as pancreatic cancer (Binnewies et al., 2018).

Camus and colleagues were the first to describe four major immune profiles: hot, altered excluded, altered immunosuppressed, and cold (Figure 1.6). These observations were made in primary colorectal cancers and allowed a classification according to the balance between tumour escape and immune coordination. The “altered excluded” phenotype represents the ability of the immune system to mount a T-cell mediated immune response, as well as the ability of the tumour cells to escape this response by physically impeding T cell infiltration. The “altered immunosuppressed” phenotype reflects the presence of an immunosuppressive environment that limits further recruitment and expansion of immune cells, without physical barriers being present

(Camus *et al.*, 2009). This system may provide a better means of identifying patients at high risk of recurrence and the best approaches to their treatment.

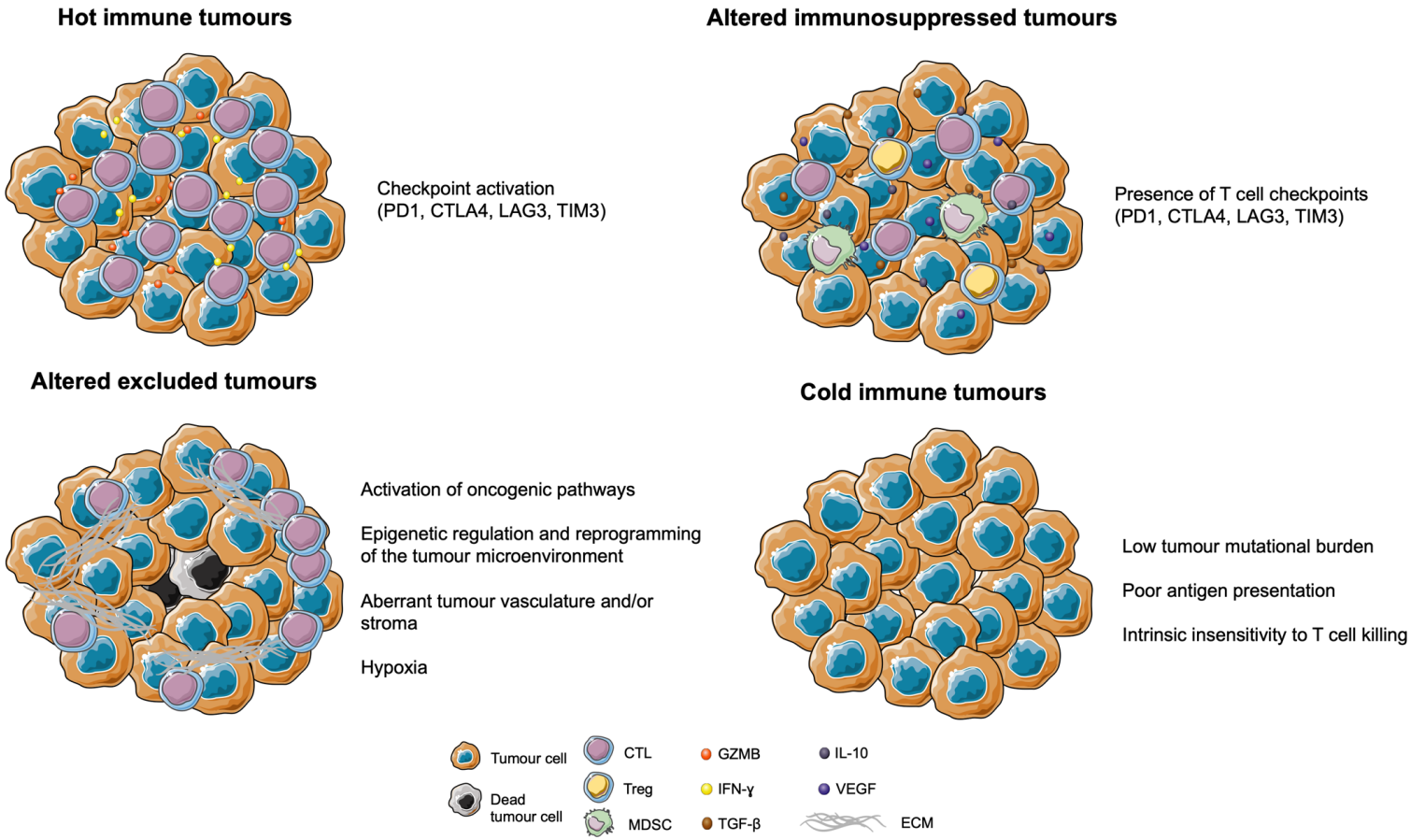

Figure 1.6|Immune-based classification of tumours.
Hot immune tumours are characterised mainly by their high degree of T cell infiltration and immune checkpoint activation. Altered immunosuppressed tumours have poor T cell infiltration, soluble immunosuppressive proteins (e.g. TGF-β, IL-10 and VEGF), and immunosuppressive cells in the TME. T cell checkpoints are also

present in this type of tumours. Altered excluded tumours have no T cell infiltration in the tumour core, and accumulation of T cells at the margin. Oncogenic pathways are activated, there is an epigenetic regulation and reprograming of the TME, the vasculature is aberrant, and hypoxic cores are often found. Cold tumours are devoid of T-cells, both at the core and margins. These exhibit low mutational burden, poor antigen presentation and intrinsic insensitivity to T cell killing. Adapted from Galon and Bruni, 2019.

Immunosuppressive mechanisms in the TME block both the natural host immune responses and the efficacy of cancer immunotherapies. There are two main types of immunosuppression mechanisms in the TME; a tumour intrinsic and a local adaptive immunosuppression. Tumour intrinsic immunosuppression may be induced by genetic alterations of the tumour, involving activation of several oncogenic pathways. These include the WNT-β-catenin (Yaguchi *et al.*, 2012, Spranger et al., 2015), mitogen-activated protein kinase (MAPK) (Sumimoto *et al.*, 2004, Sumimoto *et al.*, 2006), Janus kinase (JAK) –STAT3 (Iwata-Kajihara *et al.*, 2011) and nuclear factor-κB (NF-κB) (Nishio *et al.*, 2014) signalling pathways. The activation of each of these pathways results in expression of cytokines and chemokines that contribute to T cell exclusion from the TME or repression of factors that facilitate T cell recruitment. This mechanism can result in a cold, "altered excluded" or "altered immunosuppressed" tumour. In the case where there is local adaptive immunosuppression, TILs produce IFN-γ that induces immune checkpoint molecules, such as PD-L1, or immunosuppressive factors, such as IDO1. Therefore, this type of mechanism can result in either a hot or an altered immunosuppressed tumour, depending on the power of the driving mechanisms (Galon and Bruni, 2019).

Different types of cancer can present a great diversity in the TME composition, however, this diversity can also be observed among patients with the same cancer type and even in different tumour sites within the same patient (Mlecnik *et al.*, 2017, Zhang *et al.*, 2018). The occurrence of specific driver mutations (Spranger et al., 2015), the deregulation of oncogenes in cancer cells (Yoshida *et al.*, 2016), the load and quality of passenger mutations in cancer cells (Camus et al., 2009, McFarland *et al.*, 2017), the presence of immunosuppressive elements in the TME (Tauriello *et al.*, 2018), factors directing immune attraction (van der Woude *et al.*, 2017), and factors that mediate CTL expansion and proliferation (Mlecnik *et al.*, 2016) can all contribute to this diversity. Moreover, the TME also evolves with tumour progression and disease recurrence (Bindea et al., 2013). Although some patients show durable responses to therapies, others do not respond or acquire resistance due to significant remodelling of the TME in response to treatment.

Over a number of years, our laboratory has been using Foxp3DTR mice to investigate the impact of depleting Treg on tumour immunity. In this model, the formation of fibrosarcomas is achieved by injecting MCA in the hind leg of these mice, and, once tumours become palpable, $Foxp3^+$ Tregs are ablated by administering diphtheria toxin (DT), as already shown by Kim and colleagues (Kim et al., 2007). Previous studies

published by the group have reported that after depletion of Treg approximately half of the mice show control of established tumours. These mice, named “responders”, were shown to be distinct from “non-responders” by the development of intratumoural HEVs and a significantly higher number of TILs (Hindley et al., 2012, Colbeck *et al.*, 2017b). This study set out to compare responders and non-responder in more detail. Considering the crucial role of the TME in modulating anti-tumour immune responses, it was deemed important to focus on the TME and to specifically address whether the TME influences the response to Treg depletion. Revealing such differences could define new TME remodelling strategies to improve anti-tumour immune responses.

1.5. Hypothesis and Aims

The hypothesis of this project states that TME profile prior to immunotherapy can predict response to therapy. This hypothesis was tested according to the following aims:

1. Determine TME profiles in untreated tumours, and in non-responders and responder tumours after Treg depletion in a mouse model.
2. Investigate whether the tumour ECM predicts the response to Treg depletion.
3. Define the alterations in the TME following Treg depletion in both responders and non-responders.

Chapter 2

Methods

2.1. Mouse work

2.1.1. Mice

Genetically engineered Foxp3^{DTR} mice were gratefully received from Professor Alexander Rudensky and have been previously described (Kim et al., 2007). These mice were backcrossed with C57BL/6 mice for ≥ 10 generations by our lab. Mice were housed in accordance with UK Home Office regulations, and isolator-bred before being housed in filter-top cages for the duration of experiments.

2.1.2. Tumour induction, diphtheria toxin administration and monitoring

For tumour induction, Foxp3^{DTR} mice, aged 8 to 15 weeks, were anesthetized and injected subcutaneously with 400μg of 3-MCA (Sigma Aldrich) suspended in 100 μL of olive oil into the left hind leg, as previously described (Hindley et al., 2011). Mice were then monitored for tumour development weekly for up to 18 weeks. Tumour-bearing mice were sacrificed before their tumours reached 1.5 cm in diameter, or if tumours caused apparent discomfort.

For *in vivo* depletion of Foxp3^{+} Tregs, DT diluted to a 5 μg/kg concentration in Phosphate Buffered Saline (PBS; Gibco Life Technogies) was administered every other day by intra-peritoneal (i.p.) injection, after development of a palpable tumour.

To monitor tumour growth, tumour size was measured in mm, every other day, using calipers. Tumour leg width, non-tumour leg width, tumour width and tumour height measurements were taken. Tumour growth rate (k, days^{-1}) was calculated using the difference between the tumour and non-tumour leg diameters, by the equation for exponential growth $Y=Y0 \times exp\ (k \times X)$, using the statistical software package Prism 7 (GraphPad).

2.1.4. Dissection of Tissues

Once tumours reached the established size limit, or signs of discomfort were observed, mice were sacrificed and tumours carefully removed to avoid muscle and other normal tissues, particularly the local popliteal lymph node. Tumours were split,

whenever possible, and half was fixed in a neutral-buffered formalin solution (NBFS) and embedded in paraffin, and the other half was embedded in optimal cutting temperature (OCT) compound (CellPath) and frozen in dry ice. The inguinal lymph nodes on the tumour side (tumour draining lymph node – dLN) and on the non-tumour side (non-tumour draining lymph node – ndLN) of tumour bearing mice were taken for cell culture.

2.2. Histology

2.2.1. Immunofluorescence

2.2.1.1. Frozen sections

Five μm thick sections were cut from tumours embedded in OCT, using a cryostat machine. These were fixed for 10 minutes in ice-cold acetone and then air dried at RT (Table 2.1). Acetone fixed sections were washed in 1x PBS (3x 3 minutes). Non-specific antibody binding was blocked with incubation in 2.5% Normal Horse Serum Blocking Solution (VectorLabs) for 30 minutes at RT. After 3x 3-minute washes in PBS, sections were incubated in the primary antibody diluted to the appropriate concentration (Table 2.1) in 1% Bovine Serum Albumin (BSA) in PBS overnight at 4°C. The following day, sections were washed 3x 3 minutes in PBS, and incubated in a fluorophore-conjugated secondary antibody solution, which was diluted to the appropriate concentration in 1% BSA in PBS, for 45 minutes at RT (Table 2.1). Sections were washed 3x 3 minutes in PBS, incubated in a solution of 1 μg/mL Hoechst (Thermo Fisher Scientific) in PBS, and after a final wash in PBS, mounted using ProLong Gold Antifade Mountant (ThermoFisher) and glass coverslips. Slides were left to cure overnight at RT, protected from light, and then were imaged using a Zeiss slide scanner (Zeiss Axioscan Z.1). Images were analysed using Zen software Blue edition.

2.2.1.2. Formalin fixed paraffin embedded sections

Five μm thick sections of tumours embedded in paraffin were cut on a microtome and mounted on glass slides. Slides were dried at 37°C overnight and then baked at 60°C for 1 hour. Sections were dewaxed in xylene (3 x 5 minutes) and rehydrated via an alcohol gradient (2 x 3 minutes at 100% Methanol (MeOH), 3 minutes at 90% MeOH, 3

minutes at 70% MeOH and 5 minutes in running water). After being washed in distilled water (dH_2O), sections were cooked on a pressure cooker for 20 minutes in either Tris-EDTA (10 mmol/L Tris, 1 mmol/L – pH 9) or Sodium Citrate (10 μM/L Tris Sodium Citrate dihydrate – pH 6) antigen retrieval solution, depending on the antibody specificities (Table 2.1), cooled for 30 minutes and washed in PBS 3x 3 minutes. Non-specific antibody binding was blocked by incubating slides in 2.5% Normal Horse Serum Blocking Solution (VectorLabs) for 30 minutes at RT. Sections were incubated with primary antibody diluted to the appropriate concentration (Table 2.1) in 1% BSA in PBS overnight at 4°C. After this incubation, sections were processed as described above (Section 2.2.1.1).

Table 2.1|Antibodies used in Immunofluorescent staining.

Target Antigen	Sample type	Tissue fixative solution	Antigen retrieval	Final concentration (μg/mL)	Clone	Conjugate	Isotype	Supplier
Primary Antibodies								
TNC	FFPE	Formalin	HIER-Tris	1	EPR4219	-	Rabbit IgG	Abcam
	OCT	Acetone	-					
LUM	OCT	Acetone	-	0.4	Polyclonal	-	Goat IgG	R&D Systems
COL3A1	OCT	Acetone	-	0.5	Polyclonal	-	Rabbit IgG	Abcam
CD31	OCT	Acetone	-	0.4	Polyclonal	-	Goat IgG	R&D Systems
CD3	OCT	Acetone	-	2	Polyclonal	-	Rabbit IgG	Dako
CD4	OCT	Acetone	-	1	RM4-5	-	Rat IgG2a	eBioscience
CD8a	OCT	Acetone	-	1	53-6.7	-		eBioscience
GZMB	OCT	Acetone	-	0.4	Polyclonal	-	Goat IgG	R&D Systems
PNAd	OCT	Acetone	-	2.5	MECA-79	-	Rat IgM	BD Pharmingen
LYVE-1	FFPE	Formalin	HIER-Tris	1	ALY7	-	Rat IgG1	e-Bioscience

CCL21	FFPE	Formalin	HIER-Tris	5	Polyclonal	-	Goat IgG	R&D Systems
ZEB-1	FFPE	Formalin	HIER-Tris	0.2	Polyclonal	-	Rabbit IgG	Atlas Antibodies

Table is continued on the next page

Secondary Antibodies

Anti-Rabbit IgG	-	-	-	1	Polyclonal	AF 488	Donkey IgG	Invitrogen
Anti-Goat IgG	-	-	-	1	Polyclonal	AF 594	Donkey IgG	Invitrogen
Anti-Rat IgG	-	-	-	1	Polyclonal	AF 594	Donkey IgG	Invitrogen
Anti-Rat IgM	-	-	-	1	Polyclonal	AF 594	Goat IgG	Invitrogen
Anti-Rat IgG	-	-	-	1	Polyclonal	AF 647	Chicken IgY	Invitrogen
Anti-Rabbit IgG	-	-	-	1	Polyclonal	AF 647	Donkey IgG	Invitrogen

HIER – Heat Induced Epitope Retrieval; AF – Alexa Fluor

2.2.2. Immunohistochemistry

Tumours embedded in paraffin were cut in 5 μm sections on a microtome and mounted on glass slides. Sections were dried, baked, dewaxed, rehydrated, and antigen retrieval was done as described above (Section 2.2.1.2). After cooling for 30 minutes and washed in PBS 3x 3 minutes, endogenous peroxidase activity was quenched by incubation in Bloxall (VectorLabs) for 5 minutes at RT. Non-specific antibody binding was blocked by incubating slides in 2.5% Normal Horse Serum Blocking Solution (VectorLabs) for 30 minutes at RT. Sections were incubated in the primary antibody diluted to the appropriate concentration (Table 2.2) in 1% BSA in PBS overnight at 4°C. The following day, sections were washed in PBS 3x 3 minutes, and antibodies were detected with a 30-minute incubation of the relevant ImmPRESS™ Horseradish Peroxidase (HRP) Polymer Detection kit, and subsequently visualized by brief incubation in either Impact DAB (3, 3'-diaminobenzidine, brown) or Vector Very Intense Purple (VIP, purple) HRP substrate (VectorLabs) (specific incubation times for each antibody are specified in Table 2.2). After detection, sections were rinsed in dH_2O and counterstained in Mayers haematoxylin (SLS) for 3 minutes. A bluing solution (0.1% Sodium Bicarbonate) was used for 3 minutes to stain the nuclei. Sections were then washed in dH_2O and dehydrated with an alcohol series (3 minutes at 70% MeOH, 3 minutes at 90% MeOH, 2x 3 minutes at 100% MeOH) and then with xylene (3x 5 minutes). Mounting was performed using a specific media (distyrene, a plasticizer, and xylene – DPX) and glass coverslips. Sections were allowed to dry overnight at RT, and then imaged using the previously mentioned slide scanner. Images were analysed using Zen software Blue edition.

Table 2.2|Antibodies used in Immunohistochemical staining.

Target Antigen	Antigen Retrieval	Final concentration (μg/mL)	Chromogen incubation time (minutes)	Clone	Isotype	Supplier
TNC	HIER-Tris	0.2	3	EPR4219	Rabbit IgG	Abcam
KI67	HIER-Tris	0.03	3	Polyclonal	Rabbit IgG	Abcam
CASP3	HIER-Tris	0.025	3	Polyclonal	Rabbit IgG	R&D Systems
P16	HIER-Citrate	0.06	5	EPR20418	Rabbit IgG	Abcam
FOXP3	HIER-Tris	10	3	FJK-16s	Rat	eBioscience
CD3	HIER-Tris	0.24	3	Polyclonal	Rabbit IgG	Dako

HIER – Heat Induced Epitope Retrieval

2.2.3. Quantification of immune cell infiltration

Frozen tumour sections were stained with antibodies targeting $CD3^+CD4^+$ and $CD3^+CD8^+$ cells by immunofluorescence. Sections were viewed on a fluorescence microscope and double positive cells were counted by eye per high power field of view. For each sample, two serial tumour sections were stained, and 10 random high-power fields of view (area of each field of view = 0.13 mm^2) in each section were enumerated and averaged. As a control for observer bias, the samples used were the same as previously analysed samples by other members of the lab.

2.3. Positron Emission Tomography-Computed Tomography (PET-CT) scans

The timeline of PET-CT scans and injections is represented in Figure 2.1. Radiosynthesis of zirconium-89 (^{89}Zr) oxalate, antibody modification, labelling of the antibody and confirmation of its purity were done by Stephen Paisey, and methods for these techniques can be found in the Appendix (See Appendix, Methods section).

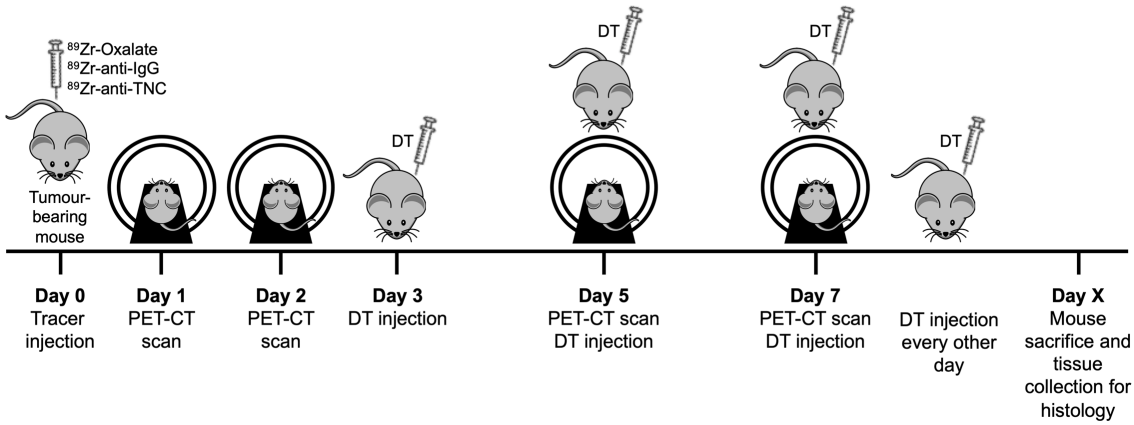

Figure 2.1|Experimental timeline used to assess TNC expression over the course of Treg depletion.
Once tumours were palpable, mice were injected i.v. with either anti-TNC antibody labelled with Zirconium, or with the negative controls, Zirconium Oxalate or anti-IgG antibody labelled with Zirconium. Mice were scanned at day 1, 2, 5 and 7, and DT treatment started at day 3, being the mice injected i.p. every other day, as described in Methods. Day X represents the day of mice sacrifice, which happened before tumours reached 1.5 cm in diameter or mice developed autoimmunity.

2.3.1. Scanning

For PET-CT imaging, mice with palpable tumours were transferred into the Wales Research and Diagnostic Positron Emission Tomography Imaging Centre (PETIC) up to 3 days before scanning. Each mouse was anaesthetised with 3-3.5% isofluorane (Teva Hospitals) delivered through a nose cone, placed on a heating pad and injected via the tail vein with a specific solution, depending on the condition to run. Experimental mice were injected with 1-3 MBq of ^{89}Zr labelled anti-TNC antibody (Abcam, clone EPR4219) in a 50 μL solution, whilst negative controls were injected with 1-3 MBq of ^{89}Zr-labelled anti-IgG (Abcam), 1-3 MBq of zirconium-oxalate, or, as a blocking experiment, cold anti-TNC antibody was injected 28h before 1-3 MBq of ^{89}Zr-labelled anti-TNC. Mice were then returned to their cages for 24h. Tail vein injections were performed by Stephen Paisey or Awen Gallimore.

On the day of scanning, the scanner (nanoScan122S PET CTMediso Preclinical Imaging System) was calibrated using a Na_{22} point source of 1 MBq. Each mouse was injected i.p., 10 minutes before acquisition, with 100 μL of iopamidol (Niopam 300, Bracco), a CT contrast agent, and anaesthetised with isofluorane. Once anaesthetised, mice were placed in the prone position on a warmed mouse bed in the scanner. Up to 3 mice were scanned at a time using the Mediso Multicell 3 mouse animal bed. Oxygen and isofluorane were supplied via a facemask through entire image acquisition. Respiration was monitored with pressure pads during the entire 75 minutes whole body PET-CT examination. Scans were performed up to 5 times for each mouse at 24, 48, 120, 142 and 192 hours post injection. Emission data were collected for 60 minutes followed by a 5-minute CT scan. Upon completion of the PET scan, mice were removed from the bed and placed in the heated recovery chamber until waking. All scanned mice were kept in individually ventilated Scantainer cages until the end of the experiment when mice were culled.

2.3.2. Analysis of PET-CT scans

For quantitative analysis and image rendering, Vivoquant™ software (v3.5, Invicro) was used. A whole mouse region of interest (ROI) was placed over each mouse from a pre-prepared template file. An entire skeleton ROI was selected from the CT scan for each mouse using the connected threshold tool. A tumour ROI was then selected from

the PET scan using the same connected threshold tool within a bounding box set to cover the entire leg of the mouse to contain the ROI to the tumour region. Tumour ROI concentrations in Becquerel (Bq)/mL were decay corrected back to the original injection time. For each ROI, the maximum Standardised Uptake Value (SUVmax) was calculated according to the following equation:

$$SUVmax\ (g/mL) = \frac{Image\ derived\ radioactivity\ concentration}{\frac{Decay\ corrected\ injected\ dose}{Body\ weight}}$$

2.4. TNC knockdown cell line

The complete process of using shRNAs to knockdown TNC in tumours is represented in Figure 2.2.

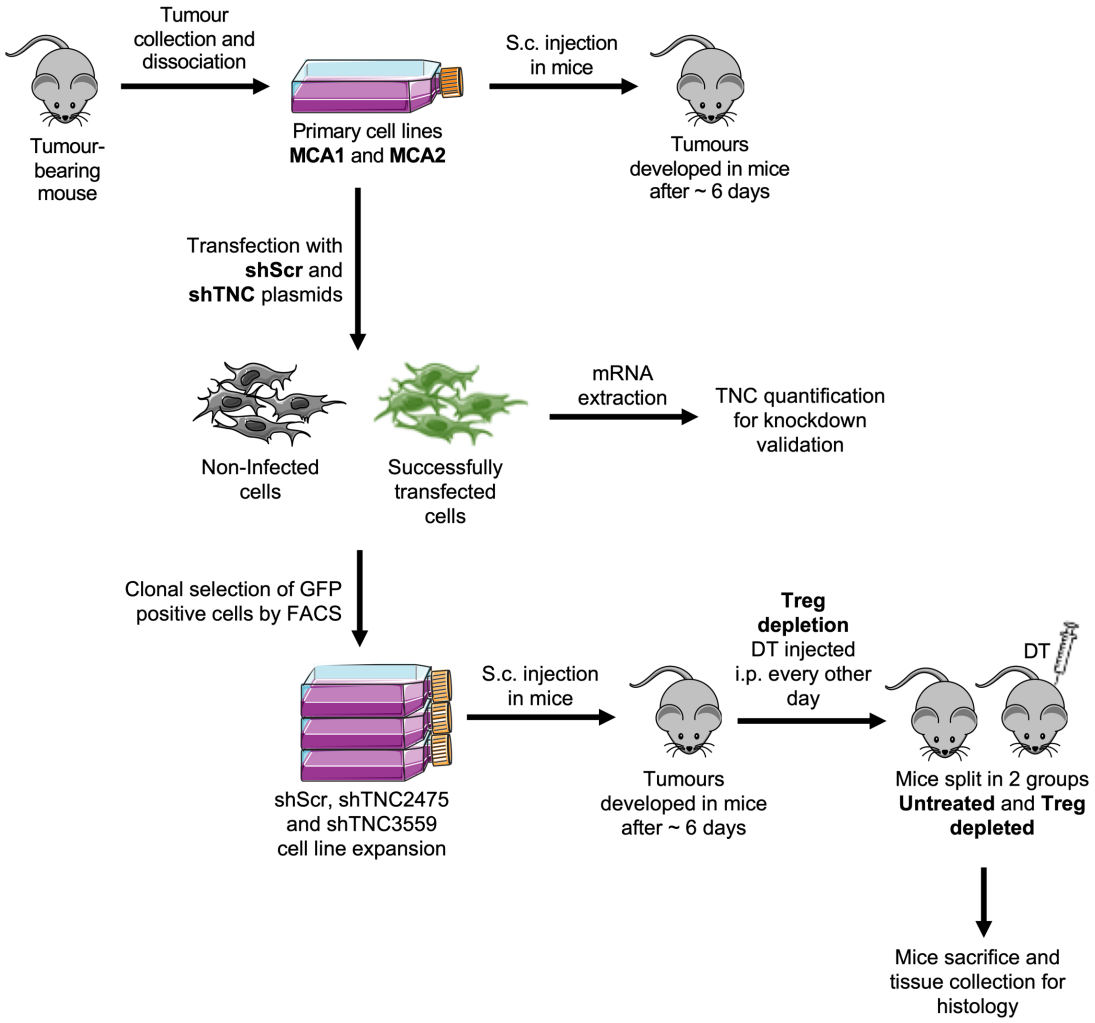

Figure 2.2|TNC knockdown of primary cell lines by shRNA and tumour induction in mice. Tumours from untreated mice were collected and dissociated to single cells. These gave rise to two different primary cell lines, MCA1 and MCA2 after 1 week of culture. Each cell line was injected in mice to test the capacity for tumour development. Tumours were palpable after ~ 6 days. Both cell lines were transfected with plasmids containing shRNAs coding for specific sites of TNC gene (shTNC) and a scrambled (shScr) sequence as control. Effectiveness of transfection was measured by GFP expression: green cells were successfully transfected; grey cells were not. mRNA was extracted from all conditions to assess TNC expression. GFP positive cells were FACS purified for each condition, and posteriorly expanded in culture. shScr and shTNC cells were used to induce tumours in mice, and these were split into two treatment groups – one left untreated and other Treg depleted. Once mice developed signs of autoimmunity or discomfort, they were sacrificed, and tumours were collected for further analysis.

2.4.1. Cell line establishment

To establish cell lines derived from MCA-induced tumours, two untreated tumours were dissected and chopped into small pieces and incubated in a cell culture flask with R10 media (RPMI media (Gibco) supplemented with 10% Foetal Calf Serum (FCS, Gibco) and L-glutamine and penicillin/streptomycin) at 37°C and 5% CO_2. On the following day, pieces of tissue were removed, and media was replaced, to exclude cells that did not attach to the flask, leaving tumour cells only to grow. When cells were confluent, the supernatant was removed from the flask and cells were washed with 1x PBS to remove any excess media. Cells were then incubated in 3 ml of Trypsin EDTA for 5-10 minutes. After this, 7 mL of R10 media was added to inactivate the enzyme. The resulting cell suspension was then centrifuged at 1200 rpm for 5 minutes, the cell pellet was re-suspended in 10 mL of R10 media and centrifuged again, under the same conditions. The cell pellet was finally re-suspended in 5 mL of R10 media. This cell suspension was added to 30 mL of R10 media in a T175 flask and split up to 3 times a week. Once the number of cells was expanded, cells were frozen at -80°C, in single vials of 10^7 cells/mL of freezing media (FCS with 10% DMSO (Sigma)). Cell lines (MCA1 and MCA2) were grown from each tumour. These were left to grow for 3-6 passages before being injected into mice.

2.4.2. Tumour induction

On injection day, cells were counted using a haemocytometer and resuspended in PBS at a concentration of 0.5 x 10^7 cells/mL. Mice were anaesthetised and injected s.c. with 0.5 x 10^6 cells (100μL of cell suspension) in the hind leg. Tumours were measured from day 6 up to 3 times per week until the mouse was sacrificed. Both the normal and tumour leg were measured, and the difference was calculated as described above (section 2.1.2).

2.4.3. shRNA knockdown

Oligonucleotide pairs for shTNC (sequences in Table 2.3) were ligated into pENTR/U6 Gateway system entry vector (Invitrogen) according to the manufacturers' instructions. A scrambled plasmid was also generated as a control. GFP was included

in the constructs to facilitate clonal selection of successful transduced cells. Hairpin sequences were verified and transferred, and viral supernatants were generated as described in (Soady *et al.*, 2017). MCA1 and MCA2 cells were resuspended at 10^6 cells/mL in virus supernatant and plated at 1 mL/well in ultra-low attachment 24-well plates (Corning). After 16 hours, cells were washed and replated in R10 media. After 48 hours, cells were transferred to normal tissue culture plastic and maintained in growth media for one week. After this time, cells were trypsinised and flow sorted to isolate GFP^+ cells for qPCR analysis. This process gave rise to originated three different cell lines; one comprising a scrambled sequence as control (shScr) and two comprising TNC sequences (shTNC2475 and shTNC3559).

Table 2.3|Oligonucleotide sequences for TNC shRNAs.

	Top Strand	Bottom Strand
shTNC2475	CACCGCCCTTGGCTGA	AAAAGCCCTTGGCTGA
	GAATTGATACGAACTAT	AATTGATAGTTCGCTAT
	CAATTTCAGCCAAGGGC	CAATTTCAGCCAAGGGC
shTNC3559	CACCGCTCCAGAAGGA	AAAAGCTCCAGAAGGA
	GCCTATAAGCGAACTTAT	GCCTATAAGTTCGCTTAT
	AGGCTCCTTCTGGAGC	AGGCTCCTTCTGGAGC

2.4.4. Quantitative Real-Time Polymerase Chain Reaction (qRT-PCR) validation

A sample of each cell line was collected, and cells were disrupted with 500 μL of RLT buffer. RNA was purified with RNeasy Plus mini kits (QIAGEN), according to the manufacturers' instructions. Resulting RNA was quantified using a NanoDrop 2000 spectophotometer (ThermoFisher Scientific) and stored at -80ºC, being posteriorly transcribed to generate complementary DNA (cDNA) using High-Capacity RNA-to-cDNA

kit (Applied Biosystems). The qRT-PCR reaction was performed in a final volume of 20 μL, containing 2 μL of cDNA sample, 10 μL of Gene Expression TaqMan® Master Mix (Applied Biosystems) and 1 μL of TaqMan® Gene Expression Assay probes (Applied Biosystems). Probes used are indicated in Table 2.4. Reactions were performed on an Applied Biosystems QuantStudio 3 Real Time Machine. Relative expression of mRNA was calculated using the ΔΔCt method.

Table 2.4|TaqMan® qRT-PCR probes.

Gene	Identification	Species
Actb	(DQ) Mix 20x	*Mus musculus*
Tnc	Mm00495662_m1	*Mus musculus*

2.5. RNAscope

RNascope for TNC mRNA transcripts detection was done accordingly to the manufacturer's instructions (ACD Bio). Before starting RNAscope, FFPE sections were baked in a dry oven for 1 hour at 60°C. After that, slides were dewaxed by immersion in fresh xylene, twice, for 5 minutes each, and in 100% fresh EtOH, twice, for 1 minute each. Slides were left to air dry for 5 minutes at RT.

To block the activity of endogenous peroxidases, tissue was covered with RNAscope Hydrogen Peroxide (ACD Bio) for 10 minutes at RT. After that, slides were washed twice for 5 minutes in dH_2O and then placed in pre-warmed dH_2O at approximately 100°C for 10 seconds to acclimate, before transferring to a pre-warmed RNAscope Target Retrieval solution (ACD Bio) for 15 or 30 minutes in a steamer. The target retrieval incubation time was optimised for each sample using positive and negative control probes. Slides were carefully removed and washed in dH_2O twice for 15 seconds. These were then transferred to fresh EtOH for 3 minutes and dried at RT. A circle around the tissue section was then drawn using an ImmEdge PAP pen (ACD Bio).

Sections were covered with RNAscope Protease Plus (ACD Bio) and incubated at 40°C for 30 minutes in HybEZ™ Oven (ACD Bio). After this time, slides were washed with dH_2O. The TNC probe (mm-Tnc, ACD Bio) was added to the slides and these were placed in the HybEZ™ Oven at 40°C for 2 hours. A negative (dapB, ACD Bio) and a positive (mmPpib, ACD Bio) control were also included in each run. Slides were then washed twice in RNAscope wash buffer (ACD Bio) for 2 minutes.

Signal amplification was performed using the RNAscope 2.5HD detection reagent kit – RED. The conditions for the amplification steps are detailed in Table 2.5. Between each step, slides were washed twice for 2 minutes in wash buffer. After the RED solution being applied for 10 minutes at RT, slides were washed in tap water and submerged in 50% Gill's Haematoxylin (SLS) for 2 minutes at RT. Slides were washed again in water, and then briefly dipped in 0.02% ammonia water. After being washed in water, sections were left at 60°C in a dry oven for 45 minutes.

Mounting was done by dipping each slide in fresh xylene, placing them in a coverslip with 2 drops of EcoMount media (BioCare) and leaving them to dry at RT. Sections were then imaged using Zeiss Axioscan Z.1, and images were analysed using Zen software Blue edition.

Table 2.5|RNAscope amplification step conditions.

Amplification Step	Time (minutes)	Temperature (°C)
AMP1	30	40
AMP2	15	40
AMP3	30	40
AMP4	15	40
AMP5	30	RT
AMP6	15	RT

2.6. Senescence-associated β-galactosidase staining

Primary cell lines obtained from tumours were incubated in 6-well plates in R10 media, at 37°C and 5% CO_2. When cells were confluent, cells were fixed and stained using the Senescence-Associated β-Galactosidase Staining Kit (Cell Signaling). In brief, media was removed, and cells were washed once with PBS. A fixative solution was added, and cells were incubated for 10-15 minutes at RT. After this, cells were washed twice with PBS, and β-Galactosidase Staining Solution was added. Plates were incubated at 37°C in a dry incubator overnight. On the following day, the development of a blue colour was checked under a microscope, and pictures were taken using an EVOS XL Core Cell Imaging System.

2.7. Telomere associated foci staining

Staining for telomere associated phosphorylated histone H2AX (γH2AX) foci (TAF) was performed in 5 μm thick tumour sections. These were initially deparaffinised in xylene (2 x 5 minutes) and rehydrated in an alcohol gradient (10 minutes in 100% ethanol, 5 minutes in 90% ethanol, 5 minutes in 70% ethanol, rinsed in tap water and 2 x 5 minutes in dH_2O). Sections were cooked on a pressure cooker for 20 minutes in Sodium Citrate antigen retrieval solution, cooled for 20 minutes at 4°C, and washed in dH_2O for 5 minutes and in PBS-TT (PBS, 0.1% Triton X-100, 0.5% Tween-20) for 5 minutes. Non-specific antibody binding was blocked by incubating slides in a solution of PBS-TT containing 8% BSA for 1 hour at RT. After a 5-minute wash in PBS-TT, sections were incubated in a primary antibody solution (PBS, 1% BSA, 1:60 Normal Goat Serum (NGS, Vectastain Rabbit IgG kit (Vector)), 1:250 anti-γH2AX (Ser139, Cell Signalling)) at 4°C overnight. The following day, sections were washed in PBS-TT, 2 x 5 minutes, incubated in a secondary antibody solution (PBS, 1% BSA, 1:60 NGS, 1:250 biotinylated anti-rabbit IgG1) for 1 hour at RT, and washed again 2 x 5 minutes in PBS-TT. Samples were incubated for 20 minutes with DSC-Fluorescein (Vector), washed for 5 minutes in PBS-TT and for another 5 minutes in PBS. In order to fix the staining, sections were cross-linked in 4% PFA/PBS for 20 minutes and washed 3 x 5 minutes in PBS. This was followed by tissue dehydration with an ice-cold ethanol gradient (70%, 90%, 100%), for 3 minutes each. Sections were air dried and incubated with the hybridisation mix (71.1% formamide, 13.7% dH_2O, 1% 1 M Tris pH 7.2, 8.7% magnesium chloride buffer (25 mM magnesium chloride, 9 mM citric acid, 82 mM sodium hydrogen phosphate), 5.1%

blocking buffer (Roche), 0.4% TelC Cy3 probe (Panagene)) and denatured for 10 min at 80°C. Probe hybridisation was subsequently achieved in a humidified chamber for 2 hours, at RT. Sections were washed 10 minutes in a 70% formamide/2x SSC (Sigma) solution, then 2 x 10 minutes in 2x SSC, and finally 3 x 10 minutes in PBS. Mounting was performed with ProLong Gold Antifade Mountant (ThermoFisher) and glass coverslips. Slides were left to cure overnight at RT, protected from light, and then were imaged using a Zeiss LSM800 confocal laser scanning microscope. Imaging consisted of obtaining Z-stacks with a step-size of 0.5 μm of random fields of view, using the 62x objective. Images were analysed with ImageJ software, where cells with overlap of telomere and γH2AX signal were considered senescent, and their percentage per field of view was calculated.

2.8. Tumoursphere assay

Tumours were chopped into small pieces and further processed using a McIlwain tissue chopper (Campden Instruments Ltd.). Pieces were transferred to a 50 mL falcon with 5 mL of a Liberase TL/DNase solution (HBSS (Thermo Fisher Scientific), 4% Liberase TL (Roche), 0.4% DNase I (Sigma-Aldrich)). This solution was incubated for 30 minutes at 37°C with shaking at 300 rpm. After incubation, the solution was centrifuged at 1500 rpm for 5 minutes and the supernatant was discarded. The pellet was then resuspended in 5 mL of red blood cell lysis buffer (BioLegend) and incubated for 5 minutes at room temperature (RT). Cells were then centrifuged at 1500 rpm for 5 minutes, and the resulting pellet was resuspended in 5 mL of RPMI culture media. In order to obtain a single cell suspension, cells were sieved with a strainer to a 50 mL falcon tube and centrifuged at 1500 rpm for 5 minutes. Two rounds of PBS washes were followed, and after the second round the pellet was resuspended in 5 mL of tumoursphere media (DMEM/F12 (Thermo Fisher Scientific), 10 ng/mL fibroblast growth factor (Thermo Fisher Scientific), 10 ng/mL EGF (Thermo Fisher Scientific), 1x N2 (Thermo Fisher Scientific)). The culture was made in ultra-low attachment 96-well plates (Corning), where cells were seeded at a concentration of 10^3 cells/well. After 7 days, spheres were counted under an inverted phase contrast microscope and passaged. After 14 days, the spheres were counted again, under the same conditions. Tumoursphere efficiency formation was calculated as percentage of the seeded cells that could form a tumoursphere.

2.9. Metastasis analysis

Both dLN and ndLN were taken from mice, mashed and sieved through a 70 μm strainer in order to obtain a single cell suspension. Cells were cultured in 6-well plates in R10 media, at 37°C and 5% CO_2. Cultures were checked daily for the presence of tumour cells, and media was replaced every other day.

2.10. Gene Expression Analysis

Taken from Colbeck et. al "Probe intensity values were corrected by background subtraction using Genome Studio software and subsequently log-2 and baseline (median) transformed using Genespring software (Agilent) before analysis of genes." Differential expression analysis was carried out using Limma (Ritchie *et al.*, 2015), probes with the highest baseline average were used in heatmaps and later analysis. R and the parallelDist package (https://cran.r-project.org/package=parallelDist) were used to perform Manhattan distance analysis of all genes. Heatmaps were created using the pheatmap (https://cran.r-project.org/package=pheatmap) R package (hierarchical clustering method "ward.D2", Manhattan clustering distance). Methods for the analysis of RNAseq data from The Cancer Genome Atlas (TCGA) can be found in the Appendix chapter. This analysis was performed by Alexander Greenshields-Watson.

2.11. Statistical analysis

All statistical analyses were performed using GraphPad Prism™ software. A P-value < 0.05 was considered significant. Details of statistical tests used are shown in Figure legends.

Chapter 3

Examining the reciprocal relationship between the tumour microenvironment and an effective anti-tumour T cell response

3.1. Introduction

Variable responses to cancer immunotherapies are well documented both amongst and within different cancer types (Emens *et al.*, 2017, Lohmueller and Finn, 2017). Whilst the extent of T cell activation and the availability of targets are significant factors in treatment success, it is also likely that other features of the TME act either as barriers or enablers of immune attack.

In order to characterise the relationship between the TME, TILs and control of tumour growth, a mouse model of carcinogen-induced fibrosarcomas was used (as described in Methods) to examine the impact of depleting Tregs on tumour growth (Hindley et al., 2012, Colbeck et al., 2017b). Using this model, it was previously reported that depleting Tregs results in significant T cell-mediated control of tumour growth in approximately half of the tumour-bearing mice. These mice, termed “responders” could be distinguished from “non-responder” mice by the development of intratumoural HEV and a significantly higher number of TILs (Figure 3.1-A) (Hindley et al., 2012, Colbeck et al., 2017b). Non-Responders, on the other hand, despite having a slightly reduced tumour growth rate compared to untreated tumours, do not develop HEVs, which results in a lower number of TILs compared to responder tumours (Figure 3.1-B). Furthermore, it was shown that neogenesis of HEV, regarded as an enabler of tumour immunity in this model, was critically dependent on activated T cells (Colbeck et al., 2017b), demonstrating that reciprocal interactions between immune cells and the tumour vasculature can drive conditions favourable to tumour destruction.

Besides tumour blood vessels and activation of T cells, it is possible that the type of stromal cells present and the composition of the ECM also play a role in the ability of T cells to infiltrate solid tumours (Hindley et al., 2012, Colbeck et al., 2017b, Allen *et al.*, 2017, Kraman *et al.*, 2010, Salmon *et al.*, 2012, Peske *et al.*, 2015). Thus, the ability of T cells to destroy tumours may depend not only on their specificity and activation status but also the composition of the TME.

Since features of the TME have, in some studies, been shown to associate with the effectiveness of immunotherapy, the study presented in this chapter was set up to compare the TME in responding and non-responding tumours, focusing on profiling specific ECM proteins with respect to lymphocyte infiltration and activation, and blood vessel formation. Identification of these distinguishing features may open new avenues for remodelling the TME as a way of creating a more permissive environment for immune

cells induced by immunotherapy. The hypothesis that the TME influences the success of Treg-targeted immunotherapy was explored.

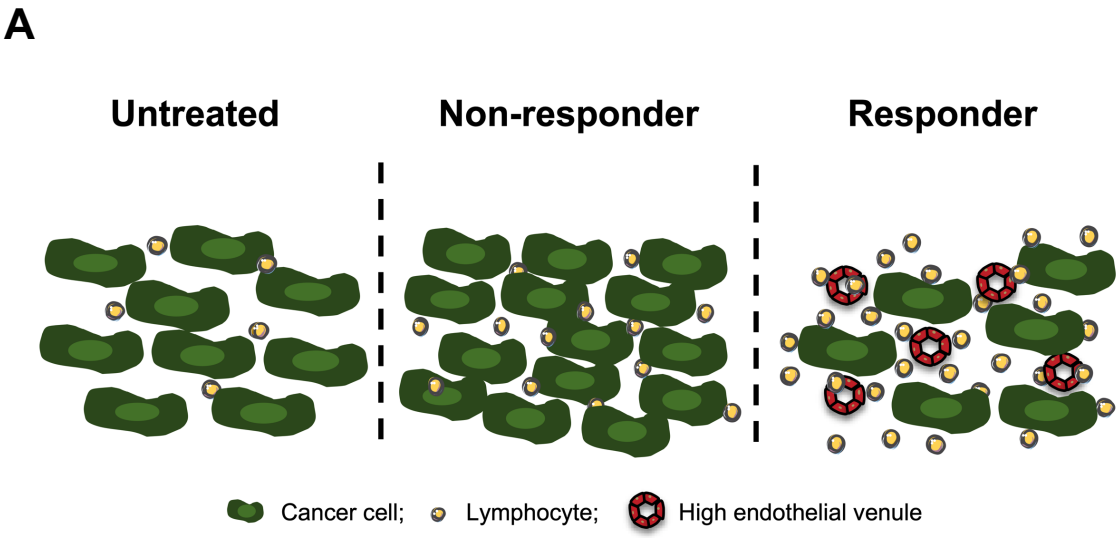

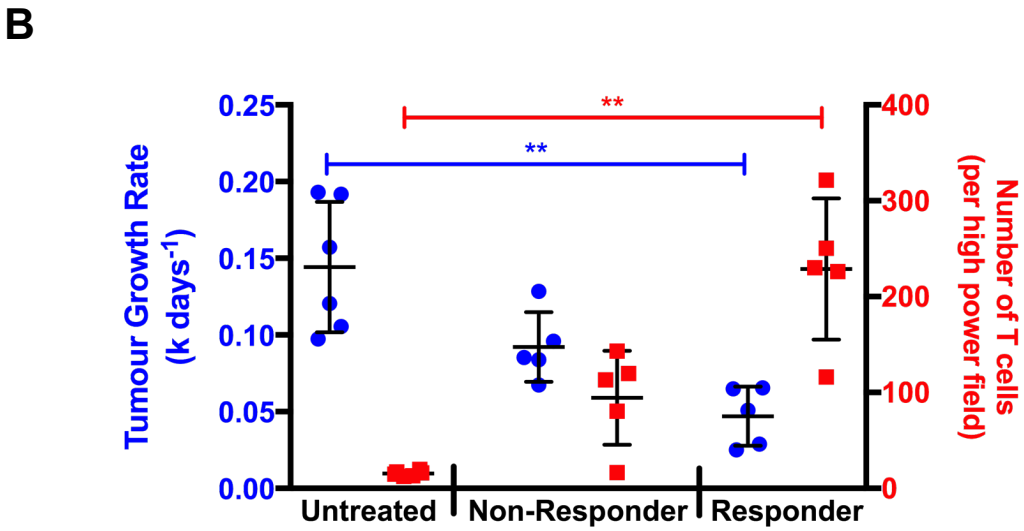

Figure 3.1| Schematic representation of the response to Treg depletion in fibrosarcoma-bearing mice.
A, Model explaining the differences in T cell numbers and development of HEVs between Untreated (Treg+), Non-Responder ($Treg^{-}HEV^{-}$), and Responder ($Treg^{-}HEV^{+}$) tumours, as previously extensively described by the group (Colbeck et al., 2017b, Hindley et al., 2012). **B,** Tumour growth rate (left axis, blue) and number of intra-tumoural $CD3^{+}$ cells (right axis, red) in Untreated (Treg+), Non-Responder ($Treg^{-}HEV^{-}$), and Responder ($Treg^{-}HEV^{+}$) tumours. Data are presented as individual data points (individual mice) plus median and standard error of the mean. Statistical significance was determined by Kruskal-Wallis One-Way ANOVA and Dunn's multiple comparisons tests (** = P≤ 0.01).

3.2. Results

3.2.1. Expression patterns of ECM proteins in mouse fibrosarcomas

In order to identify differences between tumour types beyond tumour growth rate, presence of HEVs and number of TILs, a bioinformatician in the lab (Alexander Greenshields-Watson) compared transcriptomes of untreated, responder and non-responder tumours (data originally generated by James Hindley, Gallimore lab). This analysis revealed that there are no genes differentially expressed between non-responders and untreated tumours (Figure 3.2-A), whilst 20 genes were significantly higher in non-responders when compared to responder tumours (Figure 3.2-B). From this list, TNC was most differentially expressed (adjusted p-value = 0.025, logFC = 2.365). As described previously, TNC is known to have important roles in embryonic development and wound healing, is thought to impede T cell function and is often associated with poor cancer prognosis, local recurrence and metastasis (Oskarsson *et al.*, 2011, Lowy and Oskarsson, 2015, Gocheva *et al.*, 2017, Onion *et al.*, 2018).

When the transcriptomes of responder and non-responder tumours were compared, 74 genes emerged as having significantly higher expression in responder *versus* non-responder tumours (Figure 3.2-C). These genes were associated with a strong and significant enrichment of immune pathways (Figure 3.2-D). *Cd6* (adjusted p-value = 0.019, logFC = -2.189), a T cell adhesion gene, and *Zap70 (0.019, -1.85), Cd3d (0.019, -2.38), Cd3g (0.030, -2.28)* and *Cd3e (0.020, -2.20),* key mediators of TCR signalling, were among the most significant differentially expressed genes (Figure 3.2-C). This bioinformatic finding was not surprising since as previously described, after Treg depletion, there is a negative correlation between tumour growth rates and T cell infiltrate (Hindley et al., 2011). Treg depleted tumours contain a higher number of $CD4^+$ and particularly $CD8^+$ T cells when compared to Treg replete tumours and non-responders (Figure 3.3). Indeed, as described above, T cells are critical for mediating tumour rejection in responder mice (Colbeck et al., 2017b).

Whilst there was a clear T cell immune signature present in the differentially expressed genes of responder mice (Figure 3.2-D), no pathways were significantly enriched in the non-responder gene list in which *Tnc* was most highly expressed. Analysis of gene expression patterns relative to *Tnc* using a Manhattan distance metric (Figure 3.2-E and Table 3.1) indicated that *Tnc* and *Zap70* consistently had opposing

expression patterns across all samples with the largest Manhattan distance value (21.08).

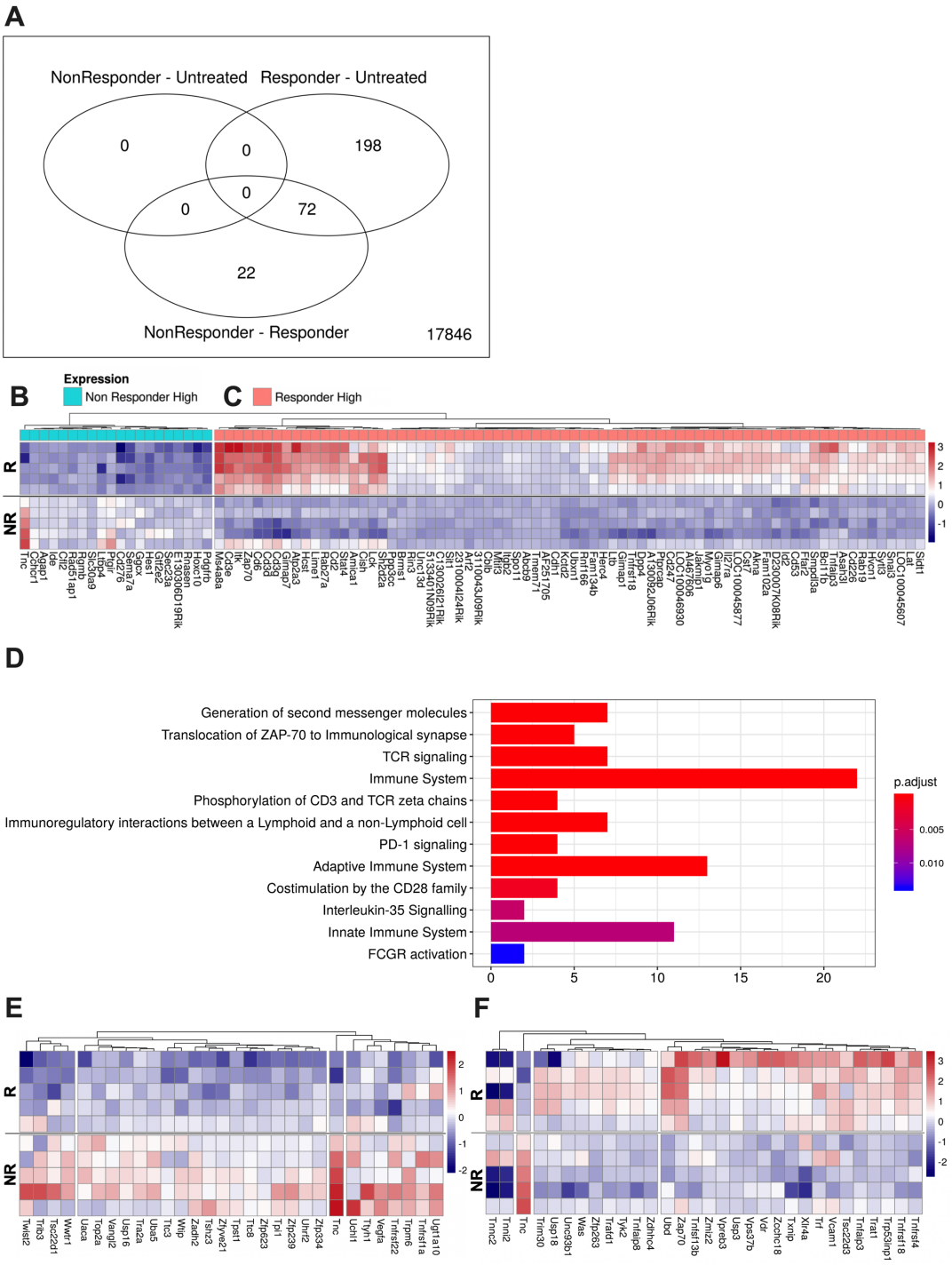

Figure 3.2| Bioinformatic transcriptome analysis of untreated, non-responder and responder tumours.

A, Differential expression analysis of microarray data comparing untreated, responding and non-responding tumours using the R package limma. Venn diagrams show the number of significantly differentially expressed genes (adjusted p-value < 0.05) for each group comparison (gene significant in both are at the intersect of the comparison circles). Heatmaps showing differentially expressed genes which are upregulated (**B)**, or downregulated (**C**), in non-responder mice tumours relative to responding mice. **D**, Analysis of genes significantly higher in non-responders (n = 74, padj < 0.05, logFC < 0). No pathways were significantly enriched in from the gene list of differentiated expressed genes higher in non-responders (n = 20, p < 0.05, logFC > 0). **E**, Manhattan Distance Analysis of Tumour Expression Against *Tnc*. Left, Top 30 genes with the

lowest Manhattan distances from *Tnc* calculated using median normalised gene expression values between responding and non-responding mice. Right, Corresponding bottom 30 genes with the furthest distance from *Tnc*.

Table 3.1|Top 30 genes with opposing expressing patterns to *Tnc*.

Manhattan Distance	Gene
21.08	*Zap70*
20.81	*Tnnc2*
20.45	*Ubd*
19.99	*Tnni2*
19.04	*Xlr4a*
18.84	*Tnfrsf4*
18.62	*Txnip*
18.39	*Tnfaip3*
18.33	*Tnfrsf18*
17.23	*Tsc22d3*
17.19	*Trp53inp1*
16.97	*Trat1*
16.5	*Zcchc18*
16.29	*Vdr*
16.18	*Usp18*
16.16	*Trim30*
15.94	*Vcam1*
15.68	*Vpreb3*
15.51	*Tnfsf13b*
15.47	*Trf*
15.37	*Trafd1*
15.36	*Zfp263*
15.35	*Tnfaip8*
15.33	*Usp3*
15.32	*Was*
15.14	*Unc93b1*
15.06	*Tyk2*
14.85	*Zdhhc4*
14.84	*Vps37b*
14.77	*Zmiz2*

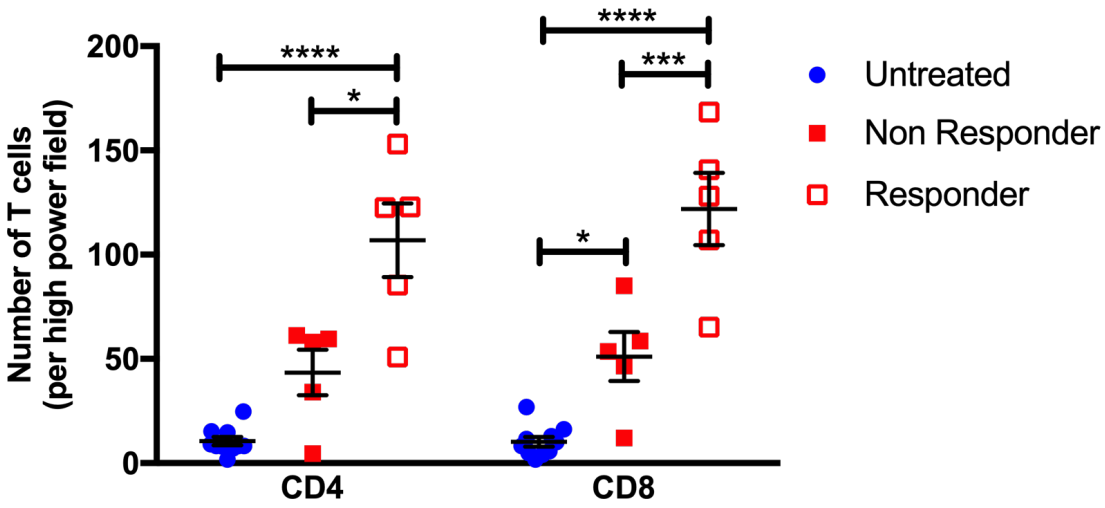

Figure 3.3| Tumour-infiltrating T cells are more abundant in responding tumours after Treg depletion.
Number of $CD3^+$ cells in tumours of Untreated (Treg+), Non-Responder ($Treg^-HEV^-$), and Responder ($Treg^-HEV^+$) $Foxp3^{DTR}$ animals. Data are presented as individual data points (individual mice) plus median and standard error of the mean. *n*=5 per group. Statistical significance was determined by Two-way ANOVA test with Tukey's multiple comparison test (*, P < 0.05; **, P < 0.01; ***, P < 0.001; ****, P < 0.0001).

Individual analysis of genes encoding ECM proteins revealed that other proteins follow the same trend as *Tnc* – lumican (*Lum*) and collagen type III alpha 1 (*Col3a1*) were also differentially expressed after Treg depletion (Figure 3.4). A significantly higher expression of *Tnc* and *Col3a1* was observed in non-responder tumours when compared to responders, whilst a range of expression is observed in untreated tumours. Although not significant, expression of *Lum* followed the same pattern.

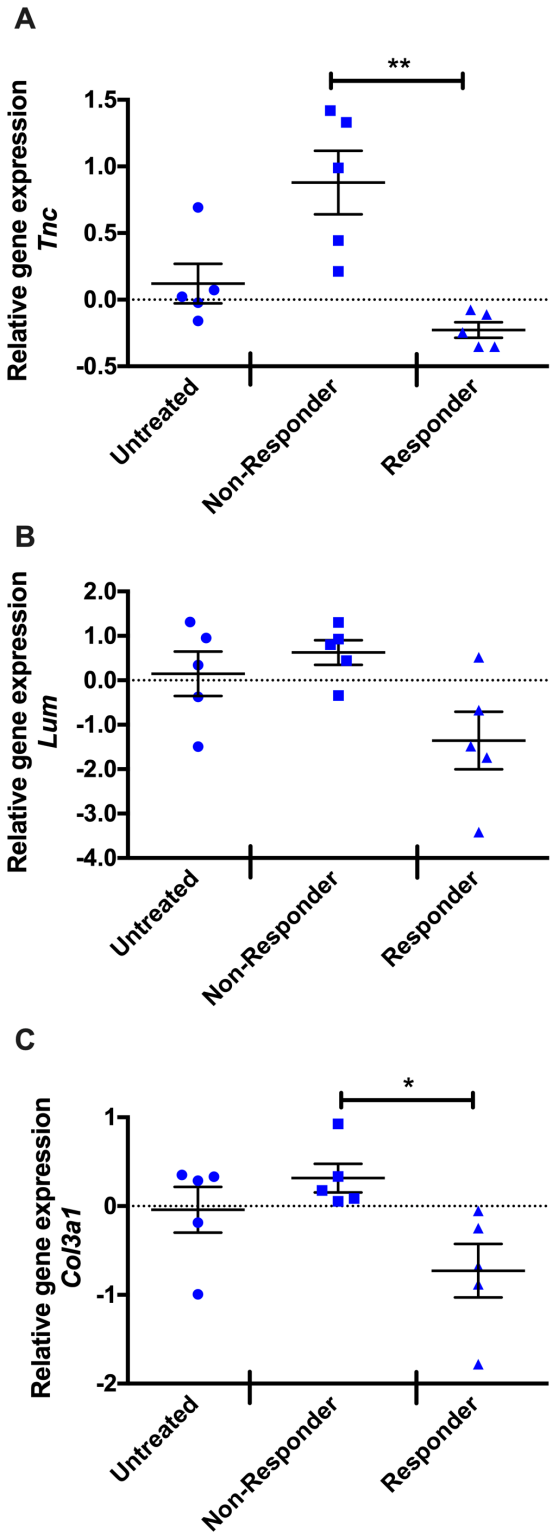

Figure 3.4| Differential expression of extracellular matrix genes after Treg depletion. Relative gene expression of tenascin-C (*Tnc*, A), lumican (*Lum*, B) and collagen, type III, alpha 1 (*Col3a1*, C) in tumours of Untreated (Treg+), Non-Responder ($Treg^{-}HEV^{-}$), and Responder ($Treg^{-}HEV^{+}$) $Foxp3^{DTR}$ animals. Data are presented as individual data points (individual mice) plus median and standard error of the mean. *n*=5 per group. Statistical significance was determined by Kruskal-Wallis test with Dunn's multiple comparison test (*, $P < 0.05$; **, $P < 0.01$)

The first aim of this study was to validate these results by immunofluorescence staining of frozen tumour sections (Figure 3.5). Both TNC and Lum protein levels clearly mirrored the gene expression pattern, where non-responder tumours present the highest levels of protein, compared with responders that have very low to no detectable protein present, and untreated tumours that show an intermediate amount of protein present in the TME (Figure 3.5-A and -B, respectively). Even though this pattern is not as evident for Col3a1 at a low power visualisation (Figure 3.5-C bottom), the same trend is observed on close inspection of the tissue at higher power (Figure 3.5-C top).

These data indicate that responder tumours can be characterised as HEV^{+}, T cell high and ECM low. Since the data above indicated that TNC and Zap70 were the genes with the most opposing expression profiles in non-responder and responder tumours and since there is a body of evidence indicating that TNC interferes with the accumulation and function of T cells, the significance of TNC in untreated and non-responder tumours was further analysed.

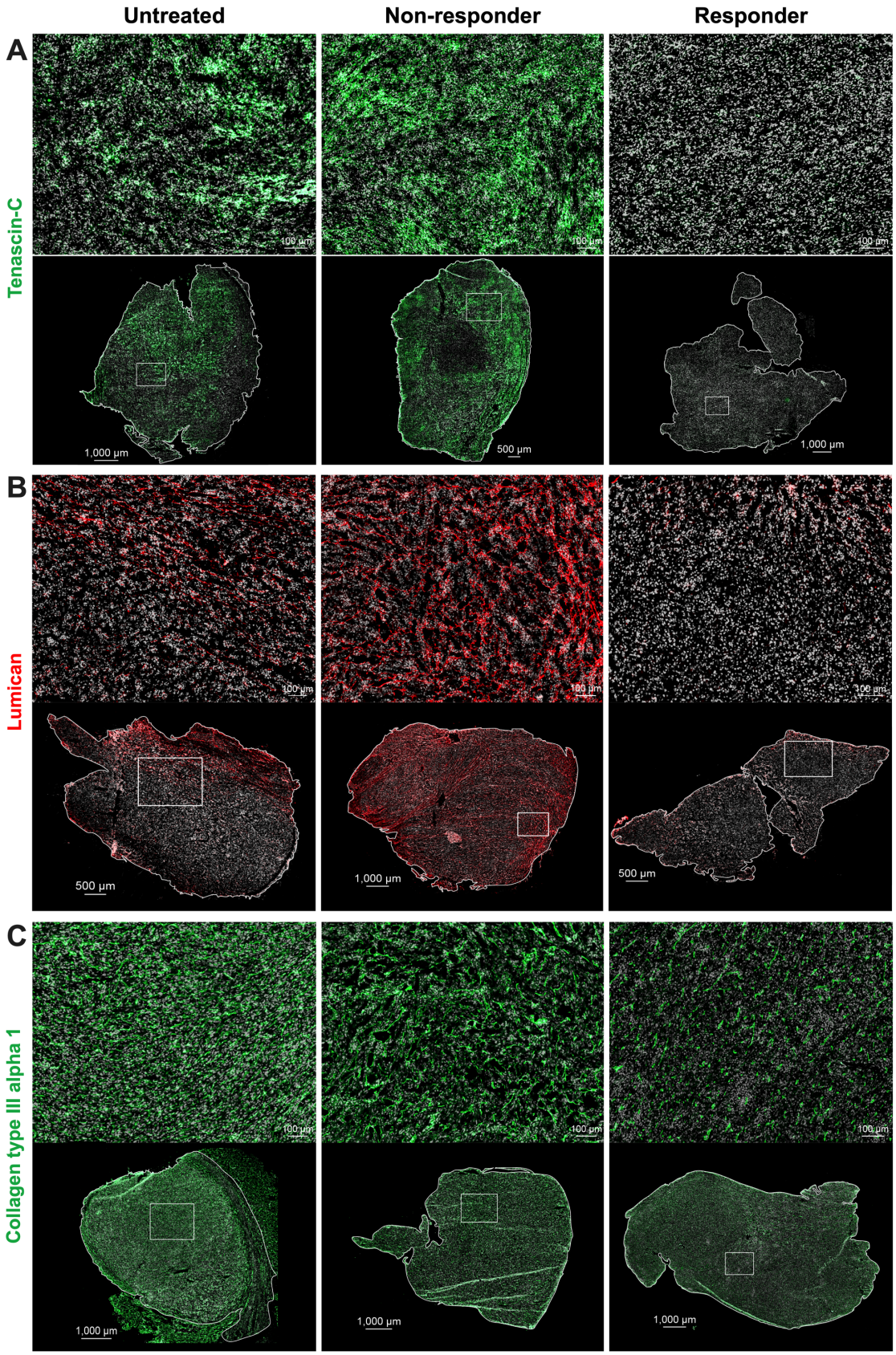

Figure 3.5|Immunofluorescent staining of ECM proteins validates gene expression data. Representative high-power images with corresponding low power images of whole tumour sections stained for TNC (A, green), LUM (B, red) and COL3A1 (C, green) prepared from tumours

of Untreated (Treg+), Non-Responder ($Treg^{-}HEV^{-}$), and Responder ($Treg^{-}HEV^{+}$) $Foxp3^{DTR}$ animals. Images include the nuclear stain Hoechst (grey).

3.2.2. TNC in the tumour microenvironment

TNC is a large oligomeric glycoprotein composed by 6 monomers (Figure 3.6). Each monomer has 4 distinct domains which can bind to different molecules, such as pathogenic components, matrix constituents, soluble factors and cell surface proteins, driving processes such as cell migration, matrix assembly, protease and pro-inflammatory cytokine synthesis (Orend and Chiquet-Ehrismann, 2006, Giblin and Midwood, 2015). Its expression in many cancers is associated with poor prognosis and tumour progression (Gocheva et al., 2017, Onion et al., 2018, Oskarsson et al., 2011, Lowy and Oskarsson, 2015).

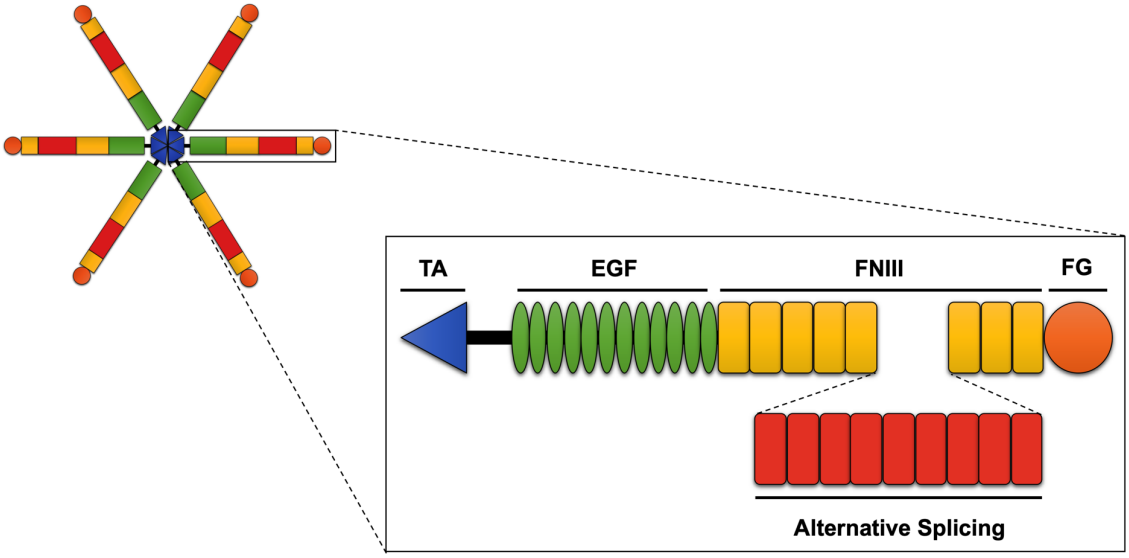

Figure 3.6|Structure and active domains of Tenascin-C.
TNC is an oligomeric protein constituted by 6 monomers. Each monomer comprises an amino terminal tenascin assembly (TA), 14.5 EGF-like domains, 8 constitutive FN-type III homologous domains and a fibrinogen (FG)-like carboxy-terminal part. Additional FN-type III domains can be added to the structure due to alternative splicing.

TNC deposition in TNC rich tumour sections unveiled a more abundant expression at the tumour periphery compared to the tumour centre, as observed in the low power image in Figure 3.4. When zoomed in (Figure 3.7-1), two different patterns emerged, a more fibrillar and better organised pattern closer to the edge of the tumour (Figure 3.7-2), and a more chaotic and less abundant staining pattern in the tumour centre (Figure 3.7-3). Similar TNC distribution has been reported in other tumours where it has been associated with stiffer matrices, implicated in limiting infiltration of immune cells or in helping tumour cells escape the primary tumour and metastasise to different sites (Cox and Erler, 2011, Acerbi *et al.*, 2015, Laklai *et al.*, 2016, Seager *et al.*, 2017, Northey *et al.*, 2017, Valkenburg *et al.*, 2018).

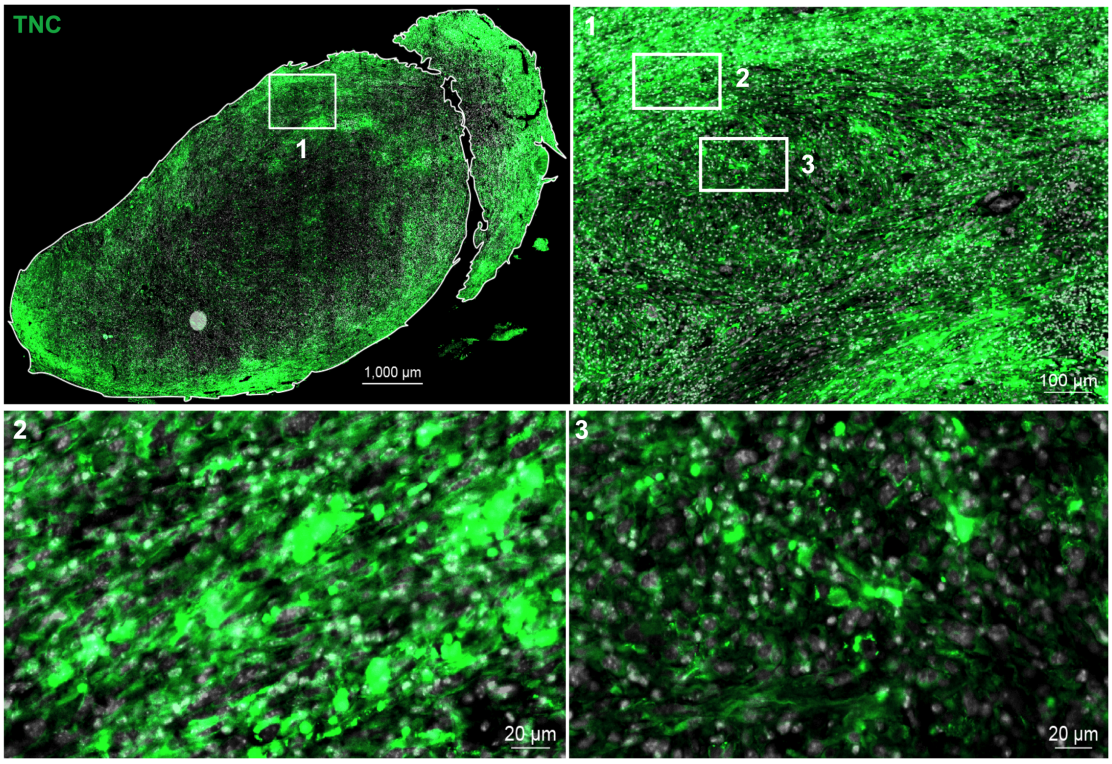

Figure 3.7| TNC presents different expression patterns within the same tumour.
Representative images of TNC expression pattern (green) in tumours. A low power image of a section through a whole tumour (left) shows TNC highly concentrated on the edges. A zoomed in medium power image (centre, 1) shows different patterns as TNC is found more towards the edge (right, 2) or the core (right, 3) of the tumour.

Since TNC has been shown to promote angiogenesis (Midwood *et al.*, 2011, Orend and Chiquet-Ehrismann, 2006, Rupp *et al.*, 2016, Radwanska *et al.*, 2017), its expression was assessed with respect to tumour vasculature. Sections of tumours from each untreated, non-responder and responder mice were co-stained for CD31 and TNC (Figure 3.8), and areas with low and high TNC were examined. Whilst this study cannot rule out a role for TNC in blood vessel function, it is evident that blood vessels can develop in areas with and without TNC, and no specific TNC staining was found close to CD31, suggesting no clear association between TNC expression and blood vessel development in this model.

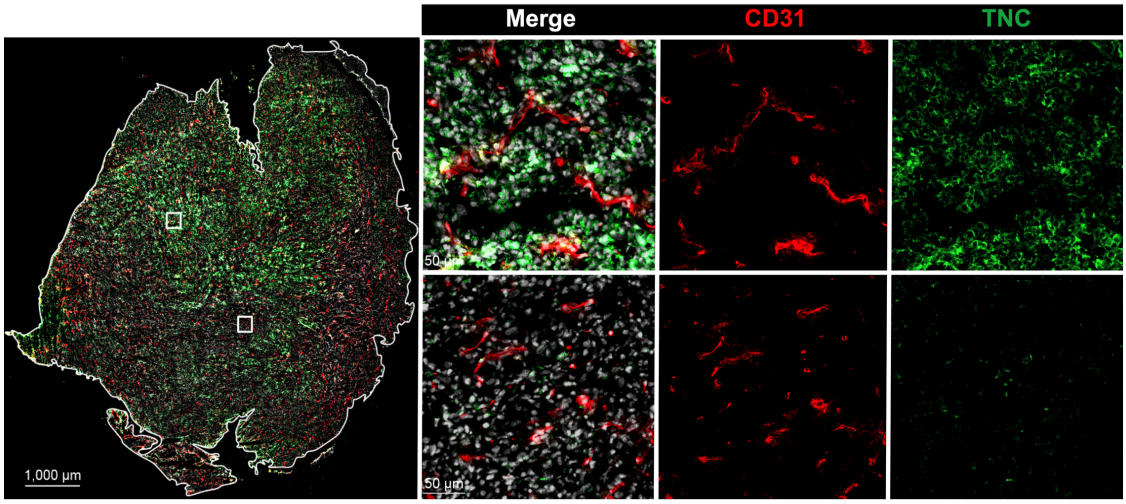

Figure 3.8|Blood vessel pattern does not correlate with TNC expression.
Representative low power image (left) of TNC (green) association with blood vessels (red), with magnifications of a TNC high area (top panel) and TNC low (bottom panel).

3.2.3. Distribution of TNC and T cells in tumours

Several studies document a role for TNC in influencing immune function. TNC has been shown to drive tumour-promoting inflammation, by activating TLR4 (Midwood *et al.*, 2009, Zuliani-Alvarez *et al.*, 2017), whilst other studies show that TNC can negatively affect T cell proliferation, activation, motility and function, potentially inhibiting adaptive immune response (Rupp et al., 2016, Radwanska et al., 2017, Salmon et al., 2012, Mirzaei *et al.*, 2018, Parekh *et al.*, 2005, Puente Navazo *et al.*, 2001). Since the data presented herein indicates that TNC is associated with non-response to Treg depletion, it was considered possible that TNC acts as a barrier to successful immunotherapy. To explore the relationship between TNC and TIL, intra-tumoural T cells were analysed with respect to the distribution of TNC. For each tumour, TNC high and TNC low regions were defined and analysed for T cell numbers. Figure 3.9 represents how these regions were identified, based on a subjective evaluation of protein present in random fields of views. High power images of TNC high and low regions (Figure 3.10-A) show that T cells can be found in both areas, in both Treg replete and depleted tumours. Enumeration of T cells revealed that, even though not significant, numbers were slightly elevated in TNC high areas (Figure 3.10-B). These results indicate that T cells are found in TNC rich areas of tumours.

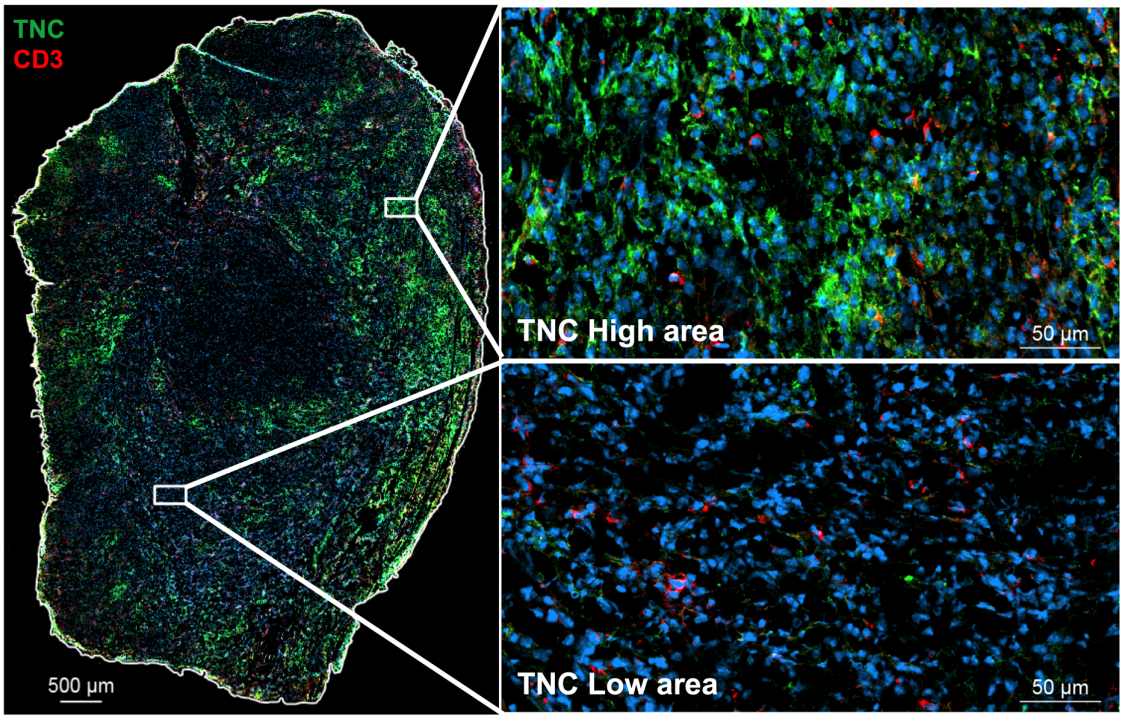

Figure 3.9| Definition of TNC high and low areas.
Tumours were individually observed and areas with high or low concentrations of TNC (green) were defined for further analysis.

A

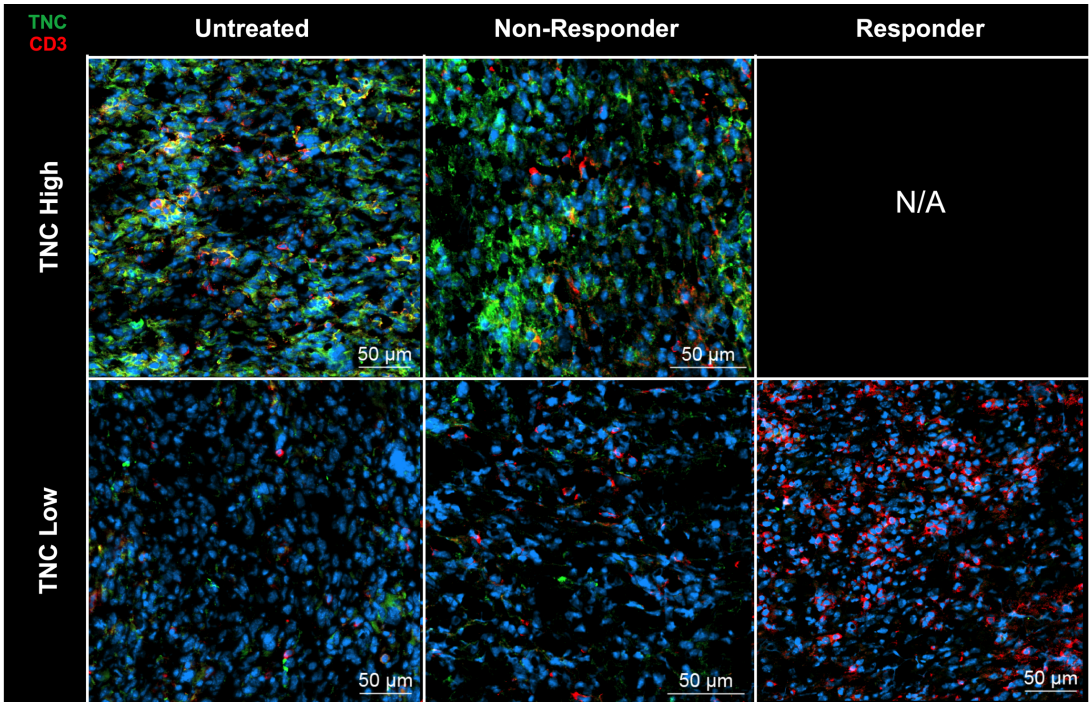

B

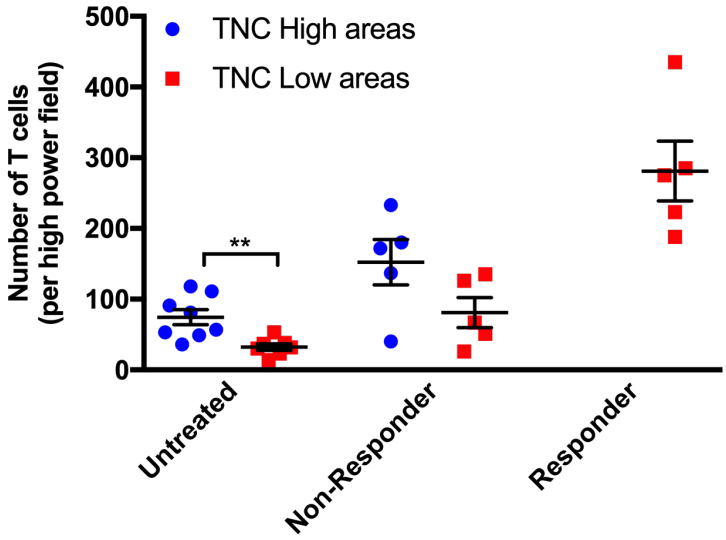

Figure 3.10|TNC expression does not exclude T cells from tumours.
A, High power images of TNC positive (green, upper panel) and TNC low (bottom panel) areas with T cell infiltrates (red) in tumours of Treg^{+}, Treg^{-}HEV^{-} and Treg^{-}HEV^{+} Foxp3^{DTR} animals. Images include the nuclear stain Hoechst (grey in A and B, blue in C). **B**, Number of intratumoural CD3^{+} cells in TNC positive and low areas in tumours of Treg^{+}, Treg^{-}HEV^{-} and Treg^{-}HEV^{+} Foxp3^{DTR} animals. Data are presented as individual data points (individual mice) plus median and standard error of the mean. *n*=5 per group. Statistical significance was determined with Mann-Whitney test.

3.2.4. T cell activity

Since T cells were found in both TNC high and TNC low areas of the tumours, the next step was to determine whether the phenotype of T cells was also similar in both areas. For this, GZMB expression was assessed by immunofluorescence (Figure 3.11-A), and $CD8^+$ cells that are either $GZMB^-$ (yellow arrowhead) or $GZMB^+$ (orange arrowhead), as well as $GZMB^+$ cells that are $CD8^-$ (red arrowhead) were detected in all tumours, and enumerated (Figure 3.11-B). This data revealed that even though there is no change in the amount of $GZMB^-CD8^+$ cells, there are significantly more $GZMB^+CD8^+$ T cells in TNC high areas than in TNC low areas of non-responder tumours, suggesting that high levels of TNC might be associated with less degranulation of T cells in poorly controlled tumours.

A

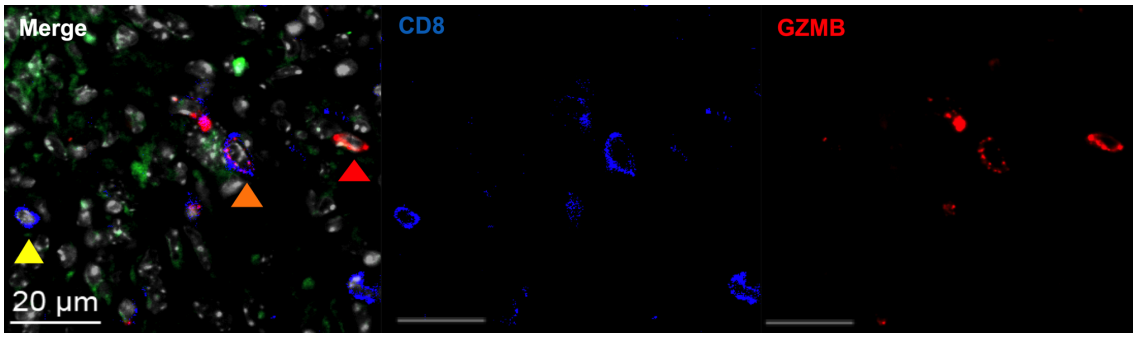

B

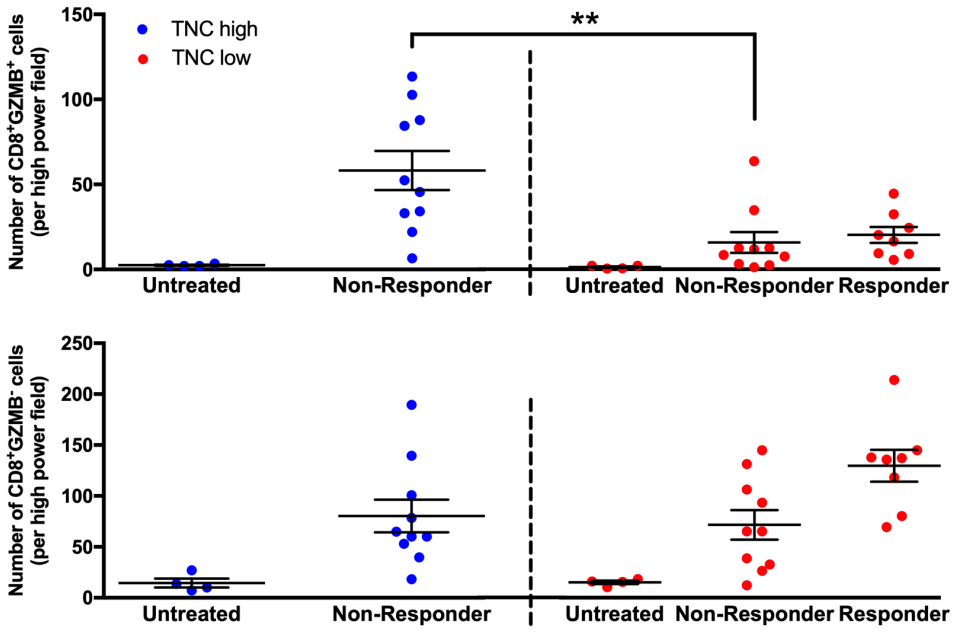

Figure 3.11|Granzyme-B is located in the cytoplasm of T cells in tumours with poor response to Treg depletion.
A, High power representative image of a $CD8^+GZMB^-$ cell (yellow arrowhead), $CD8^+GZMB^+$ cell (orange arrowhead) and $CD8^-GZMB^+$ cell (red arrowhead). Merged image includes the nuclear staining Hoechst (grey). CD8, blue; GZMB, red; TNC, green. Scale bars, 20 µm. **B**, Number of $CD8^+$ $GZMB^-$ and $CD8^+$ $GZMB^+$ cells in TNC high and low areas, in tumours of $Treg^+$, $Treg^-HEV^-$ and $Treg^-HEV^+$ $Foxp3^{DTR}$ animals. Data are presented as individual data points (individual mice) plus median and standard error of the mean. Statistical significance was determined by Mann-Whitney test.

3.2.5. Effect of TNC in response to immunotherapy

As indicated above, this study sought to address whether TNC inhibits successful Treg-targeted immunotherapy. Given that TNC is variably expressed in untreated tumours, it was considered possible that levels of TNC pre-treatment dictates whether tumours respond to immunotherapy or not. Conversely, it was also possible that TNC levels alter as a result of the response to immunotherapy.

3.2.5.1. Exploring alterations in TNC expression during Treg depletion of tumour-bearing mice

In order to understand how levels of TNC change in the microenvironment of single tumours over time, with and without Treg depletion, immuno-PET (antibody-based PET-CT imaging) was used. An antibody specific for TNC was labelled with ^{89}Zr to generate a PET tracer and injected in mice with MCA-induced tumours.

The first step was to determine whether the ^{89}Zr-labelled anti-TNC antibody would specifically label tumours. Twelve mice used in this study, the details of which can be found in Table 3.2. In brief, 4 were used as negative controls, of which one had no tumour, 3 were left untreated, and 5 were Treg depleted. Negative controls included 2 mice injected with ^{89}Zr-oxalate (1 tumour-bearing and 1 naïve), 1 mouse injected with a ^{89}Zr labelled IgG antibody (polyclonal, raised in rabbit in order to match the anti-TNC antibody), and 1 mouse injected with a mixture of hot and cold TNC antibody (1:1 ratio). Scan data was obtained for all 12 mice, but due to anaesthesia related complications, histology was performed on only 6 of the 8 experimental mice.

Table 3.2|Breakdown of mice used in PET-CT scans.

Group	Mouse	Tracer injected	Tumour	Treg depletion	Histology	Fate
Negative Control	1	^{89}Zr-Oxalate	No	No	No	PET-CT negative controls only
	2	^{89}Zr-Oxalate	Yes	No	No	
	3	^{89}Zr-anti-IgG	Yes	No	No	
	4	anti-TNC + ^{89}Zr-anti-TNC	Yes	No	No	
Experimental	5	^{89}Zr-anti-TNC	Yes	No	Yes	-
	6	^{89}Zr-anti-TNC	Yes	No	Yes	-
	7	^{89}Zr-anti-TNC	Yes	No	No	Death while scanning
	8	^{89}Zr-anti-TNC	Yes	Yes	Yes	-
	9	^{89}Zr-anti-TNC	Yes	Yes	Yes	-
	10	^{89}Zr-anti-TNC	Yes	Yes	Yes	-
	11	^{89}Zr-anti-TNC	Yes	Yes	Yes	-
	12	^{89}Zr-anti-TNC	Yes	Yes	No	Death while scanning

To analyse the images, radioactivity uptake in different ROIs was quantified, and Bq/mL values were converted to SUV (Figure 3.12). This conversion allows a normalisation of the data to the decay of the tracer and weight of the mouse, at different timepoints. In order to identify when the peak of the signal took place, biodistribution of the activity was analysed in the skeleton, liver, muscle and tumour, of untreated mice

injected with ^{89}Zr-anti-TNC, at 24, 48, 120, 142 and 192 hours (Figure 3.12-A). Tissue associated activity in the tumour indicates that the highest tumour uptake was observed at 120 hours. Moreover, radiotracer uptake in the tumour was higher than in the muscle and liver, suggesting specificity of antibody binding to the target. However, high skeleton uptake suggests that the ^{89}Zr-anti-TNC-IgG complex is unstable *in vivo*, since free zirconium salts exhibit tropism to the bone. This effect was confirmed by the activity distribution of ^{89}Zr-Oxalate negative controls in Figure 3.12-B, where accumulation of activity was clearly observed in the skeleton at 120h.

Analysis of activity uptake at 120h in negative controls (Figure 3.12-B) shows levels of activity uptake similar to treatment groups, especially in the tumour, in which both ^{89}Zr-Oxalate and ^{89}Zr-anti-IgG uptake is higher than ^{89}Zr-anti-TNC-IgG. Furthermore, no difference was observed in the tumour associated activity of ^{89}Zr-anti-TNC-IgG between untreated mice, non-responders and responders. Therefore, unlike the biodistribution data, these data indicate that activity uptake is not specific to the target.

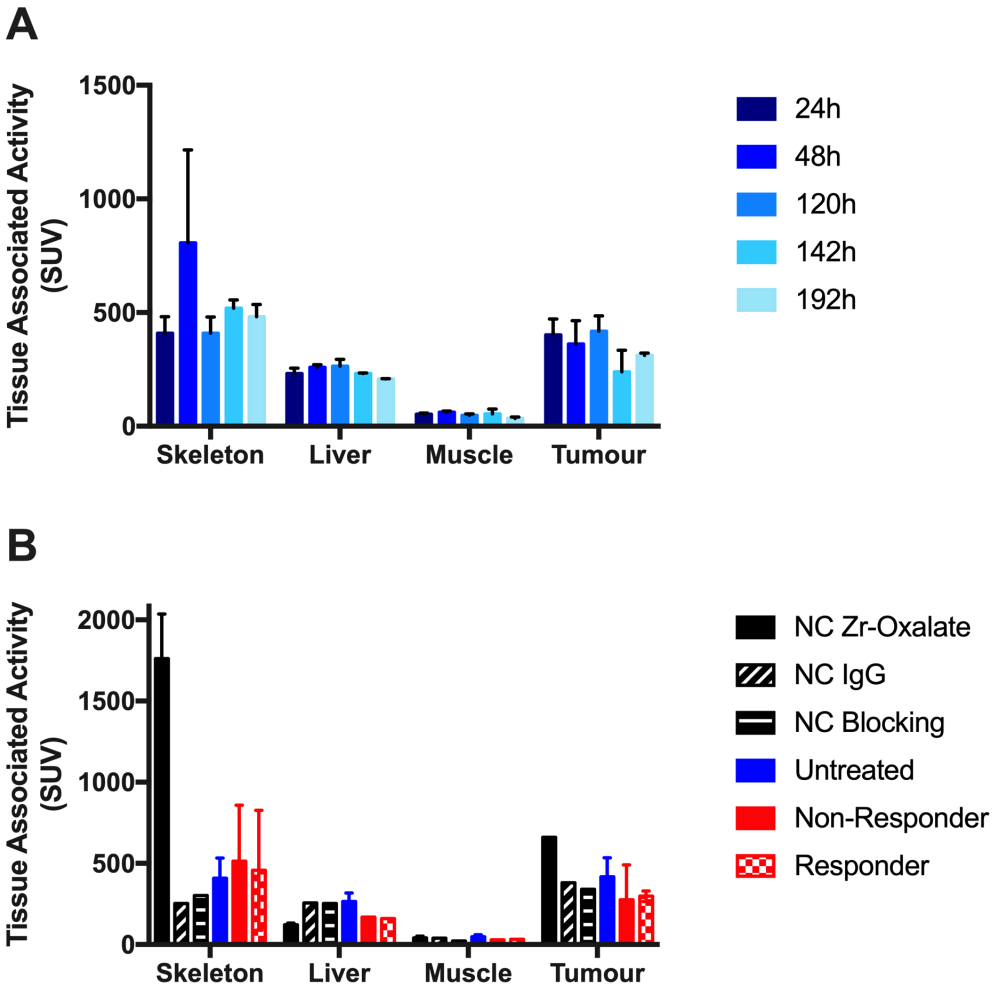

Figure 3.12|No difference in radioactivity uptake was observed between negative controls, untreated tumours and Treg depleted tumours.
A, Tissue associated activity in the skeleton, liver, muscle and tumour of untreated mice injected with ^{89}Zr-anti-TNC. **B**, Tissue associated activity in the skeleton, liver, muscle and tumour of mice injected with negative control (NC) tracers or ^{89}Zr-anti-TNC, untreated or Treg depleted (non-responders and responders). Data are presented as median and standard error of the mean. Statistical significance was determined with Mann-Whitney test.

Whilst the lack of target specificity meant that it would not be possible to draw solid conclusions from this experiment regarding TNC content in the tumours, the 4 Treg-depleted tumours were analysed in more detail to determine whether the level of ^{89}Zr-anti-TNC-IgG in individual tumours changed with time. It was possible to split the 4 Treg depleted tumours in 2 responders and 2 non-responders, based on tumour growth rates, T cell counts and presence of HEVs. Responding tumours had a lower growth rate (Figure 3.13-A) and a higher T cell count (Figure 3.13-B) when compared to non-responder and untreated tumours, and, as expected, HEVs were only present in tumours with lower growth rates and higher T cell counts (Figure 3.13-C).

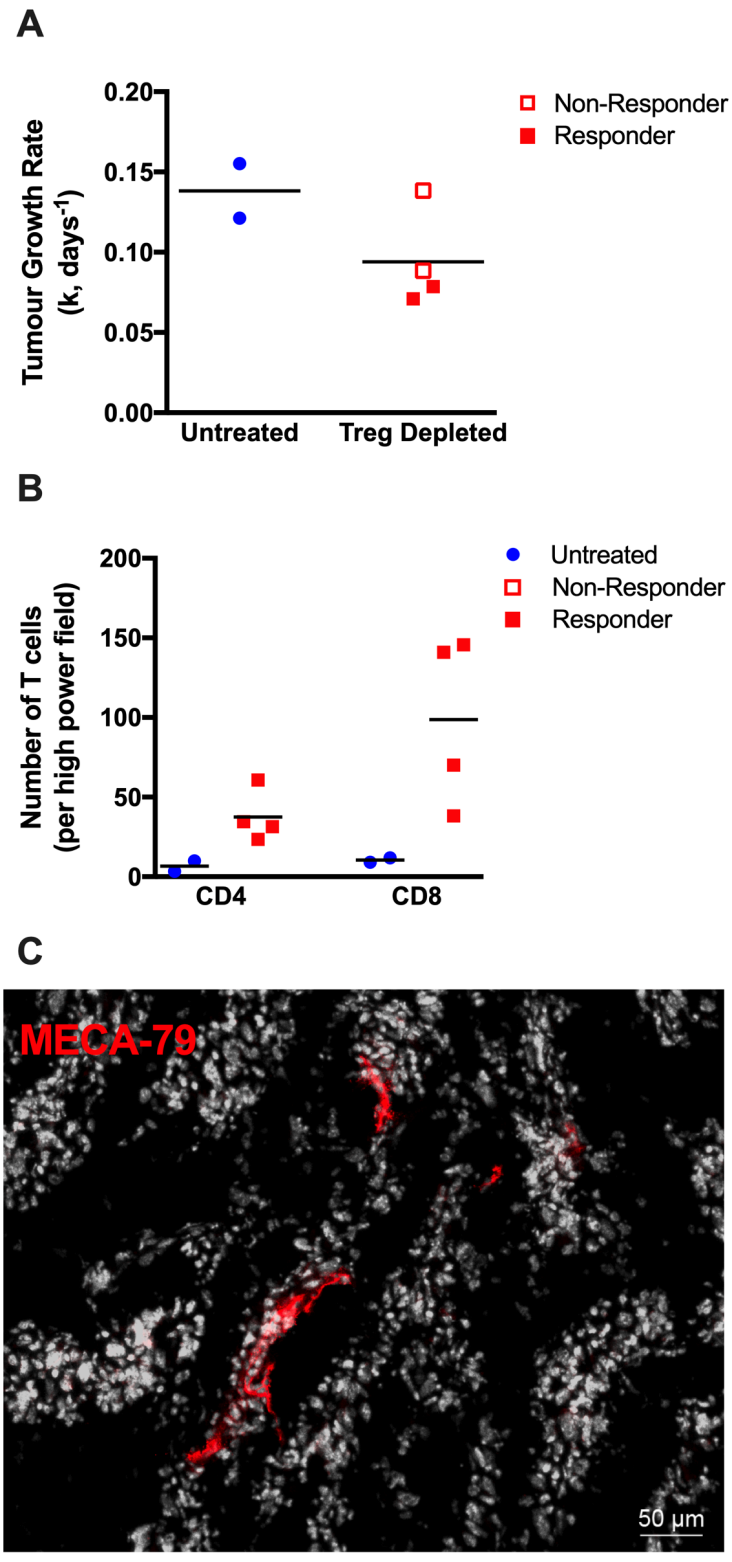

Figure 3.13|Features of tumours scanned by PET-CT.
Tumour growth rates (**A**; k, per day) and number of $CD4^+$ and $CD8^+$ cells (**B**) from tumours of Untreated (Treg+), Non-Responder ($Treg^-HEV^-$), and Responder ($Treg^-HEV^+$) $Foxp3^{DTR}$ animals. Data are presented as individual data points (individual mice) plus median and standard error of the mean. Statistical significance was determined by Kruskal-Wallis test. **C**, Representative low power image of HEVs ($MECA\text{-}79^+$ blood vessels; red) found in responders only.

Images obtained from PET-CT scans were analysed and compared with histology data (Figure 3.14). Radioactivity uptake was measured in becquerel/mL (BQML) and the concentration represented in different colours – dark blue represents lower uptake whilst yellow represents higher uptake (coloured scale bars in the figure). Figure 3.14-A shows the difference in radioactivity uptake between a tumour-bearing mouse injected with the negative control ^{89}Zr-oxalate (left) and a tumour-bearing mouse injected with ^{89}Zr-anti-TNC-IgG (right). Even though radioactivity uptake was apparent in the joints and skeleton of both mice, a difference in the tumour uptake was observed, where the tumour uptake of ^{89}Zr-anti-TNC-IgG mouse was higher than the negative control. A closer observation of the tumours pre-Treg depletion (Figure 3.14-B, left) indicates that both responders and non-responders exhibited high levels of radioactivity uptake, possibly representing high levels of TNC in early stages of tumour development. Immunofluorescent staining of the excised tumours for TNC (Figure 3.14-B, right) possibly indicating that levels of TNC change in responders as a consequence of Treg depletion. Whilst these data are compatible with the hypothesis that TNC levels pre-Treg depletion do not impact outcome after Treg-depletion, the specificity problems associated with this experimental design prevent any conclusions from being drawn.

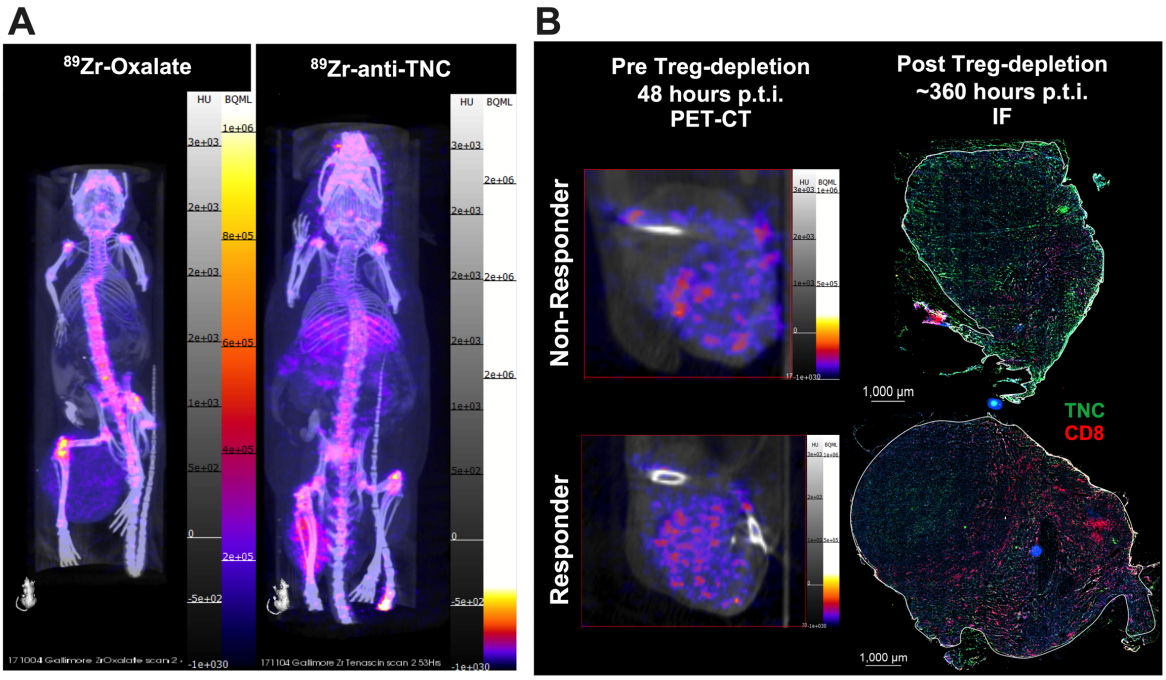

Figure 3.14|Signal obtained in PET-CT scans correspond to TNC staining in *ex-vivo* tumours.
A, Examples of PET-CT scans of tumour-bearing mice injected with ^{89}Zr-Oxalate (left) and ^{89}Zr-anti-TNC (right). **B**, Examples of PET-CT scans of mice injected with ^{89}Zr-anti-TNC (left), either non-responders (upper panel) or responders (lower panel) to Treg depletion. Images are zoomed in the tumour area, showing an example of scans 48 hours post tracer injection (p.t.i.), pre-Treg depletion. Representative high-power images of whole tumour (right) stained for TNC (green) and CD8 (red).

3.2.5.2. Effect of knocking down TNC in a cell line inducing tumour model

Since the data obtained using PET-CT was inconclusive, another method was selected to determine whether TNC in tumours prevents or diminishes the response to Treg-targeted immunotherapy. First, fibrosarcoma cell-lines were generated from carcinogen-induced tumours and interference RNA subsequently used to knockdown TNC expression in these cells. Cell lines expressing or not expressing TNC were subsequently used to examine the role of initial levels of TNC in response to Treg depletion. The cell lines were named MCA1 and MCA2.

To understand if the cell lines established from MCA-induced tumours could mimic the normal behaviour of MCA-induced tumours, $0.5x10^6$ cells were injected s.c. in the hind leg of mice and they were closely monitored. Once tumours were palpable, Treg were depleted in half of the animals and all tumours measured over time. Figure 3.15 shows that tumours derived from both cell lines grew at a similar rate (mean values of 0.10 mm/day for MCA1 and 0.16 mm/day for MCA2) and when compared to the rate previously described for untreated MCA-induced tumours (0.15 mm/day, Colbeck *et al*., 2017). All Treg depleted mice efficiently controlled tumour growth, presenting lower tumour growth rates (mean values of -0.02 mm/day for MCA1 and 0.01 mm/day for MCA2) than previously described for Treg depleted MCA-induced tumours (0.10 mm/day for non-responders and 0.06 mm/day for responders, Colbeck *et al*., 2017).

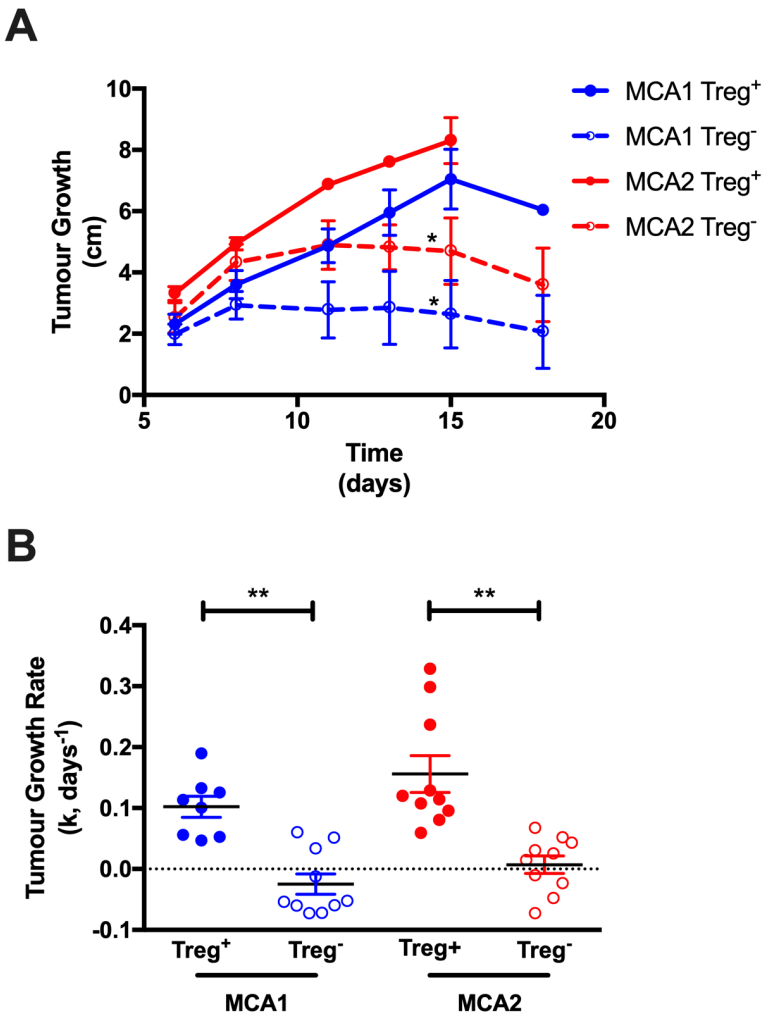

Figure 3.15|Primary cell lines derived from MCA-induced tumours grow at a similar rate *in vivo*, even when Treg depleted.
A, Tumour growth curves of MCA1 and MCA2 cell line-induced tumours, untreated ($Treg^+$) and Treg depleted ($Treg^-$). Data are presented as median and standard error of the mean. *n*=8-10. **B**, Tumour growth rates (k, per day) of MCA1 and MCA2 cell line-induced tumours, untreated ($Treg^+$) and Treg depleted ($Treg^-$). Statistical significance was determined by Kruskal-Wallis test with Dunn's multiple comparison test (*, $P < 0.05$; **, $P < 0.01$).

Both cell lines were then transfected with plasmids for a scrambled sequence, as control, and two complementary sequences for TNC. Since the plasmids had GFP as a marker gene, it was possible to distinguish successfully transfected cells (green) from cells that were not transfected. Figure 3.16-A shows that transfection was more efficient on MCA2 cells, having achieved up to 85.7% of infection as opposed to 0.1% in MCA1, hence, the following experiments were conducted using these cells. Flow cytometry plots of infection results can be found in the Appendix (Supplementary Figure 6). Cell line infection and subsequent assessment of infection efficiency by flow cytometry was done by Howard Kendrick, from the European Cancer Stem Cell Research Institute, Cardiff University. shScr, shTNC2475 and shTNC3559 cells were expanded and tested for the efficiency of TNC knockdown. By comparing *Tnc* fold change levels normalised to the house keeping gene (*Actb*), it was possible to determine that shScr cells expressed 3 times less *Tnc*, shTNC2475 expressed 24 times less *Tnc* and shTNC3559 expressed 28 times less *Tnc* than non-infected cells (Figure 3.16-B). Given these results, shTNC3559 was used in further experiments. TNC knockdown was also validated by immunofluorescence, after shScr and shTNC cells were injected in mice and the resulting tumours excised and stained for TNC expression. Figure 3.16-C shows that shScr tumours have high expression of TNC, whereas shTNC tumours have no TNC in their stroma.

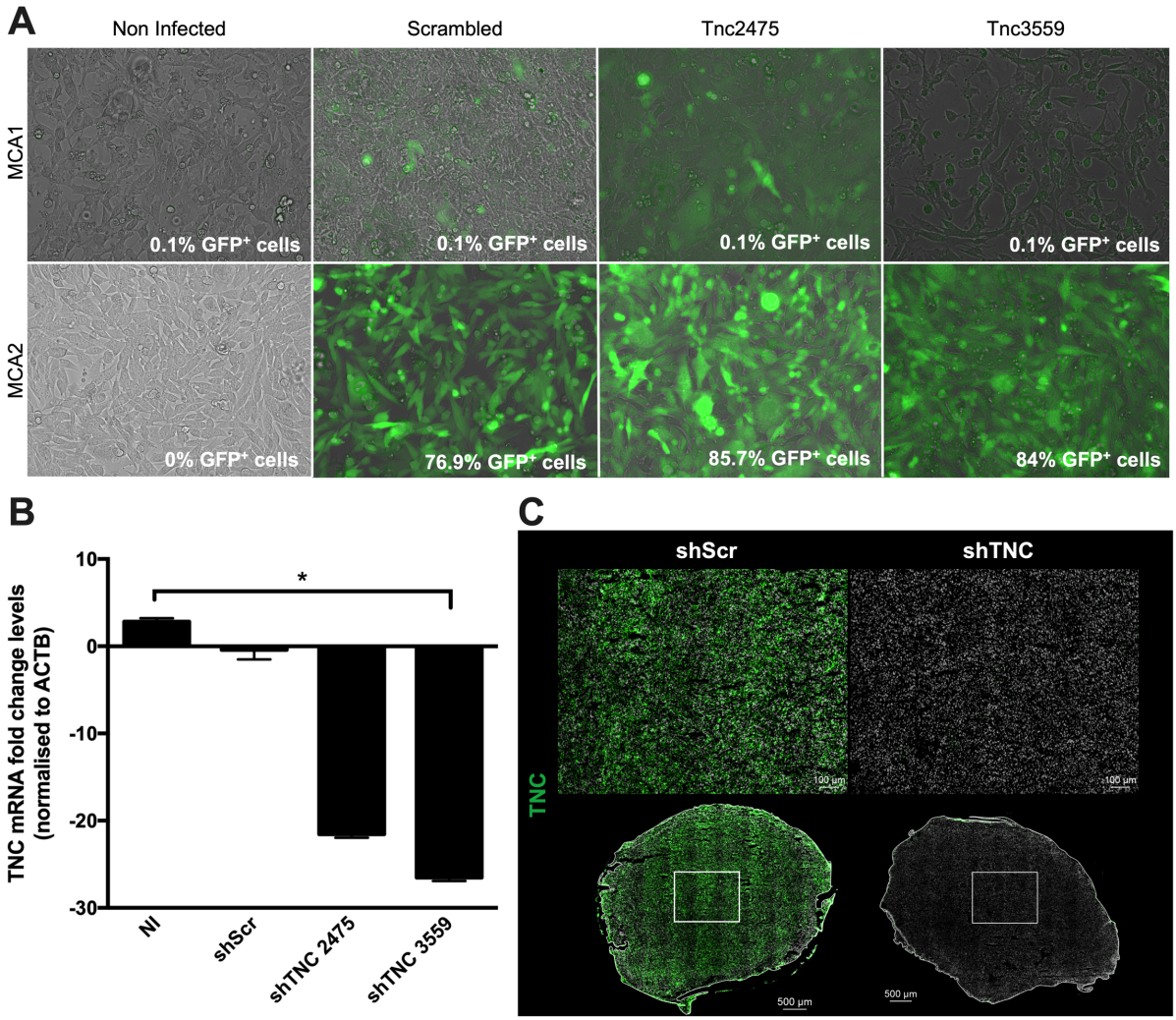

Figure 3.16|Silencing of TNC expression through shRNAs was successful both *in vitro* and *in vivo*.

A, Representative images of cell lines MCA1 and MCA2 post shRNA transfection. Green cells represent cells successfully transfected. Percentage of GFP^+ cells was obtained by flow cytometry (plots in Appendix). **B**, Relative gene expression of TNC in Non-Infected (NI) cells, cells that were transfected with a Scrambled plasmid (shScr), with shTNC 2475 and shTNC 3559 plasmids. Data are presented as median and standard error of the mean. The experiment was performed in triplicate. Kruskal-Wallis test with Dunn's multiple comparison test was performed indicating a statistically significant difference between every group ($P < 0.05$). **C**, Representative low power images of TNC (green) expression in tumours of mice injected with shScr and shTNC cells. Images include the nuclear stain Hoechst (grey).

shScr and shTNC cells were then injected in mice, tumour growth was monitored, and Tregs-depleted in half of the group once tumours were palpable. TNC expression did not appear to affect tumour growth rate in either untreated or Treg depleted tumours, since Treg depletion resulted in a reduction in tumour growth rate in both shScr and shTNC tumours (Figure 3.17-A). Comparable to the MCA-induced tumours, a loss of TNC expression was observed in tumours responding to Treg-depletion, whilst untreated tumours maintained high expression levels (Figure 3.17-B). These results indicate that TNC levels before Treg depletion do not impact on response, but loss of TNC appears to be a consequence of an effective immune response.

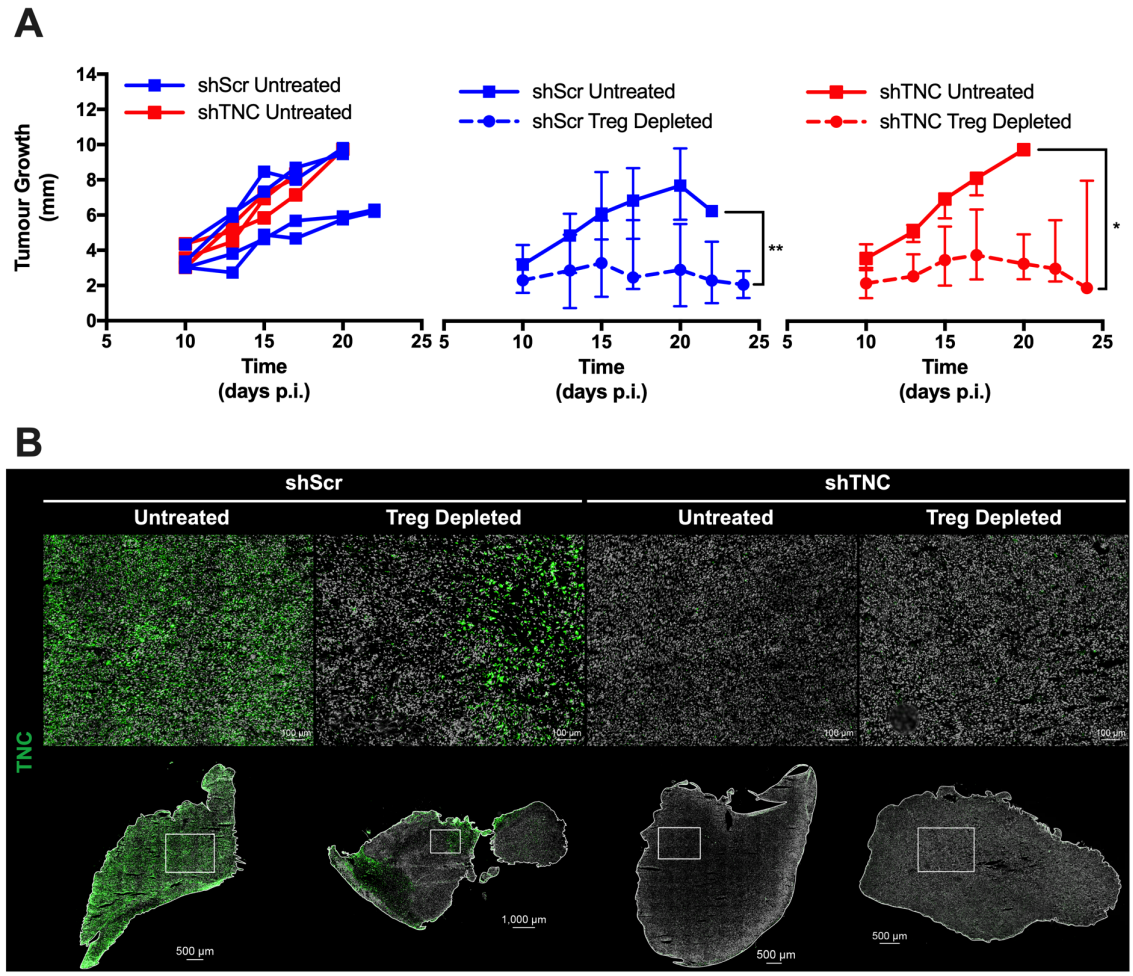

Figure 3.17| Cell line derived tumours respond to Treg depletion regardless of initial TNC expression.

A, Tumour growth curves of shScr and shTNC tumours, untreated and Treg depleted. Data are presented as individual curves (individual mice, left) or as median and standard error of the mean (centre and right). *n*=4 shScr Untreated, Treg depleted and shTNC Treg depleted groups; *n*=3 shTNC untreated group. Statistical significance was determined by Kruskal-Wallis test with Dunn's multiple comparison test (*, $P < 0.05$; **, $P < 0.01$). **B**, Representative low power images of TNC (green) expression and T-cell (CD3, red) infiltration in tumours of mice injected with shScr and shTNC cells, untreated and Treg depleted. Images include the nuclear stain Hoechst (grey).

3.2.6. Mechanism of TNC clearance from the TME

The next question arising from these data related to how TNC is cleared from the ECM. Since activated T cells and NK cells can produce enzymes which degrade ECM proteins, it was possible that the ECM was digested as a direct consequence of immune activation. Alternatively, loss of ECM proteins could be due to a change in gene expression by the tumour cells. The latter hypothesis was supported by the microarray data indicating a global decrease in TNC expression in responder tumours. This possibility was therefore tested first. RNAscope technology was used to visualise single mRNA TNC molecules in untreated, non-responder and responder tumours, by *in situ* hybridization of TNC-specific probes. Figure 3.18 shows the difference of TNC mRNA transcripts production between groups. Overall, less TNC mRNA transcripts are observed in responder tumours, when compared to both untreated and non-responders. TNC transcripts were concentrated around the edges of untreated and non-responders, compatible with the observations described in section 3.2.3, in which TNC protein was more visible at the tumour periphery.

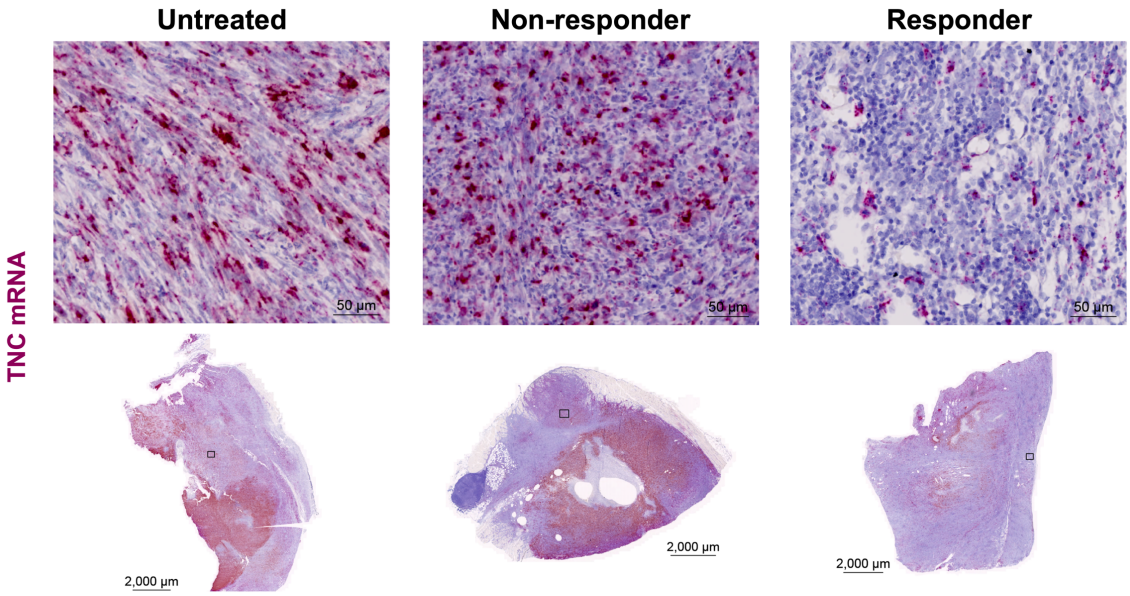

Figure 3.18|Responding tumours to therapy express less TNC mRNA transcripts than other groups.
Representative high-power images with corresponding low power image of whole tumour stained for TNC mRNA transcripts (pink) expression in tumours of Untreated ($Treg^{+}$), Non-Responder ($Treg^{-}HEV^{-}$), and Responder ($Treg^{-}HEV^{+}$) $Foxp3^{DTR}$ animals. Images include haematoxylin counterstain (blue).

A closer observation of these sections shows that the TNC mRNA signal surrounds the nuclei of the largest cells (Figure 3.19), a feature indicative of tumour cells.

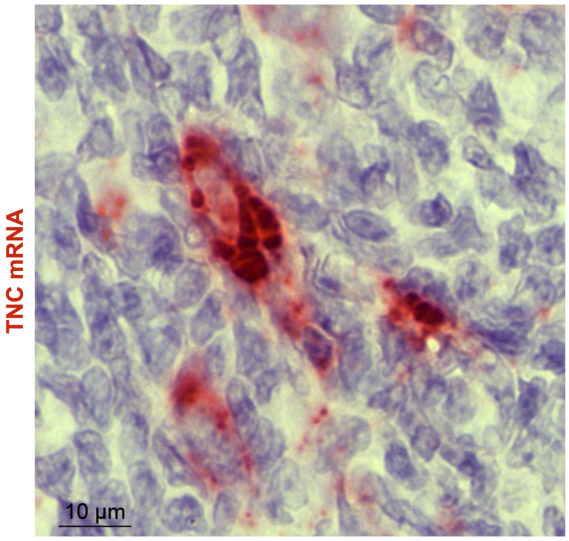

Figure 3.19| TNC is expressed mainly in tumour cells.
Representative high-power image of TNC mRNA transcripts (red) located on the cytoplasm of a tumour cell. Image includes haematoxylin counterstain (blue).

3.3. Discussion

Even though there are several new immunotherapies available for cancer patients, the responders are still a minority. Hence, it is important to understand what distinguishes responders from non-responders. The study described in this chapter focussed on comparing tumours from fibrosarcoma-bearing mice which were either Treg-replete or depleted of Tregs. Within the Treg-depleted group were responders and non-responders, as described in detail above. Features of the tumour microenvironment found to be significantly different in responders and non-responders were identified and characterised.

Transcriptome analyses, performed by a previous member of the lab (James Hindley) and more recently by a bioinformatician, Alexander Greenshields-Watson, revealed significant differences in expression of several ECM genes, most notably TNC. Subsequent immunostaining of tumours from untreated, non-responding and responding to Treg depletion mice confirmed that there is a loss of extracellular matrix proteins in responder tumours. *Tnc*, *Lum* and *Col3a1* were differentially expressed, presenting the same pattern of high expression in non-responders, almost absent in responders, and a range of expression in untreated tumours. These findings are of note since it is clear from other studies that ECM plays an important role in providing structural support enabling cancer progression. It has been demonstrated that the expression of certain ECM proteins is associated with poor prognosis and worse outcome (Gocheva et al., 2017, Onion et al., 2018, Oskarsson et al., 2011, Lowy and Oskarsson, 2015). However, this relationship between ECM proteins and patient outcome has not been reported in the context of immunotherapy yet.

As described above, TNC is an ECM protein which is highly expressed during embryonic development, but its expression is downregulated in the adult organism, being activated only during wound healing, inflammation or cancer (Midwood *et al.*, 2016). Because TNC expression in cancer is described to be involved in suppressing T cell responses (Puente Navazo et al., 2001, Parekh et al., 2005), it was considered possible that TNC might negatively affect immunotherapies. Thus, the role of TNC in these tumours was further closely analysed, either alone or in combination with other components of the TME, such as immune cells and blood vessels.

Early studies on TNC deposition indicate a specific staining pattern consisting of parallel fibre forming bands, commonly found in the stroma surrounding invading tumour

fronts, and a more diffuse and interstitial pattern in poorly differentiated tumours (Iskaros *et al.*, 1997). Later studies revealed that the ECM is more rigid at the invasive front of the lesion (Acerbi et al., 2015). These observations are in line with the results described above for TNC deposition in the MCA-induced fibrosarcomas, where tumours with high levels of TNC expression have different deposition patterns, depending on whether the TNC is at the periphery or in the core of the tumour.

Previous studies show TNC expressed close to blood vessels and, therefore, associated with angiogenesis (Lange *et al.*, 2007, Midwood et al., 2011, Saupe *et al.*, 2013). Rupp and colleagues revealed that TNC induces both pro- and anti-angiogenic activities, which results in the formation of a denser but less functional vessel network. This study shows no clear association between TNC and CD31 expression, since blood vessels are present in areas with and without TNC. However, further studies are needed to dissect blood vessel integrity and function in TNC rich and poor areas of the tumour.

The expression pattern of matrix proteins across groups highlights the inverse correlation between ECM proteins and T cell infiltration, since tumours with higher expression levels of TNC, Lum and Col3a1 (non-responders) have lower numbers of $CD4^+$ and $CD8^+$ T cells, and responding tumours, which have almost no expression of ECM proteins, usually contain 2 to 3 times more T cells. The Manhattan distance metric, used to rank genes according to how similar or opposing/inverse their expression pattern was against *Tnc*, revealed that genes involved in immune pathways, such as *Zap70*, a mediator of TCR signalling, had the furthest distance from *Tnc*, supporting the inverse correlation between ECM proteins and T cell infiltration. This suggests that a richer ECM might exclude T cells or trap them in between the fibres, preventing an effective intratumoural immune response, whilst in responders, T cells can enter freely in the tumour stroma, where they may kill tumour cells more efficiently. Whilst not significant, a comparison of T cells in TNC high and low areas indicated a slightly higher number of T cells in TNC high areas compared to TNC low areas.

Also, as part of a collaboration with the group of Matt Smalley (European Cancer Stem Cell Research Institute), the distribution of TNC and T cells was assessed in breast cancers developing spontaneously in mice with conditional deletions in *Brca2* and *p53* genes in mammary epithelial cells (Hay *et al.*, 2009). Excised tumours were stained for CD3, Foxp3 and TNC. Images in Figure 3.20 show that T cells (purple) are mainly on the outer side of the tumour nests (delineated by a green dashed line) where TNC is located, corroborating the idea that TNC might be a barrier to tumour infiltrating T cells.

The few T cells that are found inside the tumour nests, marked with red arrows, were mainly found within TNC fibres, in line with the results described in this Chapter. These data are also in line with a previous study indicating that immune cells can infiltrate tumours with rich matrices, but those matrices prevent direct contact between immune and tumour cells, establishing the importance of the T cell location in the tumour for an efficient antitumoral effect to be achieved (Salmon et al., 2012). Also, the organization of the matrix fibres (spacing and orientation) was shown to limit T cell movement in the stroma (Salmon et al., 2012, Salmon and Donnadieu, 2012).

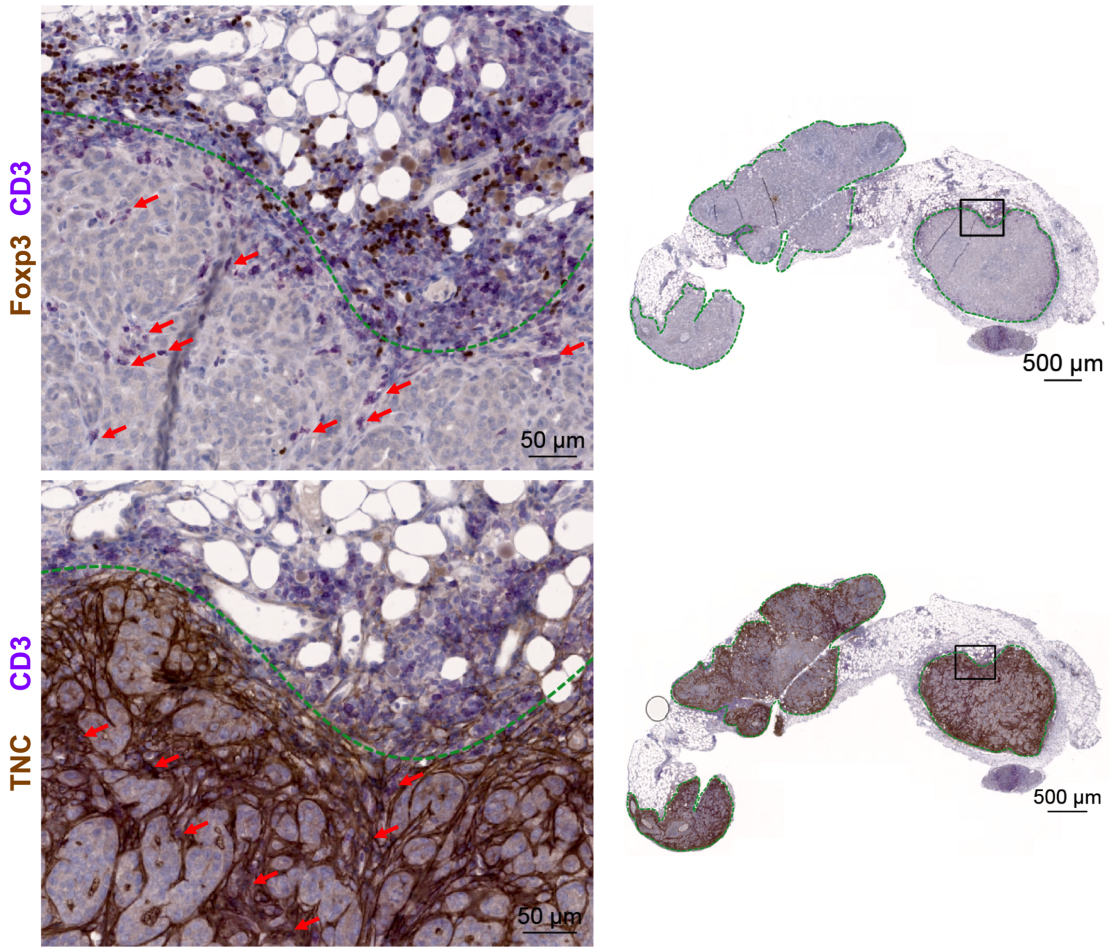

Figure 3.20|T cell infiltration in spontaneous mammary tumours.
Representative high-power images with corresponding low power image of whole tumour stained for Foxp3 (brown) and CD3 (purple) on the top panel, and TNC (brown) and CD3 (purple) expression in spontaneous mammary tumours from conditionally deleted Brca2 and p53 within the mammary epithelium. Green dashed line represents tumour nests delimitation. Red arrows represent T cell infiltration in the tumour nest.

In addition to the physical characteristics of matrix, TNC has been shown to modulate the production of inflammatory cytokines, affecting T cell recruitment. TNC is an activator of TLR4 (Zuliani-Alvarez et al., 2017), which stimulates a pro-inflammatory phenotype, recruiting fibroblasts and macrophages. Recruitment of these cells is thought to drive a self-amplifying loop resulting in a thicker matrix and sustained TAM and CAF recruitment. Furthermore, CAFs secrete CCL2 and upregulate SMAD signalling, which increases the recruitment of pro-tumourigenic macrophages to the tumour stroma. Once there, these macrophages secrete TGF-β, making the environment more immunosuppressive (Lowy and Oskarsson, 2015, Acerbi et al., 2015, Seager et al., 2017, Wehrhan *et al.*, 2004).

Given the body of evidence indicating a negative effect of TNC on T cell activity, the distribution of T cells and TNC was assessed in non-responder tumours. Findings revealed that there were more $GZMB^{+}CD8^{+}$ cells in TNC high areas than in TNC low areas in non-responding tumours possibly pointing to a lack of degranulation of T cells in TNC rich areas. It has been shown *in vitro* that specific regions of TNC can inhibit T cell activation by downregulating specific genes in phospholipase C, the calcium protein kinase C, the Jak-Stat pathway and the nuclear factor of activated T cells (NFAT) pathways (Puente Navazo et al., 2001, Parekh et al., 2005). All these pathways are involved in T cell activation and degranulation, especially the calcium protein kinase, that is needed for MAPK/ERK activation and triggering degranulation (Berg *et al.*, 1998, Macian, 2005, Puente *et al.*, 2006, Kabanova *et al.*, 2018). This inhibition may occur through interactions between TNC and integrins on the T cell surface. Mirzaei and colleagues showed that TNC carried on exosomes released by brain tumour-initiating cells can interact with T cell integrin receptors α5β1 and αvβ6; an interaction which results in reduction of T cell proliferation, activation and cytokine production (Mirzaei et al., 2018).

Since it is likely that TNC exerts inhibitory effects on T cell response, this study sought to address whether TNC prevented a successful response to Treg-targeted immunotherapy. Staining of untreated tumours revealed that whilst most tumours were positive for TNC, there appeared to be a range of expression supporting the hypothesis that TNC low tumours may respond better to immunotherapy than TNC high tumours i.e. do initial levels of TNC in the TME predict a response to Treg depletion? To answer this question, an immuno-PET based strategy was attempted with the objective of generating a zirconium labelled anti-TNC antibody to detect regions of TNC expression *in vivo*. Such

an approach should enable identification of TNC-rich and TNC-low tumours pre and post Treg-depletion.

Immuno-PET has been widely used in preclinical studies, where monoclonal antibodies, usually used in therapy, are bound to a positron radionuclide to detect primary tumours and metastasis (van de Watering *et al.*, 2014). The use of a radionuclide gives clear advantages when compared to fluorodeoxyglucose (FDG), since it can characterize and quantify specific antigen expression, whilst FDG can only measure glucose metabolism (Natarajan *et al.*, 2012). Zirconium-89 has been considered one of the most promising radionuclides to be used in conjugation with antibodies, due to its long half-life (78.4 h) and its low translational energy of the emitted positron, contributing to higher resolution images (Nayak and Brechbiel, 2009).

For this study, an anti-TNC antibody was labelled with ^{89}Zr to generate a PET tracer to track TNC protein content in tumours of untreated, non-responders and responder mice. Visual observation of the normalised PET images showed no difference between pre-Treg depletion tumours of non-responders and responders. Immunofluorescence stain of the excised tumours revealed that TNC was lost after Treg depletion in responders. However, signal quantification showed that mice injected with ^{89}Zr-anti-TNC had the same level of uptake as mice injected with negative control tracers, especially ^{89}Zr-anti-IgG. The enhanced permeability and retention (EPR) effect, which is the mechanism by which high molecular-weight molecules accumulate in tissues with increased vascular permeability, such as site of inflammation and tumours (Matsumura and Maeda, 1986), may explain this observation. The fact that activity uptake is constant in tumours over time is also a good indicator of this effect. Various studies conducted to assess this effect in more detail revealed that molecules > 48 kDa are prone to tumour-selected retention (Maeda *et al.*, 2016). Since the molecular weights of the antibodies used for ^{89}Zr labelling were around 241 kDa around 150 kDa for anti-TNC-IgG and for control IgG (polyclonal antibody) respectively, it is very likely that these were retained in the tumour interstitium.

The EPR effect has been exploited for heightened therapeutic results over the years, with groups resorting to different techniques to increase the molecular weight of drugs to facilitate extravasation and retention in the tumour interstitium (Iyer *et al.*, 2006). However, since this was a study designed to track the protein content in a tumour, the EPR effect was not desirable. The use of lower molecular weight molecules, such as single domain antibodies and small proteins based on FN domains (Wu, 2009), instead

of whole antibodies would be a possibility to overcome this limitation. In fact, a study conducted by Jacobson and colleagues successfully showed that a single-stranded DNA aptamer can be labelled and used to target TNC in tumours of mice by PET (Jacobson *et al.*, 2015). Improved approaches should therefore be considered for future studies as immune-PET is undoubtedly a potentially powerful technique for these types of studies.

Over the last decade, interference RNAs have been extensively explored as a tool for personalised cancer therapies, since they can naturally silence the expression of target genes (Rao *et al.*, 2009). This selective knockdown has the capacity of improving personalised therapies by knocking down aberrantly overexpressed molecular targets that are crucial for cancer progression (Rao et al., 2009). However, these molecules are also extensively used in scientific research, permitting the study of specific genes or proteins, and their roles in health and disease (Downward, 2004). In this study, TNC knockdown by shRNA was used to directly test the impact of the initial TNC content in response to therapy.

In order to achieve TNC knockdown in the tumour site, it was necessary to establish cell lines derived from MCA-induced tumours. Growth rates showed that tumours derived from cell lines behaved similarly to MCA-induced tumours, with the difference that cell line induced tumours all respond to Treg depletion. It has been reported that tumours derived from cells in culture develop faster, lacking the architectural and cellular complexity that characterise *in situ* tumours (Becher and Holland, 2006). The lack of HEVs in all these tumours, even the ones that respond to Treg depletion, supports the lack of complexity of cell line induced tumours when compared to *in situ* tumours.

Results obtained after tumour induction with a shTNC and a shScr cell line showed that lack of TNC does not affect tumour growth rate. This phenomenon was already reported by Talts and colleagues, who observed no differences in growth rate or number of proliferating and apoptotic cells in TNC-null mice when compared to wild type or heterozygous genotype for TNC (Talts *et al.*, 1999). The use of GFP as a selection marker could have enhanced the immunogenicity of these tumours. However, Skelton and colleagues have demonstrated that this protein is not immunogenic in C57BL/6 mice (Skelton *et al.*, 2001), supporting observations described here, where tumours grew at a similar rate as *in situ* tumours, suggesting that the presence of this protein did not affect the anti-tumour immune response. The lack of TNC in shTNC tumours indicates that tumour cells are the main source of TNC. It was also noticeable that TNC was no longer

detectable in the same extent in shScr tumour stroma after Treg depletion, indicating that TNC expression before Treg depletion does not predict response to treatment, but loss of this protein is a consequence of a successful immune response.

Overall, the data described above indicate that whilst TNC can inhibit T cell responses, this effect can be overcome, since it does not always prevent a successful immunotherapeutic response. However, it is still possible that clearance of TNC is crucial for immunotherapy to be successful. This hypothesis is further supported by the observation that rejection of TNC-expressing cell lines after Treg-depletion was also associated with loss of TNC. One intriguing possibility is that activated tumour-infiltrating T cells can degrade ECM proteins themselves. In support of this hypothesis, Ahrends and colleagues showed that a key feature of T cell help to cytotoxic T cells is to increase their expression of MMPs thereby endowing them with the ability to digest and invade tumour tissue (Ahrends *et al.*, 2017). Similarly, a study by Putz *et al*. demonstrated that heparanase production by NK cells contributes to control of tumour growth in mice, including MCA-induced fibrosarcomas, due to degradation of the ECM and improved immune anti-tumour response (Ahrends et al., 2017, Putz *et al.*, 2017). However, the detection of mRNA TNC transcripts by RNAscope revealed that tumours no longer express TNC when subjected to a robust anti-tumour immune response. Since this is an effect observed at later timepoints, the observation does not exclude the possibility that proteolytic enzymes produced by T cells and/or NK cells contribute to the degradation of TNC in early stages, after Treg depletion (Figure 3.21). Further studies are needed to address this question.

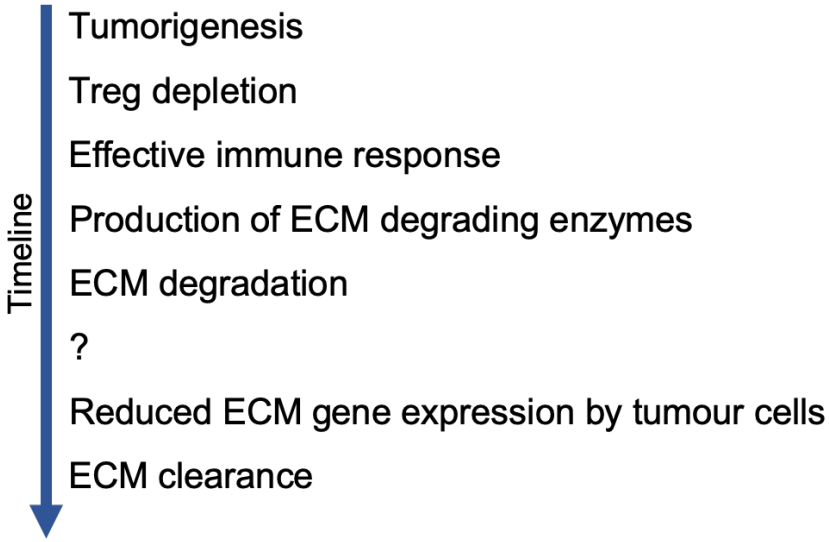

Figure 3.21| Proposed mechanism for ECM clearance in responders TME.
Question mark represents an unknown step between early ECM degradation and loss of ECM production by tumour cells at a later stage.

Lastly, a closer observation of these samples allowed identification of larger cells, with large nuclei and scarce cytoplasm as the source of TNC. These characteristics, are coincident with the morphology of tumour cells where large nuclei are present due to high proliferation rates (Zink *et al.*, 2004). Together with the data described in section 3.7.2. in which tumours forming after inoculation of shTNC cell line all lacked TNC, gives strongly indicates that tumour cells are the source of TNC in this model. Moreover, tumour cells have been proven to be a source of TNC in many types of cancer, such as breast cancer and glioblastoma (Oskarsson et al., 2011, Thakur and Mishra, 2016). However, it is clear that for some cancers, stromal cells also produce TNC and for this reason, TNC is often considered as a marker for CAFs (Ni *et al.*, 2017, Yang *et al.*, 2017). Thus, the possible contribution of these cells to the TNC content in the tumour stroma should not be ignored.

Overall, the results described in this chapter demonstrate that there is a difference in the composition of the TME of responders (Figure 3.22-C) and non-responder tumours (Figure 3.22-D) to immunotherapy, specifically pointing to a loss of matrix proteins as a marker of a successful anti-tumour immune response (Figure 3.22). This loss of ECM is mainly due to lack of gene expression by tumour cells during the process of rejection, but it may be initiated by degradation of the initial ECM present in the tumour at an earlier stage of the immune response (Figure 3.22-B). These data are similar to those obtained in human cancers, when RNAseq datasets from primary tumours in The Cancer Genome Atlas (TCGA) were analysed in order to determine whether there was a link between favourable CTL gene signature and TNC expression. This analysis revealed that whilst *TNC* expression had no impact on survival within CTL low tumours, low *TNC* expression was associated with a highly significant increase in survival within CTL high tumours (See Appendix, “Analysis of RNAseq datasets from primary tumours in TCGA” section).

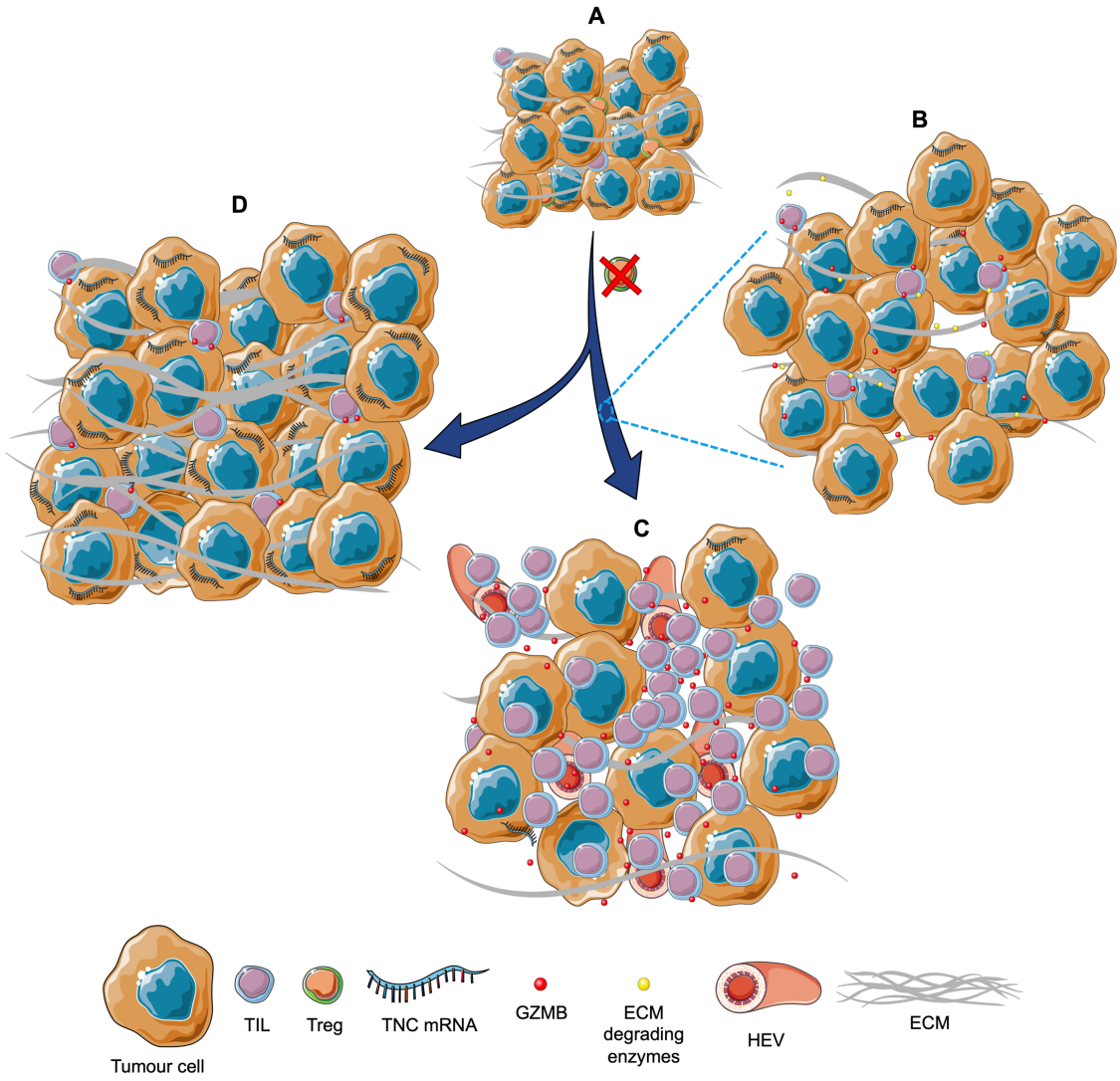

Figure 3.22|Schematic representation of response to Treg depletion in murine fibrosarcomas.
When a tumour arises due to carcinogen induction (**A**), once Tregs are depleted it can follow two paths: become a responder (**B**, with a hypothetical intermediate stage **C**) or a non-responder (**D**). The image represents all the alterations in the tumour microenvironment described in this Chapter, including changes in ECM content and TIL activity.

Given that ECM is known to affect the genotype, phenotype and function of several TME components, the study described in the next chapter explored the hypothesis that alterations to the tumour matrix is indicative of widescale remodelling of the TME.

Chapter 4

Exploring the Properties of the TME in Treg-Depleted Responder and Non-Responder Tumours

4.1. Introduction

There is accumulating evidence pointing to the importance of ECM in the TME for tumour progression. Uncontrolled proliferation in growing tumours promotes tissue stiffness due to accumulation of structural components, such as tumour and stromal cells and ECM. Tumour stiffening due to accumulation of ECM proteins results in fluid and solid stress in the TME (Walker et al., 2018), which can affect the tumour vasculature, as well as intrinsic properties of the cancer cells.

Solid stress created by the non-fluid components of the TME, compresses blood and lymphatic vessels during tumour formation, which creates fluid stress on the surrounding epithelial tissue. This decreases perfusion rates in the tissue, limiting the ability of lymphatic vessels to remove excess fluid from the tumour (Sabine et al., 2016). Compression of blood and lymphatic vessels induced by solid stress creates a hypoxic environment, which is highly associated with tumour progression (Walker et al., 2018). This solid stress can also induce CAF contraction, increasing TGF-β and ECM protein secretion by these cells. Whilst TGF-β secretion promotes an immunosuppressive environment, ECM protein secretion, as well as ECM remodelling proteins (e.g. MMPs and lysyl oxidase), increases matrix stiffness and realignment, promoting directional migration of CAF. These migratory CAFs use proteases to lead collective tumour cell invasion (Swartz and Lund, 2012).

Cancer cells sense matrix stiffness through integrin clusters at the cell surface and focal adhesions via a process known as mechanotransduction. Mechanotranduction therefore describes the process by which signalling events, which regulate the levels and activity of distinct transcription factors, are transmitted between the ECM and the interacting cells (Chin *et al.*, 2016). Key examples are Snail, ZEB and Twist; transcription factors that regulate EMT, promoting cancer cell plasticity, triggering tumour initiating and metastatic spread (Puisieux *et al.*, 2014). In addition, the same transcription factors regulate programmes affecting cell stemness and fate (Nieto and Cano, 2012). The Hippo pathway is also known to be activated due to ECM stiffness. Increased stiffness upregulates Yes-associated protein (YAP) and transcriptional coactivator with PDZ-binding motif (TAZ) and their translocation to the nucleus. Once there, they promote the expression of genes associated with proliferation and tissue remodelling, such as *ICAM* and *VCAM (Broders-Bondon et al., 2018)*. This process can lead to the accumulation in the TME of aggressive mesenchymal-like tumour cells, with increased motility and

invasive properties as well as stem-like tumour cells, with the capacity to repopulate new tissues (Cox and Erler, 2011, Lu et al., 2011, Northey et al., 2017).

The ECM has, therefore, a fundamental role in driving tumour progression. This is supported by the data presented in Chapter 3 which shows that ECM proteins are associated with tumour growth and a lack of response to Treg depletion. Moreover, the study showed that loss of ECM proteins, especially TNC, occurs as a result of an effective anti-tumour response. Due to the structural influence that ECM proteins have in the TME, the study described in this Chapter tests the hypothesis that the ECM is associated with widescale changes to the TME including changes to the lymphatic vasculature, to the intrinsic properties of the cancer cells, and in invasion of other tissues.

4.2. Results

4.2.1. The Lymphatic Network in ECM-Rich and ECM-Poor Tumours

Since dense tumour matrix is known to affect intratumoural interstitial flow, the lymphatic networks in Treg-depleted responder and non-responder tumours were compared. Specific antibodies for LYVE-1 (green) were used to stain lymphatic vessels, and the results, shown in Figure 4.1, indicate striking difference in the appearance of lymphatic vessels across groups, as responder tumours present a more extensive and well-organised lymphatic network than untreated and non-responder tumours.

Dendritic cells deliver tumour antigens to local lymph nodes via afferent lymphatic vessels in a CCL21-dependent manner. Well-functioning lymphatics are likely therefore to contribute to the efficiency with which tumour antigen-specific T cells are primed. (Russo *et al.*, 2016). Sections were then co-stained for CCL21 (red) and LYVE-1, and results show CCL21 staining in close proximity to LYVE-1 positive lymphatic vessels in responder tumours, but not in non-responder or untreated tumours (Figure 4.1). This indicates the possibility that these vessels guide tumour egress of dendritic cells, contributing to priming of antigen-specific T cells in draining lymph nodes.

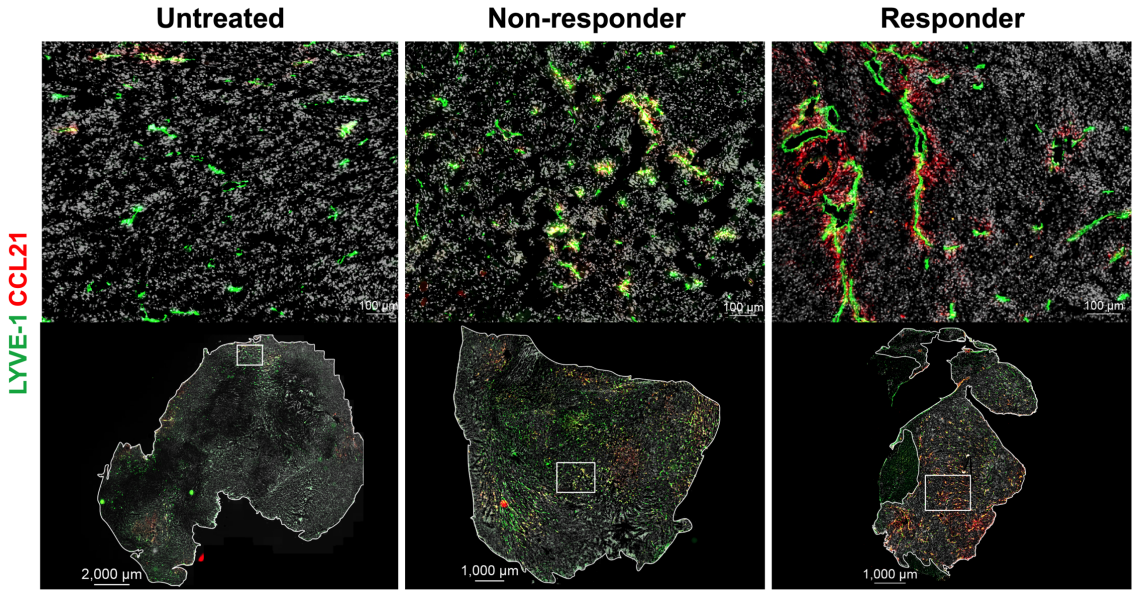

Figure 4.1|Responder tumours exhibit improved lymphatic vessels, with expression of CCL21.

Representative high-power images with corresponding low power image of whole tumour stained for LYVE-1 (green) and CCL21 (red) expression in tumours of Untreated ($Treg^{+}$), Non-Responder ($Treg^{-}HEV^{-}$), and Responder ($Treg^{-}HEV^{+}$) $Foxp3^{DTR}$ animals. Images include the nuclear stain Hoechst (grey).

4.2.2. Properties of Cancer Cells In ECM-Rich and ECM-Poor Tumours

4.2.2.1. Cell proliferation

Tumour progression is characterised by a dynamic interaction between the microenvironment and resident cells, where tumour cell proliferation induces architectural changes in the ECM. These alterations include increased deposition of ECM proteins, which interfere with cell-cell adhesion and cell polarity, culminating with increased growth factor signalling (Walker et al., 2018). With this in mind, cell fate was compared in ECM-low responder tumours and ECM-high non-responder tumours.

Cell proliferation was analysed by staining sections from untreated, non-responder and responder tumours for the cell proliferation marker, Ki67 (Figure 4.2). These data indicate that there is no striking difference when comparing Ki67 expression between the different groups, however, slightly fewer positive cells were observed in responder tumours (Figure 4.2-A). Enumeration of positive cells confirmed this trend with responders having a lower percentage of $Ki67^+$ cells than non-responders, whilst a larger range was observed in untreated tumours (Figure 4.2-B). To investigate a possible relationship between ECM proteins and cell proliferation, TNC was co-stained with Ki67 on the same samples. Within the same tumour, areas with high expression of TNC contained more $Ki67^+$ cells than TNC low areas (Figure 4.2-C), implying an association between Ki67 and TNC expression. Further studies are needed to investigate whether Ki67 positive cells are tumour or immune cells, and whether the identity of the cells is the same across the different tumour types.

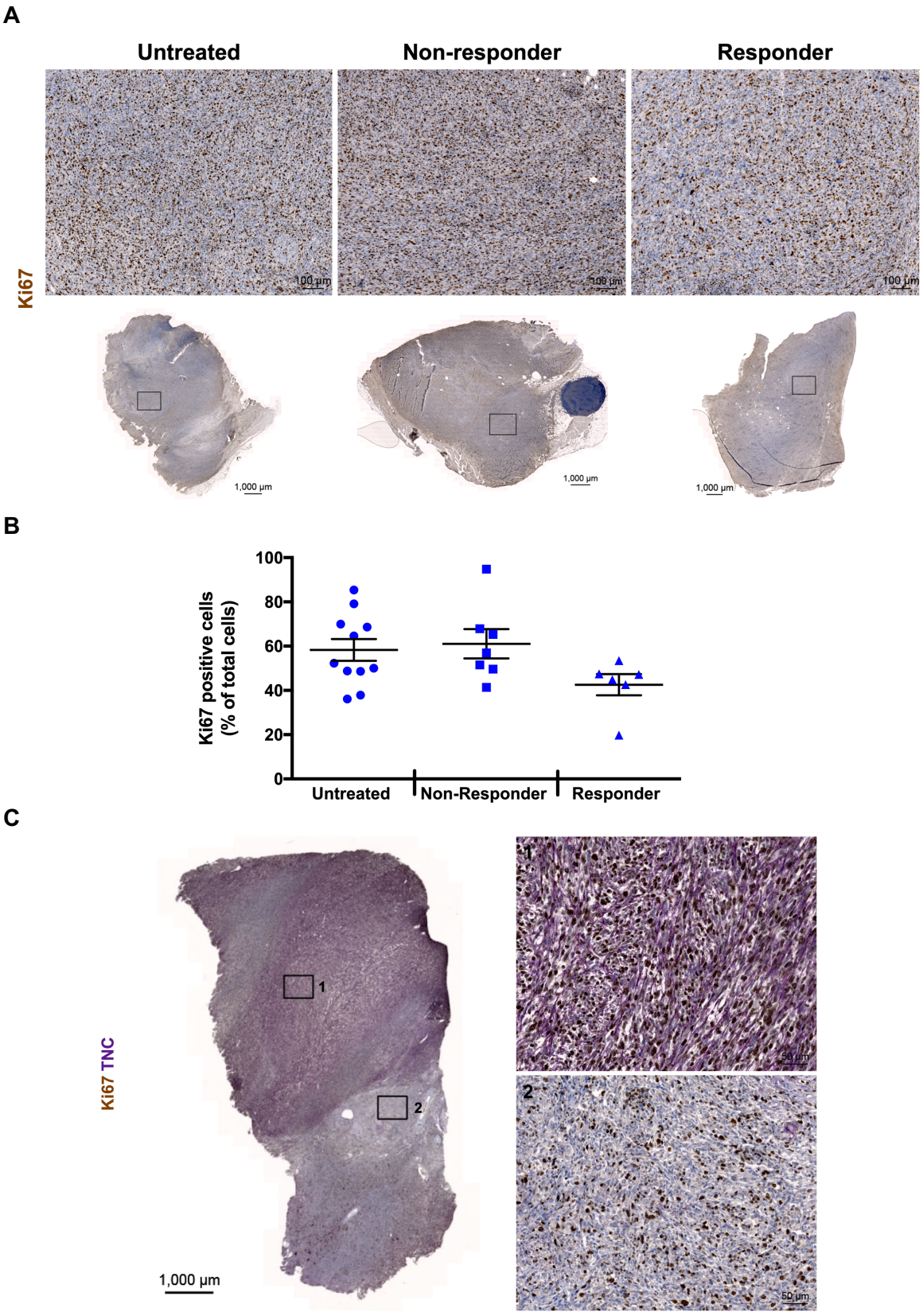

Figure 4.2| Ki67 and TNC expression in the TME.

A, Representative high-power images with corresponding low power image of whole tumour stained for Ki67 (brown) expression in tumours of Untreated (Treg+), Non-Responder (Treg^{-}HEV^{-}

), and Responder ($Treg^{-}HEV^{+}$) $Foxp3^{DTR}$ animals. Images include haematoxylin counterstain (blue). **B**, Percentage of $Ki67^{+}$ cells in tumours of Untreated (Treg+), Non-Responder ($Treg^{-}HEV^{-}$), and Responder ($Treg^{-}HEV^{+}$) $Foxp3^{DTR}$ animals. Data are presented as individual data points (individual mice) plus mean and standard error of the mean (no statistical significance was observed, Kruskal-Wallis test). **C**, Representative low power image (left) of TNC (purple) and $Ki67^{+}$ cells (brown) with magnifications of a TNC high area (top right) and TNC low (bottom right). Images include haematoxylin counterstain (blue).

4.2.2.2. Cell death

Tumour cell death was analysed in sections from untreated tumours, non-responders, and responders by staining for Caspase 3 (Casp3) expression (Figure 4.3). In all groups little Casp3 expression was observed (Figure 4.3-A), with fewer Casp3 cells observed in responders when compared to other groups (Figure 4.3-B). Co-staining with anti-TNC antibody indicated no association between Casp3 and TNC expression (Figure 4.3-C).

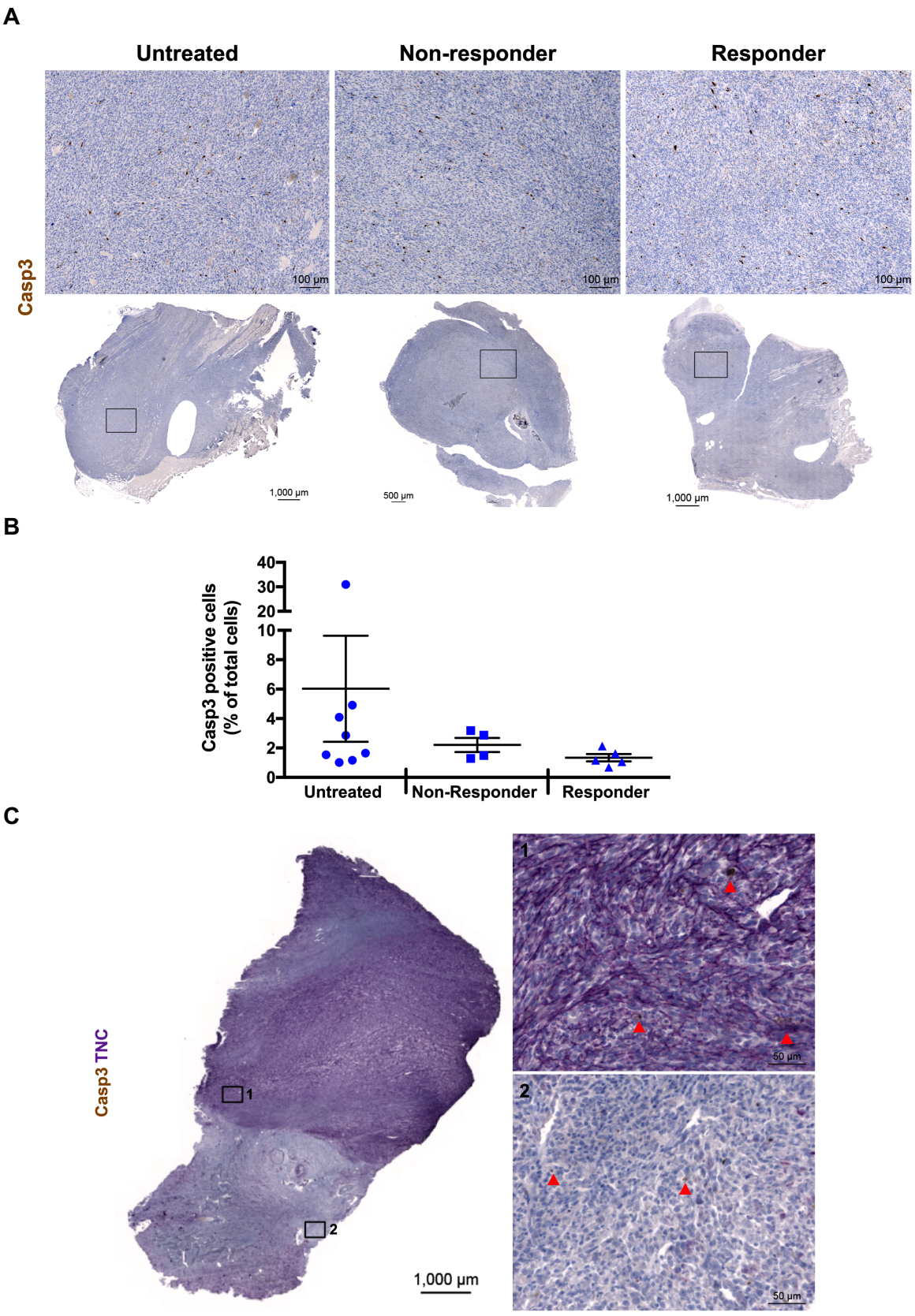

Figure 4.3| Cell death in untreated, non-responder and responder tumours.

A, Representative high-power images with corresponding low power image of whole tumour stained for Casp3 (brown) expression in tumours of Untreated (Treg+), Non-Responder (Treg-

HEV$^-$), and Responder (Treg$^-$HEV$^+$) Foxp3^{DTR} animals. Images include haematoxylin counterstain (blue). **B**, Percentage of Casp3$^+$ cells in tumours of Untreated (Treg+), Non-Responder (Treg$^-$ HEV$^-$), and Responder (Treg$^-$HEV$^+$) Foxp3^{DTR} animals. Data are presented as individual data points (individual mice) plus mean and standard error of the mean. **C**, Representative low power image (left) of TNC (purple) and Casp3$^+$ cells (brown, red arrowheads) with magnifications of a TNC high area (top right) and TNC low (bottom right). Images include haematoxylin counterstain (blue).

4.2.2.3. CSCs

As part of the bioinformatic analysis performed by Alexander Greenshields-Watson, the expression pattern of *Tnc* was mapped against all other genes in the microarray analysis using a Manhattan distance metric. Genes were ranked according to how similar or opposing/inverse their expression pattern was against *Tnc*. As mentioned in the previous Chapter (section 3.2.1), this analysis revealed that *Zap70* had the furthest distance (opposing expression pattern) from *Tnc*. In contrast, those with a similar pattern to *Tnc* included several cancer-associated (*Vegfa*, *Trib3*, *Uck2*) and stem cell/EMT genes (*Ttc3*, and *Twist2*) (Figure 3.2-E).

Given that dense ECM has been associated with the emergence of aggressive cancer cells with mesenchymal stem-like properties (Laklai et al., 2016, Northey et al., 2017) and that TNC has itself been reported as a potential marker for CSCs (He *et al.*, 2010, Pezzolo *et al.*, 2011, Nie *et al.*, 2015), these bioinformatic findings prompted an analysis of CSC-associated gene expression (Zhang *et al.*, 2015) in responders and non-responder tumour types. The data clearly indicate that CSC genes are over-represented in non-responder compared to responder tumours (Figure 4.4).

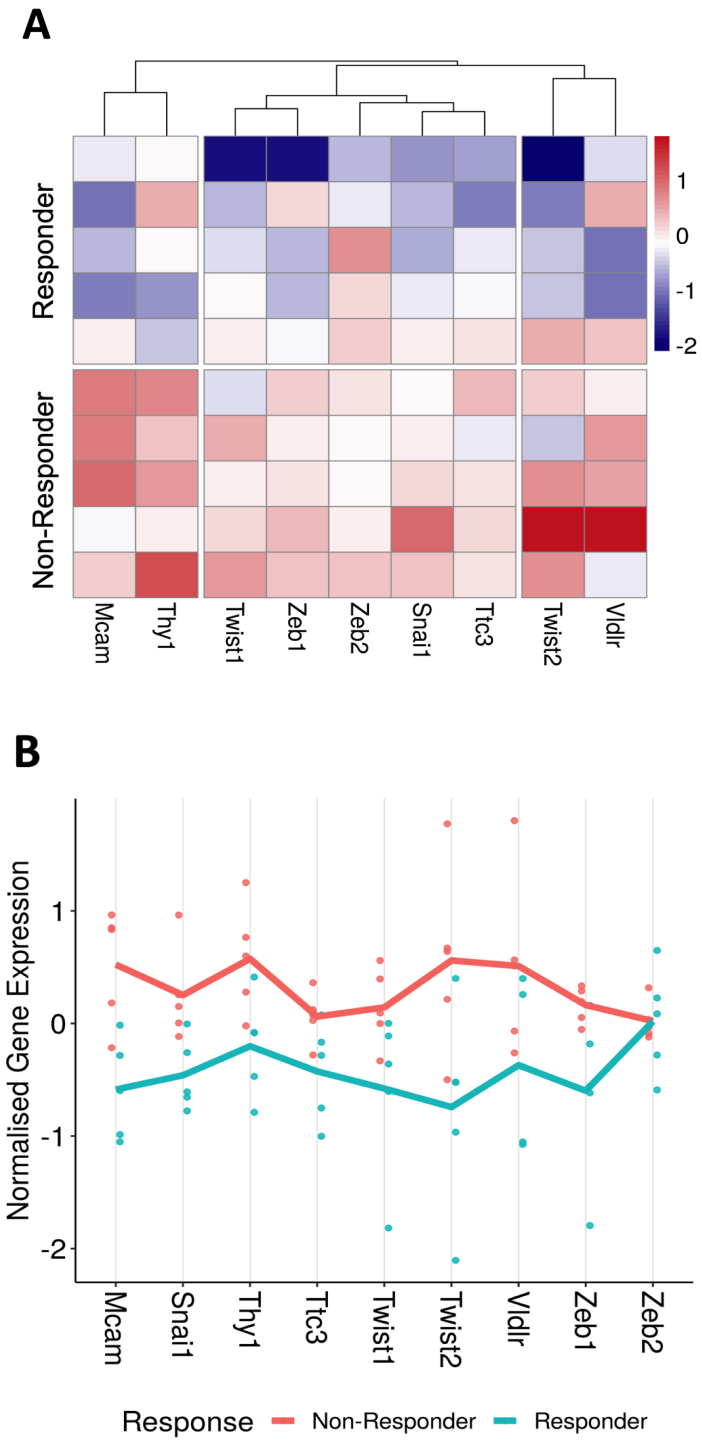

Figure 4.4| Non-responder tumours exhibited enhanced gene expression associated with cancer stem cells.

A, Gene expression of several genes associated with cancer stem cells in responding and non-responding tumours. **B**, Comparison of median normalised gene expression levels of CSC genes in responder (blue) and non-responder (red) tumours. Individual values are shown as points while the mean expression for each group is plotted by the connecting line.

As previously mentioned in section 1.2.1, CSCs are important in tumour progression. Their self-renewing and tumour initiating capacity is heavily supported by the ECM, which provides not only protection from immune attack, but is also a reservoir of important factors needed for CSC sustenance (Nallanthighal *et al.*, 2019). Therefore, to understand the role of CSCs in this model, and how they are affected by alterations in the ECM content after an effective response to immunotherapy, the expression of individual genes associated with stemness was compared in untreated, non-responder and responder tumours, using the transcriptome analysis data generated by a former member of the lab, James Hindley (Hindley et al., 2012). This analysis revealed a trend for lower expression of EMT related genes, including *Zeb1*, *Zeb2*, *Twist1* and *Twist2*, and significantly lower expression of *Snai1* in responder compared to non-responder tumours (Figure 4.5). Although not significant, *Snai1* expression was also lower in untreated tumours when compared to non-responders (Figure 4.5).

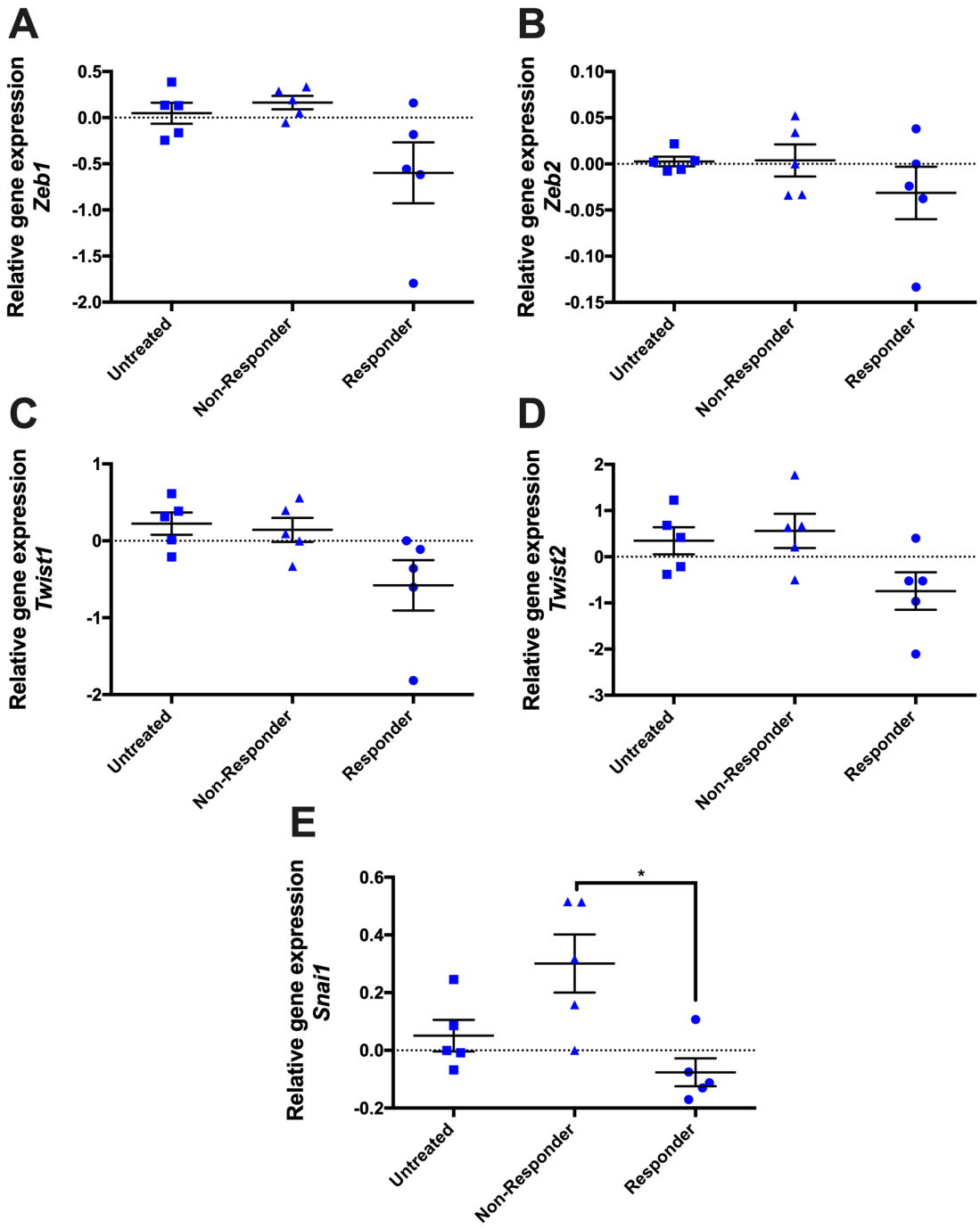

Figure 4.5|EMT markers associated with CSC phenotype are differentially expressed between tumour groups.

Relative gene expression of *Zeb1* (**A**), *Zeb2* (**B**), *Twist1* (**C**), *Twist2* (**D**) and *Snai1* (**E**) in tumours of Untreated (Treg+), Non-Responder ($Treg^{-}HEV^{-}$), and Responder ($Treg^{-}HEV^{+}$) $Foxp3^{DTR}$ animals. Data are presented as individual data points (individual mice) plus mean and standard error of the mean. *n*=5 per group. Statistical significance was determined by Kruskal-Wallis test (*, $P < 0.05$).

Untreated, non-responders and responder tumours were stained for Zeb1 expression. The data (Figure 4.6) clearly indicates a high level of Zeb1 expression in non-responders compared to a dramatic decrease in responder tumours. The increased intensity of Zeb1 stain in non-responders compared to untreated tumours, together with a lower *Snai1* expression in untreated tumours (Figure 4.5-E), suggests that EMT induced by these transcription factors is increased in non-responder tumours.

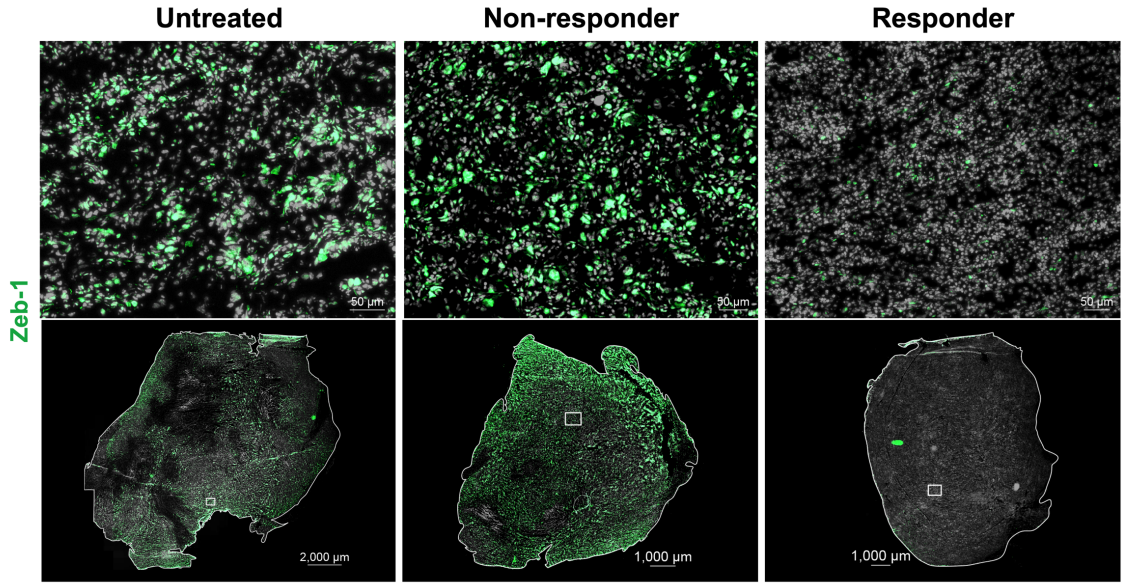

Figure 4.6| Zeb1 expression in untreated, non-responder and responder tumours.

Representative high-power images with corresponding low power image of whole tumour stained for Zeb-1 (green) expression in tumours of Untreated ($Treg^{+}$), Non-Responder ($Treg^{-}HEV^{-}$), and Responder ($Treg^{-}HEV^{+}$) $Foxp3^{DTR}$ animals. Images include the nuclear stain Hoechst (grey).

Even though a specific fibrosarcoma CSC marker has not been identified yet, studies have pointed to a set of surface antigens that may represent these cells (Augsburger *et al.*, 2017, Hatina *et al.*, 2019). The transcriptomic dataset was used again to compare the gene expression of CD24 (*Cd24a*), CD90 (*Thy1*), CD133 (*Prom1*) and CD146 (*Mcam*) in untreated, non-responders, and responder tumours (Figure 4.7). All cell surface markers, except *Prom1* (Figure 4.7-C), were expressed at a lower level in responder compared to non-responder tumours, with a significant difference observed for *Mcam* (Figure 4.7-D). Altogether, these findings suggest that a robust immune response can contribute to a genetic reprogramming of tumour cells. Although not significant, it is noteworthy that untreated tumours expressed less of the same three markers when compared to non-responders, suggesting that tumours that fail to respond to Treg depletion have an increase in CSC content.

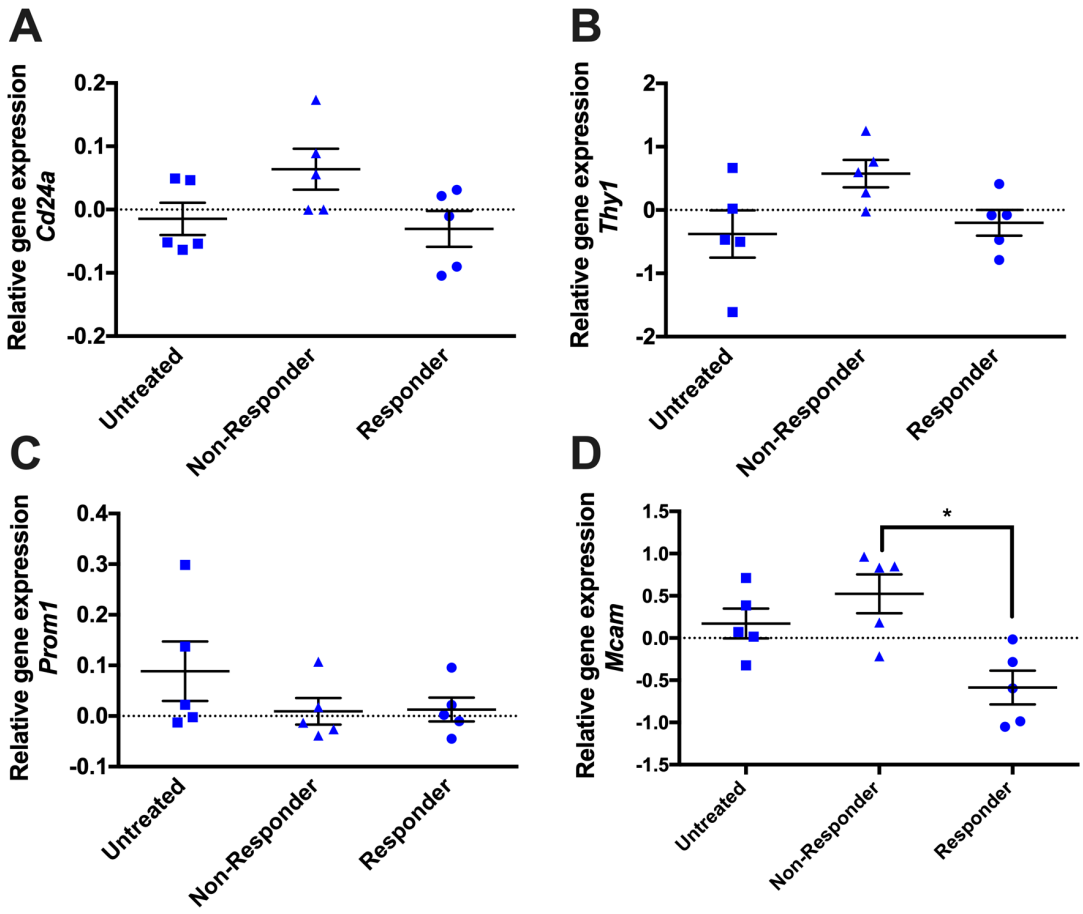

Figure 4.7| Fibrosarcoma associated CSC markers are differentially expressed between groups.

Relative gene expression of *Cd24a* (**A**), *Thy1* (**B**), *Prom1* (**C**) and *Mcam* (**D**) in tumours of Untreated (Treg+), Non-Responder ($Treg^{-}HEV^{-}$), and Responder ($Treg^{-}HEV^{+}$) $Foxp3^{DTR}$ animals. Data are presented as individual data points (individual mice) plus median and standard error of the mean. *n*=5 per group. Statistical significance was determined by Kruskal-Wallis test with Dunn's multiple comparison test.

Since a key feature of a CSC is the ability to self-renew, a tumoursphere formation assay was performed using single cells from untreated, non-responder and responder tumours. With this assay it is possible to determine the presence of cancer stem cells or progenitor cells, since only these type of cells are able to survive and proliferate in serum-free, non-adherent conditions (Johnson *et al.*, 2013). Briefly, after a single cell suspension from each type of tumour is obtained, cells are plated at a low density in the specific conditions mentioned above. Cultures are left undisturbed for 7 days, spheres are passaged and left undisturbed for another 7 days, when tumourspheres are counted. In the experiment described herein, tumourspheres bigger than 50μm were counted, and the results, shown in Figure 4.8, show that a good response to Treg depletion significantly reduces the capacity for tumoursphere formation (Figure 4.8-B), whilst a poor response to treatment induces formation of bigger spheres when compared to untreated tumour-derived spheres (Figure 4.8-A). This indicates not only that a successful immune response is associated with loss of cancer stemness, but also that failure to respond gives rise to more aggressive CSCs, with faster repopulating capacity.

A

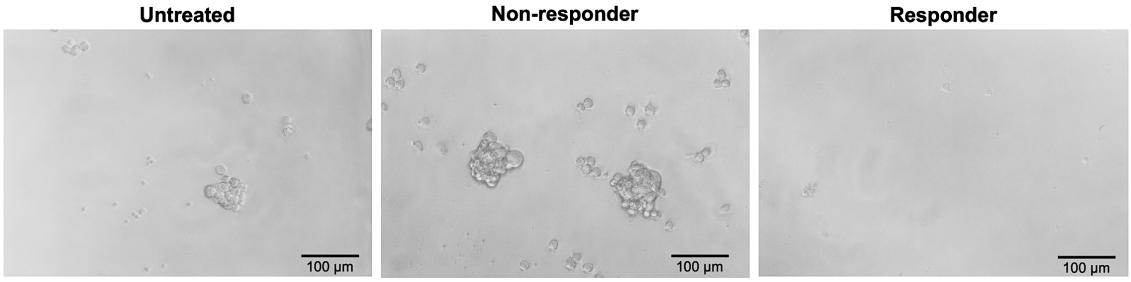

B

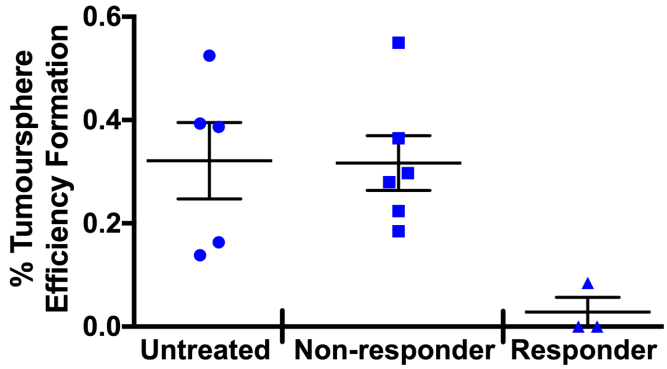

Figure 4.8|Cancer stem cells are affected by an effective response to Treg depletion.

A, Tumoursphere formation in cultures from tumours of Untreated ($Treg^{+}$), Non-Responder ($Treg^{-}HEV^{-}$), and Responder ($Treg^{-}HEV^{+}$) $Foxp3^{DTR}$ animals. **B,** Tumoursphere efficiency formation, per 10^4 cells seeded obtained from tumours of Untreated ($Treg^{+}$), Non-Responder ($Treg^{-}HEV^{-}$), and Responder ($Treg^{-}HEV^{+}$) $Foxp3^{DTR}$ animals. Data are presented as individual data points (individual mice) plus median and standard error of the mean. Statistical significance was determined by Mann-Whitney test.

4.2.3. Cell Invasion in Untreated, Non-Responder and Responder Mice

To investigate the metastatic capacity of tumours with CSCs, dLN and ndLN of untreated and non-responder tumour-bearing mice were collected, dissociated to single cell suspensions and left in culture. After 2 days in culture, cells with a flat and elongated morphology (fibroblast-like) were observed in some cultures (cells indicated in Figure 4.9-B by an arrow). For the purpose of comparing the presence of these cells in lymph nodes from untreated and non-responder mice, cultures with fibroblast-like cells were labelled “positive”, and the ones where these cells were absent were labelled “negative”. Positive cultures were generated from 100% of both lymph nodes in non-responder mice but only 66% of dLNs and 33% of ndLNs from untreated mice (Figure 4.9-A). Some of the positive cultures presented with proliferation rates that allowed for the establishment of cell lines, which are now cryopreserved and will be used in future experiments to confirm the potential cancer origin of these cells. Should this be the case, their potential invasive and metastatic capacity will be assessed. Since tumour cells from responder mice comprise significantly fewer CSCs, it is hypothesised that lymph node invasion will not be observed in these animals. This part of the study is ongoing.

A

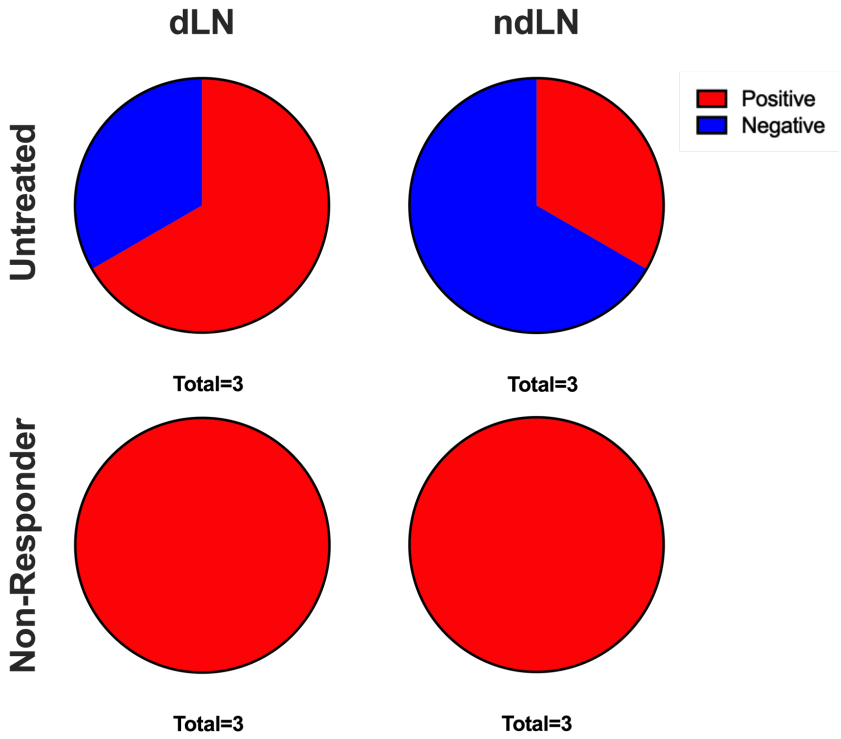

B

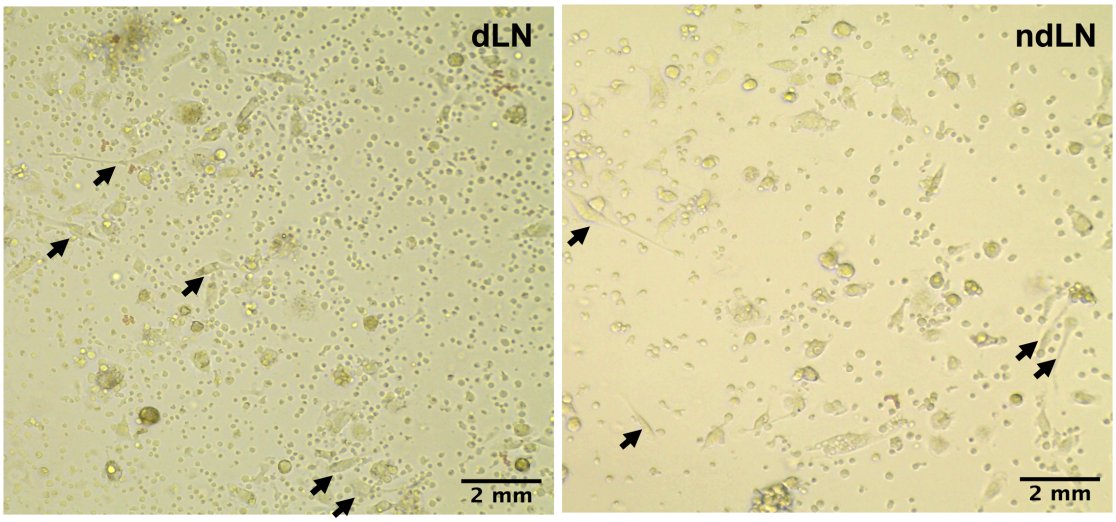

Figure 4.9|Fibroblast-like cells can be found in draining and non-draining lymph nodes of all non-responder mice.

A, Graphical representation of the proportion of lymph nodes derived from untreated and non-responder tumour-bearing mice, with (positive) and without (negative) fibroblast-like cells. **B,** Representative images of cultured dLN and ndLN derived from non-responding animals. Fibroblast-like cells (black arrows) can be found in both lymph nodes 2 days after culture.

4.2.4. Cellular Senescence in Untreated, Non-Responder and Responder Tumours

Several studies have shown that a Th1 immune response is capable of inducing senescence of cancer cells (Braumüller *et al.*, 2013, Hubackova *et al.*, 2016, Li *et al.*, 2017). This process is characterised by an irreversible loss of proliferation due to a persistent cell-cycle arrest and unresponsiveness to growth factors (Sun *et al.*, 2018). Regardless of the mechanisms inducing senescence, once a cell senses a critical level of damage or dysfunction the senescent program is activated. Apart from an arrest in proliferation, senescent cells are metabolically active and undergo extensive changes in gene expression, downregulating the expression of some genes and upregulating others. This new secretory phenotype is specific for senescent cells and is often referred to as senescence associated secretory phenotype (SASP) (Campisi and d'Adda di Fagagna, 2007, Gorgoulis *et al.*, 2019). Changes in gene expression can include insoluble proteins, particularly ECM proteins (Coppé *et al.*, 2010a). With this in mind, senescence was assessed as a possible mechanism for loss of expression of ECM genes in tumour cells.

One characteristic of senescent cells is the upregulation of lysosomal proteins and consequent increased lysosomal content, and one of the most common markers of this change is increased activity of senescence-associated β-galactosidase (SA-β-Gal) (Hernandez-Segura *et al.*, 2018, Gorgoulis et al., 2019). Therefore, primary cell lines from untreated, non-responder and responder tumours were established and SA-β-Gal activity assessed. Figure 4.10 indicates the striking difference in SA-β-Gal activity between groups; being highly upregulated in responders thereby pointing to a greater degree of senescence in these tumours.

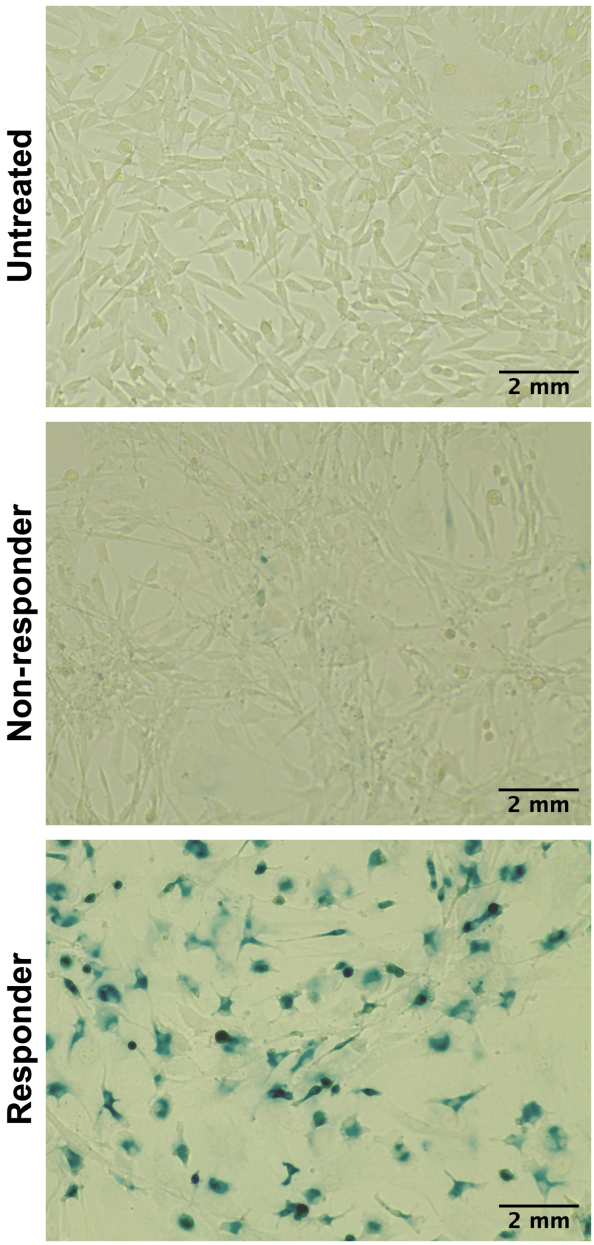

Figure 4.10|Cells derived from responding tumours to Treg depletion have high SA-β-Gal activity *in vitro*.

Representative images of cells in culture derived from untreated, non-responding and responding tumours to Treg depletion, stained for SA-β-Gal activity (blue).

Another hallmark of senescence is telomere shortening (Gorgoulis et al., 2019). Telomeres are specialised structures which protect the ends of chromosomes and which are themselves protected by a complex of proteins named shelterin. In the absence of shelterin, uncapped telomeres are recognised as damaged DNA and a DNA damage response (DDR) is induced. (d'Adda di Fagagna *et al.*, 2003, d'Adda di Fagagna *et al.*, 2004, de Lange, 2005). This response involves the activation of sensor kinases, formation of DNA damage foci containing phosphorylated histone H2AX (γH2AX), and induction of checkpoint proteins which promote cell-cycle arrest, widely associated with a senescent phenotype (d'Adda di Fagagna et al., 2003). To validate the results obtained from SA-β-Gal stain, immuno-FISH was performed in tumour sections from untreated, non-responders and responders to detect telomere associated foci (TAF). TAF can be identified by the overlap of telomere and γH2AX signals (Figure 4.11-A), Although not statistically significant (possibly reflecting reduced sample size), these data indicate a trend for more γH2AX positive cells in responder tumours (Figure 4.11-B), representing higher activation of DDR; and higher number of TAF (Figure 4.11-C), and, therefore, a higher percentage of senescent cells, when compared to untreated tumours. Most of the positive cells are those with the larger nuclei, further suggesting that the positive cells are indeed tumour cells. Further studies will be required to confirm this, as well as to increase in sample size. In addition, it will be important to determine whether cells identified as senescent no longer express ECM genes, such as TNC.

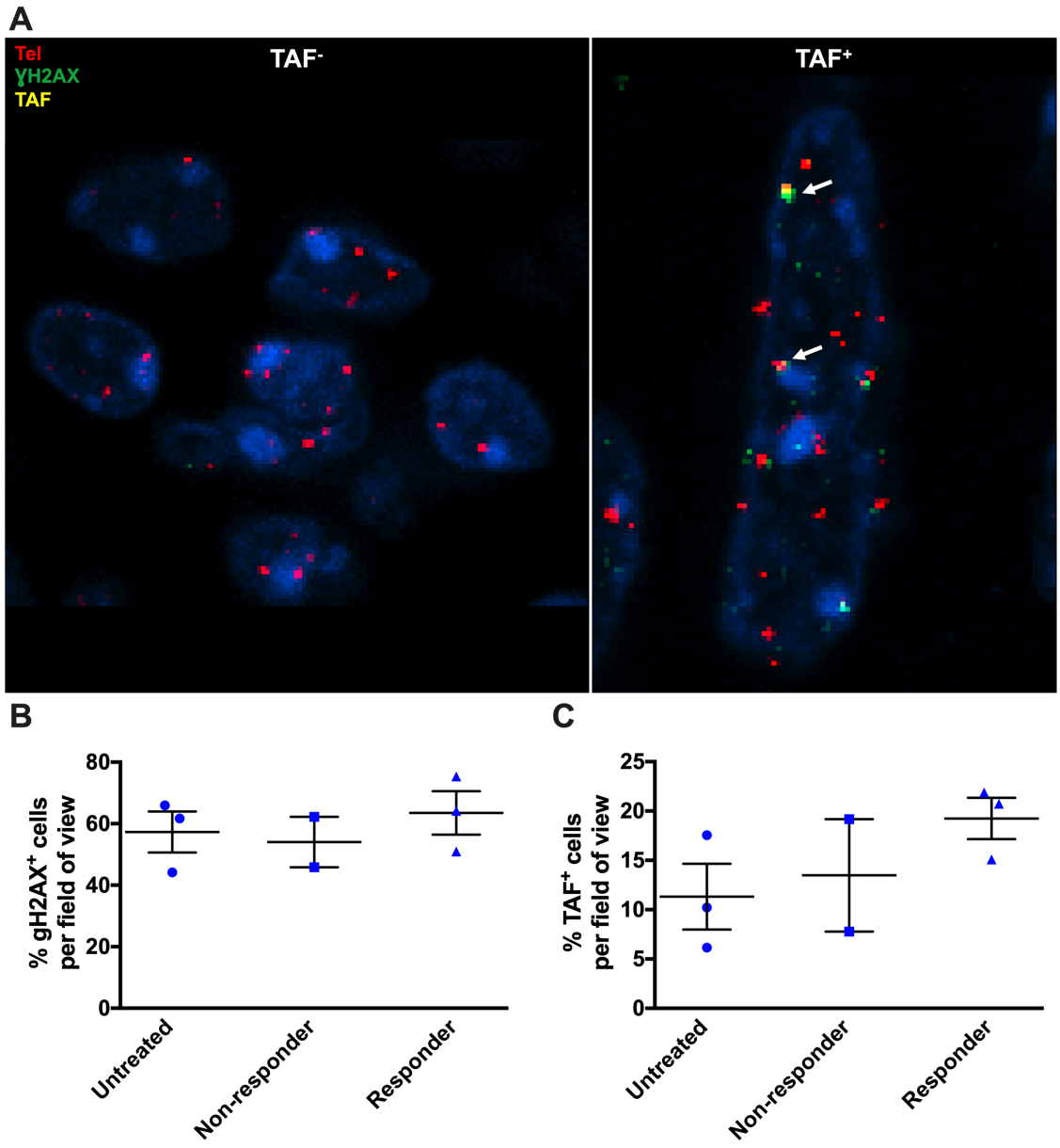

Figure 4.11| TAF$^+$ cells in untreated, non-responder and responder tumours.

A, Representative high-power images of cells negative and positive for TAF (white arrows, overlap (yellow) of γH2AX (green) and telomere (red) stain). Images include the nuclear stain Hoechst (blue). Percentage of γH2AX$^+$ (**B**) and TAF$^+$ (**C**) cells per field of view in tumour sections of Untreated (Treg+), Non-Responder (Treg$^-$HEV$^-$), and Responder (Treg$^-$HEV$^+$) Foxp3^{DTR} animals. Data are presented as individual data points (individual mice) plus median and standard error of the mean.

4.3. Discussion

The ECM is one of the most important regulators of tissue function in the body, and disturbance of its homeostasis can contribute to progression of several diseases, including cancer. There is a clear correlation between tumour density and poor prognosis, thus it is important to know how changes in the matrix affect tumour progression. With this in mind, the study described in this Chapter examined the association between loss of matrix proteins induced by an effective immune response and the genotype, phenotype and behaviour of the cancer cells.

Mechanical forces in the TME are proven as important for tumour progression, since solid and fluid stress influence angiogenesis and lymphangiogenesis. Analysis of lymphatic vessels in this study revealed a striking difference in their appearance in responders when compared to non-responders and untreated tumours. Lymphatics appear better organised, denser and surrounded by CCL21 in responder tumours when compared to untreated and non-responder tumours. Solid tumours comprise many different types of cells, including blood endothelial cells, smooth muscle cells, tumour cells and tumour associated stromal cells, all of which can secrete lymphangiogenic factors into the environment. However, since the mass of cells is disordered, there is no clear formation of a lymphangiogenic growth gradient, and the resultant lymphatic vessels are often described as patchy and randomly distributed within the TME (Li and Li, 2015). This is compatible with the observations of non-responder and untreated tumours in this study, where random staining is present without formation of clear individual vessels or networks.

The beneficial role of lymphatics in the TME is controversial in the literature. Many studies support the idea that lymphatic vessels promote tumour progression by enabling tumour cell dissemination via lymph (Ma *et al.*, 2018) and indirectly by promoting immunosuppression (Lund *et al.*, 2012, Steinskog *et al.*, 2016). Recent studies have shown that even though intra-tumoural lymphatic vessel density is associated with expression of immunosuppressive molecules, it is also associated with higher numbers of infiltrating $CD8^+$ T cells (Lund *et al.*, 2016, Bordry *et al.*, 2018). There is also evidence indicating that generation of tertiary lymphoid structures in tumours is associated with a positive response to immunotherapy using co-inhibitory receptor blockade (Johansson-Percival *et al.*, 2017, Allen et al., 2017). Hence, depending on the constitution of the TME, lymphatic vessels may either hamper or stimulate development of anti-tumour immune responses. Results presented in this Chapter are compatible with a scenario

whereby loss of ECM is associated with improved lymphatic function, which may both relieve intra-tumoural interstitial pressure and improve T cell responses. This can occur by increased migration of antigen-presenting $CCR7^+$ dendritic cells to draining lymph nodes for priming tumour-specific T cell responses (Russo et al., 2016), or by recruitment of naïve T cells into the TME through afferent lymphatics, guided by the CCL21-CCR7 axis (Ondondo *et al.*, 2014, Fankhauser *et al.*, 2017). As mentioned above, findings described in this Chapter open up the possibility that cancer cells from untreated and non-responder tumours invade draining lymph nodes. Given that lymphatic networks appear better developed in responder tumours, it is possible that these vessels serve as a conduit by which remaining malignant cells from responder tumours also invade the draining lymph nodes. This hypothesis is currently under investigation.

Since the ECM is such a critical component of the TME, having the power to control multiple hallmarks of cancer in tumour cells, the effect of a richer or poorer ECM in tumour cell proliferation was assessed. For this, TNC was used as a marker for a rich ECM, and Ki67 expression was analysed in all tumours. Although not significant, a trend for more $Ki67^+$ cells in non-responder tumours was observed, together with a higher coverage of positive staining in TNC high areas. This is corroborated by several studies showing that TNC induces tumour cell proliferation (Saupe et al., 2013). In 2006, it was suggested that TNC blocks the interaction between syndecan-4 and integrin $\alpha5\beta1$, inhibiting the tumour-suppressing activity of this integrin (Orend and Chiquet-Ehrismann, 2006). Lange and colleagues confirmed that the interaction of TNC with this coreceptor results in the inhibition of RhoA protein, FAK and tropomyocin-1 activity (Lange *et al.*, 2008). There is also evidence that TNC regulates mechanisms enabling escape from compliance with cell cycle checkpoints, promoting cell cycle progression from G1 phase to S phase by inhibiting Cyclin D1 (Orend and Chiquet-Ehrismann, 2006, Cai *et al.*, 2018). Nevertheless, the reason why there was no significant difference in the number of proliferating cells in this study might be explained with the lack of specific tumour cell markers, and many of the positive cells identified in the responder tumours may be immune cells and not tumour cells. This will be addressed in the future by enumerating and comparing $Ki67^+$ immune cells and $Ki67^+FAP^+$ cells between groups by immunofluorescence, taking into account that CAFs may also express FAP.

A possible correlation between lack of TNC in the TME and tumour cell death was also examined. Staining for the apoptotic marker Casp3 showed no difference between groups, with an overall percentage of positive cells not higher than 5%. Effective

clearance of dead cells from the TME by phagocytic cells, might however hamper assessment of cell death in tumours preventing any solid conclusions from being drawn.

The biomechanical signalling cues induced by accumulation of ECM proteins in the TME, including TNC, have been shown to result in alterations of tumour cell gene expression patterns, mainly affecting transcription factors associated to EMT (Chin et al., 2016). YAP and TAZ, which are the key transcriptional regulators in the Hippo pathway, are regulated by mechanical cues. Dupont and colleagues proved that this regulation requires stress fibres and skeletal tension induced by ECM stiffness and cell spreading (Dupont *et al.*, 2011). Although YAP is not a key direct regulator of EMT, it has been implicated in EMT induction. A study performed by Shao and colleagues revealed that KRAS and YAP1 have a similar mechanism, of action since they converge on the transcription factor FOS (Fos Proto-Oncogene, AP-1 Transcription Factor Subunit) and activate the transcriptional program involved in EMT (Shao *et al.*, 2014). In 2015, Wei and colleagues described the first molecular pathway directly linking matrix stiffness to EMT. They demonstrated that increasing matrix stiffness induces integrin-dependent phosphorylation events which promotes release of TWIST1 from its cytoplasmatic anchor, GTPase activating protein (SH3 domain) binding protein 2 (G3BP2). This leads to constitutive TWIST1 nuclear localisation, driving transcriptional events of EMT and invasion (Wei *et al.*, 2015).

Gene expression analysis of transcription factors associated with EMT in the present study revealed that they are mostly under-expressed in responders, when compared to non-responders and untreated tumours. The same transcription factors presented a similar expression between untreated and non-responder tumours, apart from *Snai1*, which was increased in non-responders. *Snai3* expression presents a different pattern; its expression is significantly increased in responders when compared to non-responders and untreated tumours. According to the literature, Snail3 usually behaves as a poor EMT-inducer and performs a different function to its two related transcription factor proteins, Snail1 and Snail2 (Gras *et al.*, 2014).

EMT in cancer is highly associated with the emergence of CSCs in the microenvironment, since stem cells have many characteristics of the mesenchymal cell state. Mani and colleagues demonstrated this phenomenon when, by inducing EMT in mammary epithelial cells, these cells formed mammospheres, which were self-renewable and capable of transmitting the EMT phenotype for many generations (Mani *et al.*, 2008). Taking this into account, the gene expression of cell surface markers

previously associated with fibrosarcoma CSCs (Augsburger et al., 2017, Hatina et al., 2019) was analysed. Three out of four markers, *Cd24a*, *Thy1* and *Mcam* but not *Prom1*, presented higher expression in non-responders comparing to responders, where expression levels were similar to untreated tumours, or lower. These results are indicative of genetic reprogramming of cancer cells in responder tumours which are associated with alterations in matrix composition and a good immune response. Since CSCs have the capacity to repopulate new tumours and possess unique mechanisms enabling escape from immunosurveillance, loss of CSCs in responder tumours most likely contributes to control of cancer progression. On the other side, the fact that the same three markers were under-expressed in untreated tumours compared to non-responders could suggest that these tumours contain more CSCs.

To assess the number of CSCs present in untreated, non-responder and responder tumours, a tumoursphere assay was performed. The specific composition of the sphere growth medium creates an environment for stem cell growth only, allied to the observation that only CSCs have the capacity to self-renew and survive through multiple passages (Dontu and Wicha, 2005). Using this assay, it was clear that responder tumours lose their stem cell content, since almost no spheres are formed. On the other hand, cells derived from non-responder tumours have the same capacity of forming spheres as untreated tumours, forming even larger spheres. This difference suggests that CSCs from non-responder tumours have higher proliferation rates, possibly being associated with a more aggressive phenotype. The association of higher numbers of CSCs in tumours with tumour proliferation and aggression is extensively described in the literature, especially in the case of brain and mammary tumours (Zhang *et al.*, 2016, Richichi *et al.*, 2016, Donnarumma *et al.*, 2017).

To investigate if the presence of CSCs in tumours from non-responders promoted a more aggressive phenotype, lymph nodes from untreated mice and non-responders were collected and left in culture. The presence of fibroblast-like cells in some lymph node cultures raised the possibility that these are cancer cells that have migrated from the tumour to the lymph node (further studies are underway to confirm this). If this is true, the observation that 100% of cultured dLNs and ndLNs from non-responders contained fibroblast-like cells, compared to just 66% of dLNs and 33% of ndLNs from untreated mice, suggests that non-responder tumours are more invasive. Moreover, the presence of tumour cells in ndLNs would suggest that non-responder tumours have an enhanced capacity to spread to distant organs (Figure 4.12). The MCA model has not been explored as a metastatic model despite its widespread use, since only two 40 year-old

studies mention the capacity of MCA tumours to metastasise – one in rats (Pimm *et al.*, 1980), and the other in which lung metastases were analysed 50 days after amputation of the mouse legs (Wexler and Rosenberg, 1979). Hence, the findings described herein might open up the possibility for further exploration of dissemination routes and how they may be controlled.

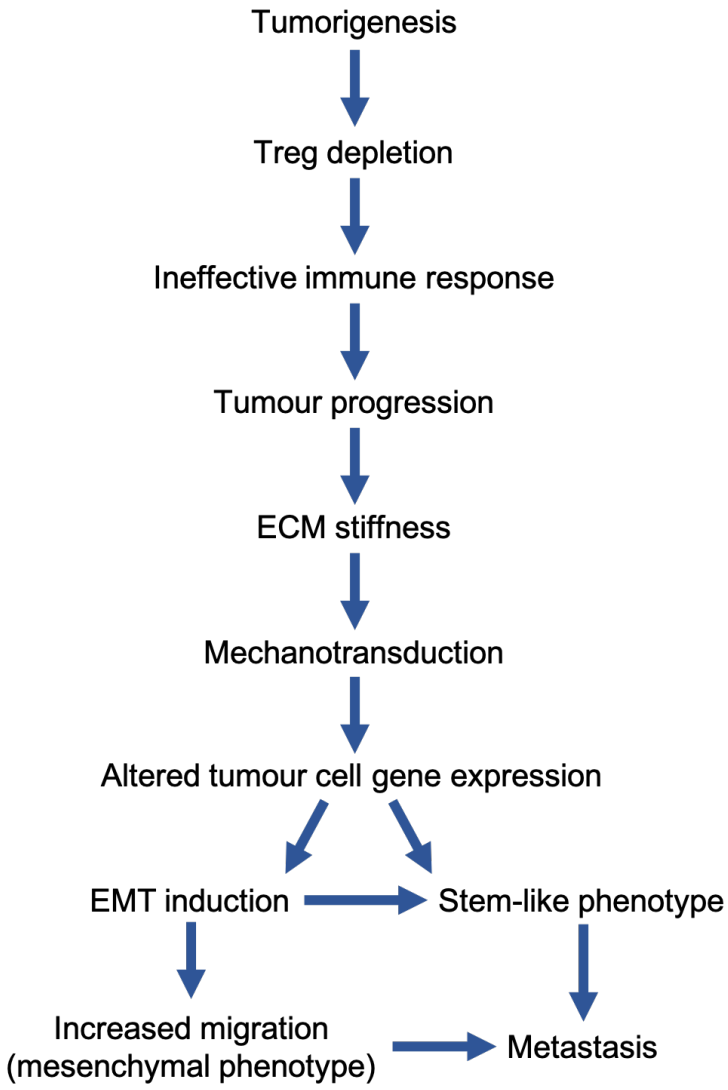

Figure 4.12| Events occurring in the TME of a non-responding tumour to Treg depletion.

Flow of events occurring in the TME after an initial ineffective immune response.

As previously mentioned, it has been shown that an effective Th1 response can induce cell senescence (Braumüller et al., 2013, Li et al., 2017). Components of the SASP released by senescent cells can include pro-inflammatory cytokines and chemokines, such as CCL5, which may increase the recruitment of TILs, promoting an anti-tumour immune response (Hubackova et al., 2016, Gorgoulis et al., 2019). By analysing the number of senescent cells in untreated, non-responder and responder tumours, it was possible to observe a trend for a larger number of senescent cells in tumours responding to Treg depletion, hence, senescent cells are associated with slower tumour growth and regression in the study described herein.

Results in the previous Chapter demonstrated that there is a downregulation of ECM related gene expression in tumours that respond to Treg depletion. Since senescent cells change their normal secretory phenotype to a senescence-associated one, including altering ECM protein expression, the emergence of senescent cells in these tumours might explain the downregulation of ECM protein expression in responder tumours. Whilst expression of some ECM proteins have been reported to be increased in senescent cells (Kumazaki *et al.*, 1991, Korybalska *et al.*, 2012), an association between senescence and loss of ECM has also been reported. A study conducted by Li and colleagues demonstrated that senescence induced by TNF-α in nucleus pulposus cells *in vitro* induces downregulation of aggrecan and collagen II expression by these cells (Li et al., 2017). Moreover, many reports point to the presence of matrix degrading enzymes as components of the SASP. MMPs (Coppé *et al.*, 2010b, Mavrogonatou *et al.*, 2019) and ADAMTSs (A disintegrin and metalloproteinase with thrombospondin motifs) (Le Maitre *et al.*, 2007, Dimozi *et al.*, 2015), can be expressed and released into the extracellular space via this mechanism. Furthermore, tissue inhibitors of MMPs (TIMPs) were shown to be downregulated in different types of senescent cells, particularly TIMP-1 in fibroblasts (Bizot-Foulon *et al.*, 1995), contributing to a shift in balance towards ECM catabolism. Hence, senescent cells may contribute to loss of ECM in responder tumours by two mechanisms: loss of ECM protein expression due to the extensive changes in gene expression patterns, and degradation of the existing matrix by releasing remodelling enzymes into the TME. The proposed mechanisms of ECM clearance in responder tumours, based on the findings of this study, are represented in Figure 4.13.

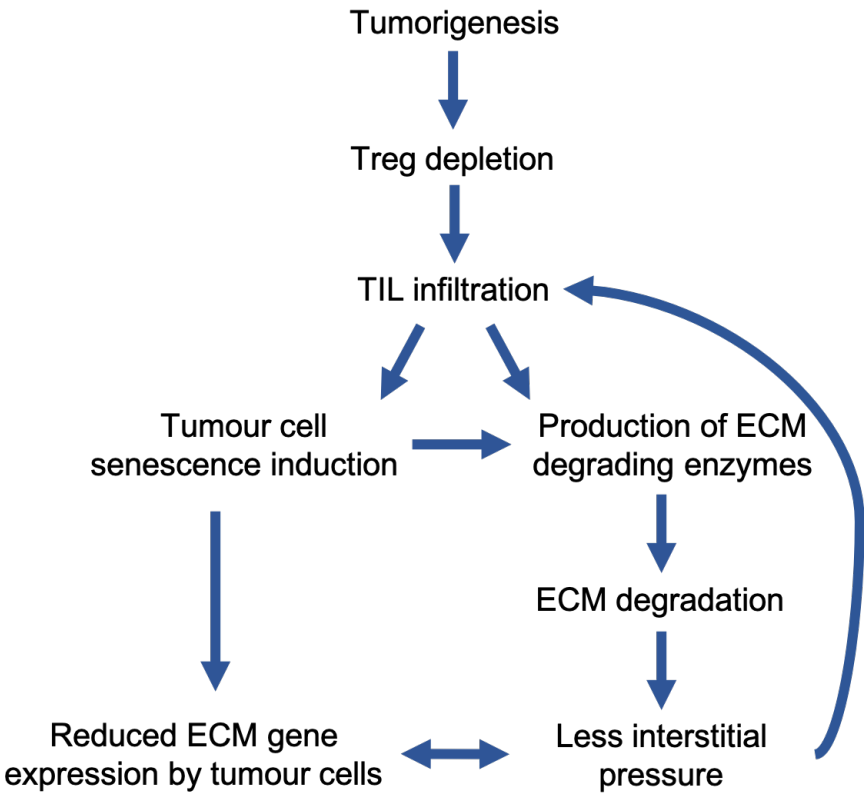

Figure 4.13|Proposed mechanism for anti-tumour response regulated by ECM clearance.

Flow of events occurring in the TME after an initial effective immune response.

It is important to note that senescent cells, although in lower numbers, were also present in non-responder tumours. In the absence of a robust immune response, it is possible that senescent cells are associated with cancer progression. The composition of the SASP in pre-senescent cells has been associated with activation of NOTCH and TGF-β signalling, which drives a shift into full senescence and paracrine senescence, either by cell-cell contacts to NOTCH receptor positive neighbouring cells, or through release of TGF-β-driven secreted growth factors. NOTCH-TGF-β activity promotes an immunosuppressive environment, permissive for tumour development (Lee and Schmitt, 2019). This process promotes accumulation of mutations in senescent cells, reprograming them towards a stem-like phenotype and enabling re-entry in the cell cycle (Milanovic *et al.*, 2018). Remodelling of the ECM by SASP-mediated mechanisms may, in this context, increase tumour cell motility, invasion and metastasis (Coppé et al., 2010a, Laberge *et al.*, 2012, Pazolli *et al.*, 2012, Cahu *et al.*, 2012, Laberge *et al.*, 2015).

In conclusion, the results in this chapter support a model whereby matrix remodelling contributes to either tumour elimination (Figure 4.14-B) or tumour progression (Figure 4.14-C). On the one hand, loss of ECM gives may result in the formation of a more functional lymphatic network, facilitating T cell priming in the draining lymph node. Enhanced T cell activation may then drive intratumoural HEV development and increased frequency of TILs. It is reasonable to hypothesise that the resulting immune response would drive tumour cell senescence and, through production of matrix remodelling enzymes, degradation of the ECM. These processes would serve to establish a self-amplifying loop driving both tumour destruction and tumour immunity. In addition, loss of ECM may drive cancer cell intrinsic changes facilitating loss of cancer stem cells. On the other hand, an increase of matrix stiffness due to an inadequate immune response at an initial stage of tumour progression, may promote activation of mechanotransduction pathways that support EMT and accumulation of cancer stem cells, possibly promoting aggression and invasion (Figure 4.14-D).

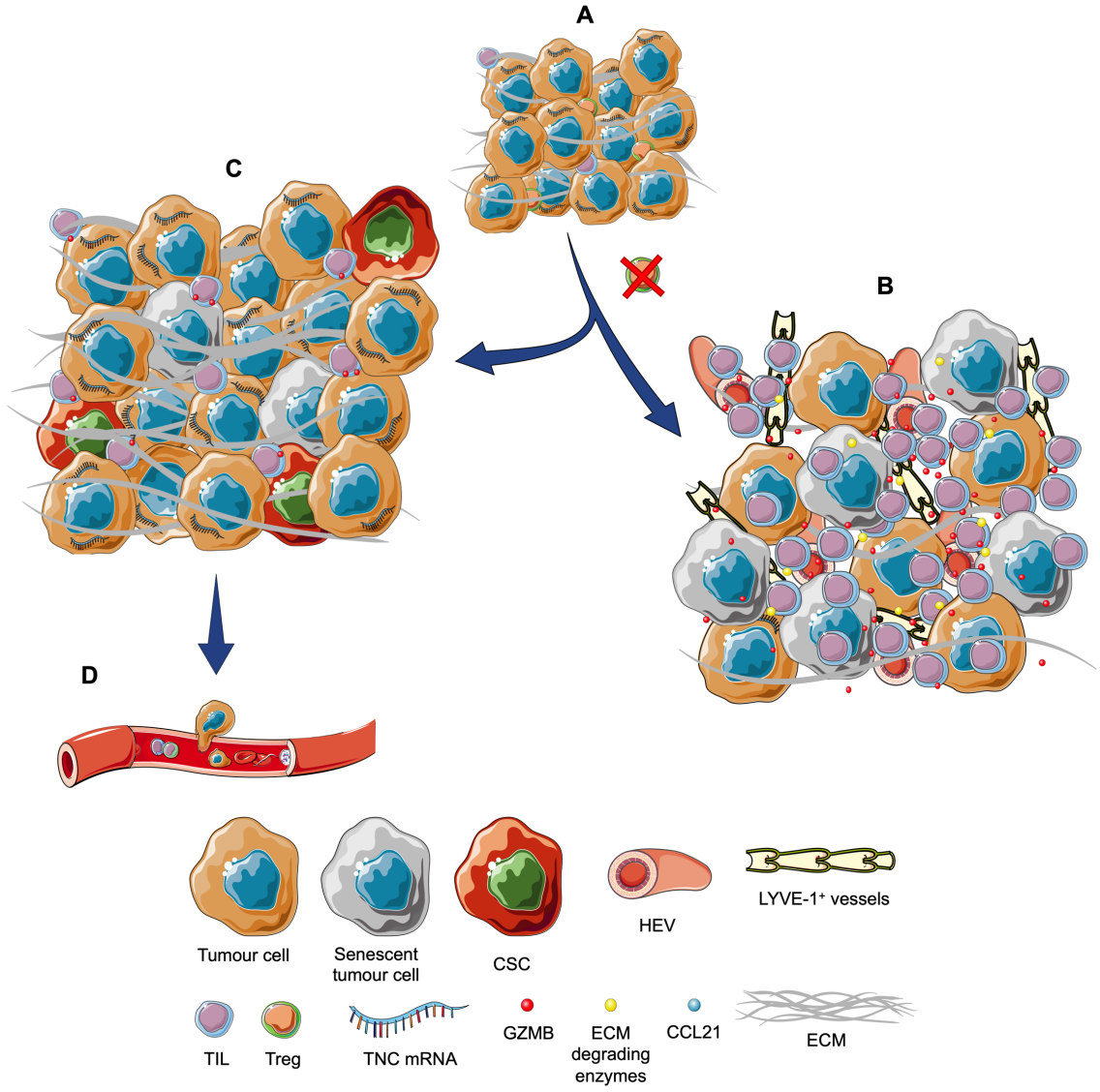

Figure 4.14|Final representation of response to Treg depletion in murine fibrosarcomas.

When a tumour arises due to carcinogen induction (**A**), once Tregs are depleted it can follow two paths: become a responder (**B**) or a non-responder (**C**). The image represents an adaptation of Figure 3.20, including all the alterations in the tumour microenvironment described in this chapter, including the emergence of senescent cells and CSCs, and a final stage of metastatic dissemination (**D**).

Chapter 5

Discussion

Despite a large number of scientific advances, cancer remains a disease that causes millions of deaths worldwide. Early research was mainly focused on targeting cancer cells, until an important landmark in cancer research was achieved when it was recognised that a tumour is not just a mass of tumour cells, but that there are many types of cells and structures that constitute the TME and contribute to tumour progression. This realisation allowed the development of new therapies to target the tumour supporting environment, to be used in combination with tumour cell targeting therapies already in place. One example of this strategy is the use of Bevacizumab, a monoclonal antibody against VEGF, in combination with chemotherapy regimens. This antibody was approved by the FDA in 2004, and in 2006, Sandler and colleagues demonstrated in a phase II trial that the combination of bevacizumab with chemotherapeutic agents (paclitaxel and carboplatin) significantly improved survival of patients with non-small-cell lung cancer (Sandler *et al.*, 2006). Similar studies were performed in other types of cancer, such as breast cancer (Miller *et al.*, 2005), renal cell carcinoma (Escudier *et al.*, 2007) and head and neck cancer (Seiwert *et al.*, 2008).

Recent key advances have revealed how tumours can evade immune mediated destruction. This knowledge has enabled the emergence of immunotherapy, which involves the manipulation of immune cells in order to reduce tumour-driven immunosuppression and promote anti-tumour immunity. Although these new approaches of tackling cancer, either by directly targeting tumour cells and/or other cells or structures in the TME, have improved patient survival, the majority of patients still do not respond to treatment and eventually relapse and succumb to the disease. Thus, it is important to understand why some patients respond to current treatments whilst others do not. There is accumulating evidence that differences in the TME can influence immunotherapy. For this reason, it is important to understand what distinguishes the TME of responders from non-responders in order to inform new strategies for overcoming barriers to immunotherapy in non-responders.

The work presented in this thesis focused on testing the hypothesis that a specific TME profile influences the ability of an immune response, activated as a result of Treg-depletion, to control tumour growth. The hypothesis was tested through three linked aims.

The first aim was to determine TME profiles in untreated, non-responder and responder tumours to Treg depletion. A bioinformatic analysis was performed revealing

significant differences in expression of ECM genes, with TNC being the most notable. This data was validated by immunofluorescence staining of tumours of each group, clearly indicating higher expression of ECM proteins and fewer T cell in non-responder and untreated tumours compared to responder tumours. Furthermore, experiments performed suggested that certain ECM proteins, such as TNC, can inhibit TIL degranulation, preventing an effective anti-tumour immune response in non-responders. From this data, it is possible to define responder tumours as being low in ECM content, with high infiltration of functional T cells, whilst non-responders present high levels of ECM proteins, with an intermediate infiltration of potentially non-functional T cells. Untreated tumours seem to have an intermediate and more variable phenotype, with some tumours expressing more ECM proteins than others.

The second aim of this project investigated whether the tumour ECM predicts the response to Treg depletion. To address this question, experiments were performed using shRNA to knockdown TNC in a fibrosarcoma-derived cell line. These experiments revealed that an effective anti-tumour immune response, with control of tumour growth, can still be achieved in conditions with pre-determined high expression of this protein in the TME. This indicates that even if TNC suppresses the activity of TIL, this effect can be overcome since activated T cells, stimulated following Treg-depletion, can still control TNC-rich tumours. It remains possible however, that in the case of a weaker T cell response, dense ECM, might still represent an impediment to a successful anti-tumour immune response.

The final aim was to define the alterations in the TME following Treg depletion in both responders and non-responders. Analysis of the lymphatic vasculature revealed that lymphatic vessels appear better organised in responders, showing a clear network of vessels, as opposed to non-responders, where lymphatic vessels are compatible with observations made by other groups describing patchy and randomly distributed vessels within the TME due to the lack of lymphangiogenic growth gradients (Li and Li, 2015). CCL21 has been described to guide and help DCs transmigration to lymphatic vessels (Vaahtomeri *et al.*, 2017), as well as guiding migration of these cells to draining lymph nodes (Russo et al., 2016). This chemokine was also shown to be involved in recruitment of naïve T cells into the TME through afferent lymphatics (Ondondo et al., 2014, Fankhauser et al., 2017). Results presented in this thesis showed high CCL21 levels in the stroma of responders, mainly found in the vicinity of lymphatic vessels, implying increased functionality of these vessels in this group.

Taking into account studies pointing to a role for dense ECM in driving gene expression changes in tumour cells, the intrinsic properties of cancer cells were also assessed. A trend for a higher number of proliferating cells was observed in non-responder ECM-rich tumours, when compared to the almost ECM-free responder tumours. No difference was observed in the number of apoptotic cells. Furthermore, a lower expression of genes related to EMT and CSC markers in responders suggested a lower content of aggressive, stem cell-like cells in these tumours, when compared to non-responders. This was validated in tumoursphere assays showing that there are fewer cells capable of forming new colonies in responder than non-responder tumours. The presence of fibroblast-like cells in cultures derived from draining and non-draining lymph nodes of all non-responder mice analysed, suggests that non-responder tumours might have a greater potential to disseminate to distant organs than untreated tumours. Studies are ongoing to determine the nature of these fibroblast-like cells. Assessment of potential lymph node invasion from responder tumours cells is also ongoing. It is hypothesised that invasion of draining lymph nodes will not be observed in the case of these tumours, since they are clearly well controlled by the immune system. It is important however to confirm that this is indeed the case especially as lymphatic networks, which are well developed in these tumours, could serve as conduits by which any remaining malignant cells from responder tumours reach and invade the draining lymph nodes (Stacker *et al.*, 2002).

Finally, potential mechanisms to explain the loss of ECM in the TME were explored. Use of RNAscope indicated that TNC transcription was reduced in cells in responder tumours. The observed trend for higher numbers of senescent cells in responder tumours might also contribute to the lack of ECM proteins in these tumours due to alterations in gene expression patterns in these cells. Moreover, it is also possible that senescent cells contribute to loss of ECM through the expression of matrix degrading enzymes. Many reports have mentioned that these enzymes, particularly MMPs and ADAMs, are included in the SASP (Le Maitre et al., 2007, Coppé et al., 2010b, Dimozi et al., 2015, Mavrogonatou et al., 2019). Matrix remodelling enzymes can also be expressed by other types of cells. Ahrends and colleagues have demonstrated that helper T cells can induce MMP expression by cytotoxic T cells, enhancing their ability to digest and invade tumour tissue (Ahrends et al., 2017). Similarly, Putz *et al*. demonstrated that heparanase production by NK cells contributes to control of tumour growth in mice, due to degradation of the ECM and improved immune anti-tumour response (Putz et al., 2017). Macrophages are also known to be major contributors of

stromal proteases, secreting a variety of MMPs (Varol and Sagi, 2018) as well as cathepsin proteases (Gocheva *et al.*, 2010). Thus, it will be important in future experiments to evaluate the involvement of matrix remodelling enzymes in ECM clearance, as well as identifying the source of these enzymes.

In conclusion, the data presented in this thesis demonstrate that a successful immune response after Treg depletion is capable of inducing alterations in the TME, enabling a switch from an immunosuppressive environment to an immunostimulatory one, therefore, disproving the initial null hypothesis. The resultant model proposed by this work states that if a strong immune response is unleashed after Treg depletion, the immune system may act in three ways: 1) by producing ECM degrading enzymes and clearing the ECM present in the tumour; 2) by inducing tumour cell senescence, contributing to a reduction in ECM content, 3) by clearing CSCs, eliminating their repopulating capacity. It is further hypothesised that the resultant loss of matrix would reduce interstitial pressure in tumours, enabling the development of functional lymphatic vasculature and increasing TIL infiltration in tumours. This promotes HEV development, intensifying robust and sustainable anti-tumour immune responses. If, on the other hand, the immune response after Treg depletion is sub-optimal, the function of the few infiltrating T cells may be hampered by the matrix-dense ECM resulting in overall poor control of tumour growth. It is tempting to speculate that such a sub-optimal immune response may drive adaptation of the tumour cells under attack; adaptations which include greater production of matrix resulting in increased tumour stiffness, vessel compression and emergence of tumour stem cells with the capacity to promote cell migration and invasion.

The above hypothesis is supported by data presented in this thesis which points to some differences between non-responder and untreated tumours. Both gene expression and abundance patterns of ECM proteins suggest an upregulation in non-responder compared to untreated tumours (Figures 3.4 and 3.5). Although not significant, there is also an increased expression of genes related to EMT (Figure 4.5) and CSCs (Figure 4.7) in non-responders, and tumourspheres obtained from these tumours are consistently bigger than those from untreated tumours (Figure 4.8). Collectively, these preliminary data imply that a sub-optimal anti-tumour immune response drives tumour aggression. Despite durable responses being observed with immunotherapies in some patients, most patients eventually exhibit resistance to treatment. This can be divided into primary resistance, adaptive immune resistance and acquired resistance. The adaptive immune resistance mechanism occurs when a tumour

is recognised by the immune system but protects itself by adapting to the immune response (Sharma *et al.*, 2017). Adaptations can be achieved through tumour cell intrinsic and extrinsic mechanisms. Genetic changes in the antigen processing and presentation machinery, such as mutations in the JAK-STAT signalling, loss of tumour antigen expression and loss of HLA expression, are common tumour cell intrinsic factors (Marincola *et al.*, 1999, Sucker *et al.*, 2014, Zaretsky *et al.*, 2016) involved in resistance. On the other hand, the TME plays an important role as a tumour cell extrinsic factor. The presence of immunosuppressive cells in the TME, such as MDSCs and TAMs, as well as other inhibitory immune checkpoints may contribute to inhibition of anti-tumour immune responses (Sharma et al., 2017). It has also been recently described that CSCs that resist to immunotherapy can modulate a CTL attack through expression of CD80 (Miao *et al.*, 2019). Therefore, it will be important to understand in the future if the potential increase of tumour aggression observed in non-responders are tumour adaptations to the weak anti-tumour immune response.

A key question which remains unanswered is why some mice become responders after Treg depletion whilst others do not. Previous work performed by former members of the lab, James Hindley and Emily Colbeck clearly indicated that Tregs are depleted to the same extent in all treated mice therefore the difference cannot be explained by differential effects of the DT administration (Hindley et al., 2012, Colbeck et al., 2017b). It was previously suggested that HEV development in responder tumours, which then promotes anti-tumour immunity, might only occur after sufficient antigen stimulation overcomes local immunosuppression (Colbeck et al., 2017b). MCA is highly mutagenic and can induce thousands of mutations in the cancer cells (Schumacher and Schreiber, 2015, Alspach *et al.*, 2019), generating potential neoantigens for recognition by T cells. It is possible that responder tumours have high numbers of neoantigens than non-responder tumours before treated starts. Supporting this hypothesis, a recent study performed by Joshi and colleagues, in patients with non-small-cell lung cancer, sampled non-synonymous mutations in several tumour biopsies as well as TCR sequences from the same site. They found that the number of nonsynonymous mutations in the tumour correlated with the numbers of TCR sequences selectively expanded in the tumour thereby suggesting that TCR expansion reflects the mutational landscape of the tumour (Joshi *et al.*, 2019). By the same mechanisms, differential neoantigen loads in responders and non-responders could explain the split in response after Treg depletion. Other components of the stromal compartment may also inhibit immune infiltration and activation (Turley *et al.*, 2015) e.g. tumour blood endothelial cells, which have been

shown not only to modulate T cell activation and cytolysis (Mazanet and Hughes, 2002, Rodig *et al.*, 2003, Huang *et al.*, 2010), but also to induce apoptosis of T cells (Motz *et al.*, 2014). MDSC are another type of stromal cell that have been shown to interfere with anti-tumour immunity. These have been shown to inhibit cytotoxic T cell killing of tumour cells in an IL-10-dependent manner, as well as to induce downregulation of MHC class I on tumour cells (Montesinos *et al.*, 2013). CAFs are also known to be major regulators of immune function. These cells are the main producers of TGF-β, a cytokine that can attenuate cytotoxicity of T cells (Ahmadzadeh and Rosenberg, 2005) and promote macrophages recruitment (Byrne *et al.*, 2008). CAFs have also been reported to release cytokines that promote polarisation of Th2 cells (De Monte *et al.*, 2011) and M2 macrophages (Kim *et al.*, 2012), contributing to an immunosuppressive environment. It may therefore be important to evaluate whether these cell types are differentially represented in non-responder versus responder tumours and whether their presence or absence prior to Treg depletion affects generation of an effective T cell response.

These findings open new possibilities to improve current available therapies. It is now known that a good anti-tumour immune response can create the right conditions to control tumour progression. By altering the TME, it may be possible to tip the balance in favour of these conditions, even when the T cell response is not optimal. Therefore, it may be important to combining immunotherapies with therapies targeting components of the TME, such as the ECM. One approach that is being explored is the use of CARs to promote matrix degradation. Caruana and colleagues have tested the use of CAR T cells engineered to express heparinase, an enzyme that degrades heparan sulphate proteoglycans which are highly present in the matrix. They have shown that these CAR T cells have improved capacity to degrade the ECM, promoting TIL infiltration and anti-tumour activity (Caruana *et al.*, 2015). CARs have also been engineered in other immune cells for the same purpose. Zhang and collaborators modified macrophages with a CAR that would trigger CD147 signalling, increasing expression of MMPs by these cells (Zhang *et al.*, 2019). This approach could be explored in the model studied in this thesis in order to improve and accelerate the first steps of TME remodelling. This would help to decrease tumour interstitial pressure, facilitating formation of functional vasculature, lymphatic and HEVs, improving the infiltration of higher numbers of TILs.

Since TNC is an ECM protein absent from healthy tissues, but whose expression in solid tumours is frequently associated with poor prognosis, it may prove an ideal target for conditioning the TME in order to improve anti-tumour immune responses. Through the use of different experimental models, TNC has been shown to affect several

processes which drive tumour progression, such as tumour proliferation (Saupe et al., 2013), angiogenesis (Tanaka *et al.*, 2004, Rupp et al., 2016), migration (Oskarsson et al., 2011) and tissue stiffness (Northey et al., 2017). TNC can also affect immune responses by inhibiting T cells (Puente Navazo et al., 2001, Parekh et al., 2005, Mirzaei et al., 2018) , and also through driving tumour-promoting inflammation (Midwood et al., 2009, Zuliani-Alvarez et al., 2017). Through engaging TLR4, TNC can polarize TAMs towards a pathogenic-immunosuppressive phenotype (Deligne *et al.*, 2020). Promoting TNC degradation could therefore represent a useful way to reduce tumour aggressiveness, decreasing invasion as well as promoting a more effective anti-tumour immune response. Interfering RNAs were used for the first time by Zukiel and colleagues to inhibit TNC synthesis in glioma patients, resulting in suppression of tumour growth (Zukiel *et al.*, 2006). This approach combined with immunotherapy might potentiate an effective anti-tumour immune response.

The specificity of TNC expression in tumour tissue also supports its usefulness as a means of targeting tumours to deliver therapeutic agents. It was shown that it is possible to deliver cytokines to the tumour, if these are expressed as fusion proteins with a single chain variable fragment of TNC antibodies (Brack *et al.*, 2006, Silacci *et al.*, 2006). Similarly, a more recent study showed that TNC antibody-drug conjugates that can only be activated in the TME, could be used to deliver chemotherapeutic agents (Dal Corso et al., 2017). Recently, after identifying a peptide that interacts with TNC (PL3), Lingasamy and colleagues developed PL3-guided nanoparticles, that after systemic administration accumulated in tumour xenografts in mice. These nanoparticles were useful for enabling tumour detection and imaging, as well as serving as tumour-seeking carriers for proapoptotic payloads to be delivered in the tumour (Lingasamy *et al.*, 2020).

To conclude, the study described in this thesis has presented a body of evidence indicating that reciprocal interactions between different components of the TME can support or hinder adaptive immune responses. Several pathways, most notably, production and degradation of the ECM, have been highlighted as important features of an immune “receptive” TME. Future challenges include 1. the need to further explore the molecular mechanisms underpinning the observations described and 2. evaluating the impact of modulating the TME of primary tumours on invasion and metastasis to secondary organs. Addressing these challenges should facilitate the design of novel therapies based on altering the ECM to improve anti-tumour immunity. To address these challenges, future work will include assessment of the consequences of a weak anti-tumour immune response in non-responders; analysis of the TCR repertoire in untreated,

non-responder and responder tumours; evaluation of the role of stromal cells and other immunosuppressive components in the TME in the response to Treg depletion; and investigation of new therapeutic avenues to promote ECM degradation and TIL infiltration.

Appendix

Methods

Radiosynthesis of ^{89}Zr Oxalate

^{89}Zr was produced in house by the ^{89}Y(p,2n) ^{88}Zr reaction via an adaptation of the methods of Walther and colleagues (Walther *et al.*, 2011). Briefly, a disk of natural abundance ^{89}Y foil (300μm thick, Goodfellow) in a costume made aluminium holder was loaded into a COSTIS Solid Target System (STS) fitted to an IBA Cyclone (18/9) cyclotron equipped with a 400 μm thick niobium beam degrader. The disk was irradiated for 4 hours with a beam energy of 40 μA. The irradiated disk was left in the cyclotron for 12 hours to allow any short lived ^{89m}Zr to decay to ^{89}Zr before removal for purification (activity 1.5-2 GBq). As described in Walther et al., the disk was dissolved in 2 M HCl with stirring and heat, and the ^{89}Zr was isolated by flowing over a hydroxamate functionalised ion exchange resin column (prepared in house freshly for each separation). The column was rinsed with 2M HCl and water to remove ^{89}Y before ^{89}Zr being liberated with 1 M oxalic acid in 3 fractions of 1 mL. The most concentrated fraction contained 800-1000 MBq.

Antibody Modification with p-SCN-Bn-DFO

Antibody modifications and radiolabelling procedures were carried out via an adaptation of the methods of Vosjan and colleagues (Vosjan *et al.*, 2010). To a solution of anti-TNC antibody in 0.1 M $NaHCO_3$ (pH 8.9) was added 10 M equivalents of p-SCN-Bn-DFO in anhydrous DMSO. The volume of the p-SCN-Bn-DFO solution transferred to the antibody solution was kept below 10% (v/v). The reaction mixture was incubated at 37°C for 60 minutes with shaking (550rpm) and the excess p-SCN-Bn-DFO was removed by Sephadex-G50 size exclusion chromatography, eluting with 100 μL fractions of PBS. After combining the fractions which corresponded to the DFO-modified antibody, the sample was washed twice with PBS and concentrated using an Amicon Ultra-0.5 mL centrifugal filter (30 kDa MWT cut-off, Merck Millipore).

Preparation of ^{89}Zr-labeled TNC antibody

A solution of ^{89}Zr in 1 M oxalic acid was adjusted to pH 7 by the addition of 1 M sodium carbonate. The resulting solution was added to the DFO-anti-TNC solution to achieve the ratio of 0.1 MBq to 1μg of antibody. The reaction mixture was incubated at room temperature for 1 hour, and the radiolabelling efficiency was determined by iTLC using an eluent of 50 mM EDTA (pH 6) and radio-HPLC. The solution was then centrifuged in a 0.5 mL Amicon 30 MWCO centrifugal concentrator (12,000 rcf, 8 minutes) in order to remove excess salt in solution. Flow-through was discarded and the concentrated protein fraction was diluted in PBS and centrifuged using the same Amicon concentrator. This was followed by a wash in PBS and another centrifugation. The concentrated ^{89}Zr-labelled antibody solution was recovered from the concentrator and diluted to the appropriate injection volume in PBS.

Radio-TLC

Five μL of the reaction mixture was spotted onto a 12 x 1 cm strip of Salicylic acid impregnated glass fibre ITLC paper (Agilent Technologies), and strips were developed for 5-10 minutes with 50mM DTPA solution adjusted to pH 7.4. The developed strips were read with a Canberra iSCAN radio TLC reader, controlled by Laura version 4.14.

Radio-HPLC

Radio-HPLC was carried out using an Agilent 1200 series machine, equipped with a refractive index detector, a single wavelength UV detector set to 254nm, a Lablogic Gamma-Ram 4 radiodetector and a Superdex 200 10/300 GL size exclusion column (GE Healthcare LifeSciences). Phosphate buffer eluent was prepared as described by Vosjan (Vosjan et al., 2010). Samples were eluted at 0.5 mL/min for 60 minutes at 35°C.

Bioinformatic analyses – Human data

Level 3 (raw counts, htseq.counts.gz) RNAseq data, and sample meta data (GDC sample sheet and clinical cart files) were download from the TCGA GDC portal

(https://portal.gdc.cancer.gov/) on 3-October-2019 for twenty-one cancer types (Supplementary Figure 1). All datasets were normalised as one matrix within the DESeq2 Bioconductor package (Love *et al.*, 2014) in R and the DESeq2 normalised counts were used for all analyses.

Only data from primary tumours was used for analysis. Patient information (GDC sample sheet - vital status, days to death, days to last follow up) was used for Kaplan Meier survival analysis (R packages: survminer and survival, https://cran.r-project.org/package=survminer). Data was censored at days-to-last-follow-up or days-to-death and log-rank p values calculated between two curves. Medoids clustering was performed using the ClusterR package (https://cran.r-project.org/package=ClusterR). Clustering was carried out on expression data, centre and scaled by each gene, using the Manhattan distance metric to obtain two clusters. RNAseq data from distinct cancers was not combined to perform clustering, this ensured gene expression levels from different cancer types were not unfairly compared.

To cluster on cytotoxic T cells alone, a meta gene signature from Marisa et al 2018 (Marisa *et al.*, 2018) was used (CTL genes – CD3G, CD3E, CD3D, PTPRC, CD8A; cytotoxicity genes – PRF1, GZMH, GNLY, GZMB, GZMK, GZMA) in each cancer type. Sixteen cancers in which CTL signature was prognostic of survival, based on visual inspection of survival curves (Supplementary Figure 1), were taken forward for TNC clustering. CTL high and CTL low clusters were separated, and a second round of medoids clustering was performed on based expression of TNC resulting in four groups (diagram shown in Supplementary Figure 4).

Analysis of RNAseq datasets from primary tumours in TCGA

TNC Gene Expression Significantly Impacts Patient Survival in the Presence of a CTL Gene Signature

T cell infiltration of tumours (particularly with cytotoxic T lymphocytes (CTL)) (Galon et al., 2006) and presence of TNC (Gocheva et al., 2017, Mirzaei et al., 2018) demonstrate opposing correlations with survival in human cancers. However, aside from the data presented above, evidence of an antagonistic relationship between T cells and TNC has solely been demonstrated *in vitro* (Mirzaei et al., 2018). We investigated whether there was a relationship between CTL gene signatures and TNC gene expression in the context of survival, specifically searching for trends analogous to those revealed by our *in vivo* mouse data. For this purpose, we examined RNAseq datasets from primary tumours in The Cancer Genome Atlas (TCGA), to determine whether there was a link between a favourable CTL gene signature and expression of TNC.

We identified 14 cancers where survival correlated with a CTL gene signature (Marisa et al., 2018) in patients' primary tumours (6 statistically significant, Supplementary Figure 1). This was performed using an unbiased medoids clustering approach where we first clustered the datasets based on expression of CTL genes (Supplementary Figure 1), followed by expression of TNC within each individual cancer (Supplementary Figure 2 and Supplementary Figure 3). This approach ensured that we were comparing expression of CTL genes or *TNC* within and not across different cancer types (extra detail in methods). We used this analysis to generate groups of CTL high and CTL low tumours (Supplementary Figure 4-A) which were then separately clustered by *TNC* expression (Supplementary Figure 4-B,C). This analysis revealed that whilst *TNC* expression had no impact on survival within CTL low tumours ($P = 0.57$, Fig. 2C), low *TNC* expression was associated with a highly significant increase in survival within CTL high tumours ($P = 0.00025$, Fig. 2B). When we reversed the analysis, clustering *TNC* high/low first, followed by CTL high/low, the same effect was apparent (Supplementary Figure 5). These data are similar to those obtained in the mouse model above in that they clearly indicate that a successful T cell response is associated with low *TNC* expression. The key question is whether TNC impinges on CTL activity in patients and mice resulting in poorer survival/outcome, or whether effective CTL activity results in loss of TNC.

Supplementary Figures

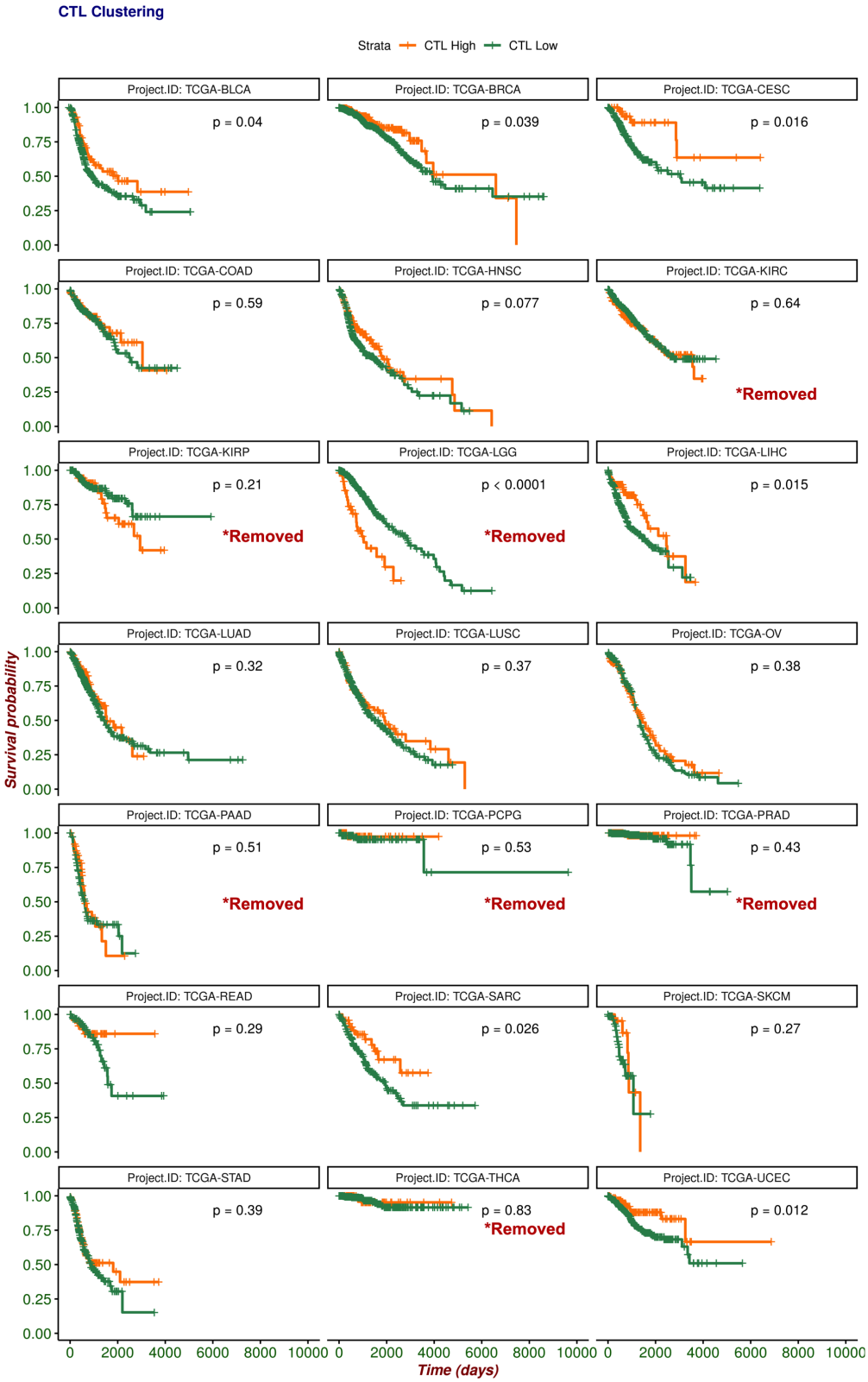

Supplementary Figure 1|Individual data for each cancer corresponding to Supplementary Figure 4-A.
Cancers were removed (red text with *) if survival did not visually correlate with expression of the CTL gene signature. Only cancers which were left were included in the analysis shown in Supplementary Figure 4-A.

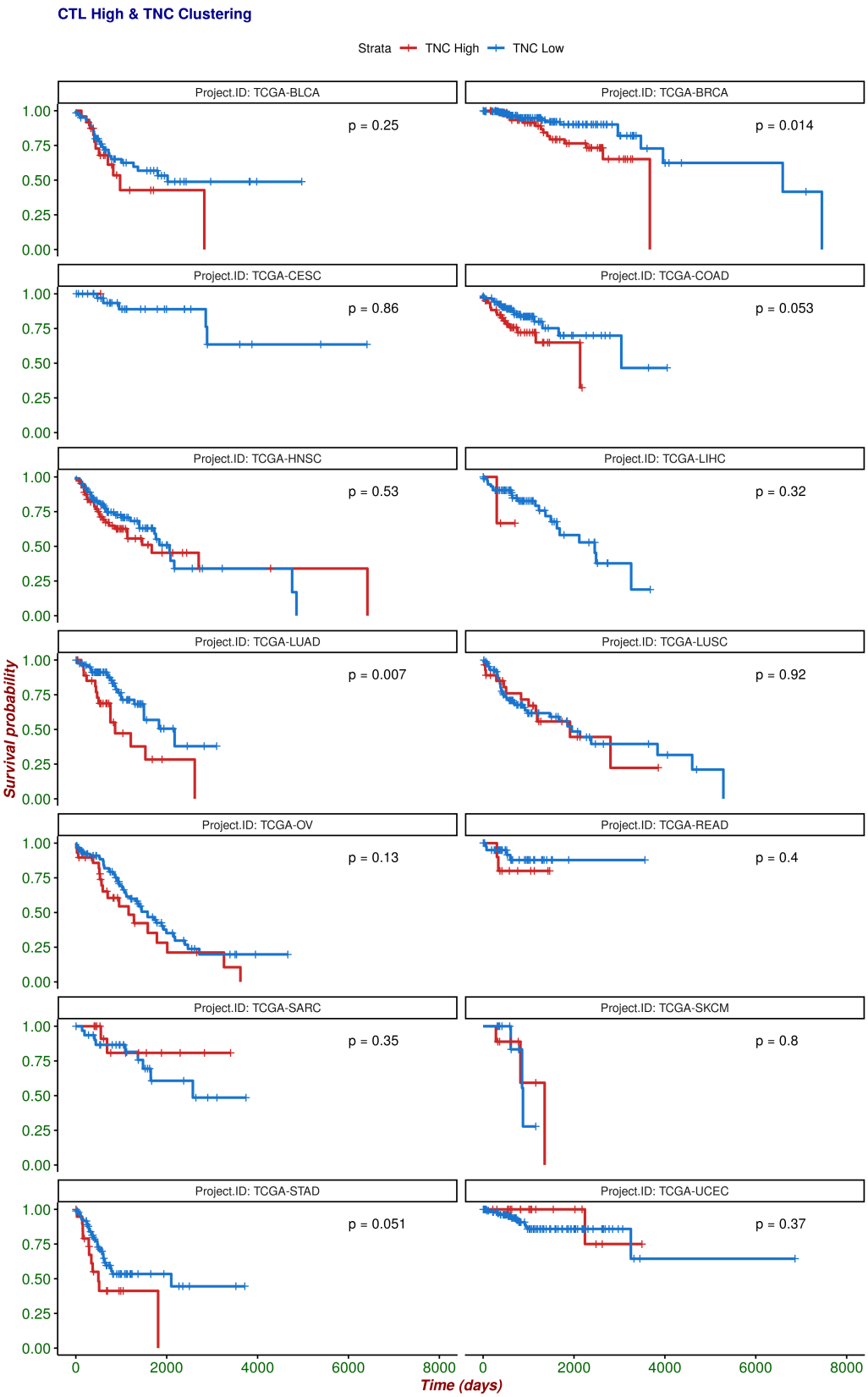

Supplementary Figure 2|Individual data for each cancer corresponding to Supplementary Figure 4-B.
Each group corresponds the orange CTL-High line in Supplementary Figure 1.

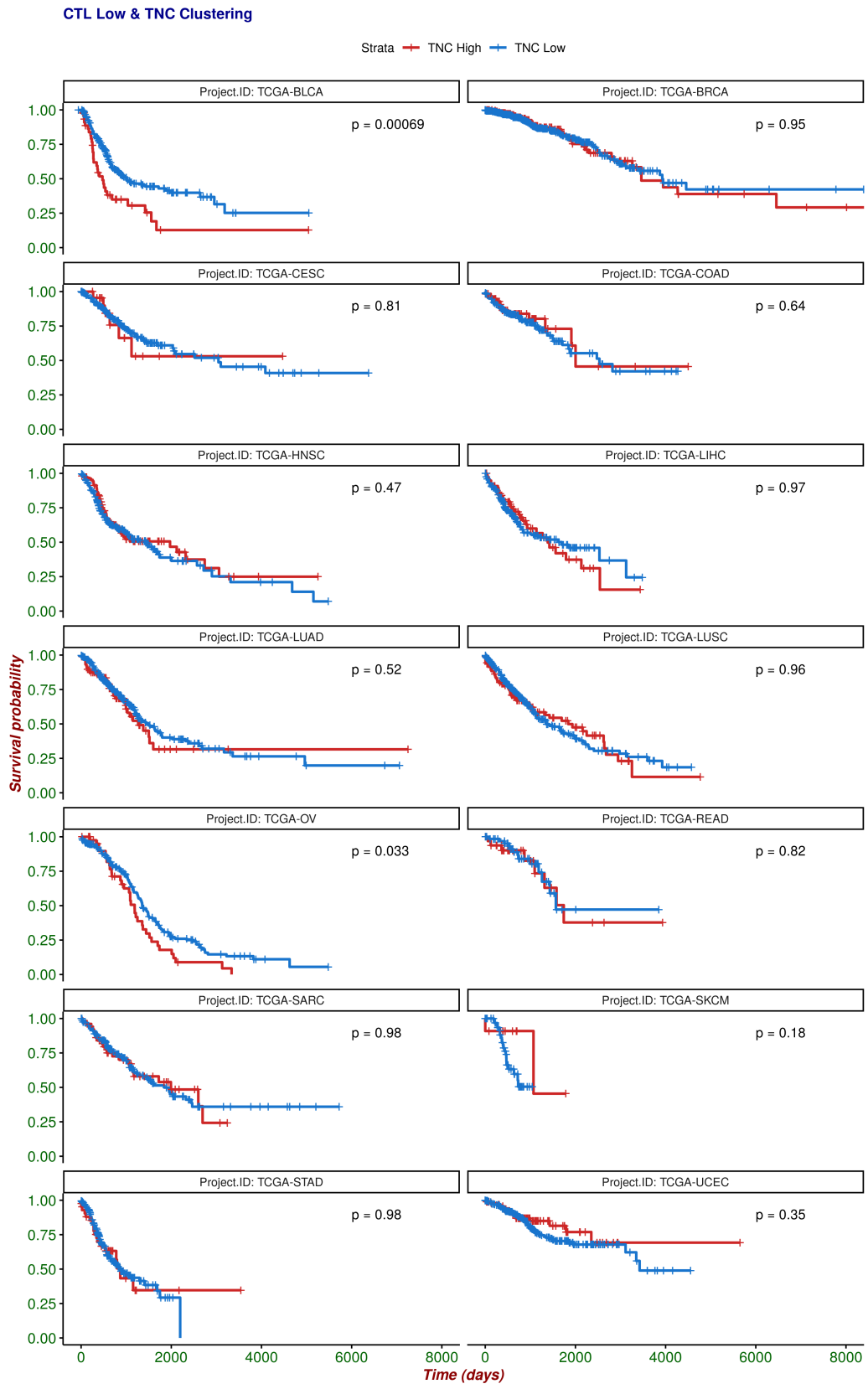

Supplementary Figure 3|Individual data for each cancer corresponding to Supplementary Figure 4-C.
Each group corresponds the green CTL-Low line in Supplementary Figure 1.

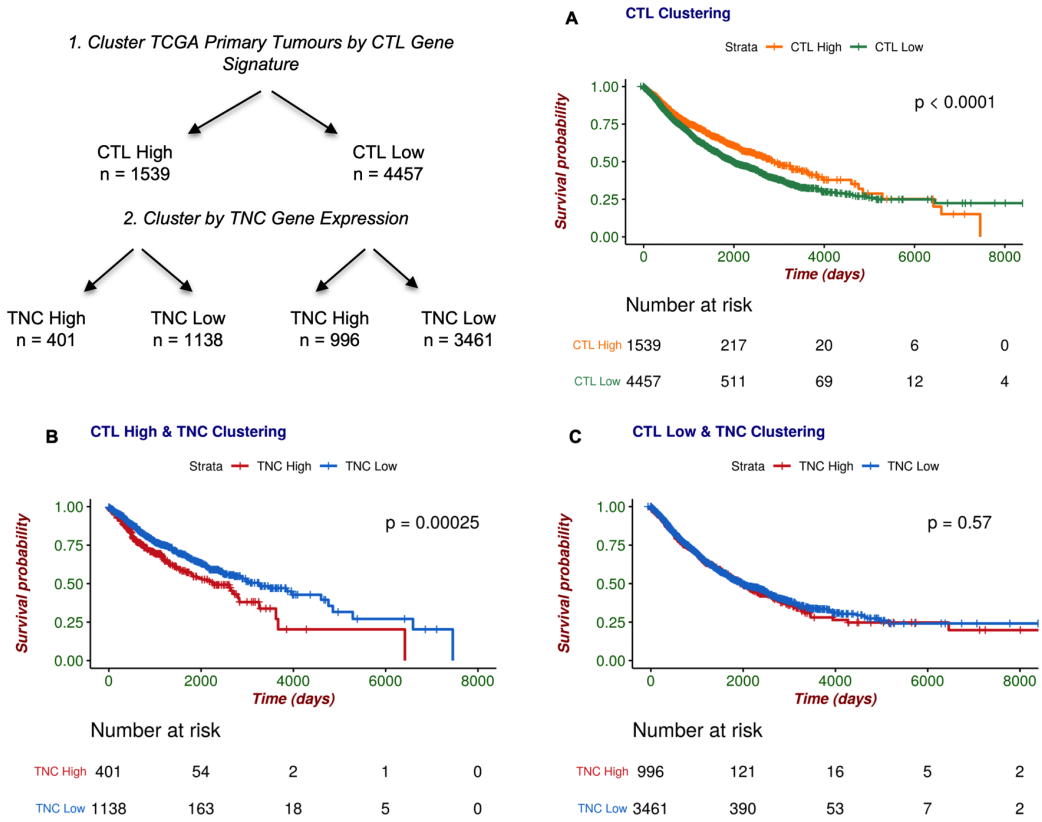

Supplementary Figure 4|Low TNC expression correlates with patient survival only in tumours that have high expression of a cytotoxic gene signature.

A, Kaplan Meier (KM) survival analysis of 14 cancers in which a CTL gene signature was associated with longer survival (based on survival curves shown in Fig. S 3), patients have been clustered by CTL gene expression in their primary tumour. Medoids clustering and patient classification was performed within each cancer separately to ensure that gene expression patterns in tumour types did not skew the analysis to certain cancer types rather than groups within each cancer. CTL High tumours (orange line) were taken forward and used to cluster patients in **B**, by TNC expression. Blue lines represent TNC Low primary tumours and red represent TNC high. CTL Low tumours (green) were taken forward and clustered patients by TNC expression shown in **C**. Individual plots for each cancer are shown in Fig. Ss 4-6.

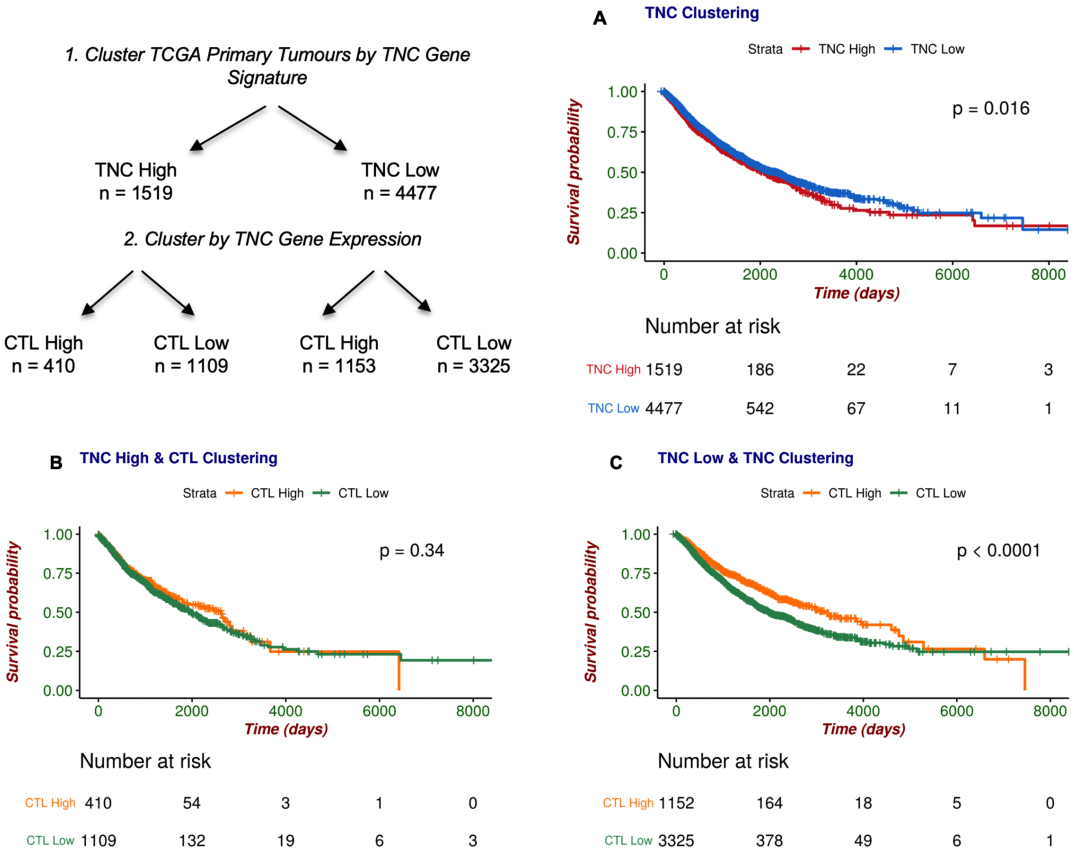

Supplementary Figure 5|Reverse Analysis of TCGA data, clustering by TNC followed by a CTL gene signature.

Analysis is the same as that performed in Supplementary Figure 4, however with reversed order. **A**, KM analysis of patients clustered (within each cancer) by relative expression of TNC, followed by clustering of **B**, TNC-High and **C**, TNC-Low primary tumour groups by the expression of a CTL gene signature.

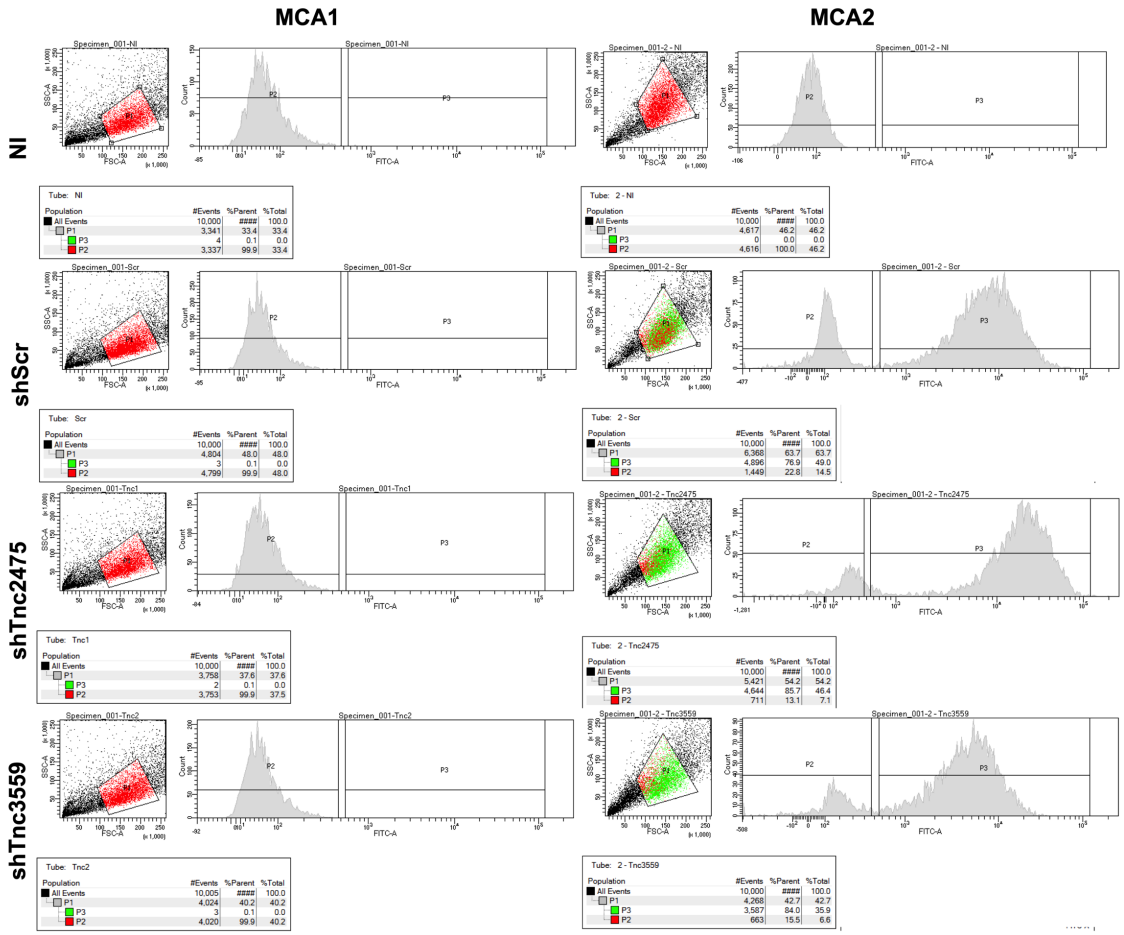

Supplementary Figure 6|Infection rate assessment by flow cytometry.

MCA1 and MCA2 cells, non-infected (NI) or infected with either a scrambled shRNA or a TNC specific shRNA (shTnc2475 or shTnc3559), were analysed by flow cytometry in order to assess the successfulness of the infection. This is translated in the amount of GFP^+ cells. Cells were first gated on the size of interest (P1), and those were posteriorly analysed for negativity (P2) or positivity (P3) of GFP (detected on the FITC channel).

References

ACERBI, I., CASSEREAU, L., DEAN, I., SHI, Q., AU, A., PARK, C., CHEN, Y. Y., LIPHARDT, J., HWANG, E. S. & WEAVER, V. M. 2015. Human breast cancer invasion and aggression correlates with ECM stiffening and immune cell infiltration. *Integr Biol (Camb),* 7**,** 1120-34.

AGER, A. & MAY, M. J. 2015. Understanding high endothelial venules: Lessons for cancer immunology. *Oncoimmunology,* 4**,** e1008791.

AHMAD, S., ABU-EID, R., SHRIMALI, R., WEBB, M., VERMA, V., DOROODCHI, A., BERRONG, Z., SAMARA, R., RODRIGUEZ, P. C., MKRTICHYAN, M. & KHLEIF, S. N. 2017. Differential PI3Kδ Signaling in CD4⁺ T-cell Subsets Enables Selective Targeting of T Regulatory Cells to Enhance Cancer Immunotherapy. *Cancer Research,* 77**,** 1892-1904.

AHMADZADEH, M. & ROSENBERG, S. A. 2005. TGF-β1 Attenuates the Acquisition and Expression of Effector Function by Tumor Antigen-Specific Human Memory CD8 T Cells. *The Journal of Immunology,* 174**,** 5215-5223.

AHRENDS, T., SPANJAARD, A., PILZECKER, B., BĄBAŁA, N., BOVENS, A., XIAO, Y., JACOBS, H. & BORST, J. 2017. CD4+ T Cell Help Confers a Cytotoxic T Cell Efector Program Including Coinhibitory Receptor Downregulation and Increased Tissue Invasiveness. *Immunity,* 47**,** 848-861.e5.

AKALU, Y. T., ROTHLIN, C. V. & GHOSH, S. 2017. TAM receptor tyrosine kinases as emerging targets of innate immune checkpoint blockade for cancer therapy. *Immunological Reviews,* 276**,** 165-177.

AKINO, T., HIDA, K., HIDA, Y., TSUCHIYA, K., FREEDMAN, D., MURAKI, C., OHGA, N., MATSUDA, K., AKIYAMA, K., HARABAYASHI, T., SHINOHARA, N., NONOMURA, K., KLAGSBRUN, M. & SHINDOH, M. 2009. Cytogenetic Abnormalities of Tumor-Associated Endothelial Cells in Human Malignant Tumors. *The American Journal of Pathology,* 175**,** 2657-2667.

AL-HAJJ, M., WICHA, M. S., BENITO-HERNANDEZ, A., MORRISON, S. J. & CLARKE, M. F. 2003. Prospective identification of tumorigenic breast cancer cells. *Proceedings of the National Academy of Sciences,* 100**,** 3983-3988.

ALI, K., SOOND, D. R., PINEIRO, R., HAGEMANN, T., PEARCE, W., LIM, E. L., BOUABE, H., SCUDAMORE, C. L., HANCOX, T., MAECKER, H., FRIEDMAN, L., TURNER, M., OKKENHAUG, K. & VANHAESEBROECK, B. 2014. Inactivation of PI(3)K p110δ breaks regulatory T-cell-mediated immune tolerance to cancer. *Nature,* 510**,** 407-411.

ALLEN, E., JABOUILLE, A., RIVERA, L. B., LODEWIJCKX, I., MISSIAEN, R., STERI, V., FEYEN, K., TAWNEY, J., HANAHAN, D., MICHAEL, I. P. & BERGERS, G. 2017. Combined antiangiogenic and anti-PD-L1 therapy stimulates tumor immunity through HEV formation. *Sci Transl Med,* 9.

ALOISI, F. & PUJOL-BORRELL, R. 2006. Lymphoid neogenesis in chronic inflammatory diseases. *Nature Reviews Immunology,* 6**,** 205-217.

ALSPACH, E., LUSSIER, D. M., MICELI, A. P., KIZHVATOV, I., DUPAGE, M., LUOMA, A. M., MENG, W., LICHTI, C. F., ESAULOVA, E., VOMUND, A. N., RUNCI, D., WARD, J. P., GUBIN, M. M., MEDRANO, R. F. V., ARTHUR, C. D., WHITE, J. M., SHEEHAN, K. C. F., CHEN, A., WUCHERPFENNIG, K. W., JACKS, T., UNANUE, E. R., ARTYOMOV, M. N. & SCHREIBER, R. D. 2019. MHC-II neoantigens shape tumour immunity and response to immunotherapy. *Nature,* 574**,** 696-701.

ALVARADO, A. G., THIAGARAJAN, P. S., MULKEARNS-HUBERT, E. E., SILVER, D. J., HALE, J. S., ALBAN, T. J., TURAGA, S. M., JARRAR, A., REIZES, O., LONGWORTH, M. S., VOGELBAUM, M. A. & LATHIA, J. D. 2017. Glioblastoma Cancer Stem Cells Evade Innate Immune Suppression of Self-Renewal through Reduced TLR4 Expression. *Cell Stem Cell,* 20**,** 450-461.e4.

ANGELL, H. & GALON, J. 2013. From the immune contexture to the Immunoscore: the role of prognostic and predictive immune markers in cancer. *Curr Opin Immunol,* 25**,** 261-7.

ANTONY, P. A., PICCIRILLO, C. A., AKPINARLI, A., FINKELSTEIN, S. E., SPEISS, P. J., SURMAN, D. R., PALMER, D. C., CHAN, C.-C., KLEBANOFF, C. A., OVERWIJK, W. W., ROSENBERG, S. A. & RESTIFO, N. P. 2005. CD8+ T Cell Immunity Against a Tumor/Self-Antigen Is Augmented by CD4+ T Helper Cells and Hindered by Naturally Occurring T Regulatory Cells. *The Journal of Immunology,* 174**,** 2591-2601.

APONTE, P. M. & CAICEDO, A. 2017. Stemness in Cancer: Stem Cells, Cancer Stem Cells, and Their Microenvironment. *Stem Cells International,* 2017**,** 5619472.

ARCE VARGAS, F., FURNESS, A. J. S., SOLOMON, I., JOSHI, K., MEKKAOUI, L., LESKO, M. H., MIRANDA ROTA, E., DAHAN, R., GEORGIOU, A., SLEDZINSKA, A., BEN AISSA, A., FRANZ, D., WERNER SUNDERLAND, M., WONG, Y. N. S., HENRY, J. Y., O'BRIEN, T., NICOL, D., CHALLACOMBE, B., BEERS, S. A., SPAIN, L., WOTHERSPOON, A., FRANCIS, N., SMITH, M., STRAUSS, D., HAYES, A., SOULTATI, A., STARES, M., SPAIN, L., LYNCH, J., FOTIADIS, N., FERNANDO, A., HAZELL, S., CHANDRA, A., PICKERING, L., RUDMAN, S., CHOWDHURY, S., SWANTON, C., JAMAL-HANJANI, M., VEERIAH, S., SHAFI, S., CZYZEWSKA-KHAN, J., JOHNSON, D., LAYCOCK, J., BOSSHARD-CARTER, L., GOH, G., ROSENTHAL, R., GORMAN, P., MURUGAESU, N., HYNDS, R. E., WILSON, G., BIRKBAK, N. J., WATKINS, T. B. K., MCGRANAHAN, N., HORSWELL, S., MITTER, R., ESCUDERO, M., STEWART, A., VAN LOO, P., ROWAN, A., XU, H., TURAJLIC, S., HILEY, C., ABBOSH, C., GOLDMAN, J., STONE, R. K., DENNER, T., MATTHEWS, N., ELGAR, G., WARD, S., BIGGS, J., COSTA, M., BEGUM, S., PHILLIMORE, B., CHAMBERS, T., NYE, E., GRACA, S., AL BAKIR, M., HARTLEY, J. A., LOWE, H. L., HERRERO, J., LAWRENCE, D., HAYWARD, M., PANAGIOTOPOULOS, N., KOLVEKAR, S., FALZON, M., BORG, E., SIMEON, C., HECTOR, G., SMITH, A., ARANDA, M., NOVELLI, M., OUKRIF, D., JANES, S. M., THAKRAR, R., FORSTER, M., AHMAD, T., LEE, S. M., PAPADATOS-PASTOS, D., CARNELL, D., MENDES, R., et al. 2017. Fc-Optimized Anti-CD25 Depletes Tumor-Infiltrating Regulatory T Cells and Synergizes with PD-1 Blockade to Eradicate Established Tumors. *Immunity,* 46**,** 577-586.

ARIKAWA-HIRASAWA, E., WATANABE, H., TAKAMI, H., HASSELL, J. R. & YAMADA, Y. 1999. Perlecan is essential for cartilage and cephalic development. *Nature Genetics,* 23**,** 354-358.

ASANO, M., TODA, M., SAKAGUCHI, N. & SAKAGUCHI, S. 1996. Autoimmune disease as a consequence of developmental abnormality of a T cell subpopulation. *Journal of Experimental Medicine,* 184**,** 387-396.

AUGSBURGER, D., NELSON, P. J., KALINSKI, T., UDELNOW, A., KNÖSEL, T., HOFSTETTER, M., QIN, J. W., WANG, Y., GUPTA, A. S., BONIFATIUS, S., LI, M., BRUNS, C. J. & ZHAO, Y. 2017. Current diagnostics and treatment of fibrosarcoma -perspectives for future therapeutic targets and strategies. *Oncotarget,* 8**,** 104638-104653.

AWWAD, M. & NORTH, R. J. 1988. Immunologically mediated regression of a murine lymphoma after treatment with anti-L3T4 antibody. A consequence of removing L3T4+ suppressor T cells from a host generating predominantly Lyt-2+ T cell-mediated immunity. *The Journal of experimental medicine,* 168**,** 2193-2206.

BALKWILL, F. R., CAPASSO, M. & HAGEMANN, T. 2012. The tumor microenvironment at a glance. *J Cell Sci,* 125**,** 5591-6.

BARBER, D. L., WHERRY, E. J., MASOPUST, D., ZHU, B., ALLISON, J. P., SHARPE, A. H., FREEMAN, G. J. & AHMED, R. 2006. Restoring function in exhausted CD8 T cells during chronic viral infection. *Nature,* 439**,** 682-687.

BATES, G. J., FOX, S. B., HAN, C., LEEK, R. D., GARCIA, J. F., HARRIS, A. L. & BANHAM, A. H. 2006. Quantification of Regulatory T Cells Enables the Identification of High-Risk Breast Cancer Patients and Those at Risk of Late Relapse. *Journal of Clinical Oncology,* 24**,** 5373-5380.

BATLLE, E. & CLEVERS, H. 2017. Cancer stem cells revisited. *Nat Med,* 23**,** 1124-1134.

BECHER, O. J. & HOLLAND, E. C. 2006. Genetically engineered models have advantages over xenografts for preclinical studies. *Cancer Res,* 66**,** 3355-8, discussion 3358-9.

BENGSCH, B., JOHNSON, A. L., KURACHI, M., ODORIZZI, P. M., PAUKEN, K. E., ATTANASIO, J., STELEKATI, E., MCLANE, L. M., PALEY, M. A., DELGOFFE, G. M. & WHERRY, E. J. 2016. Bioenergetic Insufficiencies Due to Metabolic Alterations Regulated by the Inhibitory Receptor PD-1 Are an Early Driver of CD8+ T Cell Exhaustion. *Immunity,* 45**,** 358-373.

BENNETT, C. L., CHRISTIE, J., RAMSDELL, F., BRUNKOW, M. E., FERGUSON, P. J., WHITESELL, L., KELLY, T. E., SAULSBURY, F. T., CHANCE, P. F. & OCHS, H. D. 2001. The immune dysregulation, polyendocrinopathy, enteropathy, X-linked syndrome (IPEX) is caused by mutations of FOXP3. *Nature Genetics,* 27**,** 20-21.

BERG, N. N., PUENTE, L. G., DAWICKI, W. & OSTERGAARD, H. L. 1998. Sustained TCR signaling is required for mitogen-activated protein kinase activation and degranulation by cytotoxic T lymphocytes. *J Immunol,* 161**,** 2919-24.

BETTS, G., TWOHIG, J., VAN DEN BROEK, M., SIERRO, S., GODKIN, A. & GALLIMORE, A. 2007. The impact of regulatory T cells on carcinogen-induced sarcogenesis. *British journal of cancer,* 96**,** 1849-1854.

BEVAN, M. J. 1976. Cross-priming for a secondary cytotoxic response to minor H antigens with H-2 congenic cells which do not cross-react in the cytotoxic assay. *Journal of Experimental Medicine,* 143**,** 1283-1288.

BEVAN, M. J. 2004. Helping the CD8+ T-cell response. *Nature Reviews Immunology,* 4**,** 595-602.

BINDEA, G., MLECNIK, B., TOSOLINI, M., KIRILOVSKY, A., WALDNER, M., OBENAUF, ANNA C., ANGELL, H., FREDRIKSEN, T., LAFONTAINE, L., BERGER, A., BRUNEVAL, P., FRIDMAN, WOLF H., BECKER, C., PAGÈS, F., SPEICHER, MICHAEL R., TRAJANOSKI, Z. & GALON, J. 2013. Spatiotemporal Dynamics of Intratumoral Immune Cells Reveal the Immune Landscape in Human Cancer. *Immunity,* 39**,** 782-795.

BINNEWIES, M., ROBERTS, E. W., KERSTEN, K., CHAN, V., FEARON, D. F., MERAD, M., COUSSENS, L. M., GABRILOVICH, D. I., OSTRAND-ROSENBERG, S., HEDRICK, C. C., VONDERHEIDE, R. H., PITTET, M. J., JAIN, R. K., ZOU, W., HOWCROFT, T. K., WOODHOUSE, E. C., WEINBERG, R. A. & KRUMMEL, M. F. 2018. Understanding the tumor immune microenvironment (TIME) for effective therapy. *Nat Med,* 24**,** 541-550.

BISSELL, M. J., HALL, H. G. & PARRY, G. 1982. How does the extracellular matrix direct gene expression? *J Theor Biol,* 99**,** 31-68.

BISWAS, S. K. & MANTOVANI, A. 2010. Macrophage plasticity and interaction with lymphocyte subsets: cancer as a paradigm. *Nature Immunology,* 11**,** 889-896.

BIZOT-FOULON, V., BOUCHARD, B., HORNEBECK, W., DUBERTRET, L. & BERTAUX, B. 1995. Uncoordinate expressions of type I and III collagens, collagenase and tissue inhibitor of matrix metalloproteinase 1 along in vitro proliferative life span of human skin fibroblasts. *Cell Biology International,* 19**,** 129-136.

BLANPAIN, C. 2013. Tracing the cellular origin of cancer. *Nature Cell Biology,* 15**,** 126-134.

BONNET, D. & DICK, J. E. 1997. Human acute myeloid leukemia is organized as a hierarchy that originates from a primitive hematopoietic cell. *Nature Medicine,* 3**,** 730-737.
BORDRY, N., BROGGI, M. A. S., DE JONGE, K., SCHAEUBLE, K., GANNON, P. O., FOUKAS, P. G., DANENBERG, E., ROMANO, E., BAUMGAERTNER, P., FANKHAUSER, M., WALD, N., CAGNON, L., ABED-MAILLARD, S., MABY-EL HAJJAMI, H., MURRAY, T., IOANNIDOU, K., LETOVANEC, I., YAN, P., MICHIELIN, O., MATTER, M., SWARTZ, M. A. & SPEISER, D. E. 2018. Lymphatic vessel density is associated with CD8. *Oncoimmunology,* 7**,** e1462878.
BRACK, S. S., SILACCI, M., BIRCHLER, M. & NERI, D. 2006. Tumor-Targeting Properties of Novel Antibodies Specific to the Large Isoform of Tenascin-C. *Clinical Cancer Research,* 12**,** 3200-3208.
BRAUMÜLLER, H., WIEDER, T., BRENNER, E., ASSMAN, S., HAHN, M., ALKHALED, M., SCHILBACH, K., ESSMANN, F., KNEILLING, M., GRIESSINGER, C., RANTA, F., ULLRICH, S., MOCIKAT, R., BRAUNGART, K., MEHRA, T., FEHRENBACHER, B., BERDEL, J., NIESSNER, H., MEIER, F., VAN DEN BROEK, M., HÄRING, H. U., HANDGRETINGER, R., QUINTANILLA-MARTINEZ, L., FEND, F., PESIC, M., BAUER, J., ZENDER, L., SCHALLER, M., SCHULZE-OSTHOFF, K. & RÖCKEN, M. 2013. T-helper-1-cell cytokines drive cancer into senescence. *Nature,* 494**,** 361-5.
BRODERS-BONDON, F., NGUYEN HO-BOULDOIRES, T. H., FERNANDEZ-SANCHEZ, M. E. & FARGE, E. 2018. Mechanotransduction in tumor progression: The dark side of the force. *J Cell Biol,* 217**,** 1571-1587.
BRONTE, V., BRANDAU, S., CHEN, S.-H., COLOMBO, M. P., FREY, A. B., GRETEN, T. F., MANDRUZZATO, S., MURRAY, P. J., OCHOA, A., OSTRAND-ROSENBERG, S., RODRIGUEZ, P. C., SICA, A., UMANSKY, V., VONDERHEIDE, R. H. & GABRILOVICH, D. I. 2016. Recommendations for myeloid-derived suppressor cell nomenclature and characterization standards. *Nature Communications,* 7**,** 12150.
BROWN, M., ASSEN, F. P., LEITHNER, A., ABE, J., SCHACHNER, H., ASFOUR, G., BAGO-HORVATH, Z., STEIN, J. V., UHRIN, P., SIXT, M. & KERJASCHKI, D. 2018. Lymph node blood vessels provide exit routes for metastatic tumor cell dissemination in mice. *Science,* 359**,** 1408-1411.
BRUNKOW, M. E., JEFFERY, E. W., HJERRILD, K. A., PAEPER, B., CLARK, L. B., YASAYKO, S.-A., WILKINSON, J. E., GALAS, D., ZIEGLER, S. F. & RAMSDELL, F. 2001. Disruption of a new forkhead/winged-helix protein, scurfin, results in the fatal lymphoproliferative disorder of the scurfy mouse. *Nature Genetics,* 27**,** 68-73.
BUOMMINO, E., TIRINO, V., DE FILIPPIS, A., SILVESTRI, F., NICOLETTI, R., CIAVATTA, M. L., PIROZZI, G. & TUFANO, M. A. 2011. 3-O-methylfunicone, from Penicillium pinophilum, is a selective inhibitor of breast cancer stem cells. *Cell Proliferation,* 44**,** 401-409.
BURNET, M. 1957. Cancer: a biological approach. III. Viruses associated with neoplastic conditions. IV. Practical applications. *Br Med J,* 1**,** 841-7.
BURTON, J. B., PRICEMAN, S. J., SUNG, J. L., BRAKENHIELM, E., AN, D. S., PYTOWSKI, B., ALITALO, K. & WU, L. 2008. Suppression of Prostate Cancer Nodal and Systemic Metastasis by Blockade of the Lymphangiogenic Axis. *Cancer Research,* 68**,** 7828-7837.
BUSSARD, K. M., MUTKUS, L., STUMPF, K., GOMEZ-MANZANO, C. & MARINI, F. C. 2016. Tumor-associated stromal cells as key contributors to the tumor microenvironment. *Breast Cancer Res,* 18**,** 84.

BUSSOLATI, B., DEAMBROSIS, I., RUSSO, S., DEREGIBUS, M. C. & CAMUSSI, G. 2003. Altered angiogenesis and survival in human tumor-derived endothelial cells. *The FASEB Journal,* 17**,** 1159-1161.
BYRNE, S. N., KNOX, M. C. & HALLIDAY, G. M. 2008. TGFβ is responsible for skin tumour infiltration by macrophages enabling the tumours to escape immune destruction. *Immunology & Cell Biology,* 86**,** 92-97.
CABARCAS, S. M., MATHEWS, L. A. & FARRAR, W. L. 2011. The cancer stem cell niche—there goes the neighborhood? *International Journal of Cancer,* 129**,** 2315-2327.
CAHU, J., BUSTANY, S. & SOLA, B. 2012. Senescence-associated secretory phenotype favors the emergence of cancer stem-like cells. *Cell Death & Disease,* 3**,** e446-e446.
CAI, J., LU, W., DU, S., GUO, Z., WANG, H., WEI, W. & SHEN, X. 2018. Tenascin-C Modulates Cell Cycle Progression to Enhance Tumour Cell Proliferation through AKT/FOXO1 Signalling in Pancreatic Cancer. *J Cancer,* 9**,** 4449-4462.
CAMPISI, J. & D'ADDA DI FAGAGNA, F. 2007. Cellular senescence: when bad things happen to good cells. *Nat Rev Mol Cell Biol,* 8**,** 729-40.
CAMUS, M., TOSOLINI, M., MLECNIK, B., PAGÈS, F., KIRILOVSKY, A., BERGER, A., COSTES, A., BINDEA, G., CHAROENTONG, P., BRUNEVAL, P., TRAJANOSKI, Z., FRIDMAN, W.-H. & GALON, J. 2009. Coordination of Intratumoral Immune Reaction and Human Colorectal Cancer Recurrence. *Cancer Research,* 69**,** 2685-2693.
CARMELIET, P. & JAIN, R. K. 2011. Molecular mechanisms and clinical applications of angiogenesis. *Nature,* 473**,** 298-307.
CARUANA, I., SAVOLDO, B., HOYOS, V., WEBER, G., LIU, H., KIM, E. S., ITTMANN, M. M., MARCHETTI, D. & DOTTI, G. 2015. Heparanase promotes tumor infiltration and antitumor activity of CAR-redirected T lymphocytes. *Nat Med,* 21**,** 524-9.
CHANG, J. C. 2016. Cancer stem cells: Role in tumor growth, recurrence, metastasis, and treatment resistance. *Medicine (Baltimore),* 95**,** S20-5.
CHANG, S. H., MIRABOLFATHINEJAD, S. G., KATTA, H., CUMPIAN, A. M., GONG, L., CAETANO, M. S., MOGHADDAM, S. J. & DONG, C. 2014. T helper 17 cells play a critical pathogenic role in lung cancer. *Proceedings of the National Academy of Sciences,* 111**,** 5664-5669.
CHEN, B., DAI, W., MEI, D., LIU, T., LI, S., HE, B., YUAN, L., ZHANG, H., WANG, X. & ZHANG, Q. 2016. Comprehensively priming the tumor microenvironment by cancer-associated fibroblast-targeted liposomes for combined therapy with cancer cell-targeted chemotherapeutic drug delivery system. *J Control Release,* 241**,** 68-80.
CHEN, DANIEL S. & MELLMAN, I. 2013. Oncology Meets Immunology: The Cancer-Immunity Cycle. *Immunity,* 39**,** 1-10.
CHEN, H.-F., HUANG, C.-H., LIU, C.-J., HUNG, J.-J., HSU, C.-C., TENG, S.-C. & WU, K.-J. 2014. Twist1 induces endothelial differentiation of tumour cells through the Jagged1-KLF4 axis. *Nature Communications,* 5**,** 4697.
CHEN, X. & SONG, E. 2019. Turning foes to friends: targeting cancer-associated fibroblasts. *Nat Rev Drug Discov,* 18**,** 99-115.
CHEN, Z., LAURENCE, A. & O'SHEA, J. J. 2007. Signal transduction pathways and transcriptional regulation in the control of Th17 differentiation. *Seminars in Immunology,* 19**,** 400-408.
CHEN, Z., VARNEY, M. L., BACKORA, M. W., COWAN, K., SOLHEIM, J. C., TALMADGE, J. E. & SINGH, R. K. 2005. Down-Regulation of Vascular Endothelial Cell Growth Factor-C Expression Using Small Interfering RNA Vectors in Mammary Tumors Inhibits Tumor Lymphangiogenesis and

Spontaneous Metastasis and Enhances Survival. *Cancer Research,* 65**,** 9004-9011.
CHESNEY, J., PUZANOV, I., COLLICHIO, F., SINGH, P., MILHEM, M. M., GLASPY, J., HAMID, O., ROSS, M., FRIEDLANDER, P., GARBE, C., LOGAN, T. F., HAUSCHILD, A., LEBBÉ, C., CHEN, L., KIM, J. J., GANSERT, J., ANDTBACKA, R. H. I. & KAUFMAN, H. L. 2018. Randomized, Open-Label Phase II Study Evaluating the Efficacy and Safety of Talimogene Laherparepvec in Combination With Ipilimumab Versus Ipilimumab Alone in Patients With Advanced, Unresectable Melanoma. *Journal of Clinical Oncology,* 36**,** 1658-1667.
CHIN, L., XIA, Y., DISCHER, D. E. & JANMEY, P. A. 2016. Mechanotransduction in cancer. *Curr Opin Chem Eng,* 11**,** 77-84.
CIRRI, P. & CHIARUGI, P. 2011. Cancer associated fibroblasts: the dark side of the coin. *American journal of cancer research,* 1**,** 482-497.
COLBECK, E. J., AGER, A., GALLIMORE, A. & JONES, G. W. 2017a. Tertiary Lymphoid Structures in Cancer: Drivers of Antitumor Immunity, Immunosuppression, or Bystander Sentinels in Disease? *Front Immunol,* 8**,** 1830.
COLBECK, E. J., JONES, E., HINDLEY, J. P., SMART, K., SCHULZ, R., BROWNE, M., CUTTING, S., WILLIAMS, A., PARRY, L., GODKIN, A., WARE, C. F., AGER, A. & GALLIMORE, A. 2017b. Treg Depletion Licenses T Cell-Driven HEV Neogenesis and Promotes Tumor Destruction. *Cancer Immunol Res,* 5**,** 1005-1015.
COLLIN, M. & BIGLEY, V. 2018. Human dendritic cell subsets: an update. *Immunology,* 154**,** 3-20.
COLLISON, L. W., WORKMAN, C. J., KUO, T. T., BOYD, K., WANG, Y., VIGNALI, K. M., CROSS, R., SEHY, D., BLUMBERG, R. S. & VIGNALI, D. A. A. 2007. The inhibitory cytokine IL-35 contributes to regulatory T-cell function. *Nature,* 450**,** 566-569.
CONLON, G. A. & MURRAY, G. I. 2019. Recent advances in understanding the roles of matrix metalloproteinases in tumour invasion and metastasis. *The Journal of Pathology,* 247**,** 629-640.
COPPÉ, J.-P., DESPREZ, P.-Y., KRTOLICA, A. & CAMPISI, J. 2010a. The Senescence-Associated Secretory Phenotype: The Dark Side of Tumor Suppression. *Annual Review of Pathology: Mechanisms of Disease,* 5**,** 99-118.
COPPÉ, J.-P., PATIL, C. K., RODIER, F., KRTOLICA, A., BEAUSÉJOUR, C. M., PARRINELLO, S., HODGSON, J. G., CHIN, K., DESPREZ, P.-Y. & CAMPISI, J. 2010b. A Human-Like Senescence-Associated Secretory Phenotype Is Conserved in Mouse Cells Dependent on Physiological Oxygen. *PLOS ONE,* 5**,** e9188.
CORTHAY, A. 2009. How do Regulatory T Cells Work? *Scandinavian Journal of Immunology,* 70**,** 326-336.
CORZO, C. A., CONDAMINE, T., LU, L., COTTER, M. J., YOUN, J.-I., CHENG, P., CHO, H.-I., CELIS, E., QUICENO, D. G., PADHYA, T., MCCAFFREY, T. V., MCCAFFREY, J. C. & GABRILOVICH, D. I. 2010. HIF-1α regulates function and differentiation of myeloid-derived suppressor cells in the tumor microenvironment. *Journal of Experimental Medicine,* 207**,** 2439-2453.
COSTELL, M., GUSTAFSSON, E., ASZÓDI, A., MÖRGELIN, M., BLOCH, W., HUNZIKER, E., ADDICKS, K., TIMPL, R. & FÄSSLER, R. 1999. Perlecan Maintains the Integrity of Cartilage and Some Basement Membranes. *Journal of Cell Biology,* 147**,** 1109-1122.
COX, T. R. & ERLER, J. T. 2011. Remodeling and homeostasis of the extracellular matrix: implications for fibrotic diseases and cancer. *Dis Model Mech,* 4**,** 165-78.

CROSS, W. C. H., GRAHAM, T. A. & WRIGHT, N. A. 2016. New paradigms in clonal evolution: punctuated equilibrium in cancer. *The Journal of Pathology,* 240**,** 126-136.

CROTTY, S. 2015. A brief history of T cell help to B cells. *Nature Reviews Immunology,* 15**,** 185-189.

CRUM, R., SZABO, S. & FOLKMAN, J. 1985. A new class of steroids inhibits angiogenesis in the presence of heparin or a heparin fragment. *Science,* 230**,** 1375-1378.

CUBILLOS-RUIZ, JUAN R., SILBERMAN, PEDRO C., RUTKOWSKI, MELANIE R., CHOPRA, S., PERALES-PUCHALT, A., SONG, M., ZHANG, S., BETTIGOLE, SARAH E., GUPTA, D., HOLCOMB, K., ELLENSON, LORA H., CAPUTO, T., LEE, A.-H., CONEJO-GARCIA, JOSE R. & GLIMCHER, LAURIE H. 2015. ER Stress Sensor XBP1 Controls Anti-tumor Immunity by Disrupting Dendritic Cell Homeostasis. *Cell,* 161**,** 1527-1538.

CURIEL, T. J., COUKOS, G., ZOU, L., ALVAREZ, X., CHENG, P., MOTTRAM, P., EVDEMON-HOGAN, M., CONEJO-GARCIA, J. R., ZHANG, L., BUROW, M., ZHU, Y., WEI, S., KRYCZEK, I., DANIEL, B., GORDON, A., MYERS, L., LACKNER, A., DISIS, M. L., KNUTSON, K. L., CHEN, L. & ZOU, W. 2004. Specific recruitment of regulatory T cells in ovarian carcinoma fosters immune privilege and predicts reduced survival. *Nature Medicine,* 10**,** 942-949.

CURRAN, M. A., MONTALVO, W., YAGITA, H. & ALLISON, J. P. 2010. PD-1 and CTLA-4 combination blockade expands infiltrating T cells and reduces regulatory T and myeloid cells within B16 melanoma tumors. *Proceedings of the National Academy of Sciences,* 107**,** 4275-4280.

D'ADDA DI FAGAGNA, F., REAPER, P. M., CLAY-FARRACE, L., FIEGLER, H., CARR, P., VON ZGLINICKI, T., SARETZKI, G., CARTER, N. P. & JACKSON, S. P. 2003. A DNA damage checkpoint response in telomere-initiated senescence. *Nature,* 426**,** 194-8.

D'ADDA DI FAGAGNA, F., TEO, S. H. & JACKSON, S. P. 2004. Functional links between telomeres and proteins of the DNA-damage response. *Genes Dev,* 18**,** 1781-99.

D'ANGELO, S. P., MELCHIORI, L., MERCHANT, M. S., BERNSTEIN, D., GLOD, J., KAPLAN, R., GRUPP, S., TAP, W. D., CHAGIN, K., BINDER, G. K., BASU, S., LOWTHER, D. E., WANG, R., BATH, N., TIPPING, A., BETTS, G., RAMACHANDRAN, I., NAVENOT, J.-M., ZHANG, H., WELLS, D. K., VAN WINKLE, E., KARI, G., TRIVEDI, T., HOLDICH, T., PANDITE, L., AMADO, R. & MACKALL, C. L. 2018. Antitumor Activity Associated with Prolonged Persistence of Adoptively Transferred NY-ESO-1 ^{c259}T Cells in Synovial Sarcoma. *Cancer Discovery,* 8**,** 944-957.

DAGOGO-JACK, I. & SHAW, A. T. 2018. Tumour heterogeneity and resistance to cancer therapies. *Nature Reviews Clinical Oncology,* 15**,** 81-94.

DAL CORSO, A., GÉBLEUX, R., MURER, P., SOLTERMANN, A. & NERI, D. 2017. A non-internalizing antibody-drug conjugate based on an anthracycline payload displays potent therapeutic activity in vivo. *J Control Release,* 264**,** 211-218.

DALERBA, P., DYLLA, S. J., PARK, I.-K., LIU, R., WANG, X., CHO, R. W., HOEY, T., GURNEY, A., HUANG, E. H., SIMEONE, D. M., SHELTON, A. A., PARMIANI, G., CASTELLI, C. & CLARKE, M. F. 2007. Phenotypic characterization of human colorectal cancer stem cells. *Proceedings of the National Academy of Sciences,* 104**,** 10158-10163.

DAY, C. L., KAUFMANN, D. E., KIEPIELA, P., BROWN, J. A., MOODLEY, E. S., REDDY, S., MACKEY, E. W., MILLER, J. D., LESLIE, A. J., DEPIERRES, C., MNCUBE, Z., DURAISWAMY, J., ZHU, B., EICHBAUM, Q., ALTFELD, M., WHERRY, E. J., COOVADIA, H. M., GOULDER, P. J. R., KLENERMAN, P., AHMED, R., FREEMAN, G. J. & WALKER, B. D. 2006. PD-1 expression on

HIV-specific T cells is associated with T-cell exhaustion and disease progression. *Nature,* 443**,** 350-354.
DE LANGE, T. 2005. Shelterin: the protein complex that shapes and safeguards human telomeres. *Genes Dev,* 19**,** 2100-10.
DE MONTE, L., RENI, M., TASSI, E., CLAVENNA, D., PAPA, I., RECALDE, H., BRAGA, M., DI CARLO, V., DOGLIONI, C. & PROTTI, M. P. 2011. Intratumor T helper type 2 cell infiltrate correlates with cancer-associated fibroblast thymic stromal lymphopoietin production and reduced survival in pancreatic cancer. *Journal of Experimental Medicine,* 208**,** 469-478.
DE PALMA, M., BIZIATO, D. & PETROVA, T. V. 2017. Microenvironmental regulation of tumour angiogenesis. *Nat Rev Cancer,* 17**,** 457-474.
DE SIMONE, M., ARRIGONI, A., ROSSETTI, G., GRUARIN, P., RANZANI, V., POLITANO, C., BONNAL, RAOUL J. P., PROVASI, E., SARNICOLA, MARIA L., PANZERI, I., MORO, M., CROSTI, M., MAZZARA, S., VAIRA, V., BOSARI, S., PALLESCHI, A., SANTAMBROGIO, L., BOVO, G., ZUCCHINI, N., TOTIS, M., GIANOTTI, L., CESANA, G., PEREGO, ROBERTO A., MARONI, N., PISANI CERETTI, A., OPOCHER, E., DE FRANCESCO, R., GEGINAT, J., STUNNENBERG, HENDRIK G., ABRIGNANI, S. & PAGANI, M. 2016. Transcriptional Landscape of Human Tissue Lymphocytes Unveils Uniqueness of Tumor-Infiltrating T Regulatory Cells. *Immunity,* 45**,** 1135-1147.
DEAGLIO , S., DWYER , K. M., GAO , W., FRIEDMAN , D., USHEVA , A., ERAT , A., CHEN , J.-F., ENJYOJI , K., LINDEN , J., OUKKA , M., KUCHROO , V. K., STROM , T. B. & ROBSON , S. C. 2007. Adenosine generation catalyzed by CD39 and CD73 expressed on regulatory T cells mediates immune suppression. *Journal of Experimental Medicine,* 204**,** 1257-1265.
DELIGNE, C., MURDAMOOTHOO, D., GAMMAGE, A. N., GSCHWANDTNER, M., ERNE, W., LOUSTAU, T., MARZEDA, A. M., CARAPITO, R., PAUL, N., VELAZQUEZ-QUESADA, I., MAZZIER, I., SUN, Z., OREND, G. & MIDWOOD, K. S. 2020. Matrix-Targeting Immunotherapy Controls Tumor Growth and Spread by Switching Macrophage Phenotype. *Cancer Immunology Research,* 8**,** 368-382.
DENARDO, D. G., BARRETO, J. B., ANDREU, P., VASQUEZ, L., TAWFIK, D., KOLHATKAR, N. & COUSSENS, L. M. 2009. CD4+ T Cells Regulate Pulmonary Metastasis of Mammary Carcinomas by Enhancing Protumor Properties of Macrophages. *Cancer Cell,* 16**,** 91-102.
DENG, L.-J., WANG, L.-H., PENG, C.-K., LI, Y.-B., HUANG, M.-H., CHEN, M.-F., LEI, X.-P., QI, M., CEN, Y., YE, W.-C., ZHANG, D.-M. & CHEN, W.-M. 2017. Fibroblast Activation Protein α Activated Tripeptide Bufadienolide Antitumor Prodrug with Reduced Cardiotoxicity. *Journal of Medicinal Chemistry,* 60**,** 5320-5333.
DI TOMASO, T., MAZZOLENI, S., WANG, E., SOVENA, G., CLAVENNA, D., FRANZIN, A., MORTINI, P., FERRONE, S., DOGLIONI, C., MARINCOLA, F. M., GALLI, R., PARMIANI, G. & MACCALLI, C. 2010. Immunobiological Characterization of Cancer Stem Cells Isolated from Glioblastoma Patients. *Clinical Cancer Research,* 16**,** 800-813.
DIAS, J. D., HEMMINKI, O., DIACONU, I., HIRVINEN, M., BONETTI, A., GUSE, K., ESCUTENAIRE, S., KANERVA, A., PESONEN, S., LÖSKOG, A., CERULLO, V. & HEMMINKI, A. 2012. Targeted cancer immunotherapy with oncolytic adenovirus coding for a fully human monoclonal antibody specific for CTLA-4. *Gene Therapy,* 19**,** 988-998.
DIDOMENICO, J., LAMANO, J. B., OYON, D., LI, Y., VELICEASA, D., KAUR, G., AMPIE, L., CHOY, W., LAMANO, J. B. & BLOCH, O. 2018. The immune checkpoint protein PD-L1 induces and maintains regulatory T cells in glioblastoma. *OncoImmunology,* 7**,** e1448329.

DIEFENBACH, A., JAMIESON, A. M., LIU, S. D., SHASTRI, N. & RAULET, D. H. 2000. Ligands for the murine NKG2D receptor: expression by tumor cells and activation of NK cells and macrophages. *Nature Immunology,* 1**,** 119-126.
DIGHE, A. S., RICHARDS, E., OLD, L. J. & SCHREIBER, R. D. 1994. Enhanced in vivo growth and resistance to rejection of tumor cells expressing dominant negative IFNγ receptors. *Immunity,* 1**,** 447-456.
DIMOZI, A., MAVROGONATOU, E., SKLIROU, A. & KLETSAS, D. 2015. Oxidative stress inhibits the proliferation, induces premature senescence and promotes a catabolic phenotype in human nucleus pulposus intervertebral disc cells. *Eur Cell Mater,* 30**,** 89-102; discussion 103.
DIRAT, B., BOCHET, L., DABEK, M., DAVIAUD, D., DAUVILLIER, S., MAJED, B., WANG, Y. Y., MEULLE, A., SALLES, B., LE GONIDEC, S., GARRIDO, I., ESCOURROU, G., VALET, P. & MULLER, C. 2011. Cancer-Associated Adipocytes Exhibit an Activated Phenotype and Contribute to Breast Cancer Invasion. *Cancer Research,* 71**,** 2455-2465.
DONG, H., STROME, S. E., SALOMAO, D. R., TAMURA, H., HIRANO, F., FLIES, D. B., ROCHE, P. C., LU, J., ZHU, G., TAMADA, K., LENNON, V. A., CELIS, E. & CHEN, L. 2002. Tumor-associated B7-H1 promotes T-cell apoptosis: A potential mechanism of immune evasion. *Nature Medicine,* 8**,** 793-800.
DONNARUMMA, E., FIORE, D., NAPPA, M., ROSCIGNO, G., ADAMO, A., IABONI, M., RUSSO, V., AFFINITO, A., PUOTI, I., QUINTAVALLE, C., RIENZO, A., PISCUOGLIO, S., THOMAS, R. & CONDORELLI, G. 2017. Cancer-associated fibroblasts release exosomal microRNAs that dictate an aggressive phenotype in breast cancer. *Oncotarget,* 8**,** 19592-19608.
DONTU, G. & WICHA, M. S. 2005. Survival of mammary stem cells in suspension culture: implications for stem cell biology and neoplasia. *J Mammary Gland Biol Neoplasia,* 10**,** 75-86.
DOUGAN, M., DRANOFF, G. & DOUGAN, S. K. 2019. Cancer Immunotherapy: Beyond Checkpoint Blockade *Annual Review of Cancer Biology,* 3**,** 1-21.
DOUGAN, M., INGRAM, J. R., JEONG, H.-J., MOSAHEB, M. M., BRUCK, P. T., ALI, L., PISHESHA, N., BLOMBERG, O., TYLER, P. M., SERVOS, M. M., RASHIDIAN, M., NGUYEN, Q.-D., VON ANDRIAN, U. H., PLOEGH, H. L. & DOUGAN, S. K. 2018. Targeting Cytokine Therapy to the Pancreatic Tumor Microenvironment Using PD-L1–Specific VHHs. *Cancer Immunology Research,* 6**,** 389-401.
DOWNWARD, J. 2004. RNA interference. *BMJ,* 328**,** 1245-8.
DU, T., SHI, G., LI, Y. M., ZHANG, J. F., TIAN, H. W., WEI, Y. Q., DENG, H. & YU, D. C. 2014. Tumor-specific oncolytic adenoviruses expressing granulocyte macrophage colony-stimulating factor or anti-CTLA4 antibody for the treatment of cancers. *Cancer Gene Therapy,* 21**,** 340-348.
DUHEN, T., GEIGER, R., JARROSSAY, D., LANZAVECCHIA, A. & SALLUSTO, F. 2009. Production of interleukin 22 but not interleukin 17 by a subset of human skin-homing memory T cells. *Nature Immunology,* 10**,** 857-863.
DUNN, G. P., BRUCE, A. T., IKEDA, H., OLD, L. J. & SCHREIBER, R. D. 2002. Cancer immunoediting: from immunosurveillance to tumor escape. *Nat Immunol,* 3**,** 991-8.
DUPONT, S., MORSUT, L., ARAGONA, M., ENZO, E., GIULITTI, S., CORDENONSI, M., ZANCONATO, F., LE DIGABEL, J., FORCATO, M., BICCIATO, S., ELVASSORE, N. & PICCOLO, S. 2011. Role of YAP/TAZ in mechanotransduction. *Nature,* 474**,** 179-83.
DVORAK, H. F. 1986. Tumors: wounds that do not heal. Similarities between tumor stroma generation and wound healing. *N Engl J Med,* 315**,** 1650-9.
EARLY BREAST CANCER TRIALISTS' COLLABORATIVE GROUP, E. 2005. Effects of radiotherapy and of differences in the extent of surgery for early breast

cancer on local recurrence and 15-year survival: an overview of the randomised trials. *The Lancet,* 366**,** 2087-2106.
EMENS, L. A., ASCIERTO, P. A., DARCY, P. K., DEMARIA, S., EGGERMONT, A. M. M., REDMOND, W. L., SELIGER, B. & MARINCOLA, F. M. 2017. Cancer immunotherapy: Opportunities and challenges in the rapidly evolving clinical landscape. *Eur J Cancer,* 81**,** 116-129.
EREZ, N., TRUITT, M., OLSON, P. & HANAHAN, D. 2010. Cancer-Associated Fibroblasts Are Activated in Incipient Neoplasia to Orchestrate Tumor-Promoting Inflammation in an NF-κB-Dependent Manner. *Cancer Cell,* 17**,** 135-147.
ESCUDIER, B., PLUZANSKA, A., KORALEWSKI, P., RAVAUD, A., BRACARDA, S., SZCZYLIK, C., CHEVREAU, C., FILIPEK, M., MELICHAR, B., BAJETTA, E., GORBUNOVA, V., BAY, J.-O., BODROGI, I., JAGIELLO-GRUSZFELD, A. & MOORE, N. 2007. Bevacizumab plus interferon alfa-2a for treatment of metastatic renal cell carcinoma: a randomised, double-blind phase III trial. *The Lancet,* 370**,** 2103-2111.
ESHHAR, Z., WAKS, T., GROSS, G. & SCHINDLER, D. G. 1993. Specific activation and targeting of cytotoxic lymphocytes through chimeric single chains consisting of antibody-binding domains and the gamma or zeta subunits of the immunoglobulin and T-cell receptors. *Proceedings of the National Academy of Sciences,* 90**,** 720-724.
EWING, J. 1928. Neoplastic Diseases: A Treatise on Tumours. By James Ewing, A.M., M.D., Sc.D., Professor of Pathology at Cornell University Medical College, N.Y.; Pathologist to the Memorial Hospital. Third edition. Royal 8vo. Pp. 1127, with 546 illustrations. 1928. Philadelphia and London: W. B. Saunders Co. Ltd. 63s. net. *BJS (British Journal of Surgery),* 16**,** 174-175.
FAHL, S. P., COFFEY, F. & WIEST, D. L. 2014. Origins of γδ T Cell Effector Subsets: A Riddle Wrapped in an Enigma. *The Journal of Immunology,* 193**,** 4289-4294.
FANKHAUSER, M., BROGGI, M. A. S., POTIN, L., BORDRY, N., JEANBART, L., LUND, A. W., DA COSTA, E., HAUERT, S., RINCON-RESTREPO, M., TREMBLAY, C., CABELLO, E., HOMICSKO, K., MICHIELIN, O., HANAHAN, D., SPEISER, D. E. & SWARTZ, M. A. 2017. Tumor lymphangiogenesis promotes T cell infiltration and potentiates immunotherapy in melanoma. *Sci Transl Med,* 9.
FEARON, E. R., BURKE, P. J., SCHIFFER, C. A., ZEHNBAUER, B. A. & VOGELSTEIN, B. 1986. Differentiation of Leukemia Cells to Polymorphonuclear Leukocytes in Patients with Acute Nonlymphocytic Leukemia. *New England Journal of Medicine,* 315**,** 15-24.
FEARON, E. R. & VOGELSTEIN, B. 1990. A genetic model for colorectal tumorigenesis. *Cell,* 61**,** 759-67.
FIDLER, I. J. 2003. The pathogenesis of cancer metastasis: the 'seed and soil' hypothesis revisited. *Nat Rev Cancer,* 3**,** 453-8.
FOLEY, E. J. 1953. Antigenic Properties of Methylcholanthrene-induced Tumors in Mice of the Strain of Origin. *Cancer Research,* 13**,** 835-837.
FOLKMAN, J. 1971. Tumor Angiogenesis: Therapeutic Implications. *New England Journal of Medicine,* 285**,** 1182-1186.
FOLKMAN, J. 1974. Tumor angiogenesis. *Adv Cancer Res,* 19**,** 331-58.
FONTENOT, J. D., GAVIN, M. A. & RUDENSKY, A. Y. 2003. Foxp3 programs the development and function of CD4+CD25+ regulatory T cells. *Nature Immunology,* 4**,** 330-336.
FRANKLIN, R. A., LIAO, W., SARKAR, A., KIM, M. V., BIVONA, M. R., LIU, K., PAMER, E. G. & LI, M. O. 2014. The cellular and molecular origin of tumor-associated macrophages. *Science,* 344**,** 921-925.

FRANTZ, C., STEWART, K. M. & WEAVER, V. M. 2010. The extracellular matrix at a glance. *J Cell Sci,* 123**,** 4195-200.
FREEMAN, G. J., LONG, A. J., IWAI, Y., BOURQUE, K., CHERNOVA, T., NISHIMURA, H., FITZ, L. J., MALENKOVICH, N., OKAZAKI, T., BYRNE, M. C., HORTON, H. F., FOUSER, L., CARTER, L., LING, V., BOWMAN, M. R., CARRENO, B. M., COLLINS, M., WOOD, C. R. & HONJO, T. 2000. Engagement of the Pd-1 Immunoinhibitory Receptor by a Novel B7 Family Member Leads to Negative Regulation of Lymphocyte Activation. *Journal of Experimental Medicine,* 192**,** 1027-1034.
GAJEWSKI, T. F., MENG, Y., BLANK, C., BROWN, I., KACHA, A., KLINE, J. & HARLIN, H. 2006. Immune resistance orchestrated by the tumor microenvironment. *Immunological Reviews,* 213**,** 131-145.
GALLIMORE, A., GLITHERO, A., GODKIN, A., TISSOT, A. C., PLÜCKTHUN, A., ELLIOTT, T., HENGARTNER, H. & ZINKERNAGEL, R. 1998. Induction and Exhaustion of Lymphocytic Choriomeningitis Virus–specific Cytotoxic T Lymphocytes Visualized Using Soluble Tetrameric Major Histocompatibility Complex Class I–Peptide Complexes. *Journal of Experimental Medicine,* 187**,** 1383-1393.
GALLIMORE, A. & GODKIN, A. 2008. Regulatory T cells and tumour immunity - observations in mice and men. *Immunology,* 123**,** 157-163.
GALON, J. & BRUNI, D. 2019. Approaches to treat immune hot, altered and cold tumours with combination immunotherapies. *Nature Reviews Drug Discovery,* 18**,** 197-218.
GALON, J., COSTES, A., SANCHEZ-CABO, F., KIRILOVSKY, A., MLECNIK, B., LAGORCE-PAGÈS, C., TOSOLINI, M., CAMUS, M., BERGER, A., WIND, P., ZINZINDOHOUÉ, F., BRUNEVAL, P., CUGNENC, P. H., TRAJANOSKI, Z., FRIDMAN, W. H. & PAGÈS, F. 2006. Type, density, and location of immune cells within human colorectal tumors predict clinical outcome. *Science,* 313**,** 1960-4.
GALON, J., MLECNIK, B., BINDEA, G., ANGELL, H. K., BERGER, A., LAGORCE, C., LUGLI, A., ZLOBEC, I., HARTMANN, A., BIFULCO, C., NAGTEGAAL, I. D., PALMQVIST, R., MASUCCI, G. V., BOTTI, G., TATANGELO, F., DELRIO, P., MAIO, M., LAGHI, L., GRIZZI, F., ASSLABER, M., D'ARRIGO, C., VIDAL-VANACLOCHA, F., ZAVADOVA, E., CHOUCHANE, L., OHASHI, P. S., HAFEZI-BAKHTIARI, S., WOUTERS, B. G., ROEHRL, M., NGUYEN, L., KAWAKAMI, Y., HAZAMA, S., OKUNO, K., OGINO, S., GIBBS, P., WARING, P., SATO, N., TORIGOE, T., ITOH, K., PATEL, P. S., SHUKLA, S. N., WANG, Y., KOPETZ, S., SINICROPE, F. A., SCRIPCARIU, V., ASCIERTO, P. A., MARINCOLA, F. M., FOX, B. A. & PAGÈS, F. 2014. Towards the introduction of the 'Immunoscore' in the classification of malignant tumours. *J Pathol,* 232**,** 199-209.
GALON, J., PAGÈS, F., MARINCOLA, F. M., ANGELL, H. K., THURIN, M., LUGLI, A., ZLOBEC, I., BERGER, A., BIFULCO, C., BOTTI, G., TATANGELO, F., BRITTEN, C. M., KREITER, S., CHOUCHANE, L., DELRIO, P., ARNDT, H., ASSLABER, M., MAIO, M., MASUCCI, G. V., MIHM, M., VIDAL-VANACLOCHA, F., ALLISON, J. P., GNJATIC, S., HAKANSSON, L., HUBER, C., SINGH-JASUJA, H., OTTENSMEIER, C., ZWIERZINA, H., LAGHI, L., GRIZZI, F., OHASHI, P. S., SHAW, P. A., CLARKE, B. A., WOUTERS, B. G., KAWAKAMI, Y., HAZAMA, S., OKUNO, K., WANG, E., O'DONNELL-TORMEY, J., LAGORCE, C., PAWELEC, G., NISHIMURA, M. I., HAWKINS, R., LAPOINTE, R., LUNDQVIST, A., KHLEIF, S. N., OGINO, S., GIBBS, P., WARING, P., SATO, N., TORIGOE, T., ITOH, K., PATEL, P. S., SHUKLA, S. N., PALMQVIST, R., NAGTEGAAL, I. D., WANG, Y., D'ARRIGO, C., KOPETZ, S., SINICROPE, F. A., TRINCHIERI, G., GAJEWSKI, T. F., ASCIERTO, P. A. &

FOX, B. A. 2012. Cancer classification using the Immunoscore: a worldwide task force. *J Transl Med,* 10**,** 205.
GAMBICHLER, T., SCHRÖTER, U., HÖXTERMANN, S., SUSOK, L., STOCKFLETH, E. & BECKER, J. C. 2020. Decline of programmed death-1-positive circulating T regulatory cells predicts more favourable clinical outcome of patients with melanoma under immune checkpoint blockade. *British Journal of Dermatology,* 182**,** 1214-1220.
GAO, Q., DONG, X., XU, Q., ZHU, L., WANG, F., HOU, Y. & CHAO, C.-C. 2019. Therapeutic potential of CRISPR/Cas9 gene editing in engineered T-cell therapy. *Cancer Medicine,* 8**,** 4254-4264.
GAO, Q., QIU, S.-J., FAN, J., ZHOU, J., WANG, X.-Y., XIAO, Y.-S., XU, Y., LI, Y.-W. & TANG, Z.-Y. 2007. Intratumoral Balance of Regulatory and Cytotoxic T Cells Is Associated With Prognosis of Hepatocellular Carcinoma After Resection. *Journal of Clinical Oncology,* 25**,** 2586-2593.
GAO, Q., WANG, X.-Y., QIU, S.-J., ZHOU, J., SHI, Y.-H., ZHANG, B.-H. & FAN, J. 2011. Tumor stroma reaction-related gene signature predicts clinical outcome in human hepatocellular carcinoma. *Cancer Science,* 102**,** 1522-1531.
GENG, Y., SHAO, Y., HE, W., HU, W., XU, Y., CHEN, J., WU, C. & JIANG, J. 2015. Prognostic Role of Tumor-Infiltrating Lymphocytes in Lung Cancer: a Meta-Analysis. *Cell Physiol Biochem,* 37**,** 1560-71.
GERSHON, R. K., COHEN, P., HENCIN, R. & LIEBHABER, S. A. 1972. Suppressor T cells. *J Immunol,* 108**,** 586-90.
GIBLIN, S. P. & MIDWOOD, K. S. 2015. Tenascin-C: Form versus function. *Cell Adh Migr,* 9**,** 48-82.
GILLEN, J., RICHARDSON, D. & MOORE, K. 2019. Angiopoietin-1 and Angiopoietin-2 Inhibitors: Clinical Development. *Current Oncology Reports,* 21**,** 22.
GINHOUX, F., GRETER, M., LEBOEUF, M., NANDI, S., SEE, P., GOKHAN, S., MEHLER, M. F., CONWAY, S. J., NG, L. G., STANLEY, E. R., SAMOKHVALOV, I. M. & MERAD, M. 2010. Fate Mapping Analysis Reveals That Adult Microglia Derive from Primitive Macrophages. *Science,* 330**,** 841-845.
GIRARD, J. P., MOUSSION, C. & FÖRSTER, R. 2012. HEVs, lymphatics and homeostatic immune cell trafficking in lymph nodes. *Nat Rev Immunol,* 12**,** 762-73.
GOCHEVA, V., NABA, A., BHUTKAR, A., GUARDIA, T., MILLER, K. M., LI, C. M., DAYTON, T. L., SANCHEZ-RIVERA, F. J., KIM-KISELAK, C., JAILKHANI, N., WINSLOW, M. M., DEL ROSARIO, A., HYNES, R. O. & JACKS, T. 2017. Quantitative proteomics identify Tenascin-C as a promoter of lung cancer progression and contributor to a signature prognostic of patient survival. *Proc Natl Acad Sci U S A,* 114**,** E5625-E5634.
GOCHEVA, V., WANG, H.-W., GADEA, B. B., SHREE, T., HUNTER, K. E., GARFALL, A. L., BERMAN, T. & JOYCE, J. A. 2010. IL-4 induces cathepsin protease activity in tumor-associated macrophages to promote cancer growth and invasion. *Genes & Development,* 24**,** 241-255.
GOMEZ PERDIGUERO, E., KLAPPROTH, K., SCHULZ, C., BUSCH, K., AZZONI, E., CROZET, L., GARNER, H., TROUILLET, C., DE BRUIJN, M. F., GEISSMANN, F. & RODEWALD, H.-R. 2015. Tissue-resident macrophages originate from yolk-sac-derived erythro-myeloid progenitors. *Nature,* 518**,** 547-551.
GONDEK, D. C., LU, L.-F., QUEZADA, S. A., SAKAGUCHI, S. & NOELLE, R. J. 2005. Cutting Edge: Contact-Mediated Suppression by CD4+CD25+ Regulatory Cells Involves a Granzyme B-Dependent, Perforin-Independent Mechanism. *The Journal of Immunology,* 174**,** 1783-1786.
GORGOULIS, V., ADAMS, P. D., ALIMONTI, A., BENNETT, D. C., BISCHOF, O., BISHOP, C., CAMPISI, J., COLLADO, M., EVANGELOU, K., FERBEYRE, G.,

GIL, J., HARA, E., KRIZHANOVSKY, V., JURK, D., MAIER, A. B., NARITA, M., NIEDERNHOFER, L., PASSOS, J. F., ROBBINS, P. D., SCHMITT, C. A., SEDIVY, J., VOUGAS, K., VON ZGLINICKI, T., ZHOU, D., SERRANO, M. & DEMARIA, M. 2019. Cellular Senescence: Defining a Path Forward. *Cell,* 179**,** 813-827.

GRAS, B., JACQUEROUD, L., WIERINCKX, A., LAMBLOT, C., FAUVET, F., LACHUER, J., PUISIEUX, A. & ANSIEAU, S. 2014. Snail family members unequally trigger EMT and thereby differ in their ability to promote the neoplastic transformation of mammary epithelial cells. *PLoS One,* 9**,** e92254.

GREAVES, M. & MALEY, C. C. 2012. Clonal evolution in cancer. *Nature,* 481**,** 306-13.

GRISERI, T., ASQUITH, M., THOMPSON, C. & POWRIE, F. 2010. OX40 is required for regulatory T cell–mediated control of colitis. *Journal of Experimental Medicine,* 207**,** 699-709.

GROSSMAN, W. J., VERBSKY, J. W., BARCHET, W., COLONNA, M., ATKINSON, J. P. & LEY, T. J. 2004. Human T Regulatory Cells Can Use the Perforin Pathway to Cause Autologous Target Cell Death. *Immunity,* 21**,** 589-601.

GU-TRANTIEN, C., LOI, S., GARAUD, S., EQUETER, C., LIBIN, M., DE WIND, A., RAVOET, M., LE BUANEC, H., SIBILLE, C., MANFOUO-FOUTSOP, G., VEYS, I., HAIBE-KAINS, B., SINGHAL, S. K., MICHIELS, S., ROTHÉ, F., SALGADO, R., DUVILLIER, H., IGNATIADIS, M., DESMEDT, C., BRON, D., LARSIMONT, D., PICCART, M., SOTIRIOU, C. & WILLARD-GALLO, K. 2013. CD4+ follicular helper T cell infiltration predicts breast cancer survival. *The Journal of Clinical Investigation,* 123**,** 2873-2892.

GUILLIAMS, M., MOVAHEDI, K., BOSSCHAERTS, T., VANDENDRIESSCHE, T., CHUAH, M. K., HÉRIN, M., ACOSTA-SANCHEZ, A., MA, L., MOSER, M., VAN GINDERACHTER, J. A., BRYS, L., DE BAETSELIER, P. & BESCHIN, A. 2009. IL-10 Dampens TNF/Inducible Nitric Oxide Synthase-Producing Dendritic Cell-Mediated Pathogenicity during Parasitic Infection. *The Journal of Immunology,* 182**,** 1107-1118.

HANAHAN, D. & COUSSENS, L. M. 2012. Accessories to the crime: functions of cells recruited to the tumor microenvironment. *Cancer Cell,* 21**,** 309-22.

HANAHAN, D. & WEINBERG, R. A. 2000. The hallmarks of cancer. *Cell,* 100**,** 57-70.

HANAHAN, D. & WEINBERG, R. A. 2011. Hallmarks of cancer: the next generation. *Cell,* 144**,** 646-74.

HANNA, E., QUICK, J. & LIBUTTI, S. K. 2009. The tumour microenvironment: a novel target for cancer therapy. *Oral Dis,* 15**,** 8-17.

HARIBHAI, D., WILLIAMS, JASON B., JIA, S., NICKERSON, D., SCHMITT, ERICA G., EDWARDS, B., ZIEGELBAUER, J., YASSAI, M., LI, S.-H., RELLAND, LANCE M., WISE, PETRA M., CHEN, A., ZHENG, Y.-Q., SIMPSON, PIPPA M., GORSKI, J., SALZMAN, NITA H., HESSNER, MARTIN J., CHATILA, TALAL A. & WILLIAMS, CALVIN B. 2011. A Requisite Role for Induced Regulatory T Cells in Tolerance Based on Expanding Antigen Receptor Diversity. *Immunity,* 35**,** 109-122.

HARRINGTON, K., FREEMAN, D. J., KELLY, B., HARPER, J. & SORIA, J.-C. 2019. Optimizing oncolytic virotherapy in cancer treatment. *Nature Reviews Drug Discovery,* 18**,** 689-706.

HATINA, J., KRIPNEROVA, M., HOUFKOVA, K., PESTA, M., KUNCOVA, J., SANA, J., SLABY, O. & RODRÍGUEZ, R. 2019. Sarcoma Stem Cell Heterogeneity. *Adv Exp Med Biol,* 1123**,** 95-118.

HAY, T., MATTHEWS, J. R., PIETZKA, L., LAU, A., CRANSTON, A., NYGREN, A. O., DOUGLAS-JONES, A., SMITH, G. C., MARTIN, N. M., O'CONNOR, M. & CLARKE, A. R. 2009. Poly(ADP-ribose) polymerase-1 inhibitor treatment regresses autochthonous Brca2/p53-mutant mammary tumors in vivo and delays tumor relapse in combination with carboplatin. *Cancer Res,* 69**,** 3850-5.

HE, J., LIU, Y., XIE, X., ZHU, T., SOULES, M., DIMECO, F., VESCOVI, A. L., FAN, X. & LUBMAN, D. M. 2010. Identification of cell surface glycoprotein markers for glioblastoma-derived stem-like cells using a lectin microarray and LC-MS/MS approach. *J Proteome Res,* 9**,** 2565-72.
HEGDE, P. S., KARANIKAS, V. & EVERS, S. 2016. The Where, the When, and the How of Immune Monitoring for Cancer Immunotherapies in the Era of Checkpoint Inhibition. *Clinical Cancer Research,* 22**,** 1865-1874.
HENNEQUIN, A., DERANGÈRE, V., BOIDOT, R., APETOH, L., VINCENT, J., ORRY, D., FRAISSE, J., CAUSERET, S., MARTIN, F., ARNOULD, L., BELTJENS, F., GHIRINGHELLI, F. & LADOIRE, S. 2016. Tumor infiltration by Tbet+ effector T cells and CD20+ B cells is associated with survival in gastric cancer patients. *OncoImmunology,* 5**,** e1054598.
HERNANDEZ-SEGURA, A., NEHME, J. & DEMARIA, M. 2018. Hallmarks of Cellular Senescence. *Trends Cell Biol,* 28**,** 436-453.
HIDA, K., HIDA, Y., AMIN, D. N., FLINT, A. F., PANIGRAHY, D., MORTON, C. C. & KLAGSBRUN, M. 2004. Tumor-Associated Endothelial Cells with Cytogenetic Abnormalities. *Cancer Research,* 64**,** 8249-8255.
HIGANO, C. S., SCHELLHAMMER, P. F., SMALL, E. J., BURCH, P. A., NEMUNAITIS, J., YUH, L., PROVOST, N. & FROHLICH, M. W. 2009. Integrated data from 2 randomized, double-blind, placebo-controlled, phase 3 trials of active cellular immunotherapy with sipuleucel-T in advanced prostate cancer. *Cancer,* 115**,** 3670-3679.
HINDLEY, J. P., FERREIRA, C., JONES, E., LAUDER, S. N., LADELL, K., WYNN, K. K., BETTS, G. J., SINGH, Y., PRICE, D. A., GODKIN, A. J., DYSON, J. & GALLIMORE, A. 2011. Analysis of the T-cell receptor repertoires of tumor-infiltrating conventional and regulatory T cells reveals no evidence for conversion in carcinogen-induced tumors. *Cancer Res,* 71**,** 736-46.
HINDLEY, J. P., JONES, E., SMART, K., BRIDGEMAN, H., LAUDER, S. N., ONDONDO, B., CUTTING, S., LADELL, K., WYNN, K. K., WITHERS, D., PRICE, D. A., AGER, A., GODKIN, A. J. & GALLIMORE, A. M. 2012. T-cell trafficking facilitated by high endothelial venules is required for tumor control after regulatory T-cell depletion. *Cancer Res,* 72**,** 5473-82.
HODI, F. S., O'DAY, S. J., MCDERMOTT, D. F., WEBER, R. W., SOSMAN, J. A., HAANEN, J. B., GONZALEZ, R., ROBERT, C., SCHADENDORF, D., HASSEL, J. C., AKERLEY, W., VAN DEN EERTWEGH, A. J. M., LUTZKY, J., LORIGAN, P., VAUBEL, J. M., LINETTE, G. P., HOGG, D., OTTENSMEIER, C. H., LEBBÉ, C., PESCHEL, C., QUIRT, I., CLARK, J. I., WOLCHOK, J. D., WEBER, J. S., TIAN, J., YELLIN, M. J., NICHOL, G. M., HOOS, A. & URBA, W. J. 2010. Improved Survival with Ipilimumab in Patients with Metastatic Melanoma. *New England Journal of Medicine,* 363**,** 711-723.
HOFHEINZ, R. D., AL-BATRAN, S. E., HARTMANN, F., HARTUNG, G., JÄGER, D., RENNER, C., TANSWELL, P., KUNZ, U., AMELSBERG, A., KUTHAN, H. & STEHLE, G. 2003. Stromal Antigen Targeting by a Humanised Monoclonal Antibody: An Early Phase II Trial of Sibrotuzumab in Patients with Metastatic Colorectal Cancer. *Oncology Research and Treatment,* 26**,** 44-48.
HONKANEN, T. J., TIKKANEN, A., KARIHTALA, P., MÄKINEN, M., VÄYRYNEN, J. P. & KOIVUNEN, J. P. 2019. Prognostic and predictive role of tumour-associated macrophages in HER2 positive breast cancer. *Scientific Reports,* 9**,** 10961.
HOY, A. J., BALABAN, S. & SAUNDERS, D. N. 2017. Adipocyte-Tumor Cell Metabolic Crosstalk in Breast Cancer. *Trends Mol Med,* 23**,** 381-392.
HUANG, A., GOLUMBEK, P., AHMADZADEH, M., JAFFEE, E., PARDOLL, D. & LEVITSKY, H. 1994. Role of bone marrow-derived cells in presenting MHC class I-restricted tumor antigens. *Science,* 264**,** 961-965.

HUANG, X., BAI, X., CAO, Y., WU, J., HUANG, M., TANG, D., TAO, S., ZHU, T., LIU, Y., YANG, Y., ZHOU, X., ZHAO, Y., WU, M., WEI, J., WANG, D., XU, G., WANG, S., MA, D. & ZHOU, J. 2010. Lymphoma endothelium preferentially expresses Tim-3 and facilitates the progression of lymphoma by mediating immune evasion. *Journal of Experimental Medicine,* 207**,** 505-520.

HUBACKOVA, S., KUCEROVA, A., MICHLITS, G., KYJACOVA, L., REINIS, M., KOROLOV, O., BARTEK, J. & HODNY, Z. 2016. IFNγ induces oxidative stress, DNA damage and tumor cell senescence via TGFβ/SMAD signaling-dependent induction of Nox4 and suppression of ANT2. *Oncogene,* 35**,** 1236-49.

HUGHES, E., SCURR, M., CAMPBELL, E., JONES, E., GODKIN, A. & GALLIMORE, A. 2018. T-cell modulation by cyclophosphamide for tumour therapy. *Immunology,* 154**,** 62-68.

HUGHES, R., QIAN, B.-Z., ROWAN, C., MUTHANA, M., KEKLIKOGLOU, I., OLSON, O. C., TAZZYMAN, S., DANSON, S., ADDISON, C., CLEMONS, M., GONZALEZ-ANGULO, A. M., JOYCE, J. A., DE PALMA, M., POLLARD, J. W. & LEWIS, C. E. 2015. Perivascular M2 Macrophages Stimulate Tumor Relapse after Chemotherapy. *Cancer Research,* 75**,** 3479-3491.

HURWITZ, A. A., YU, T. F.-Y., LEACH, D. R. & ALLISON, J. P. 1998. CTLA-4 blockade synergizes with tumor-derived granulocyte– macrophage colony-stimulating factor for treatment of an experimental mammary carcinoma. *Proceedings of the National Academy of Sciences,* 95**,** 10067-10071.

HWANG, W. T., ADAMS, S. F., TAHIROVIC, E., HAGEMANN, I. S. & COUKOS, G. 2012. Prognostic significance of tumor-infiltrating T cells in ovarian cancer: a meta-analysis. *Gynecol Oncol,* 124**,** 192-8.

HYUN, K.-H., YOON, C.-H., KIM, R.-K., LIM, E.-J., AN, S., PARK, M.-J., HYUN, J.-W., SUH, Y., KIM, M.-J. & LEE, S.-J. 2011. Eckol suppresses maintenance of stemness and malignancies in glioma stem-like cells. *Toxicology and Applied Pharmacology,* 254**,** 32-40.

IMIELINSKI, M., BERGER, ALICE H., HAMMERMAN, PETER S., HERNANDEZ, B., PUGH, TREVOR J., HODIS, E., CHO, J., SUH, J., CAPELLETTI, M., SIVACHENKO, A., SOUGNEZ, C., AUCLAIR, D., LAWRENCE, MICHAEL S., STOJANOV, P., CIBULSKIS, K., CHOI, K., DE WAAL, L., SHARIFNIA, T., BROOKS, A., GREULICH, H., BANERJI, S., ZANDER, T., SEIDEL, D., LEENDERS, F., ANSÉN, S., LUDWIG, C., ENGEL-RIEDEL, W., STOELBEN, E., WOLF, J., GOPARJU, C., THOMPSON, K., WINCKLER, W., KWIATKOWSKI, D., JOHNSON, BRUCE E., JÄNNE, PASI A., MILLER, VINCENT A., PAO, W., TRAVIS, WILLIAM D., PASS, HARVEY I., GABRIEL, STACEY B., LANDER, ERIC S., THOMAS, ROMAN K., GARRAWAY, LEVI A., GETZ, G. & MEYERSON, M. 2012. Mapping the Hallmarks of Lung Adenocarcinoma with Massively Parallel Sequencing. *Cell,* 150**,** 1107-1120.

ISKAROS, B. F., TANAKA, K. E., HU, X., KADISH, A. S. & STEINBERG, J. J. 1997. Morphologic pattern of tenascin as a diagnostic biomarker in colon cancer. *J Surg Oncol,* 64**,** 98-101.

IVANOV, I. I., MCKENZIE, B. S., ZHOU, L., TADOKORO, C. E., LEPELLEY, A., LAFAILLE, J. J., CUA, D. J. & LITTMAN, D. R. 2006. The Orphan Nuclear Receptor RORbt Directs the Differentiation Program of Proinflammatory IL-17+ T Helper Cells. *Cell,* 126**,** 1121-1133.

IWATA-KAJIHARA, T., SUMIMOTO, H., KAWAMURA, N., UEDA, R., TAKAHASHI, T., MIZUGUCHI, H., MIYAGISHI, M., TAKEDA, K. & KAWAKAMI, Y. 2011. Enhanced Cancer Immunotherapy Using STAT3-Depleted Dendritic Cells with High Th1-Inducing Ability and Resistance to Cancer Cell-Derived Inhibitory Factors. *The Journal of Immunology,* 187**,** 27-36.

IYER, A. K., KHALED, G., FANG, J. & MAEDA, H. 2006. Exploiting the enhanced permeability and retention effect for tumor targeting. *Drug Discov Today,* 11**,** 812-8.

JACOBSON, O., YAN, X., NIU, G., WEISS, I. D., MA, Y., SZAJEK, L. P., SHEN, B., KIESEWETTER, D. O. & CHEN, X. 2015. PET imaging of tenascin-C with a radiolabeled single-stranded DNA aptamer. *J Nucl Med,* 56**,** 616-21.

JAMAL-HANJANI, M., HACKSHAW, A., NGAI, Y., SHAW, J., DIVE, C., QUEZADA, S., MIDDLETON, G., DE BRUIN, E., LE QUESNE, J., SHAFI, S., FALZON, M., HORSWELL, S., BLACKHALL, F., KHAN, I., JANES, S., NICOLSON, M., LAWRENCE, D., FORSTER, M., FENNELL, D., LEE, S.-M., LESTER, J., KERR, K., MULLER, S., ILES, N., SMITH, S., MURUGAESU, N., MITTER, R., SALM, M., STUART, A., MATTHEWS, N., ADAMS, H., AHMAD, T., ATTANOOS, R., BENNETT, J., BIRKBAK, N. J., BOOTON, R., BRADY, G., BUCHAN, K., CAPITANO, A., CHETTY, M., COBBOLD, M., CROSBIE, P., DAVIES, H., DENISON, A., DJEARMAN, M., GOLDMAN, J., HASWELL, T., JOSEPH, L., KORNASZEWSKA, M., KREBS, M., LANGMAN, G., MACKENZIE, M., MILLAR, J., MORGAN, B., NAIDU, B., NONAKA, D., PEGGS, K., PRITCHARD, C., REMMEN, H., ROWAN, A., SHAH, R., SMITH, E., SUMMERS, Y., TAYLOR, M., VEERIAH, S., WALLER, D., WILCOX, B., WILCOX, M., WOOLHOUSE, I., MCGRANAHAN, N. & SWANTON, C. 2014. Tracking Genomic Cancer Evolution for Precision Medicine: The Lung TRACERx Study. *PLOS Biology,* 12**,** e1001906.

JAMAL-HANJANI, M., WILSON, G. A., MCGRANAHAN, N., BIRKBAK, N. J., WATKINS, T. B. K., VEERIAH, S., SHAFI, S., JOHNSON, D. H., MITTER, R., ROSENTHAL, R., SALM, M., HORSWELL, S., ESCUDERO, M., MATTHEWS, N., ROWAN, A., CHAMBERS, T., MOORE, D. A., TURAJLIC, S., XU, H., LEE, S.-M., FORSTER, M. D., AHMAD, T., HILEY, C. T., ABBOSH, C., FALZON, M., BORG, E., MARAFIOTI, T., LAWRENCE, D., HAYWARD, M., KOLVEKAR, S., PANAGIOTOPOULOS, N., JANES, S. M., THAKRAR, R., AHMED, A., BLACKHALL, F., SUMMERS, Y., SHAH, R., JOSEPH, L., QUINN, A. M., CROSBIE, P. A., NAIDU, B., MIDDLETON, G., LANGMAN, G., TROTTER, S., NICOLSON, M., REMMEN, H., KERR, K., CHETTY, M., GOMERSALL, L., FENNELL, D. A., NAKAS, A., RATHINAM, S., ANAND, G., KHAN, S., RUSSELL, P., EZHIL, V., ISMAIL, B., IRVIN-SELLERS, M., PRAKASH, V., LESTER, J. F., KORNASZEWSKA, M., ATTANOOS, R., ADAMS, H., DAVIES, H., DENTRO, S., TANIERE, P., O'SULLIVAN, B., LOWE, H. L., HARTLEY, J. A., ILES, N., BELL, H., NGAI, Y., SHAW, J. A., HERRERO, J., SZALLASI, Z., SCHWARZ, R. F., STEWART, A., QUEZADA, S. A., LE QUESNE, J., VAN LOO, P., DIVE, C., HACKSHAW, A. & SWANTON, C. 2017. Tracking the Evolution of Non–Small-Cell Lung Cancer. *New England Journal of Medicine,* 376**,** 2109-2121.

JANSSENS, W., CARLIER, V., WU, B., VANDERELST, L., JACQUEMIN, M. G. & SAINT-REMY, J.-M. R. 2003. CD4+CD25+ T Cells Lyse Antigen-Presenting B Cells by Fas-Fas Ligand Interaction in an Epitope-Specific Manner. *The Journal of Immunology,* 171**,** 4604-4612.

JATOI, I., HILSENBECK, S. G., CLARK, G. M. & OSBORNE, C. K. 1999. Significance of Axillary Lymph Node Metastasis in Primary Breast Cancer. *Journal of Clinical Oncology,* 17**,** 2334-2334.

JOHANSSON-PERCIVAL, A., HE, B., LI, Z. J., KJELLÉN, A., RUSSELL, K., LI, J., LARMA, I. & GANSS, R. 2017. De novo induction of intratumoral lymphoid structures and vessel normalization enhances immunotherapy in resistant tumors. *Nat Immunol,* 18**,** 1207-1217.

JOHNSON, L. A., MORGAN, R. A., DUDLEY, M. E., CASSARD, L., YANG, J. C., HUGHES, M. S., KAMMULA, U. S., ROYAL, R. E., SHERRY, R. M.,

WUNDERLICH, J. R., LEE, C.-C. R., RESTIFO, N. P., SCHWARZ, S. L., COGDILL, A. P., BISHOP, R. J., KIM, H., BREWER, C. C., RUDY, S. F., VANWAES, C., DAVIS, J. L., MATHUR, A., RIPLEY, R. T., NATHAN, D. A., LAURENCOT, C. M. & ROSENBERG, S. A. 2009. Gene therapy with human and mouse T-cell receptors mediates cancer regression and targets normal tissues expressing cognate antigen. *Blood,* 114**,** 535-546.

JOHNSON, S., CHEN, H. & LO, P. K. 2013. Tumorsphere Formation Assays. *Bio Protoc,* 3.

JONES, E., DAHM-VICKER, M., SIMON, A. K., GREEN, A., POWRIE, F., CERUNDOLO, V. & GALLIMORE, A. 2002. Depletion of CD25+ regulatory cells results in suppression of melanoma growth and induction of autoreactivity in mice. *Cancer Immun,* 2**,** 1.

JONES, E., GALLIMORE, A. & AGER, A. 2018. Defining High Endothelial Venules and Tertiary Lymphoid Structures in Cancer. *Methods Mol Biol,* 1845**,** 99-118.

JORDAN, M. S., BOESTEANU, A., REED, A. J., PETRONE, A. L., HOLENBECK, A. E., LERMAN, M. A., NAJI, A. & CATON, A. J. 2001. Thymic selection of CD4+CD25+ regulatory T cells induced by an agonist self-peptide. *Nature Immunology,* 2**,** 301-306.

JOSHI, K., ROBERT DE MASSY, M., ISMAIL, M., READING, J. L., UDDIN, I., WOOLSTON, A., HATIPOGLU, E., OAKES, T., ROSENTHAL, R., PEACOCK, T., RONEL, T., NOURSADEGHI, M., TURATI, V., FURNESS, A. J. S., GEORGIOU, A., WONG, Y. N. S., BEN AISSA, A., WERNER SUNDERLAND, M., JAMAL-HANJANI, M., VEERIAH, S., BIRKBAK, N. J., WILSON, G. A., HILEY, C. T., GHORANI, E., GUERRA-ASSUNÇÃO, J. A., HERRERO, J., ENVER, T., HADRUP, S. R., HACKSHAW, A., PEGGS, K. S., MCGRANAHAN, N., SWANTON, C., QUEZADA, S. A., CHAIN, B. & CONSORTIUM, T. R. 2019. Spatial heterogeneity of the T cell receptor repertoire reflects the mutational landscape in lung cancer. *Nature Medicine,* 25**,** 1549-1559.

KABANOVA, A., ZURLI, V. & BALDARI, C. T. 2018. Signals Controlling Lytic Granule Polarization at the Cytotoxic Immune Synapse. *Front Immunol,* 9**,** 307.

KALLURI, R. 2003. Basement membranes: structure, assembly and role in tumour angiogenesis. *Nat Rev Cancer,* 3**,** 422-33.

KALLURI, R. & WEINBERG, R. A. 2009. The basics of epithelial-mesenchymal transition. *J Clin Invest,* 119**,** 1420-8.

KAMADA, T., TOGASHI, Y., TAY, C., HA, D., SASAKI, A., NAKAMURA, Y., SATO, E., FUKUOKA, S., TADA, Y., TANAKA, A., MORIKAWA, H., KAWAZOE, A., KINOSHITA, T., SHITARA, K., SAKAGUCHI, S. & NISHIKAWA, H. 2019. PD-1⁺ regulatory T cells amplified by PD-1 blockade promote hyperprogression of cancer. *Proceedings of the National Academy of Sciences,* 116**,** 9999-10008.

KAN, Z., JAISWAL, B. S., STINSON, J., JANAKIRAMAN, V., BHATT, D., STERN, H. M., YUE, P., HAVERTY, P. M., BOURGON, R., ZHENG, J., MOORHEAD, M., CHAUDHURI, S., TOMSHO, L. P., PETERS, B. A., PUJARA, K., CORDES, S., DAVIS, D. P., CARLTON, V. E. H., YUAN, W., LI, L., WANG, W., EIGENBROT, C., KAMINKER, J. S., EBERHARD, D. A., WARING, P., SCHUSTER, S. C., MODRUSAN, Z., ZHANG, Z., STOKOE, D., DE SAUVAGE, F. J., FAHAM, M. & SESHAGIRI, S. 2010. Diverse somatic mutation patterns and pathway alterations in human cancers. *Nature,* 466**,** 869-873.

KANTOFF, P. W., HIGANO, C. S., SHORE, N. D., BERGER, E. R., SMALL, E. J., PENSON, D. F., REDFERN, C. H., FERRARI, A. C., DREICER, R., SIMS, R. B., XU, Y., FROHLICH, M. W. & SCHELLHAMMER, P. F. 2010. Sipuleucel-T Immunotherapy for Castration-Resistant Prostate Cancer. *New England Journal of Medicine,* 363**,** 411-422.

KAPLAN, D. H., SHANKARAN, V., DIGHE, A. S., STOCKERT, E., AGUET, M., OLD, L. J. & SCHREIBER, R. D. 1998. Demonstration of an interferon γ-dependent tumor surveillance system in immunocompetent mice. *Proceedings of the National Academy of Sciences,* 95**,** 7556-7561.
KAPLAN, M. H., HUFFORD, M. M. & OLSON, M. R. 2015. The development and in vivo function of T helper 9 cells. *Nature Reviews Immunology,* 15**,** 295-307.
KIM, J. H., OH, S.-H., KIM, E.-J., PARK, S. J., HONG, S. P., CHEON, J. H., KIM, T. I. & KIM, W. H. 2012. The role of myofibroblasts in upregulation of S100A8 and S100A9 and the differentiation of myeloid cells in the colorectal cancer microenvironment. *Biochemical and Biophysical Research Communications,* 423**,** 60-66.
KIM, J. M. & CHEN, D. S. 2016. Immune escape to PD-L1/PD-1 blockade: seven steps to success (or failure). *Annals of Oncology,* 27**,** 1492-1504.
KIM, J. M., RASMUSSEN, J. P. & RUDENSKY, A. Y. 2007. Regulatory T cells prevent catastrophic autoimmunity throughout the lifespan of mice. *Nat Immunol,* 8**,** 191-7.
KISSICK, H. T. & SANDA, M. G. 2015. The role of active vaccination in cancer immunotherapy: lessons from clinical trials. *Current Opinion in Immunology,* 35**,** 15-22.
KLAGES, K., MAYER, C. T., LAHL, K., LODDENKEMPER, C., TENG, M. W. L., NGIOW, S. F., SMYTH, M. J., HAMANN, A., HUEHN, J. & SPARWASSER, T. 2010. Selective Depletion of Foxp3+ Regulatory T Cells Improves Effective Therapeutic Vaccination against Established Melanoma. *Cancer Research,* 70**,** 7788-7799.
KNUDSON, A. G. 1971. Mutation and cancer: statistical study of retinoblastoma. *Proc Natl Acad Sci U S A,* 68**,** 820-3.
KOEBEL, C. M., VERMI, W., SWANN, J. B., ZERAFA, N., RODIG, S. J., OLD, L. J., SMYTH, M. J. & SCHREIBER, R. D. 2007. Adaptive immunity maintains occult cancer in an equilibrium state. *Nature,* 450**,** 903-907.
KOJIMA, Y., ACAR, A., EATON, E. N., MELLODY, K. T., SCHEEL, C., BEN-PORATH, I., ONDER, T. T., WANG, Z. C., RICHARDSON, A. L., WEINBERG, R. A. & ORIMO, A. 2010. Autocrine TGF-β and stromal cell-derived factor-1 (SDF-1) signaling drives the evolution of tumor-promoting mammary stromal myofibroblasts. *Proceedings of the National Academy of Sciences,* 107**,** 20009-20014.
KORYBALSKA, K., KAWKA, E., KUSCH, A., AREGGER, F., DRAGUN, D., JÖRRES, A., BRĘBOROWICZ, A. & WITOWSKI, J. 2012. Recovery of Senescent Endothelial Cells From Injury. *The Journals of Gerontology: Series A,* 68**,** 250-257.
KRAMAN, M., BAMBROUGH, P. J., ARNOLD, J. N., ROBERTS, E. W., MAGIERA, L., JONES, J. O., GOPINATHAN, A., TUVESON, D. A. & FEARON, D. T. 2010. Suppression of antitumor immunity by stromal cells expressing fibroblast activation protein-alpha. *Science,* 330**,** 827-30.
KREN, L., MUCKOVA, K., LZICAROVA, E., SOVA, M., VYBIHAL, V., SVOBODA, T., FADRUS, P., SMRCKA, M., SLABY, O., LAKOMY, R., VANHARA, P., KRENOVA, Z. & MICHALEK, J. 2010. Production of immune-modulatory nonclassical molecules HLA-G and HLA-E by tumor infiltrating ameboid microglia/macrophages in glioblastomas: A role in innate immunity? *Journal of Neuroimmunology,* 220**,** 131-135.
KRESO, A. & DICK, JOHN E. 2014. Evolution of the Cancer Stem Cell Model. *Cell Stem Cell,* 14**,** 275-291.
KRISHNA PRIYA, S., NAGARE, R. P., SNEHA, V. S., SIDHANTH, C., BINDHYA, S., MANASA, P. & GANESAN, T. S. 2016. Tumour angiogenesis-Origin of blood vessels. *Int J Cancer,* 139**,** 729-35.

KRUMMEL, M. F. & ALLISON, J. P. 1995. CD28 and CTLA-4 have opposing effects on the response of T cells to stimulation. *Journal of Experimental Medicine,* 182**,** 459-465.
KRYCZEK, I., BANERJEE, M., CHENG, P., VATAN, L., SZELIGA, W., WEI, S., HUANG, E., FINLAYSON, E., SIMEONE, D., WELLING, T. H., CHANG, A., COUKOS, G., LIU, R. & ZOU, W. 2009. Phenotype, distribution, generation, and functional and clinical relevance of Th17 cells in the human tumor environments. *Blood,* 114**,** 1141-1149.
KRYCZEK, I., LIN, Y., NAGARSHETH, N., PENG, D., ZHAO, L., ZHAO, E., VATAN, L., SZELIGA, W., DOU, Y., OWENS, S., ZGODZINSKI, W., MAJEWSKI, M., WALLNER, G., FANG, J., HUANG, E. & ZOU, W. 2014. IL-22+CD4+ T Cells Promote Colorectal Cancer Stemness via STAT3 Transcription Factor Activation and Induction of the Methyltransferase DOT1L. *Immunity,* 40**,** 772-784.
KUANG, D.-M., XIAO, X., ZHAO, Q., CHEN, M.-M., LI, X.-F., LIU, R.-X., WEI, Y., OUYANG, F.-Z., CHEN, D.-P., WU, Y., LAO, X.-M., DENG, H. & ZHENG, L. 2014. B7-H1–expressing antigen-presenting cells mediate polarization of protumorigenic Th22 subsets. *The Journal of Clinical Investigation,* 124**,** 4657-4667.
KUANG, D.-M., ZHAO, Q., PENG, C., XU, J., ZHANG, J.-P., WU, C. & ZHENG, L. 2009. Activated monocytes in peritumoral stroma of hepatocellular carcinoma foster immune privilege and disease progression through PD-L1. *Journal of Experimental Medicine,* 206**,** 1327-1337.
KUMAR, V., PATEL, S., TCYGANOV, E. & GABRILOVICH, D. I. 2016. The Nature of Myeloid-Derived Suppressor Cells in the Tumor Microenvironment. *Trends in Immunology,* 37**,** 208-220.
KUMAZAKI, T., ROBETORYE, R. S., ROBETORYE, S. C. & SMITH, J. R. 1991. Fibronectin expression increases during in vitro cellular senescence: Correlation with increased cell area. *Experimental Cell Research,* 195**,** 13-19.
KUROZUMI, K., HARDCASTLE, J., THAKUR, R., YANG, M., CHRISTOFORIDIS, G., FULCI, G., HOCHBERG, F. H., WEISSLEDER, R., CARSON, W., CHIOCCA, E. A. & KAUR, B. 2007. Effect of Tumor Microenvironment Modulation on the Efficacy of Oncolytic Virus Therapy. *JNCI: Journal of the National Cancer Institute,* 99**,** 1768-1781.
KUSUDA, T., SHIGEMASA, K., ARIHIRO, K., FUJII, T., NAGAI, N. & OHAMA, K. 2005. Relative expression levels of Th1 and Th2 cytokine mRNA are independent prognostic factors in patients with ovarian cancer. *Oncol Rep,* 13**,** 1153-8.
LABERGE, R.-M., AWAD, P., CAMPISI, J. & DESPREZ, P.-Y. 2012. Epithelial-Mesenchymal Transition Induced by Senescent Fibroblasts. *Cancer Microenvironment,* 5**,** 39-44.
LABERGE, R.-M., SUN, Y., ORJALO, A. V., PATIL, C. K., FREUND, A., ZHOU, L., CURRAN, SAMUEL C., DAVALOS, A. R., WILSON-EDELL, K. A., LIU, S., LIMBAD, C., DEMARIA, M., LI, P., HUBBARD, G. B., IKENO, Y., JAVORS, M., DESPREZ, P.-Y., BENZ, C. C., KAPAHI, P., NELSON, P. S. & CAMPISI, J. 2015. MTOR regulates the pro-tumorigenic senescence-associated secretory phenotype by promoting IL1A translation. *Nature Cell Biology,* 17**,** 1049-1061.
LAKLAI, H., MIROSHNIKOVA, Y. A., PICKUP, M. W., COLLISSON, E. A., KIM, G. E., BARRETT, A. S., HILL, R. C., LAKINS, J. N., SCHLAEPFER, D. D., MOUW, J. K., LEBLEU, V. S., ROY, N., NOVITSKIY, S. V., JOHANSEN, J. S., POLI, V., KALLURI, R., IACOBUZIO-DONAHUE, C. A., WOOD, L. D., HEBROK, M., HANSEN, K., MOSES, H. L. & WEAVER, V. M. 2016. Genotype tunes pancreatic ductal adenocarcinoma tissue tension to induce matricellular fibrosis and tumor progression. *Nat Med,* 22**,** 497-505.

LANGE, K., KAMMERER, M., HEGI, M. E., GROTEGUT, S., DITTMANN, A., HUANG, W., FLURI, E., YIP, G. W., GÖTTE, M., RUIZ, C. & OREND, G. 2007. Endothelin receptor type B counteracts tenascin-C-induced endothelin receptor type A-dependent focal adhesion and actin stress fiber disorganization. *Cancer Res,* 67**,** 6163-73.
LANGE, K., KAMMERER, M., SAUPE, F., HEGI, M. E., GROTEGUT, S., FLURI, E. & OREND, G. 2008. Combined lysophosphatidic acid/platelet-derived growth factor signaling triggers glioma cell migration in a tenascin-C microenvironment. *Cancer Res,* 68**,** 6942-52.
LARKIN, J., CHIARION-SILENI, V., GONZALEZ, R., GROB, J.-J., RUTKOWSKI, P., LAO, C. D., COWEY, C. L., SCHADENDORF, D., WAGSTAFF, J., DUMMER, R., FERRUCCI, P. F., SMYLIE, M., HOGG, D., HILL, A., MÁRQUEZ-RODAS, I., HAANEN, J., GUIDOBONI, M., MAIO, M., SCHÖFFSKI, P., CARLINO, M. S., LEBBÉ, C., MCARTHUR, G., ASCIERTO, P. A., DANIELS, G. A., LONG, G. V., BASTHOLT, L., RIZZO, J. I., BALOGH, A., MOSHYK, A., HODI, F. S. & WOLCHOK, J. D. 2019. Five-Year Survival with Combined Nivolumab and Ipilimumab in Advanced Melanoma. *New England Journal of Medicine,* 381**,** 1535-1546.
LAROCCA, C. J. & WARNER, S. G. 2018. Oncolytic viruses and checkpoint inhibitors: combination therapy in clinical trials. *Clinical and Translational Medicine,* 7**,** 35.
LAU, E. Y.-T., HO, N. P.-Y. & LEE, T. K.-W. 2017. Cancer Stem Cells and Their Microenvironment: Biology and Therapeutic Implications. *Stem Cells International,* 2017**,** 3714190.
LAURENT, P., JOLIVEL, V., MANICKI, P., CHIU, L., CONTIN-BORDES, C., TRUCHETET, M.-E. & PRADEU, T. 2017. Immune-Mediated Repair: A Matter of Plasticity. *Frontiers in Immunology,* 8.
LE, D. T. & JAFFEE, E. M. 2012. Regulatory T-cell Modulation Using Cyclophosphamide in Vaccine Approaches: A Current Perspective. *Cancer Research,* 72**,** 3439-3444.
LE MAITRE, C. L., FREEMONT, A. J. & HOYLAND, J. A. 2007. Accelerated cellular senescence in degenerate intervertebral discs: a possible role in the pathogenesis of intervertebral disc degeneration. *Arthritis Research & Therapy,* 9**,** R45.
LEACH, D. R., KRUMMEL, M. F. & ALLISON, J. P. 1996. Enhancement of Antitumor Immunity by CTLA-4 Blockade. *Science,* 271**,** 1734-1736.
LEE, H. E., CHAE, S. W., LEE, Y. J., KIM, M. A., LEE, H. S., LEE, B. L. & KIM, W. H. 2008. Prognostic implications of type and density of tumour-infiltrating lymphocytes in gastric cancer. *Br J Cancer,* 99**,** 1704-11.
LEE, M., KIEFEL, H., LAJEVIC, M. D., MACAULEY, M. S., KAWASHIMA, H., O'HARA, E., PAN, J., PAULSON, J. C. & BUTCHER, E. C. 2014. Transcriptional programs of lymphoid tissue capillary and high endothelium reveal control mechanisms for lymphocyte homing. *Nature Immunology,* 15**,** 982-995.
LEE, S. & SCHMITT, C. A. 2019. The dynamic nature of senescence in cancer. *Nat Cell Biol,* 21**,** 94-101.
LEVENTAL, K. R., YU, H., KASS, L., LAKINS, J. N., EGEBLAD, M., ERLER, J. T., FONG, S. F. T., CSISZAR, K., GIACCIA, A., WENINGER, W., YAMAUCHI, M., GASSER, D. L. & WEAVER, V. M. 2009. Matrix Crosslinking Forces Tumor Progression by Enhancing Integrin Signaling. *Cell,* 139**,** 891-906.
LI, C., HEIDT, D. G., DALERBA, P., BURANT, C. F., ZHANG, L., ADSAY, V., WICHA, M., CLARKE, M. F. & SIMEONE, D. M. 2007. Identification of Pancreatic Cancer Stem Cells. *Cancer Research,* 67**,** 1030-1037.
LI, M. O., WAN, Y. Y., SANJABI, S., ROBERTSON, A.-K. L. & FLAVELL, R. A. 2006. TRANSFORMING GROWTH FACTOR-β REGULATION OF IMMUNE RESPONSES. *Annual Review of Immunology,* 24**,** 99-146.

LI, P., GAN, Y., XU, Y., SONG, L., WANG, L., OUYANG, B., ZHANG, C. & ZHOU, Q. 2017. The inflammatory cytokine TNF-α promotes the premature senescence of rat nucleus pulposus cells via the PI3K/Akt signaling pathway. *Sci Rep,* 7**,** 42938.

LI, S. & LI, Q. 2015. Cancer stem cells, lymphangiogenesis, and lymphatic metastasis. *Cancer Lett,* 357**,** 438-47.

LI, X., KOSTARELI, E., SUFFNER, J., GARBI, N. & HÄMMERLING, G. J. 2010. Efficient Treg depletion induces T-cell infiltration and rejection of large tumors. *European Journal of Immunology,* 40**,** 3325-3335.

LIAKOU, C. I., KAMAT, A., TANG, D. N., CHEN, H., SUN, J., TRONCOSO, P., LOGOTHETIS, C. & SHARMA, P. 2008. CTLA-4 blockade increases IFNγ-producing CD4⁺ICOS^{hi} cells to shift the ratio of effector to regulatory T cells in cancer patients. *Proceedings of the National Academy of Sciences,* 105**,** 14987.

LIANG, B., WORKMAN, C., LEE, J., CHEW, C., DALE, B. M., COLONNA, L., FLORES, M., LI, N., SCHWEIGHOFFER, E., GREENBERG, S., TYBULEWICZ, V., VIGNALI, D. & CLYNES, R. 2008. Regulatory T Cells Inhibit Dendritic Cells by Lymphocyte Activation Gene-3 Engagement of MHC Class II. *The Journal of Immunology,* 180**,** 5916-5926.

LINETTE, G. P., STADTMAUER, E. A., MAUS, M. V., RAPOPORT, A. P., LEVINE, B. L., EMERY, L., LITZKY, L., BAGG, A., CARRENO, B. M., CIMINO, P. J., BINDER-SCHOLL, G. K., SMETHURST, D. P., GERRY, A. B., PUMPHREY, N. J., BENNETT, A. D., BREWER, J. E., DUKES, J., HARPER, J., TAYTON-MARTIN, H. K., JAKOBSEN, B. K., HASSAN, N. J., KALOS, M. & JUNE, C. H. 2013. Cardiovascular toxicity and titin cross-reactivity of affinity-enhanced T cells in myeloma and melanoma. *Blood,* 122**,** 863-871.

LINGASAMY, P., TOBI, A., KURM, K., KOPANCHUK, S., SUDAKOV, A., SALUMÄE, M., RÄTSEP, T., ASSER, T., BJERKVIG, R. & TEESALU, T. 2020. Tumor-penetrating peptide for systemic targeting of Tenascin-C. *Scientific Reports,* 10**,** 5809.

LINSLEY, P. S., GREENE, J. L., TAN, P., BRADSHAW, J., LEDBETTER, J. A., ANASETTI, C. & DAMLE, N. K. 1992. Coexpression and functional cooperation of CTLA-4 and CD28 on activated T lymphocytes. *Journal of Experimental Medicine,* 176**,** 1595-1604.

LIOTTA, L. A. & KOHN, E. C. 2001. The microenvironment of the tumour-host interface. *Nature,* 411**,** 375-9.

LIU , W., PUTNAM , A. L., XU-YU , Z., SZOT , G. L., LEE , M. R., ZHU , S., GOTTLIEB , P. A., KAPRANOV , P., GINGERAS , T. R., DE ST. GROTH , B. F., CLAYBERGER , C., SOPER , D. M., ZIEGLER , S. F. & BLUESTONE , J. A. 2006. CD127 expression inversely correlates with FoxP3 and suppressive function of human CD4+ T reg cells. *Journal of Experimental Medicine,* 203**,** 1701-1711.

LOEFFLER, M., KRÜGER, J. A., NIETHAMMER, A. G. & REISFELD, R. A. 2006. Targeting tumor-associated fibroblasts improves cancer chemotherapy by increasing intratumoral drug uptake. *The Journal of Clinical Investigation,* 116**,** 1955-1962.

LOHMUELLER, J. & FINN, O. J. 2017. Current modalities in cancer immunotherapy: Immunomodulatory antibodies, CARs and vaccines. *Pharmacol Ther,* 178**,** 31-47.

LOVE, M. I., HUBER, W. & ANDERS, S. 2014. Moderated estimation of fold change and dispersion for RNA-seq data with DESeq2. *Genome Biol,* 15**,** 550.

LOWY, C. M. & OSKARSSON, T. 2015. Tenascin C in metastasis: A view from the invasive front. *Cell Adh Migr,* 9**,** 112-24.

LU, P., TAKAI, K., WEAVER, V. M. & WERB, Z. 2011. Extracellular matrix degradation and remodeling in development and disease. *Cold Spring Harb Perspect Biol,* 3.
LU, Y., HONG, S., LI, H., PARK, J., HONG, B., WANG, L., ZHENG, Y., LIU, Z., XU, J., HE, J., YANG, J., QIAN, J. & YI, Q. 2012. Th9 cells promote antitumor immune responses in vivo. *The Journal of Clinical Investigation,* 122**,** 4160-4171.
LUND, A. W. 2016. Rethinking Lymphatic Vessels and Antitumor Immunity. *Trends in Cancer,* 2**,** 548-551.
LUND, A. W., DURAES, F. V., HIROSUE, S., RAGHAVAN, V. R., NEMBRINI, C., THOMAS, S. N., ISSA, A., HUGUES, S. & SWARTZ, M. A. 2012. VEGF-C promotes immune tolerance in B16 melanomas and cross-presentation of tumor antigen by lymph node lymphatics. *Cell Rep,* 1**,** 191-9.
LUND, A. W., WAGNER, M., FANKHAUSER, M., STEINSKOG, E. S., BROGGI, M. A., SPRANGER, S., GAJEWSKI, T. F., ALITALO, K., EIKESDAL, H. P., WIIG, H. & SWARTZ, M. A. 2016. Lymphatic vessels regulate immune microenvironments in human and murine melanoma. *J Clin Invest,* 126**,** 3389-402.
MA, Q., DIETERICH, L. C. & DETMAR, M. 2018. Multiple roles of lymphatic vessels in tumor progression. *Curr Opin Immunol,* 53**,** 7-12.
MA, Q.-Y., HUANG, D.-Y., ZHANG, H.-J., CHEN, J., MILLER, W. & CHEN, X.-F. 2016. Function of follicular helper T cell is impaired and correlates with survival time in non-small cell lung cancer. *International Immunopharmacology,* 41**,** 1-7.
MACCIÒ, A., GRAMIGNANO, G., CHERCHI, M. C., TANCA, L., MELIS, L. & MADEDDU, C. 2020. Role of M1-polarized tumor-associated macrophages in the prognosis of advanced ovarian cancer patients. *Scientific Reports,* 10**,** 6096.
MACIAN, F. 2005. NFAT proteins: key regulators of T-cell development and function. *Nat Rev Immunol,* 5**,** 472-84.
MAEDA, H., TSUKIGAWA, K. & FANG, J. 2016. A Retrospective 30 Years After Discovery of the Enhanced Permeability and Retention Effect of Solid Tumors: Next-Generation Chemotherapeutics and Photodynamic Therapy--Problems, Solutions, and Prospects. *Microcirculation,* 23**,** 173-82.
MAKKOUK, A. & WEINER, G. J. 2015. Cancer Immunotherapy and Breaking Immune Tolerance: New Approaches to an Old Challenge. *Cancer Research,* 75**,** 5-10.
MANDRIOTA, S. J., JUSSILA, L., JELTSCH, M., COMPAGNI, A., BAETENS, D., PREVO, R., BANERJI, S., HUARTE, J., MONTESANO, R., JACKSON, D. G., ORCI, L., ALITALO, K., CHRISTOFORI, G. & PEPPER, M. S. 2001. Vascular endothelial growth factor-C-mediated lymphangiogenesis promotes tumour metastasis. *EMBO J,* 20**,** 672-82.
MANI, S. A., GUO, W., LIAO, M. J., EATON, E. N., AYYANAN, A., ZHOU, A. Y., BROOKS, M., REINHARD, F., ZHANG, C. C., SHIPITSIN, M., CAMPBELL, L. L., POLYAK, K., BRISKEN, C., YANG, J. & WEINBERG, R. A. 2008. The epithelial-mesenchymal transition generates cells with properties of stem cells. *Cell,* 133**,** 704-15.
MANTOVANI, A. & ALLAVENA, P. 2015. The interaction of anticancer therapies with tumor-associated macrophages. *Journal of Experimental Medicine,* 212**,** 435-445.
MARIE, J. C., LIGGITT, D. & RUDENSKY, A. Y. 2006. Cellular Mechanisms of Fatal Early-Onset Autoimmunity in Mice with the T Cell-Specific Targeting of Transforming Growth Factor-β Receptor. *Immunity,* 25**,** 441-454.
MARINCOLA, F. M., JAFFEE, E. M., HICKLIN, D. J. & FERRONE, S. 1999. Escape of Human Solid Tumors from T–Cell Recognition: Molecular Mechanisms and Functional Significance. *In:* DIXON, F. J. (ed.) *Advances in Immunology.* Academic Press.

MARISA, L., SVRCEK, M., COLLURA, A., BECHT, E., CERVERA, P., WANHERDRICK, K., BUHARD, O., GOLOUDINA, A., JONCHÈRE, V., SELVES, J., MILANO, G., GUENOT, D., COHEN, R., COLAS, C., LAURENT-PUIG, P., OLSCHWANG, S., LEFÈVRE, J. H., PARC, Y., BOIGE, V., LEPAGE, C., ANDRÉ, T., FLÉJOU, J. F., DÉRANGÈRE, V., GHIRINGHELLI, F., DE REYNIES, A. & DUVAL, A. 2018. The Balance Between Cytotoxic T-cell Lymphocytes and Immune Checkpoint Expression in the Prognosis of Colon Tumors. *J Natl Cancer Inst,* 110.

MARTINET, L., GARRIDO, I., FILLERON, T., LE GUELLEC, S., BELLARD, E., FOURNIE, J. J., ROCHAIX, P. & GIRARD, J. P. 2011. Human solid tumors contain high endothelial venules: association with T- and B-lymphocyte infiltration and favorable prognosis in breast cancer. *Cancer Res,* 71**,** 5678-87.

MARZO, A. L., LAKE, R. A., LO, D., SHERMAN, L., MCWILLIAM, A., NELSON, D., ROBINSON, B. W. S. & SCOTT, B. 1999. Tumor Antigens are Constitutively Presented in the Draining Lymph Nodes. *The Journal of Immunology,* 162**,** 5838-5845.

MATSUMURA, Y. & MAEDA, H. 1986. A new concept for macromolecular therapeutics in cancer chemotherapy: mechanism of tumoritropic accumulation of proteins and the antitumor agent smancs. *Cancer Res,* 46**,** 6387-92.

MAUDE, S. L., LAETSCH, T. W., BUECHNER, J., RIVES, S., BOYER, M., BITTENCOURT, H., BADER, P., VERNERIS, M. R., STEFANSKI, H. E., MYERS, G. D., QAYED, M., DE MOERLOOSE, B., HIRAMATSU, H., SCHLIS, K., DAVIS, K. L., MARTIN, P. L., NEMECEK, E. R., YANIK, G. A., PETERS, C., BARUCHEL, A., BOISSEL, N., MECHINAUD, F., BALDUZZI, A., KRUEGER, J., JUNE, C. H., LEVINE, B. L., WOOD, P., TARAN, T., LEUNG, M., MUELLER, K. T., ZHANG, Y., SEN, K., LEBWOHL, D., PULSIPHER, M. A. & GRUPP, S. A. 2018. Tisagenlecleucel in Children and Young Adults with B-Cell Lymphoblastic Leukemia. *New England Journal of Medicine,* 378**,** 439-448.

MAVROGONATOU, E., PRATSINIS, H., PAPADOPOULOU, A., KARAMANOS, N. K. & KLETSAS, D. 2019. Extracellular matrix alterations in senescent cells and their significance in tissue homeostasis. *Matrix Biology,* 75-76**,** 27-42.

MAZANET, M. M. & HUGHES, C. C. W. 2002. B7-H1 Is Expressed by Human Endothelial Cells and Suppresses T Cell Cytokine Synthesis. *The Journal of Immunology,* 169**,** 3581-3588.

MCFARLAND, C. D., YAGLOM, J. A., WOJTKOWIAK, J. W., SCOTT, J. G., MORSE, D. L., SHERMAN, M. Y. & MIRNY, L. A. 2017. The Damaging Effect of Passenger Mutations on Cancer Progression. *Cancer Research,* 77**,** 4763-4772.

MCGRANAHAN, N., ROSENTHAL, R., HILEY, C. T., ROWAN, A. J., WATKINS, T. B. K., WILSON, G. A., BIRKBAK, N. J., VEERIAH, S., VAN LOO, P., HERRERO, J., SWANTON, C., SWANTON, C., JAMAL-HANJANI, M., VEERIAH, S., SHAFI, S., CZYZEWSKA-KHAN, J., JOHNSON, D., LAYCOCK, J., BOSSHARD-CARTER, L., ROSENTHAL, R., GORMAN, P., HYNDS, R. E., WILSON, G., BIRKBAK, N. J., WATKINS, T. B. K., MCGRANAHAN, N., HORSWELL, S., MITTER, R., ESCUDERO, M., STEWART, A., VAN LOO, P., ROWAN, A., XU, H., TURAJLIC, S., HILEY, C., ABBOSH, C., GOLDMAN, J., STONE, R. K., DENNER, T., MATTHEWS, N., ELGAR, G., WARD, S., COSTA, M., BEGUM, S., PHILLIMORE, B., CHAMBERS, T., NYE, E., GRACA, S., AL BAKIR, M., JOSHI, K., FURNESS, A., BEN AISSA, A., WONG, Y. N. S., GEORGIOU, A., QUEZADA, S., HARTLEY, J. A., LOWE, H. L., HERRERO, J., LAWRENCE, D., HAYWARD, M., PANAGIOTOPOULOS, N., KOLVEKAR, S., FALZON, M., BORG, E., MARAFIOTI, T., SIMEON, C., HECTOR, G., SMITH, A., ARANDA, M., NOVELLI, M., OUKRIF, D., JANES, S. M., THAKRAR, R., FORSTER, M., AHMAD, T., LEE, S. M., PAPADATOS-PASTOS, D.,

CARNELL, D., MENDES, R., GEORGE, J., NAVANI, N., AHMED, A., TAYLOR, M., CHOUDHARY, J., SUMMERS, Y., CALIFANO, R., TAYLOR, P., SHAH, R., KRYSIAK, P., RAMMOHAN, K., FONTAINE, E., BOOTON, R., EVISON, M., CROSBIE, P., MOSS, S., IDRIES, F., JOSEPH, L., BISHOP, P., CHATURVED, A., QUINN, A. M., et al. 2017. Allele-Specific HLA Loss and Immune Escape in Lung Cancer Evolution. *Cell,* 171**,** 1259-1271.e11.

MEI, Z., LIU, Y., LIU, C., CUI, A., LIANG, Z., WANG, G., PENG, H., CUI, L. & LI, C. 2014. Tumour-infiltrating inflammation and prognosis in colorectal cancer: systematic review and meta-analysis. *Br J Cancer,* 110**,** 1595-605.

MERTENS, J. C., FINGAS, C. D., CHRISTENSEN, J. D., SMOOT, R. L., BRONK, S. F., WERNEBURG, N. W., GUSTAFSON, M. P., DIETZ, A. B., ROBERTS, L. R., SIRICA, A. E. & GORES, G. J. 2013. Therapeutic Effects of Deleting Cancer-Associated Fibroblasts in Cholangiocarcinoma. *Cancer Research,* 73**,** 897-907.

MIAO, Y., YANG, H., LEVORSE, J., YUAN, S., POLAK, L., SRIBOUR, M., SINGH, B., ROSENBLUM, M. D. & FUCHS, E. 2019. Adaptive Immune Resistance Emerges from Tumor-Initiating Stem Cells. *Cell,* 177**,** 1172-1186.e14.

MIDWOOD, K., SACRE, S., PICCININI, A. M., INGLIS, J., TREBAUL, A., CHAN, E., DREXLER, S., SOFAT, N., KASHIWAGI, M., OREND, G., BRENNAN, F. & FOXWELL, B. 2009. Tenascin-C is an endogenous activator of Toll-like receptor 4 that is essential for maintaining inflammation in arthritic joint disease. *Nat Med,* 15**,** 774-80.

MIDWOOD, K. S., CHIQUET, M., TUCKER, R. P. & OREND, G. 2016. Tenascin-C at a glance. *J Cell Sci,* 129**,** 4321-4327.

MIDWOOD, K. S., HUSSENET, T., LANGLOIS, B. & OREND, G. 2011. Advances in tenascin-C biology. *Cell Mol Life Sci,* 68**,** 3175-99.

MILANOVIC, M., FAN, D. N. Y., BELENKI, D., DÄBRITZ, J. H. M., ZHAO, Z., YU, Y., DÖRR, J. R., DIMITROVA, L., LENZE, D., MONTEIRO BARBOSA, I. A., MENDOZA-PARRA, M. A., KANASHOVA, T., METZNER, M., PARDON, K., REIMANN, M., TRUMPP, A., DÖRKEN, B., ZUBER, J., GRONEMEYER, H., HUMMEL, M., DITTMAR, G., LEE, S. & SCHMITT, C. A. 2018. Senescence-associated reprogramming promotes cancer stemness. *Nature,* 553**,** 96-100.

MILLER, K. D., CHAP, L. I., HOLMES, F. A., COBLEIGH, M. A., MARCOM, P. K., FEHRENBACHER, L., DICKLER, M., OVERMOYER, B. A., REIMANN, J. D., SING, A. P., LANGMUIR, V. & RUGO, H. S. 2005. Randomized Phase III Trial of Capecitabine Compared With Bevacizumab Plus Capecitabine in Patients With Previously Treated Metastatic Breast Cancer. *Journal of Clinical Oncology,* 23**,** 792-799.

MIRZAEI, R., SARKAR, S., DZIKOWSKI, L., RAWJI, K. S., KHAN, L., FAISSNER, A., BOSE, P. & YONG, V. W. 2018. Brain tumor-initiating cells export tenascin-C associated with exosomes to suppress T cell activity. *Oncoimmunology,* 7**,** e1478647.

MLECNIK, B., BINDEA, G., ANGELL, H. K., MABY, P., ANGELOVA, M., TOUGERON, D., CHURCH, S. E., LAFONTAINE, L., FISCHER, M., FREDRIKSEN, T., SASSO, M., BILOCQ, A. M., KIRILOVSKY, A., OBENAUF, A. C., HAMIEH, M., BERGER, A., BRUNEVAL, P., TUECH, J.-J., SABOURIN, J.-C., LE PESSOT, F., MAUILLON, J., RAFII, A., LAURENT-PUIG, P., SPEICHER, M. R., TRAJANOSKI, Z., MICHEL, P., SESBOÜE, R., FREBOURG, T., PAGÈS, F., VALGE-ARCHER, V., LATOUCHE, J.-B. & GALON, J. 2016. Integrative Analyses of Colorectal Cancer Show Immunoscore Is a Stronger Predictor of Patient Survival Than Microsatellite Instability. *Immunity,* 44**,** 698-711.

MLECNIK, B., VAN DEN EYNDE, M., BINDEA, G., CHURCH, S. E., VASATURO, A., FREDRIKSEN, T., LAFONTAINE, L., HAICHEUR, N., MARLIOT, F., DEBETANCOURT, D., PAIRET, G., JOURET-MOURIN, A., GIGOT, J.-F., HUBERT, C., DANSE, E., DRAGEAN, C., CARRASCO, J., HUMBLET, Y.,

VALGE-ARCHER, V., BERGER, A., PAGÈS, F., MACHIELS, J.-P. & GALON, J. 2017. Comprehensive Intrametastatic Immune Quantification and Major Impact of Immunoscore on Survival. *JNCI: Journal of the National Cancer Institute,* 110**,** 97-108.

MOHAMMED, R. A. A., MARTIN, S. G., GILL, M. S., GREEN, A. R., PAISH, E. C. & ELLIS, I. O. 2007. Improved Methods of Detection of Lymphovascular Invasion Demonstrate That It is the Predominant Method of Vascular Invasion in Breast Cancer and has Important Clinical Consequences. *The American Journal of Surgical Pathology,* 31**,** 1825-1833.

MONTESINOS, J. J., MORA-GARCÍA, M. D. L., MAYANI, H., FLORES-FIGUEROA, E., GARCÍA-ROCHA, R., FAJARDO-ORDUÑA, G. R., CASTRO-MANRREZA, M. E., WEISS-STEIDER, B. & MONROY-GARCÍA, A. 2013. In Vitro Evidence of the Presence of Mesenchymal Stromal Cells in Cervical Cancer and Their Role in Protecting Cancer Cells from Cytotoxic T Cell Activity. *Stem Cells and Development,* 22**,** 2508-2519.

MORRISON, B. J., STEEL, J. C. & MORRIS, J. C. 2018. Reduction of MHC-I expression limits T-lymphocyte-mediated killing of Cancer-initiating cells. *BMC Cancer,* 18**,** 469.

MOSKOPHIDIS, D., LECHNER, F., PIRCHER, H. & ZINKERNAGEL, R. M. 1993. Virus persistence in acutely infected immunocompetent mice by exhaustion of antiviral cytotoxic effector T cells. *Nature,* 362**,** 758-761.

MOTZ, G. T., SANTORO, S. P., WANG, L.-P., GARRABRANT, T., LASTRA, R. R., HAGEMANN, I. S., LAL, P., FELDMAN, M. D., BENENCIA, F. & COUKOS, G. 2014. Tumor endothelium FasL establishes a selective immune barrier promoting tolerance in tumors. *Nature Medicine,* 20**,** 607-615.

MOVAHEDI, K., GUILLIAMS, M., VAN DEN BOSSCHE, J., VAN DEN BERGH, R., GYSEMANS, C., BESCHIN, A., DE BAETSELIER, P. & VAN GINDERACHTER, J. A. 2008. Identification of discrete tumor-induced myeloid-derived suppressor cell subpopulations with distinct T cell–suppressive activity. *Blood,* 111**,** 4233-4244.

MUELLER, S. N. & AHMED, R. 2009. High antigen levels are the cause of T cell exhaustion during chronic viral infection. *Proceedings of the National Academy of Sciences,* 106**,** 8623-8628.

NAGASE, H., TAKEOKA, T., URAKAWA, S., MORIMOTO-OKAZAWA, A., KAWASHIMA, A., IWAHORI, K., TAKIGUCHI, S., NISHIKAWA, H., SATO, E., SAKAGUCHI, S., MORI, M., DOKI, Y. & WADA, H. 2017. ICOS+ Foxp3+ TILs in gastric cancer are prognostic markers and effector regulatory T cells associated with Helicobacter pylori. *International Journal of Cancer,* 140**,** 686-695.

NALLANTHIGHAL, S., HEISERMAN, J. P. & CHEON, D. J. 2019. The Role of the Extracellular Matrix in Cancer Stemness. *Front Cell Dev Biol,* 7**,** 86.

NATARAJAN, A., HABTE, F. & GAMBHIR, S. S. 2012. Development of a novel long-lived immunoPET tracer for monitoring lymphoma therapy in a humanized transgenic mouse model. *Bioconjug Chem,* 23**,** 1221-9.

NAYAK, T. K. & BRECHBIEL, M. W. 2009. Radioimmunoimaging with longer-lived positron-emitting radionuclides: potentials and challenges. *Bioconjug Chem,* 20**,** 825-41.

NEVALA, W. K., VACHON, C. M., LEONTOVICH, A. A., SCOTT, C. G., THOMPSON, M. A. & MARKOVIC, S. N. 2009. Evidence of Systemic Th2-Driven Chronic Inflammation in Patients with Metastatic Melanoma. *Clinical Cancer Research,* 15**,** 1931-1939.

NEYT, K., PERROS, F., GEURTSVANKESSEL, C. H., HAMMAD, H. & LAMBRECHT, B. N. 2012. Tertiary lymphoid organs in infection and autoimmunity. *Trends in Immunology,* 33**,** 297-305.

NI, W. D., YANG, Z. T., CUI, C. A., CUI, Y., FANG, L. Y. & XUAN, Y. H. 2017. Tenascin-C is a potential cancer-associated fibroblasts marker and predicts poor prognosis in prostate cancer. *Biochem Biophys Res Commun,* 486**,** 607-612.

NIE, S., GURREA, M., ZHU, J., THAKOLWIBOON, S., HETH, J. A., MURASZKO, K. M., FAN, X. & LUBMAN, D. M. 2015. Tenascin-C: a novel candidate marker for cancer stem cells in glioblastoma identified by tissue microarrays. *J Proteome Res,* 14**,** 814-22.

NIEMAN, K. M., KENNY, H. A., PENICKA, C. V., LADANYI, A., BUELL-GUTBROD, R., ZILLHARDT, M. R., ROMERO, I. L., CAREY, M. S., MILLS, G. B., HOTAMISLIGIL, G. S., YAMADA, S. D., PETER, M. E., GWIN, K. & LENGYEL, E. 2011. Adipocytes promote ovarian cancer metastasis and provide energy for rapid tumor growth. *Nature Medicine,* 17**,** 1498-1503.

NIETO, M. A. & CANO, A. 2012. The epithelial–mesenchymal transition under control: Global programs to regulate epithelial plasticity. *Seminars in Cancer Biology,* 22**,** 361-368.

NISHIKAWA, H. & SAKAGUCHI, S. 2010. Regulatory T cells in tumor immunity. *International Journal of Cancer,* 127**,** 759-767.

NISHIO, H., YAGUCHI, T., SUGIYAMA, J., SUMIMOTO, H., UMEZAWA, K., IWATA, T., SUSUMU, N., FUJII, T., KAWAMURA, N., KOBAYASHI, A., PARK, J., AOKI, D. & KAWAKAMI, Y. 2014. Immunosuppression through constitutively activated NF-κB signalling in human ovarian cancer and its reversal by an NF-κB inhibitor. *British journal of cancer,* 110**,** 2965-2974.

NOBEN-TRAUTH, N., HU-LI, J. & PAUL, W. E. 2000. Conventional, Naive CD4+ T Cells Provide an Initial Source of IL-4 During Th2 Differentiation. *The Journal of Immunology,* 165**,** 3620-3625.

NORELLI, M., CAMISA, B., BARBIERA, G., FALCONE, L., PUREVDORJ, A., GENUA, M., SANVITO, F., PONZONI, M., DOGLIONI, C., CRISTOFORI, P., TRAVERSARI, C., BORDIGNON, C., CICERI, F., OSTUNI, R., BONINI, C., CASUCCI, M. & BONDANZA, A. 2018. Monocyte-derived IL-1 and IL-6 are differentially required for cytokine-release syndrome and neurotoxicity due to CAR T cells. *Nature Medicine,* 24**,** 739-748.

NORTH, R. J. & BURSUKER, I. 1984. Generation and decay of the immune response to a progressive fibrosarcoma. I. Ly-1+2- suppressor T cells down-regulate the generation of Ly-1-2+ effector T cells. *Journal of Experimental Medicine,* 159**,** 1295-1311.

NORTHEY, J. J., PRZYBYLA, L. & WEAVER, V. M. 2017. Tissue Force Programs Cell Fate and Tumor Aggression. *Cancer Discov,* 7**,** 1224-1237.

NOWAK, D., STEWART, D. & KOEFFLER, H. P. 2009. Differentiation therapy of leukemia: 3 decades of development. *Blood,* 113**,** 3655-65.

NOWELL, P. C. 1976. The clonal evolution of tumor cell populations. *Science,* 194**,** 23-8.

NOWICKI, T. S., BERENT-MAOZ, B., CHEUNG-LAU, G., HUANG, R. R., WANG, X., TSOI, J., KAPLAN-LEFKO, P., CABRERA, P., TRAN, J., PANG, J., MACABALI, M., GARCILAZO, I. P., CARRETERO, I. B., KALBASI, A., COCHRAN, A. J., GRASSO, C. S., HU-LIESKOVAN, S., CHMIELOWSKI, B., COMIN-ANDUIX, B., SINGH, A. & RIBAS, A. 2019. A Pilot Trial of the Combination of Transgenic NY-ESO-1–reactive Adoptive Cellular Therapy with Dendritic Cell Vaccination with or without Ipilimumab. *Clinical Cancer Research,* 25**,** 2096-2108.

OHGA, N., ISHIKAWA, S., MAISHI, N., AKIYAMA, K., HIDA, Y., KAWAMOTO, T., SADAMOTO, Y., OSAWA, T., YAMAMOTO, K., KONDOH, M., OHMURA, H., SHINOHARA, N., NONOMURA, K., SHINDOH, M. & HIDA, K. 2012. Heterogeneity of Tumor Endothelial Cells: Comparison between Tumor

Endothelial Cells Isolated from High- and Low-Metastatic Tumors. *The American Journal of Pathology,* 180**,** 1294-1307.
ÖHLUND, D., ELYADA, E. & TUVESON, D. 2014. Fibroblast heterogeneity in the cancer wound. *The Journal of experimental medicine,* 211**,** 1503-1523.
OJALVO, L. S., WHITTAKER, C. A., CONDEELIS, J. S. & POLLARD, J. W. 2010. Gene Expression Analysis of Macrophages That Facilitate Tumor Invasion Supports a Role for Wnt-Signaling in Mediating Their Activity in Primary Mammary Tumors. *The Journal of Immunology,* 184**,** 702-712.
OLIVERAS-FERRAROS, C. V.-M., ALEJANDRO; MENENDE, JAVIER A. 2010. Pharmacological Mimicking of Caloric Restriction Elicits Epigenetic Reprogramming of Differentiated Cells to Stem-Like Self-Renewal States. *Rejuvenation Research,* 13**,** 519-526.
ONDONDO, B., JONES, E., HINDLEY, J., CUTTING, S., SMART, K., BRIDGEMAN, H., MATTHEWS, K. K., LADELL, K., PRICE, D. A., JACKSON, D. G., GODKIN, A., AGER, A. & GALLIMORE, A. 2014. Progression of carcinogen-induced fibrosarcomas is associated with the accumulation of naïve CD4+ T cells via blood vessels and lymphatics. *Int J Cancer,* 134**,** 2156-67.
ONION, D., ISHERWOOD, M., SHRIDHAR, N., XENOPHONTOS, M., CRAZE, M. L., DAY, L. J., GARCÍA-MÁRQUEZ, M. A., PINEDA, R. G., REECE-SMITH, A. M., SAUNDERS, J. H., DUFFY, J. P., ARGENT, R. H. & GRABOWSKA, A. M. 2018. Multicomponent analysis of the tumour microenvironment reveals low CD8 T cell number, low stromal caveolin-1 and high tenascin-C and their combination as significant prognostic markers in non-small cell lung cancer. *Oncotarget,* 9**,** 1760-1771.
ONISHI, Y., FEHERVARI, Z., YAMAGUCHI, T. & SAKAGUCHI, S. 2008. Foxp3+ natural regulatory T cells preferentially form aggregates on dendritic cells in vitro and actively inhibit their maturation. *Proceedings of the National Academy of Sciences,* 105**,** 10113-10118.
ONIZUKA, S., TAWARA, I., SHIMIZU, J., SAKAGUCHI, S., FUJITA, T. & NAKAYAMA, E. 1999. Tumor Rejection by in Vivo Administration of Anti-CD25 (Interleukin-2 Receptor α) Monoclonal Antibody. *Cancer Research,* 59**,** 3128.
OREND, G. & CHIQUET-EHRISMANN, R. 2006. Tenascin-C induced signaling in cancer. *Cancer Lett,* 244**,** 143-63.
ORIMO, A., GUPTA, P. B., SGROI, D. C., ARENZANA-SEISDEDOS, F., DELAUNAY, T., NAEEM, R., CAREY, V. J., RICHARDSON, A. L. & WEINBERG, R. A. 2005. Stromal Fibroblasts Present in Invasive Human Breast Carcinomas Promote Tumor Growth and Angiogenesis through Elevated SDF-1/CXCL12 Secretion. *Cell,* 121**,** 335-348.
OSKARSSON, T., ACHARYYA, S., ZHANG, X. H., VANHARANTA, S., TAVAZOIE, S. F., MORRIS, P. G., DOWNEY, R. J., MANOVA-TODOROVA, K., BROGI, E. & MASSAGUÉ, J. 2011. Breast cancer cells produce tenascin C as a metastatic niche component to colonize the lungs. *Nat Med,* 17**,** 867-74.
OSTERMANN, E., GARIN-CHESA, P., HEIDER, K. H., KALAT, M., LAMCHE, H., PURI, C., KERJASCHKI, D., RETTIG, W. J. & ADOLF, G. R. 2008. Effective Immunoconjugate Therapy in Cancer Models Targeting a Serine Protease of Tumor Fibroblasts. *Clinical Cancer Research,* 14**,** 4584-4592.
OWEN, D. L., MAHMUD, S. A., SJAASTAD, L. E., WILLIAMS, J. B., SPANIER, J. A., SIMEONOV, D. R., RUSCHER, R., HUANG, W., PROEKT, I., MILLER, C. N., HEKIM, C., JESCHKE, J. C., AGGARWAL, P., BROECKEL, U., LARUE, R. S., HENZLER, C. M., ALEGRE, M.-L., ANDERSON, M. S., AUGUST, A., MARSON, A., ZHENG, Y., WILLIAMS, C. B. & FARRAR, M. A. 2019. Thymic regulatory T cells arise via two distinct developmental programs. *Nature Immunology,* 20**,** 195-205.

PAGET, S. 1889. THE DISTRIBUTION OF SECONDARY GROWTHS IN CANCER OF THE BREAST. *The Lancet,* 133**,** 571-573.
PAPADOPOULOS, N. & LENNARTSSON, J. 2018. The PDGF/PDGFR pathway as a drug target. *Molecular Aspects of Medicine,* 62**,** 75-88.
PAREKH, K., RAMACHANDRAN, S., COOPER, J., BIGNER, D., PATTERSON, A. & MOHANAKUMAR, T. 2005. Tenascin-C, over expressed in lung cancer down regulates effector functions of tumor infiltrating lymphocytes. *Lung Cancer,* 47**,** 17-29.
PARHAM, P. 2015. *The Immune System*, New York: Garland Science
PAZOLLI, E., ALSPACH, E., MILCZAREK, A., PRIOR, J., PIWNICA-WORMS, D. & STEWART, S. A. 2012. Chromatin Remodeling Underlies the Senescence-Associated Secretory Phenotype of Tumor Stromal Fibroblasts That Supports Cancer Progression. *Cancer Research,* 72**,** 2251-2261.
PEREIRA, E. R., KEDRIN, D., SEANO, G., GAUTIER, O., MEIJER, E. F. J., JONES, D., CHIN, S.-M., KITAHARA, S., BOUTA, E. M., CHANG, J., BEECH, E., JEONG, H.-S., CARROLL, M. C., TAGHIAN, A. G. & PADERA, T. P. 2018. Lymph node metastases can invade local blood vessels, exit the node, and colonize distant organs in mice. *Science,* 359**,** 1403-1407.
PERRONE, G., RUFFINI, P. A., CATALANO, V., SPINO, C., SANTINI, D., MURETTO, P., SPOTO, C., ZINGARETTI, C., SISTI, V., ALESSANDRONI, P., GIORDANI, P., CICETTI, A., D'EMIDIO, S., MORINI, S., RUZZO, A., MAGNANI, M., TONINI, G., RABITTI, C. & GRAZIANO, F. 2008. Intratumoural FOXP3-positive regulatory T cells are associated with adverse prognosis in radically resected gastric cancer. *European Journal of Cancer,* 44**,** 1875-1882.
PESKE, J. D., WOODS, A. B. & ENGELHARD, V. H. 2015. Control of CD8 T-Cell Infiltration into Tumors by Vasculature and Microenvironment. *Adv Cancer Res,* 128**,** 263-307.
PETROVA, V., ANNICCHIARICO-PETRUZZELLI, M., MELINO, G. & AMELIO, I. 2018. The hypoxic tumour microenvironment. *Oncogenesis,* 7**,** 10.
PEZZOLO, A., PARODI, F., MARIMPIETRI, D., RAFFAGHELLO, L., COCCO, C., PISTORIO, A., MOSCONI, M., GAMBINI, C., CILLI, M., DEAGLIO, S., MALAVASI, F. & PISTOIA, V. 2011. Oct-4+/Tenascin C+ neuroblastoma cells serve as progenitors of tumor-derived endothelial cells. *Cell Res,* 21**,** 1470-86.
PFEIFFER, F., KUMAR, V., BUTZ, S., VESTWEBER, D., IMHOF, B. A., STEIN, J. V. & ENGELHARDT, B. 2008. Distinct molecular composition of blood and lymphatic vascular endothelial cell junctions establishes specific functional barriers within the peripheral lymph node. *European Journal of Immunology,* 38**,** 2142-2155.
PIMM, M. V., EMBLETON, M. J. & BALDWIN, R. W. 1980. Multiple antigenic specificities within primary 3-methylcholanthrene-induced rat sarcomas and metastases. *Int J Cancer,* 25**,** 621-9.
POLYAK, K., HAVIV, I. & CAMPBELL, I. G. 2009. Co-evolution of tumor cells and their microenvironment. *Trends Genet,* 25**,** 30-8.
POWRIE, F. & MASON, D. 1990. OX-22high CD4+ T cells induce wasting disease with multiple organ pathology: prevention by the OX-22low subset. *J Exp Med,* 172**,** 1701-8.
PRIETO-VILA, M., TAKAHASHI, R. U., USUBA, W., KOHAMA, I. & OCHIYA, T. 2017. Drug Resistance Driven by Cancer Stem Cells and Their Niche. *Int J Mol Sci,* 18.
PROVENZANO, PAOLO P., CUEVAS, C., CHANG, AMY E., GOEL, VIKAS K., VON HOFF, DANIEL D. & HINGORANI, SUNIL R. 2012. Enzymatic Targeting of the Stroma Ablates Physical Barriers to Treatment of Pancreatic Ductal Adenocarcinoma. *Cancer Cell,* 21**,** 418-429.

PUENTE, L. G., HE, J. S. & OSTERGAARD, H. L. 2006. A novel PKC regulates ERK activation and degranulation of cytotoxic T lymphocytes: Plasticity in PKC regulation of ERK. *Eur J Immunol,* 36**,** 1009-18.
PUENTE NAVAZO, M. D., VALMORI, D. & RÜEGG, C. 2001. The alternatively spliced domain TnFnIII A1A2 of the extracellular matrix protein tenascin-C suppresses activation-induced T lymphocyte proliferation and cytokine production. *J Immunol,* 167**,** 6431-40.
PUISIEUX, A., BRABLETZ, T. & CARAMEL, J. 2014. Oncogenic roles of EMT-inducing transcription factors. *Nature Cell Biology,* 16**,** 488-494.
PURWAR, R., SCHLAPBACH, C., XIAO, S., KANG, H. S., ELYAMAN, W., JIANG, X., JETTEN, A. M., KHOURY, S. J., FUHLBRIGGE, R. C., KUCHROO, V. K., CLARK, R. A. & KUPPER, T. S. 2012. Robust tumor immunity to melanoma mediated by interleukin-9–producing T cells. *Nature Medicine,* 18**,** 1248-1253.
PUTZ, E. M., MAYFOSH, A. J., KOS, K., BARKAUSKAS, D. S., NAKAMURA, K., TOWN, L., GOODALL, K. J., YEE, D. Y., POON, I. K., BASCHUK, N., SOUZA-FONSECA-GUIMARAES, F., HULETT, M. D. & SMYTH, M. J. 2017. NK cell heparanase controls tumor invasion and immune surveillance. *J Clin Invest,* 127**,** 2777-2788.
PYONTECK, S. M., AKKARI, L., SCHUHMACHER, A. J., BOWMAN, R. L., SEVENICH, L., QUAIL, D. F., OLSON, O. C., QUICK, M. L., HUSE, J. T., TEIJEIRO, V., SETTY, M., LESLIE, C. S., OEI, Y., PEDRAZA, A., ZHANG, J., BRENNAN, C. W., SUTTON, J. C., HOLLAND, E. C., DANIEL, D. & JOYCE, J. A. 2013. CSF-1R inhibition alters macrophage polarization and blocks glioma progression. *Nature Medicine,* 19**,** 1264-1272.
QIAN, B., DENG, Y., IM, J. H., MUSCHEL, R. J., ZOU, Y., LI, J., LANG, R. A. & POLLARD, J. W. 2009. A Distinct Macrophage Population Mediates Metastatic Breast Cancer Cell Extravasation, Establishment and Growth. *PLOS ONE,* 4**,** e6562.
QIAN, C.-N., RESAU, J. H. & TEH, B. T. 2007. Prospects for Vasculature Reorganization in Sentinel Lymph Nodes. *Cell Cycle,* 6**,** 514-517.
QUEZADA, S. A., PEGGS, K. S., CURRAN, M. A. & ALLISON, J. P. 2006. CTLA4 blockade and GM-CSF combination immunotherapy alters the intratumor balance of effector and regulatory T cells. *The Journal of Clinical Investigation,* 116**,** 1935-1945.
QUEZADA, S. A., PEGGS, K. S., SIMPSON, T. R. & ALLISON, J. P. 2011. Shifting the equilibrium in cancer immunoediting: from tumor tolerance to eradication. *Immunological Reviews,* 241**,** 104-118.
QUEZADA, S. A., SIMPSON, T. R., PEGGS, K. S., MERGHOUB, T., VIDER, J., FAN, X., BLASBERG, R., YAGITA, H., MURANSKI, P., ANTONY, P. A., RESTIFO, N. P. & ALLISON, J. P. 2010. Tumor-reactive CD4+ T cells develop cytotoxic activity and eradicate large established melanoma after transfer into lymphopenic hosts. *Journal of Experimental Medicine,* 207**,** 637-650.
RAAVÉ, R., VAN KUPPEVELT, T. H. & DAAMEN, W. F. 2018. Chemotherapeutic drug delivery by tumoral extracellular matrix targeting. *J Control Release,* 274**,** 1-8.
RABINOVICH, G. A., GABRILOVICH, D. & SOTOMAYOR, E. M. 2007. Immunosuppressive Strategies that are Mediated by Tumor Cells. *Annual Review of Immunology,* 25**,** 267-296.
RADWANSKA, A., GRALL, D., SCHAUB, S., DIVONNE, S. B. F., CIAIS, D., REKIMA, S., RUPP, T., SUDAKA, A., OREND, G. & VAN OBBERGHEN-SCHILLING, E. 2017. Counterbalancing anti-adhesive effects of Tenascin-C through fibronectin expression in endothelial cells. *Sci Rep,* 7**,** 12762.
RAFIQ, S., YEKU, O. O., JACKSON, H. J., PURDON, T. J., VAN LEEUWEN, D. G., DRAKES, D. J., SONG, M., MIELE, M. M., LI, Z., WANG, P., YAN, S., XIANG, J., MA, X., SESHAN, V. E., HENDRICKSON, R. C., LIU, C. & BRENTJENS, R.

J. 2018. Targeted delivery of a PD-1-blocking scFv by CAR-T cells enhances anti-tumor efficacy in vivo. *Nature Biotechnology,* 36**,** 847-856.
RAO, D. D., VORHIES, J. S., SENZER, N. & NEMUNAITIS, J. 2009. siRNA vs. shRNA: similarities and differences. *Adv Drug Deliv Rev,* 61**,** 746-59.
RAPOPORT, A. P., STADTMAUER, E. A., BINDER-SCHOLL, G. K., GOLOUBEVA, O., VOGL, D. T., LACEY, S. F., BADROS, A. Z., GARFALL, A., WEISS, B., FINKLESTEIN, J., KULIKOVSKAYA, I., SINHA, S. K., KRONSBERG, S., GUPTA, M., BOND, S., MELCHIORI, L., BREWER, J. E., BENNETT, A. D., GERRY, A. B., PUMPHREY, N. J., WILLIAMS, D., TAYTON- MARTIN, H. K., RIBEIRO, L., HOLDICH, T., YANOVICH, S., HARDY, N., YARED, J., KERR, N., PHILIP, S., WESTPHAL, S., SIEGEL, D. L., LEVINE, B. L., JAKOBSEN, B. K., KALOS, M. & JUNE, C. H. 2015. NY-ESO-1–specific TCR–engineered T cells mediate sustained antigen-specific antitumor effects in myeloma. *Nature Medicine,* 21**,** 914-921.
RECH, A. J., MICK, R., MARTIN, S., RECIO, A., AQUI, N. A., POWELL, D. J., JR., COLLIGON, T. A., TROSKO, J. A., LEINBACH, L. I., PLETCHER, C. H., TWEED, C. K., DEMICHELE, A., FOX, K. R., DOMCHEK, S. M., RILEY, J. L. & VONDERHEIDE, R. H. 2012. CD25 blockade depletes and selectively reprograms regulatory T cells in concert with immunotherapy in cancer patients. *Science translational medicine,* 4**,** 134ra62-134ra62.
REN, J., LIU, X., FANG, C., JIANG, S., JUNE, C. H. & ZHAO, Y. 2017. Multiplex Genome Editing to Generate Universal CAR T Cells Resistant to PD1 Inhibition. *Clinical Cancer Research,* 23**,** 2255-2266.
RIBAS, A. & WOLCHOK, J. D. 2018. Cancer immunotherapy using checkpoint blockade. *Science,* 359**,** 1350-1355.
RICHICHI, C., OSTI, D., DEL BENE, M., FORNASARI, L., PATANÈ, M., POLLO, B., DIMECO, F. & PELICCI, G. 2016. Tumor-initiating cell frequency is relevant for glioblastoma aggressiveness. *Oncotarget,* 7**,** 71491-71503.
RITCHIE, M. E., PHIPSON, B., WU, D., HU, Y., LAW, C. W., SHI, W. & SMYTH, G. K. 2015. limma powers differential expression analyses for RNA-sequencing and microarray studies. *Nucleic Acids Res,* 43**,** e47.
ROBBINS, P. F., KASSIM, S. H., TRAN, T. L. N., CRYSTAL, J. S., MORGAN, R. A., FELDMAN, S. A., YANG, J. C., DUDLEY, M. E., WUNDERLICH, J. R., SHERRY, R. M., KAMMULA, U. S., HUGHES, M. S., RESTIFO, N. P., RAFFELD, M., LEE, C.-C. R., LI, Y. F., EL-GAMIL, M. & ROSENBERG, S. A. 2015. A Pilot Trial Using Lymphocytes Genetically Engineered with an NY-ESO-1–Reactive T-cell Receptor: Long-term Follow-up and Correlates with Response. *Clinical Cancer Research,* 21**,** 1019-1027.
ROBBINS, P. F., MORGAN, R. A., FELDMAN, S. A., YANG, J. C., SHERRY, R. M., DUDLEY, M. E., WUNDERLICH, J. R., NAHVI, A. V., HELMAN, L. J., MACKALL, C. L., KAMMULA, U. S., HUGHES, M. S., RESTIFO, N. P., RAFFELD, M., LEE, C.-C. R., LEVY, C. L., LI, Y. F., EL-GAMIL, M., SCHWARZ, S. L., LAURENCOT, C. & ROSENBERG, S. A. 2011. Tumor Regression in Patients With Metastatic Synovial Cell Sarcoma and Melanoma Using Genetically Engineered Lymphocytes Reactive With NY-ESO-1. *Journal of Clinical Oncology,* 29**,** 917-924.
ROBERTS, E. W., BROZ, M. L., BINNEWIES, M., HEADLEY, M. B., NELSON, A. E., WOLF, D. M., KAISHO, T., BOGUNOVIC, D., BHARDWAJ, N. & KRUMMEL, M. F. 2016. Critical Role for CD103+/CD141+ Dendritic Cells Bearing CCR7 for Tumor Antigen Trafficking and Priming of T Cell Immunity in Melanoma. *Cancer Cell,* 30**,** 324-336.
ROBERTS, N., KLOOS, B., CASSELLA, M., PODGRABINSKA, S., PERSAUD, K., WU, Y., PYTOWSKI, B. & SKOBE, M. 2006. Inhibition of VEGFR-3 Activation with the Antagonistic Antibody More Potently Suppresses Lymph Node and

Distant Metastases than Inactivation of VEGFR-2. *Cancer Research,* 66**,** 2650-2657.
RODIG, N., RYAN, T., ALLEN, J. A., PANG, H., GRABIE, N., CHERNOVA, T., GREENFIELD, E. A., LIANG, S. C., SHARPE, A. H., LICHTMAN, A. H. & FREEMAN, G. J. 2003. Endothelial expression of PD-L1 and PD-L2 down-regulates CD8+ T cell activation and cytolysis. *European Journal of Immunology,* 33**,** 3117-3126.
ROMANO, E., KUSIO-KOBIALKA, M., FOUKAS, P. G., BAUMGAERTNER, P., MEYER, C., BALLABENI, P., MICHIELIN, O., WEIDE, B., ROMERO, P. & SPEISER, D. E. 2015. Ipilimumab-dependent cell-mediated cytotoxicity of regulatory T cells ex vivo by nonclassical monocytes in melanoma patients. *Proceedings of the National Academy of Sciences,* 112**,** 6140-6145.
ROSENBERG, S. A. & RESTIFO, N. P. 2015. Adoptive cell transfer as personalized immunotherapy for human cancer. *Science,* 348**,** 62-68.
ROSENTHAL, R., CADIEUX, E. L., SALGADO, R., BAKIR, M. A., MOORE, D. A., HILEY, C. T., LUND, T., TANIĆ, M., READING, J. L., JOSHI, K., HENRY, J. Y., GHORANI, E., WILSON, G. A., BIRKBAK, N. J., JAMAL-HANJANI, M., VEERIAH, S., SZALLASI, Z., LOI, S., HELLMANN, M. D., FEBER, A., CHAIN, B., HERRERO, J., QUEZADA, S. A., DEMEULEMEESTER, J., VAN LOO, P., BECK, S., MCGRANAHAN, N., SWANTON, C., SWANTON, C., JAMAL-HANJANI, M., VEERIAH, S., CZYZEWSKA-KHAN, J., JOHNSON, D., LAYCOCK, J., ROSENTHAL, R., GORMAN, P., HYNDS, R. E., WILSON, G., BIRKBAK, N. J., WATKINS, T. B. K., MCGRANAHAN, N., ESCUDERO, M., STEWART, A., VAN LOO, P., ROWAN, A., HILEY, C., ABBOSH, C., GOLDMAN, J., STONE, R. K., DENNER, T., WARD, S., NYE, E., JOSHI, K., BEN AISSA, A., WONG, Y. N. S., GEORGIOU, A., QUEZADA, S., HARTLEY, J. A., LOWE, H. L., HERRERO, J., LAWRENCE, D., HAYWARD, M., PANAGIOTOPOULOS, N., FALZON, M., BORG, E., MARAFIOTI, T., JANES, S. M., FORSTER, M., AHMAD, T., LEE, S. M., PAPADATOS-PASTOS, D., CARNELL, D., MENDES, R., GEORGE, J., AHMED, A., TAYLOR, M., CHOUDHARY, J., SUMMERS, Y., CALIFANO, R., TAYLOR, P., SHAH, R., KRYSIAK, P., RAMMOHAN, K., FONTAINE, E., BOOTON, R., EVISON, M., CROSBIE, P., MOSS, S., JOSEPH, L., BISHOP, P., QUINN, A. M., DORAN, H., LEEK, A., HARRISON, P., MOORE, K., WADDINGTON, R., NOVASIO, J., BLACKHALL, F., ROGAN, J., SMITH, E., et al. 2019. Neoantigen-directed immune escape in lung cancer evolution. *Nature,* 567**,** 479-485.
ROWSHANRAVAN, B., HALLIDAY, N. & SANSOM, D. M. 2018. CTLA-4: a moving target in immunotherapy. *Blood,* 131**,** 58-67.
ROZARIO, T. & DESIMONE, D. W. 2010. The extracellular matrix in development and morphogenesis: A dynamic view. *Developmental Biology,* 341**,** 126-140.
RUFFELL, B., CHANG-STRACHAN, D., CHAN, V., ROSENBUSCH, A., HO, CHRISTINE M. T., PRYER, N., DANIEL, D., HWANG, E. S., RUGO, HOPE S. & COUSSENS, LISA M. 2014. Macrophage IL-10 Blocks CD8+ T Cell-Dependent Responses to Chemotherapy by Suppressing IL-12 Expression in Intratumoral Dendritic Cells. *Cancer Cell,* 26**,** 623-637.
RUPP, T., LANGLOIS, B., KOCZOROWSKA, M. M., RADWANSKA, A., SUN, Z., HUSSENET, T., LEFEBVRE, O., MURDAMOOTHOO, D., ARNOLD, C., KLEIN, A., BINIOSSEK, M. L., HYENNE, V., NAUDIN, E., VELAZQUEZ-QUESADA, I., SCHILLING, O., VAN OBBERGHEN-SCHILLING, E. & OREND, G. 2016. Tenascin-C Orchestrates Glioblastoma Angiogenesis by Modulation of Pro- and Anti-angiogenic Signaling. *Cell Rep,* 17**,** 2607-2619.
RUSSO, E., TEIJEIRA, A., VAAHTOMERI, K., WILLRODT, A. H., BLOCH, J. S., NITSCHKÉ, M., SANTAMBROGIO, L., KERJASCHKI, D., SIXT, M. & HALIN,

C. 2016. Intralymphatic CCL21 Promotes Tissue Egress of Dendritic Cells through Afferent Lymphatic Vessels. *Cell Rep,* 14**,** 1723-1734.
RYBINSKI, B., FRANCO-BARRAZA, J. & CUKIERMAN, E. 2014. The wound healing, chronic fibrosis, and cancer progression triad. *Physiological Genomics,* 46**,** 223-244.
SABAT, R., OUYANG, W. & WOLK, K. 2014. Therapeutic opportunities of the IL-22–IL-22R1 system. *Nature Reviews Drug Discovery,* 13**,** 21-38.
SABINE, A., SAYGILI DEMIR, C. & PETROVA, T. V. 2016. Endothelial Cell Responses to Biomechanical Forces in Lymphatic Vessels. *Antioxid Redox Signal,* 25**,** 451-65.
SAKAGUCHI, S., SAKAGUCHI, N., ASANO, M., ITOH, M. & TODA, M. 1995. Immunologic self-tolerance maintained by activated T cells expressing IL-2 receptor alpha-chains (CD25). Breakdown of a single mechanism of self-tolerance causes various autoimmune diseases. *J Immunol,* 155**,** 1151-64.
SALGADO, R., DENKERT, C., DEMARIA, S., SIRTAINE, N., KLAUSCHEN, F., PRUNERI, G., WIENERT, S., VAN DEN EYNDEN, G., BAEHNER, F. L., PENAULT-LLORCA, F., PEREZ, E. A., THOMPSON, E. A., SYMMANS, W. F., RICHARDSON, A. L., BROCK, J., CRISCITIELLO, C., BAILEY, H., IGNATIADIS, M., FLORIS, G., SPARANO, J., KOS, Z., NIELSEN, T., RIMM, D. L., ALLISON, K. H., REIS-FILHO, J. S., LOIBL, S., SOTIRIOU, C., VIALE, G., BADVE, S., ADAMS, S., WILLARD-GALLO, K., LOI, S. & 2014, I. T. W. G. 2015. The evaluation of tumor-infiltrating lymphocytes (TILs) in breast cancer: recommendations by an International TILs Working Group 2014. *Ann Oncol,* 26**,** 259-71.
SALMON, H. & DONNADIEU, E. 2012. Within tumors, interactions between T cells and tumor cells are impeded by the extracellular matrix. *Oncoimmunology,* 1**,** 992-994.
SALMON, H., FRANCISZKIEWICZ, K., DAMOTTE, D., DIEU-NOSJEAN, M. C., VALIDIRE, P., TRAUTMANN, A., MAMI-CHOUAIB, F. & DONNADIEU, E. 2012. Matrix architecture defines the preferential localization and migration of T cells into the stroma of human lung tumors. *J Clin Invest,* 122**,** 899-910.
SANDLER, A., GRAY, R., PERRY, M. C., BRAHMER, J., SCHILLER, J. H., DOWLATI, A., LILENBAUM, R. & JOHNSON, D. H. 2006. Paclitaxel–Carboplatin Alone or with Bevacizumab for Non–Small-Cell Lung Cancer. *New England Journal of Medicine,* 355**,** 2542-2550.
SANTEGOETS, S. J. A. M., DIJKGRAAF, E. M., BATTAGLIA, A., BECKHOVE, P., BRITTEN, C. M., GALLIMORE, A., GODKIN, A., GOUTTEFANGEAS, C., DE GRUIJL, T. D., KOENEN, H. J. P. M., SCHEFFOLD, A., SHEVACH, E. M., STAATS, J., TASKÉN, K., WHITESIDE, T. L., KROEP, J. R., WELTERS, M. J. P. & VAN DER BURG, S. H. 2015. Monitoring regulatory T cells in clinical samples: consensus on an essential marker set and gating strategy for regulatory T cell analysis by flow cytometry. *Cancer Immunology, Immunotherapy,* 64**,** 1271-1286.
SATO, E., OLSON, S. H., AHN, J., BUNDY, B., NISHIKAWA, H., QIAN, F., JUNGBLUTH, A. A., FROSINA, D., GNJATIC, S., AMBROSONE, C., KEPNER, J., ODUNSI, T., RITTER, G., LELE, S., CHEN, Y.-T., OHTANI, H., OLD, L. J. & ODUNSI, K. 2005. Intraepithelial CD8+ tumor-infiltrating lymphocytes and a high CD8+/regulatory T cell ratio are associated with favorable prognosis in ovarian cancer. *Proceedings of the National Academy of Sciences of the United States of America,* 102**,** 18538-18543.
SAUPE, F., SCHWENZER, A., JIA, Y., GASSER, I., SPENLÉ, C., LANGLOIS, B., KAMMERER, M., LEFEBVRE, O., HLUSHCHUK, R., RUPP, T., MARKO, M., VAN DER HEYDEN, M., CREMEL, G., ARNOLD, C., KLEIN, A., SIMON-ASSMANN, P., DJONOV, V., NEUVILLE-MÉCHINE, A., ESPOSITO, I.,

SLOTTA-HUSPENINA, J., JANSSEN, K. P., DE WEVER, O., CHRISTOFORI, G., HUSSENET, T. & OREND, G. 2013. Tenascin-C downregulates wnt inhibitor dickkopf-1, promoting tumorigenesis in a neuroendocrine tumor model. *Cell Rep,* 5**,** 482-92.
SCHATTON, T., SCHÜTTE, U., FRANK, N. Y., ZHAN, Q., HOERNING, A., ROBLES, S. C., ZHOU, J., HODI, F. S., SPAGNOLI, G. C., MURPHY, G. F. & FRANK, M. H. 2010. Modulation of T-cell activation by malignant melanoma initiating cells. *Cancer research,* 70**,** 697-708.
SCHMIDT, A., OBERLE, N. & KRAMMER, P. 2012. Molecular Mechanisms of Treg-Mediated T Cell Suppression. *Frontiers in Immunology,* 3.
SCHNELLHARDT, S., ERBER, R., BÜTTNER-HEROLD, M., ROSAHL, M.-C., OTT, O. J., STRNAD, V., BECKMANN, M. W., KING, L., HARTMANN, A., FIETKAU, R. & DISTEL, L. 2020. Accelerated Partial Breast Irradiation: Macrophage Polarisation Shift Classification Identifies High-Risk Tumours in Early Hormone Receptor-Positive Breast Cancer. *Cancers,* 12.
SCHREIBER, R. D., OLD, L. J. & SMYTH, M. J. 2011. Cancer immunoediting: integrating immunity's roles in cancer suppression and promotion. *Science,* 331**,** 1565-70.
SCHULZ, C., PERDIGUERO, E. G., CHORRO, L., SZABO-ROGERS, H., CAGNARD, N., KIERDORF, K., PRINZ, M., WU, B., JACOBSEN, S. E. W., POLLARD, J. W., FRAMPTON, J., LIU, K. J. & GEISSMANN, F. 2012. A Lineage of Myeloid Cells Independent of Myb and Hematopoietic Stem Cells. *Science,* 336**,** 86-90.
SCHUMACHER, T. N. & SCHREIBER, R. D. 2015. Neoantigens in cancer immunotherapy. *Science,* 348**,** 69-74.
SCULLY, S., FRANCESCONE, R., FAIBISH, M., BENTLEY, B., TAYLOR, S. L., OH, D., SCHAPIRO, R., MORAL, L., YAN, W. & SHAO, R. 2012. Transdifferentiation of Glioblastoma Stem-Like Cells into Mural Cells Drives Vasculogenic Mimicry in Glioblastomas. *The Journal of Neuroscience,* 32**,** 12950-12960.
SCURR, M., GALLIMORE, A. & GODKIN, A. 2012. T cell subsets and colorectal cancer: Discerning the good from the bad. *Cellular Immunology,* 279**,** 21-24.
SCURR, M., PEMBROKE, T., BLOOM, A., ROBERTS, D., THOMSON, A., SMART, K., BRIDGEMAN, H., ADAMS, R., BREWSTER, A., JONES, R., GWYNNE, S., BLOUNT, D., HARROP, R., HILLS, R., GALLIMORE, A. & GODKIN, A. 2017a. Low-Dose Cyclophosphamide Induces Antitumor T-Cell Responses, which Associate with Survival in Metastatic Colorectal Cancer. *Clinical Cancer Research,* 23**,** 6771-6780.
SCURR, M., PEMBROKE, T., BLOOM, A., ROBERTS, D., THOMSON, A., SMART, K., BRIDGEMAN, H., ADAMS, R., BREWSTER, A., JONES, R., GWYNNE, S., BLOUNT, D., HARROP, R., WRIGHT, M., HILLS, R., GALLIMORE, A. & GODKIN, A. 2017b. Effect of Modified Vaccinia Ankara–5T4 and Low-Dose Cyclophosphamide on Antitumor Immunity in Metastatic Colorectal Cancer: A Randomized Clinical Trial. *JAMA Oncology,* 3**,** e172579-e172579.
SEAGER, R. J., HAJAL, C., SPILL, F., KAMM, R. D. & ZAMAN, M. H. 2017. Dynamic interplay between tumour, stroma and immune system can drive or prevent tumour progression. Convergent Science Physical Oncology.
SEIWERT, T. Y., HARAF, D. J., COHEN, E. E. W., STENSON, K., WITT, M. E., DEKKER, A., KOCHERGINSKY, M., WEICHSELBAUM, R. R., CHEN, H. X. & VOKES, E. E. 2008. Phase I Study of Bevacizumab Added to Fluorouracil- and Hydroxyurea-Based Concomitant Chemoradiotherapy for Poor-Prognosis Head and Neck Cancer. *Journal of Clinical Oncology,* 26**,** 1732-1741.
SELBY, M. J., ENGELHARDT, J. J., QUIGLEY, M., HENNING, K. A., CHEN, T., SRINIVASAN, M. & KORMAN, A. J. 2013. Anti-CTLA-4 Antibodies of IgG2a

Isotype Enhance Antitumor Activity through Reduction of Intratumoral Regulatory T Cells. *Cancer Immunology Research,* 1**,** 32-42.
SEN, D. R., KAMINSKI, J., BARNITZ, R. A., KURACHI, M., GERDEMANN, U., YATES, K. B., TSAO, H.-W., GODEC, J., LAFLEUR, M. W., BROWN, F. D., TONNERRE, P., CHUNG, R. T., TULLY, D. C., ALLEN, T. M., FRAHM, N., LAUER, G. M., WHERRY, E. J., YOSEF, N. & HAINING, W. N. 2016. The epigenetic landscape of T cell exhaustion. *Science,* 354**,** 1165-1169.
SENOVILLA, L., GALLUZZI, L., ZITVOGEL, L. & KROEMER, G. 2013. Immunosurveillance as a regulator of tissue homeostasis. *Trends in Immunology,* 34**,** 471-481.
SFANOS, K. S., BRUNO, T. C., MARIS, C. H., XU, L., THOBURN, C. J., DEMARZO, A. M., MEEKER, A. K., ISAACS, W. B. & DRAKE, C. G. 2008. Phenotypic Analysis of Prostate-Infiltrating Lymphocytes Reveals T_H17 and T_{reg} Skewing. *Clinical Cancer Research,* 14**,** 3254-3261.
SHACKLETON, M. 2010. Normal stem cells and cancer stem cells: similar and different. *Semin Cancer Biol,* 20**,** 85-92.
SHANKARAN, V., IKEDA, H., BRUCE, A. T., WHITE, J. M., SWANSON, P. E., OLD, L. J. & SCHREIBER, R. D. 2001. IFNγ and lymphocytes prevent primary tumour development and shape tumour immunogenicity. *Nature,* 410**,** 1107-1111.
SHAO, D. D., XUE, W., KRALL, E. B., BHUTKAR, A., PICCIONI, F., WANG, X., SCHINZEL, A. C., SOOD, S., ROSENBLUH, J., KIM, J. W., ZWANG, Y., ROBERTS, T. M., ROOT, D. E., JACKS, T. & HAHN, W. C. 2014. KRAS and YAP1 converge to regulate EMT and tumor survival. *Cell,* 158**,** 171-84.
SHARMA, P., HU-LIESKOVAN, S., WARGO, J. A. & RIBAS, A. 2017. Primary, Adaptive, and Acquired Resistance to Cancer Immunotherapy. *Cell,* 168**,** 707-723.
SHEU, B.-C., LIN, R.-H., LIEN, H.-C., HO, H.-N., HSU, S.-M. & HUANG, S.-C. 2001. Predominant Th2/Tc2 Polarity of Tumor-Infiltrating Lymphocytes in Human Cervical Cancer. *The Journal of Immunology,* 167**,** 2972-2978.
SHIAO, S. L., RUFFELL, B., DENARDO, D. G., FADDEGON, B. A., PARK, C. C. & COUSSENS, L. M. 2015. TH2-Polarized CD4+ T Cells and Macrophages Limit Efficacy of Radiotherapy. *Cancer Immunology Research,* 3**,** 518-525.
SHIMADA, H., CHATTEN, J., NEWTON, W. A., SACHS, N., HAMOUDI, A. B., CHIBA, T., MARSDEN, H. B. & MISUGI, K. 1984. Histopathologic Prognostic Factors in Neuroblastic Tumors: Definition of Subtypes of Ganglioneuroblastoma and an Age-Linked Classification of Neuroblastomas. *JNCI: Journal of the National Cancer Institute,* 73**,** 405-416.
SHIMIZU, J., YAMAZAKI, S. & SAKAGUCHI, S. 1999. Induction of Tumor Immunity by Removing CD25+CD4+ T Cells: A Common Basis Between Tumor Immunity and Autoimmunity. *The Journal of Immunology,* 163**,** 5211-5218.
SHIMIZU, J., YAMAZAKI, S., TAKAHASHI, T., ISHIDA, Y. & SAKAGUCHI, S. 2002. Stimulation of CD25+CD4+ regulatory T cells through GITR breaks immunological self-tolerance. *Nature Immunology,* 3**,** 135-142.
SIGAL, L. J., CROTTY, S., ANDINO, R. & ROCK, K. L. 1999. Cytotoxic T-cell immunity to virus-infected non-haematopoietic cells requires presentation of exogenous antigen. *Nature,* 398**,** 77-80.
SILACCI, M., BRACK, S. S., SPÄTH, N., BUCK, A., HILLINGER, S., ARNI, S., WEDER, W., ZARDI, L. & NERI, D. 2006. Human monoclonal antibodies to domain C of tenascin-C selectively target solid tumors in vivo. *Protein Engineering, Design and Selection,* 19**,** 471-478.
SIMPSON, T. R., LI, F., MONTALVO-ORTIZ, W., SEPULVEDA, M. A., BERGERHOFF, K., ARCE, F., RODDIE, C., HENRY, J. Y., YAGITA, H., WOLCHOK, J. D., PEGGS, K. S., RAVETCH, J. V., ALLISON, J. P. & QUEZADA, S. A. 2013. Fc-dependent depletion of tumor-infiltrating regulatory T

cells co-defines the efficacy of anti–CTLA-4 therapy against melanoma. *Journal of Experimental Medicine,* 210**,** 1695-1710.
SINGH, A. & SETTLEMAN, J. 2010. EMT, cancer stem cells and drug resistance: an emerging axis of evil in the war on cancer. *Oncogene,* 29**,** 4741-51.
SINGH, S. K., HAWKINS, C., CLARKE, I. D., SQUIRE, J. A., BAYANI, J., HIDE, T., HENKELMAN, R. M., CUSIMANO, M. D. & DIRKS, P. B. 2004. Identification of human brain tumour initiating cells. *Nature,* 432**,** 396-401.
SINICROPE, F. A., REGO, R. L., ANSELL, S. M., KNUTSON, K. L., FOSTER, N. R. & SARGENT, D. J. 2009. Intraepithelial Effector (CD3+)/Regulatory (FoxP3+) T-Cell Ratio Predicts a Clinical Outcome of Human Colon Carcinoma. *Gastroenterology,* 137**,** 1270-1279.
SISTIGU, A., VIAUD, S., CHAPUT, N., BRACCI, L., PROIETTI, E. & ZITVOGEL, L. 2011. Immunomodulatory effects of cyclophosphamide and implementations for vaccine design. *Seminars in Immunopathology,* 33**,** 369-383.
SKELTON, D., SATAKE, N. & KOHN, D. B. 2001. The enhanced green fluorescent protein (eGFP) is minimally immunogenic in C57BL/6 mice. *Gene Therapy,* 8**,** 1813-1814.
SKOBE, M., HAWIGHORST, T., JACKSON, D. G., PREVO, R., JANES, L., VELASCO, P., RICCARDI, L., ALITALO, K., CLAFFEY, K. & DETMAR, M. 2001. Induction of tumor lymphangiogenesis by VEGF-C promotes breast cancer metastasis. *Nat Med,* 7**,** 192-8.
SMALL, E. J., SCHELLHAMMER, P. F., HIGANO, C. S., REDFERN, C. H., NEMUNAITIS, J. J., VALONE, F. H., VERJEE, S. S., JONES, L. A. & HERSHBERG, R. M. 2006. Placebo-Controlled Phase III Trial of Immunologic Therapy with Sipuleucel-T (APC8015) in Patients with Metastatic, Asymptomatic Hormone Refractory Prostate Cancer. *Journal of Clinical Oncology,* 24**,** 3089-3094.
SMITH, M. L., GOURDON, D., LITTLE, W. C., KUBOW, K. E., EGUILUZ, R. A., LUNA-MORRIS, S. & VOGEL, V. 2007. Force-Induced Unfolding of Fibronectin in the Extracellular Matrix of Living Cells. *PLOS Biology,* 5**,** e268.
SMYTH, M. J., CROWE, N. Y. & GODFREY, D. I. 2001. NK cells and NKT cells collaborate in host protection from methylcholanthrene-induced fibrosarcoma. *International Immunology,* 13**,** 459-463.
SMYTH, M. J., NGIOW, S. F., RIBAS, A. & TENG, M. W. 2016. Combination cancer immunotherapies tailored to the tumour microenvironment. *Nat Rev Clin Oncol,* 13**,** 143-58.
SMYTH, M. J., THIA, K. Y. T., STREET, S. E. A., CRETNEY, E., TRAPANI, J. A., TANIGUCHI, M., KAWANO, T., PELIKAN, S. B., CROWE, N. Y. & GODFREY, D. I. 2000. Differential Tumor Surveillance by Natural Killer (Nk) and Nkt Cells. *Journal of Experimental Medicine,* 191**,** 661-668.
SOADY, K. J., TORNILLO, G., KENDRICK, H., MENIEL, V., OLIJNYK-DALLIS, D., MORRIS, J. S., STEIN, T., GUSTERSON, B. A., ISACKE, C. M. & SMALLEY, M. J. 2017. The receptor protein tyrosine phosphatase PTPRB negatively regulates FGF2-dependent branching morphogenesis. *Development,* 144**,** 3777-3788.
SOJKA, D. K. & FOWELL, D. J. 2011. Regulatory T cells inhibit acute IFN-γ synthesis without blocking T-helper cell type 1 (Th1) differentiation via a compartmentalized requirement for IL-10. *Proceedings of the National Academy of Sciences,* 108**,** 18336-18341.
SPAETH, E. L., DEMBINSKI, J. L., SASSER, A. K., WATSON, K., KLOPP, A., HALL, B., ANDREEFF, M. & MARINI, F. 2009. Mesenchymal Stem Cell Transition to Tumor-Associated Fibroblasts Contributes to Fibrovascular Network Expansion and Tumor Progression. *PLOS ONE,* 4**,** e4992.

SPRANGER, S., BAO, R. & GAJEWSKI, T. F. 2015. Melanoma-intrinsic β-catenin signalling prevents anti-tumour immunity. *Nature,* 523**,** 231-235.
STACKER, S. A., ACHEN, M. G., JUSSILA, L., BALDWIN, M. E. & ALITALO, K. 2002. Lymphangiogenesis and cancer metastasis. *Nature Reviews Cancer,* 2**,** 573-583.
STACKER, S. A., CAESAR, C., BALDWIN, M. E., THORNTON, G. E., WILLIAMS, R. A., PREVO, R., JACKSON, D. G., NISHIKAWA, S., KUBO, H. & ACHEN, M. G. 2001. VEGF-D promotes the metastatic spread of tumor cells via the lymphatics. *Nat Med,* 7**,** 186-91.
STACKER, S. A., WILLIAMS, S. P., KARNEZIS, T., SHAYAN, R., FOX, S. B. & ACHEN, M. G. 2014. Lymphangiogenesis and lymphatic vessel remodelling in cancer. *Nat Rev Cancer,* 14**,** 159-72.
STEINSKOG, E. S., SAGSTAD, S. J., WAGNER, M., KARLSEN, T. V., YANG, N., MARKHUS, C. E., YNDESTAD, S., WIIG, H. & EIKESDAL, H. P. 2016. Impaired lymphatic function accelerates cancer growth. *Oncotarget,* 7**,** 45789-45802.
STREUBEL, B., CHOTT, A., HUBER, D., EXNER, M., JÄGER, U., WAGNER, O. & SCHWARZINGER, I. 2004. Lymphoma-Specific Genetic Aberrations in Microvascular Endothelial Cells in B-Cell Lymphomas. *New England Journal of Medicine,* 351**,** 250-259.
STUTMAN, O. 1974. Tumor Development after 3-Methylcholanthrene in Immunologically Deficient Athymic-Nude Mice. *Science,* 183**,** 534-536.
SUCKER, A., ZHAO, F., REAL, B., HEEKE, C., BIELEFELD, N., MABEN, S., HORN, S., MOLL, I., MALTANER, R., HORN, P. A., SCHILLING, B., SABBATINO, F., LENNERZ, V., KLOOR, M., FERRONE, S., SCHADENDORF, D., FALK, C. S., GRIEWANK, K. & PASCHEN, A. 2014. Genetic Evolution of T-cell Resistance in the Course of Melanoma Progression. *Clinical Cancer Research,* 20**,** 6593-6604.
SUGIYAMA, D., NISHIKAWA, H., MAEDA, Y., NISHIOKA, M., TANEMURA, A., KATAYAMA, I., EZOE, S., KANAKURA, Y., SATO, E., FUKUMORI, Y., KARBACH, J., JÄGER, E. & SAKAGUCHI, S. 2013. Anti-CCR4 mAb selectively depletes effector-type FoxP3⁺CD4⁺ regulatory T cells, evoking antitumor immune responses in humans. *Proceedings of the National Academy of Sciences,* 110**,** 17945-17950.
SULTAN, M., VIDOVIC, D., PAINE, A. S., HUYNH, T. T., COYLE, K. M., THOMAS, M. L., CRUICKSHANK, B. M., DEAN, C. A., CLEMENTS, D. R., KIM, Y., LEE, K., GUJAR, S. A., WEAVER, I. C. G. & MARCATO, P. 2018. Epigenetic Silencing of TAP1 in Aldefluor+ Breast Cancer Stem Cells Contributes to Their Enhanced Immune Evasion. *STEM CELLS,* 36**,** 641-654.
SUMIMOTO , H., IMABAYASHI , F., IWATA , T. & KAWAKAMI , Y. 2006. The BRAF–MAPK signaling pathway is essential for cancer-immune evasion in human melanoma cells. *Journal of Experimental Medicine,* 203**,** 1651-1656.
SUMIMOTO, H., MIYAGISHI, M., MIYOSHI, H., YAMAGATA, S., SHIMIZU, A., TAIRA, K. & KAWAKAMI, Y. 2004. Inhibition of growth and invasive ability of melanoma by inactivation of mutated BRAF with lentivirus-mediated RNA interference. *Oncogene,* 23**,** 6031-6039.
SUN, Y., COPPÉ, J. P. & LAM, E. W. 2018. Cellular Senescence: The Sought or the Unwanted? *Trends Mol Med,* 24**,** 871-885.
SUTMULLER, R. P. M., VAN DUIVENVOORDE, L. M., VAN ELSAS, A., SCHUMACHER, T. N. M., WILDENBERG, M. E., ALLISON, J. P., TOES, R. E. M., OFFRINGA, R. & MELIEF, C. J. M. 2001. Synergism of Cytotoxic T Lymphocyte–Associated Antigen 4 Blockade and Depletion of Cd25+ Regulatory T Cells in Antitumor Therapy Reveals Alternative Pathways for

Suppression of Autoreactive Cytotoxic T Lymphocyte Responses. *Journal of Experimental Medicine,* 194**,** 823-832.
SWARTZ, M. A. & LUND, A. W. 2012. Lymphatic and interstitial flow in the tumour microenvironment: linking mechanobiology with immunity. *Nat Rev Cancer,* 12**,** 210-9.
SZABO, S. J., KIM, S. T., COSTA, G. L., ZHANG, X., FATHMAN, C. G. & GLIMCHER, L. H. 2000. A Novel Transcription Factor, T-bet, Directs Th1 Lineage Commitment. *Cell,* 100**,** 655-669.
SZABO, S. J., SULLIVAN, B. M., PENG, S. L. & GLIMCHER, L. H. 2003. Molecular Mechanisms RegulatinG Th1 Immune Responses. *Annual Review of Immunology,* 21**,** 713-758.
T R MOSMANN, A. & COFFMAN, R. L. 1989. TH1 and TH2 Cells: Different Patterns of Lymphokine Secretion Lead to Different Functional Properties. *Annual Review of Immunology,* 7**,** 145-173.
TADA, T., TAKEMORI, T., OKUMURA, K., NONAKA, M. & TOKUHISA, T. 1978. Two distinct types of helper T cells involved in the secondary antibody response: independent and synergistic effects of Ia- and Ia+ helper T cells. *Journal of Experimental Medicine,* 147**,** 446-458.
TAKADA, K. & TAKAHAMA, Y. 2015. Positive-selection-inducing self-peptides displayed by cortical thymic epithelial cells. *Advances in immunology,* 125**,** 87-110.
TALTS, J. F., WIRL, G., DICTOR, M., MULLER, W. J. & FÄSSLER, R. 1999. Tenascin-C modulates tumor stroma and monocyte/macrophage recruitment but not tumor growth or metastasis in a mouse strain with spontaneous mammary cancer. *J Cell Sci,* 112 (Pt 12)**,** 1855-64.
TANAKA, K., HIRAIWA, N., HASHIMOTO, H., YAMAZAKI, Y. & KUSAKABE, M. 2004. Tenascin-C regulates angiogenesis in tumor through the regulation of vascular endothelial growth factor expression. *International Journal of Cancer,* 108**,** 31-40.
TANG, C.-H. & TSAI, C.-C. 2012. CCL2 increases MMP-9 expression and cell motility in human chondrosarcoma cells via the Ras/Raf/MEK/ERK/NF-κB signaling pathway. *Biochemical Pharmacology,* 83**,** 335-344.
TANG, Q.-L., ZHAO, Z.-Q., LI, J.-C., LIANG, Y., YIN, J.-Q., ZOU, C.-Y., XIE, X.-B., ZENG, Y.-X., SHEN, J.-N., KANG, T. & WANG, J. 2011. Salinomycin inhibits osteosarcoma by targeting its tumor stem cells. *Cancer Letters,* 311**,** 113-121.
TAURIELLO, D. V. F., PALOMO-PONCE, S., STORK, D., BERENGUER-LLERGO, A., BADIA-RAMENTOL, J., IGLESIAS, M., SEVILLANO, M., IBIZA, S., CAÑELLAS, A., HERNANDO-MOMBLONA, X., BYROM, D., MATARIN, J. A., CALON, A., RIVAS, E. I., NEBREDA, A. R., RIERA, A., ATTOLINI, C. S.-O. & BATLLE, E. 2018. TGFβ drives immune evasion in genetically reconstituted colon cancer metastasis. *Nature,* 554**,** 538-543.
TAWARA, I., TAKE, Y., UENAKA, A., NOGUCHI, Y. & NAKAYAMA, E. 2002. Sequential Involvement of Two Distinct CD4+ Regulatory T Cells during the Course of Transplantable Tumor Growth and Protection from 3–Methylcholanthrene-induced Tumorigenesis by CD25–depletion. *Japanese Journal of Cancer Research,* 93**,** 911-916.
TAYLOR, S. & FOLKMAN, J. 1982. Protamine is an inhibitor of angiogenesis. *Nature,* 297**,** 307-312.
TENG, M. W. L., NGIOW, S. F., VON SCHEIDT, B., MCLAUGHLIN, N., SPARWASSER, T. & SMYTH, M. J. 2010. Conditional Regulatory T-Cell Depletion Releases Adaptive Immunity Preventing Carcinogenesis and Suppressing Established Tumor Growth. *Cancer Research,* 70**,** 7800-7809.

THAKUR, R. & MISHRA, D. P. 2016. Matrix reloaded: CCN, tenascin and SIBLING group of matricellular proteins in orchestrating cancer hallmark capabilities. *Pharmacol Ther,* 168**,** 61-74.
THORNTON, A. M. & SHEVACH, E. M. 1998. CD4+CD25+ Immunoregulatory T Cells Suppress Polyclonal T Cell Activation In Vitro by Inhibiting Interleukin 2 Production. *Journal of Experimental Medicine,* 188**,** 287-296.
TOGO, S., POLANSKA, U. M., HORIMOTO, Y. & ORIMO, A. 2013. Carcinoma-associated fibroblasts are a promising therapeutic target. *Cancers (Basel),* 5**,** 149-69.
TOSOLINI, M., KIRILOVSKY, A., MLECNIK, B., FREDRIKSEN, T., MAUGER, S., BINDEA, G., BERGER, A., BRUNEVAL, P., FRIDMAN, W.-H., PAGÈS, F. & GALON, J. 2011. Clinical Impact of Different Classes of Infiltrating T Cytotoxic and Helper Cells (Th1, Th2, Treg, Th17) in Patients with Colorectal Cancer. *Cancer Research,* 71**,** 1263-1271.
TRIFARI, S., KAPLAN, C. D., TRAN, E. H., CRELLIN, N. K. & SPITS, H. 2009. Identification of a human helper T cell population that has abundant production of interleukin 22 and is distinct from TH-17, TH1 and TH2 cells. *Nature Immunology,* 10**,** 864-871.
TRIPATHI, S. K. & LAHESMAA, R. 2014. Transcriptional and epigenetic regulation of T-helper lineage specification. *Immunological Reviews,* 261**,** 62-83.
TURK, M. J., GUEVARA-PATIÑO, J. A., RIZZUTO, G. A., ENGELHORN, M. E., SAKAGUCHI, S. & HOUGHTON, A. N. 2004. Concomitant tumor immunity to a poorly immunogenic melanoma is prevented by regulatory T cells. *The Journal of experimental medicine,* 200**,** 771-782.
TURLEY, S. J., CREMASCO, V. & ASTARITA, J. L. 2015. Immunological hallmarks of stromal cells in the tumour microenvironment. *Nature Reviews Immunology,* 15**,** 669-682.
UENO, H., BANCHEREAU, J. & VINUESA, C. G. 2015. Pathophysiology of T follicular helper cells in humans and mice. *Nature Immunology,* 16**,** 142-152.
VAAHTOMERI, K., BROWN, M., HAUSCHILD, R., DE VRIES, I., LEITHNER, A. F., MEHLING, M., KAUFMANN, W. A. & SIXT, M. 2017. Locally Triggered Release of the Chemokine CCL21 Promotes Dendritic Cell Transmigration across Lymphatic Endothelia. *Cell Rep,* 19**,** 902-909.
VALKENBURG, K. C., DE GROOT, A. E. & PIENTA, K. J. 2018. Targeting the tumour stroma to improve cancer therapy. *Nat Rev Clin Oncol,* 15**,** 366-381.
VAN DE WATERING, F. C., RIJPKEMA, M., PERK, L., BRINKMANN, U., OYEN, W. J. & BOERMAN, O. C. 2014. Zirconium-89 labeled antibodies: a new tool for molecular imaging in cancer patients. *Biomed Res Int,* 2014**,** 203601.
VAN DEN BROEK, M. E., KÄGI, D., OSSENDORP, F., TOES, R., VAMVAKAS, S., LUTZ, W. K., MELIEF, C. J., ZINKERNAGEL, R. M. & HENGARTNER, H. 1996. Decreased tumor surveillance in perforin-deficient mice. *Journal of Experimental Medicine,* 184**,** 1781-1790.
VAN DER BRUGGEN, P., TRAVERSARI, C., CHOMEZ, P., LURQUIN, C., DE PLAEN, E., VAN DEN EYNDE, B., KNUTH, A. & BOON, T. 1991. A gene encoding an antigen recognized by cytolytic T lymphocytes on a human melanoma. *Science,* 254**,** 1643-1647.
VAN DER WOUDE, L. L., GORRIS, M. A. J., HALILOVIC, A., FIGDOR, C. G. & DE VRIES, I. J. M. 2017. Migrating into the Tumor: a Roadmap for T Cells. *Trends in Cancer,* 3**,** 797-808.
VAN LEEUWEN, E. M. M., REMMERSWAAL, E. B. M., VOSSEN, M. T. M., ROWSHANI, A. T., WERTHEIM-VAN DILLEN, P. M. E., VAN LIER, R. A. W. & TEN BERGE, I. J. M. 2004. Emergence of a CD4+CD28− Granzyme B+, Cytomegalovirus-Specific T Cell Subset after Recovery of Primary Cytomegalovirus Infection. *The Journal of Immunology,* 173**,** 1834-1841.

VAN NEERVEN, S. M., TIEKEN, M., VERMEULEN, L. & BIJLSMA, M. F. 2016. Bidirectional interconversion of stem and non-stem cancer cell populations: A reassessment of theoretical models for tumor heterogeneity. *Mol Cell Oncol,* 3**,** e1098791.
VAN NIEKERK, G., DAVIDS, L. M., HATTINGH, S. M. & ENGELBRECHT, A. M. 2017. Cancer stem cells: A product of clonal evolution? *Int J Cancer,* 140**,** 993-999.
VAN VLOTEN, J. P., WORKENHE, S. T., WOOTTON, S. K., MOSSMAN, K. L. & BRIDLE, B. W. 2018. Critical Interactions between Immunogenic Cancer Cell Death, Oncolytic Viruses, and the Immune System Define the Rational Design of Combination Immunotherapies. *The Journal of Immunology,* 200**,** 450-458.
VAROL, C. & SAGI, I. 2018. Phagocyte—extracellular matrix crosstalk empowers tumor development and dissemination. *The FEBS Journal,* 285**,** 734-751.
VERMEULEN, L., DE SOUSA E MELO, F., RICHEL, D. J. & MEDEMA, J. P. 2012. The developing cancer stem-cell model: clinical challenges and opportunities. *The Lancet Oncology,* 13**,** e83-e89.
VERMEULEN, L., DE SOUSA E MELO, F., VAN DER HEIJDEN, M., CAMERON, K., DE JONG, J. H., BOROVSKI, T., TUYNMAN, J. B., TODARO, M., MERZ, C., RODERMOND, H., SPRICK, M. R., KEMPER, K., RICHEL, D. J., STASSI, G. & MEDEMA, J. P. 2010. Wnt activity defines colon cancer stem cells and is regulated by the microenvironment. *Nature Cell Biology,* 12**,** 468-476.
VESALAINEN, S., LIPPONEN, P., TALJA, M. & SYRJÄNEN, K. 1994. Histological grade, perineural infiltration, tumour-infiltrating lymphocytes and apoptosis as determinants of long-term prognosis in prostatic adenocarcinoma. *Eur J Cancer,* 30A**,** 1797-803.
VIGL, B., AEBISCHER, D., NITSCHKÉ, M., IOLYEVA, M., RÖTHLIN, T., ANTSIFEROVA, O. & HALIN, C. 2011. Tissue inflammation modulates gene expression of lymphatic endothelial cells and dendritic cell migration in a stimulus-dependent manner. *Blood,* 118**,** 205-215.
VISVADER, J. E. 2011. Cells of origin in cancer. *Nature,* 469**,** 314-322.
VOSJAN, M. J., PERK, L. R., VISSER, G. W., BUDDE, M., JUREK, P., KIEFER, G. E. & VAN DONGEN, G. A. 2010. Conjugation and radiolabeling of monoclonal antibodies with zirconium-89 for PET imaging using the bifunctional chelate p-isothiocyanatobenzyl-desferrioxamine. *Nat Protoc,* 5**,** 739-43.
WAITZ, R., FASSÒ, M. & ALLISON, J. P. 2012. CTLA-4 blockade synergizes with cryoablation to mediate tumor rejection. *OncoImmunology,* 1**,** 544-546.
WALKER, C., MOJARES, E. & DEL RÍO HERNÁNDEZ, A. 2018. Role of Extracellular Matrix in Development and Cancer Progression. *Int J Mol Sci,* 19.
WALTHER, M., GEBHARDT, P., GROSSE-GEHLING, P., WÜRBACH, L., IRMLER, I., PREUSCHE, S., KHALID, M., OPFERMANN, T., KAMRADT, T., STEINBACH, J. & SALUZ, H. P. 2011. Implementation of 89Zr production and in vivo imaging of B-cells in mice with 89Zr-labeled anti-B-cell antibodies by small animal PET/CT. *Appl Radiat Isot,* 69**,** 852-7.
WALUNAS, T. L., LENSCHOW, D. J., BAKKER, C. Y., LINSLEY, P. S., FREEMAN, G. J., GREEN, J. M., THOMPSON, C. B. & BLUESTONE, J. A. 1994. CTLA-4 can function as a negative regulator of T cell activation. *Immunity,* 1**,** 405-413.
WANG, J., LU, F., REN, Q., SUN, H., XU, Z., LAN, R., LIU, Y., WARD, D., QUAN, J., YE, T. & ZHANG, H. 2011. Novel Histone Demethylase LSD1 Inhibitors Selectively Target Cancer Cells with Pluripotent Stem Cell Properties. *Cancer Research,* 71**,** 7238-7249.
WANG, L., YI, T., KORTYLEWSKI, M., PARDOLL, D. M., ZENG, D. & YU, H. 2009. IL-17 can promote tumor growth through an IL-6–Stat3 signaling pathway. *Journal of Experimental Medicine,* 206**,** 1457-1464.
WANG, Z. & HAN, W. 2018. Biomarkers of cytokine release syndrome and neurotoxicity related to CAR-T cell therapy. *Biomarker Research,* 6**,** 4.

WEHRHAN, F., RÖDEL, F., GRABENBAUER, G. G., AMANN, K., BRÜCKL, W. & SCHULTZE-MOSGAU, S. 2004. Transforming growth factor beta 1 dependent regulation of Tenascin-C in radiation impaired wound healing. *Radiother Oncol,* 72**,** 297-303.

WEI, S. C., FATTET, L., TSAI, J. H., GUO, Y., PAI, V. H., MAJESKI, H. E., CHEN, A. C., SAH, R. L., TAYLOR, S. S., ENGLER, A. J. & YANG, J. 2015. Matrix stiffness drives epithelial-mesenchymal transition and tumour metastasis through a TWIST1-G3BP2 mechanotransduction pathway. *Nat Cell Biol,* 17**,** 678-88.

WEI, X., ZHANG, J., GU, Q., HUANG, M., ZHANG, W., GUO, J. & ZHOU, X. 2017. Reciprocal Expression of IL-35 and IL-10 Defines Two Distinct Effector Treg Subsets that Are Required for Maintenance of Immune Tolerance. *Cell Reports,* 21**,** 1853-1869.

WEIR, B. A., WOO, M. S., GETZ, G., PERNER, S., DING, L., BEROUKHIM, R., LIN, W. M., PROVINCE, M. A., KRAJA, A., JOHNSON, L. A., SHAH, K., SATO, M., THOMAS, R. K., BARLETTA, J. A., BORECKI, I. B., BRODERICK, S., CHANG, A. C., CHIANG, D. Y., CHIRIEAC, L. R., CHO, J., FUJII, Y., GAZDAR, A. F., GIORDANO, T., GREULICH, H., HANNA, M., JOHNSON, B. E., KRIS, M. G., LASH, A., LIN, L., LINDEMAN, N., MARDIS, E. R., MCPHERSON, J. D., MINNA, J. D., MORGAN, M. B., NADEL, M., ORRINGER, M. B., OSBORNE, J. R., OZENBERGER, B., RAMOS, A. H., ROBINSON, J., ROTH, J. A., RUSCH, V., SASAKI, H., SHEPHERD, F., SOUGNEZ, C., SPITZ, M. R., TSAO, M.-S., TWOMEY, D., VERHAAK, R. G. W., WEINSTOCK, G. M., WHEELER, D. A., WINCKLER, W., YOSHIZAWA, A., YU, S., ZAKOWSKI, M. F., ZHANG, Q., BEER, D. G., WISTUBA, I. I., WATSON, M. A., GARRAWAY, L. A., LADANYI, M., TRAVIS, W. D., PAO, W., RUBIN, M. A., GABRIEL, S. B., GIBBS, R. A., VARMUS, H. E., WILSON, R. K., LANDER, E. S. & MEYERSON, M. 2007. Characterizing the cancer genome in lung adenocarcinoma. *Nature,* 450**,** 893-898.

WEXLER, H. & ROSENBERG, S. A. 1979. Pulmonary metastases from autochthonous 3-methylcholanthrene-induced murine tumors. *J Natl Cancer Inst,* 63**,** 1393-5.

WHERRY, E. J. & AHMED, R. 2004. Memory CD8 T-Cell Differentiation during Viral Infection. *Journal of Virology,* 78**,** 5535-5545.

WHERRY, E. J. & KURACHI, M. 2015. Molecular and cellular insights into T cell exhaustion. *Nature Reviews Immunology,* 15**,** 486-499.

WHITESIDE, T. L. 2012. What are regulatory T cells (Treg) regulating in cancer and why? *Seminars in Cancer Biology,* 22**,** 327-334.

WISE, S. G. & WEISS, A. S. 2009. Tropoelastin. *The International Journal of Biochemistry & Cell Biology,* 41**,** 494-497.

WU, A. M. 2009. Antibodies and antimatter: the resurgence of immuno-PET. *J Nucl Med,* 50**,** 2-5.

WU, X., PENG, M., HUANG, B., ZHANG, H., WANG, H., HUANG, B., XUE, Z., ZHANG, L., DA, Y., YANG, D., YAO, Z. & ZHANG, R. 2013. Immune microenvironment profiles of tumor immune equilibrium and immune escape states of mouse sarcoma. *Cancer Letters,* 340**,** 124-133.

XIONG, Y.-Q., SUN, H.-C., ZHANG, W., ZHU, X.-D., ZHUANG, P.-Y., ZHANG, J.-B., WANG, L., WU, W.-Z., QIN, L.-X. & TANG, Z.-Y. 2009. Human Hepatocellular Carcinoma Tumor–derived Endothelial Cells Manifest Increased Angiogenesis Capability and Drug Resistance Compared with Normal Endothelial Cells. *Clinical Cancer Research,* 15**,** 4838-4846.

YAGUCHI, T., GOTO, Y., KIDO, K., MOCHIMARU, H., SAKURAI, T., TSUKAMOTO, N., KUDO-SAITO, C., FUJITA, T., SUMIMOTO, H. & KAWAKAMI, Y. 2012. Immune Suppression and Resistance Mediated by Constitutive Activation of

Wnt/β-Catenin Signaling in Human Melanoma Cells. *The Journal of Immunology,* 189**,** 2110-2117.
YAKISICH, J. S. 2012. Challenges and limitations of targeting cancer stem cells and/or the tumour microenvironment. *Drugs and Therapy Studies,* 2**,** e10.
YAMASHINA, T., BAGHDADI, M., YONEDA, A., KINOSHITA, I., SUZU, S., DOSAKA-AKITA, H. & JINUSHI, M. 2014. Cancer Stem-like Cells Derived from Chemoresistant Tumors Have a Unique Capacity to Prime Tumorigenic Myeloid Cells. *Cancer Research,* 74**,** 2698-2709.
YANG, F., TUXHORN, J. A., RESSLER, S. J., MCALHANY, S. J., DANG, T. D. & ROWLEY, D. R. 2005. Stromal Expression of Connective Tissue Growth Factor Promotes Angiogenesis and Prostate Cancer Tumorigenesis. *Cancer Research,* 65**,** 8887-8895.
YANG, L., QI, Y., HU, J., TANG, L., ZHAO, S. & SHAN, B. 2012a. Expression of Th17 Cells in Breast Cancer Tissue and Its Association with Clinical Parameters. *Cell Biochemistry and Biophysics,* 62**,** 153-159.
YANG, Y.-P., CHANG, Y.-L., HUANG, P.-I., CHIOU, G.-Y., TSENG, L.-M., CHIOU, S.-H., CHEN, M.-H., CHEN, M.-T., SHIH, Y.-H., CHANG, C.-H., HSU, C.-C., MA, H.-I., WANG, C.-T., TSAI, L.-L., YU, C.-C. & CHANG, C.-J. 2012b. Resveratrol suppresses tumorigenicity and enhances radiosensitivity in primary glioblastoma tumor initiating cells by inhibiting the STAT3 axis. *Journal of Cellular Physiology,* 227**,** 976-993.
YANG, Z., NI, W., CUI, C., FANG, L. & XUAN, Y. 2017. Tenascin C is a prognostic determinant and potential cancer-associated fibroblasts marker for breast ductal carcinoma. *Exp Mol Pathol,* 102**,** 262-267.
YE, Z.-J., ZHOU, Q., GU, Y.-Y., QIN, S.-M., MA, W.-L., XIN, J.-B., TAO, X.-N. & SHI, H.-Z. 2010. Generation and Differentiation of IL-17–Producing CD4+ T Cells in Malignant Pleural Effusion. *The Journal of Immunology,* 185**,** 6348-6354.
YEO, E.-J., CASSETTA, L., QIAN, B.-Z., LEWKOWICH, I., LI, J.-F., STEFATER, J. A., SMITH, A. N., WIECHMANN, L. S., WANG, Y., POLLARD, J. W. & LANG, R. A. 2014. Myeloid WNT7b Mediates the Angiogenic Switch and Metastasis in Breast Cancer. *Cancer Research,* 74**,** 2962-2973.
YEWDELL, J. W. & HAERYFAR, S. M. M. 2005. UNDERSTANDING PRESENTATION OF VIRAL ANTIGENS TO CD8+ T CELLS IN VIVO: The Key to Rational Vaccine Design. *Annual Review of Immunology,* 23**,** 651-682.
YONG, C. S. M., DARDALHON, V., DEVAUD, C., TAYLOR, N., DARCY, P. K. & KERSHAW, M. H. 2017. CAR T-cell therapy of solid tumors. *Immunology & Cell Biology,* 95**,** 356-363.
YOSHIDA, G. J. & SAYA, H. 2016. Therapeutic strategies targeting cancer stem cells. *Cancer Sci,* 107**,** 5-11.
YOSHIDA, M., TAGUCHI, A., KAWANA, K., ADACHI, K., KAWATA, A., OGISHIMA, J., NAKAMURA, H., FUJIMOTO, A., SATO, M., INOUE, T., NISHIDA, H., FURUYA, H., TOMIO, K., ARIMOTO, T., KOGA, K., WADA-HIRAIKE, O., ODA, K., NAGAMATSU, T., KIYONO, T., OSUGA, Y. & FUJII, T. 2016. Modification of the Tumor Microenvironment in KRAS or c-MYC-Induced Ovarian Cancer-Associated Peritonitis. *PLOS ONE,* 11**,** e0160330.
YOUNGBLOOD, B., HALE, J. S., KISSICK, H. T., AHN, E., XU, X., WIELAND, A., ARAKI, K., WEST, E. E., GHONEIM, H. E., FAN, Y., DOGRA, P., DAVIS, C. W., KONIECZNY, B. T., ANTIA, R., CHENG, X. & AHMED, R. 2017. Effector CD8 T cells dedifferentiate into long-lived memory cells. *Nature,* 552**,** 404-409.
YUAN, X., ZHANG, J., LI, D., MAO, Y., MO, F., DU, W. & MA, X. 2017. Prognostic significance of tumor-associated macrophages in ovarian cancer: A meta-analysis. *Gynecologic Oncology,* 147**,** 181-187.
ZAJAC, A. J., BLATTMAN, J. N., MURALI-KRISHNA, K., SOURDIVE, D. J. D., SURESH, M., ALTMAN, J. D. & AHMED, R. 1998. Viral Immune Evasion Due

to Persistence of Activated T Cells Without Effector Function. *Journal of Experimental Medicine,* 188**,** 2205-2213.
ZARETSKY, J. M., GARCIA-DIAZ, A., SHIN, D. S., ESCUIN-ORDINAS, H., HUGO, W., HU-LIESKOVAN, S., TORREJON, D. Y., ABRIL-RODRIGUEZ, G., SANDOVAL, S., BARTHLY, L., SACO, J., HOMET MORENO, B., MEZZADRA, R., CHMIELOWSKI, B., RUCHALSKI, K., SHINTAKU, I. P., SANCHEZ, P. J., PUIG-SAUS, C., CHERRY, G., SEJA, E., KONG, X., PANG, J., BERENT-MAOZ, B., COMIN-ANDUIX, B., GRAEBER, T. G., TUMEH, P. C., SCHUMACHER, T. N. M., LO, R. S. & RIBAS, A. 2016. Mutations Associated with Acquired Resistance to PD-1 Blockade in Melanoma. *New England Journal of Medicine,* 375**,** 819-829.
ZAUNDERS, J. J., DYER, W. B., WANG, B., MUNIER, M. L., MIRANDA-SAKSENA, M., NEWTON, R., MOORE, J., MACKAY, C. R., COOPER, D. A., SAKSENA, N. K. & KELLEHER, A. D. 2004. Identification of circulating antigen-specific CD4+ T lymphocytes with a CCR5+, cytotoxic phenotype in an HIV-1 long-term nonprogressor and in CMV infection. *Blood,* 103**,** 2238-2247.
ZHANG, A. W., MCPHERSON, A., MILNE, K., KROEGER, D. R., HAMILTON, P. T., MIRANDA, A., FUNNELL, T., LITTLE, N., DE SOUZA, C. P. E., LAAN, S., LEDOUX, S., COCHRANE, D. R., LIM, J. L. P., YANG, W., ROTH, A., SMITH, M. A., HO, J., TSE, K., ZENG, T., SHLAFMAN, I., MAYO, M. R., MOORE, R., FAILMEZGER, H., HEINDL, A., WANG, Y. K., BASHASHATI, A., GREWAL, D. S., BROWN, S. D., LAI, D., WAN, A. N. C., NIELSEN, C. B., HUEBNER, C., TESSIER-CLOUTIER, B., ANGLESIO, M. S., BOUCHARD-CÔTÉ, A., YUAN, Y., WASSERMAN, W. W., GILKS, C. B., KARNEZIS, A. N., APARICIO, S., MCALPINE, J. N., HUNTSMAN, D. G., HOLT, R. A., NELSON, B. H. & SHAH, S. P. 2018. Interfaces of Malignant and Immunologic Clonal Dynamics in Ovarian Cancer. *Cell,* 173**,** 1755-1769.e22.
ZHANG, D., PARK, D., ZHONG, Y., LU, Y., RYCAJ, K., GONG, S., CHEN, X., LIU, X., CHAO, H. P., WHITNEY, P., CALHOUN-DAVIS, T., TAKATA, Y., SHEN, J., IYER, V. R. & TANG, D. G. 2016. Stem cell and neurogenic gene-expression profiles link prostate basal cells to aggressive prostate cancer. *Nat Commun,* 7**,** 10798.
ZHANG, J.-P., YAN, J., XU, J., PANG, X.-H., CHEN, M.-S., LI, L., WU, C., LI, S.-P. & ZHENG, L. 2009. Increased intratumoral IL-17-producing cells correlate with poor survival in hepatocellular carcinoma patients. *Journal of Hepatology,* 50**,** 980-989.
ZHANG, P., SUN, Y. & MA, L. 2015. ZEB1: at the crossroads of epithelial-mesenchymal transition, metastasis and therapy resistance. *Cell Cycle,* 14**,** 481-7.
ZHANG, S., BALCH, C., CHAN, M. W., LAI, H.-C., MATEI, D., SCHILDER, J. M., YAN, P. S., HUANG, T. H.-M. & NEPHEW, K. P. 2008. Identification and Characterization of Ovarian Cancer-Initiating Cells from Primary Human Tumors. *Cancer Research,* 68**,** 4311-4320.
ZHANG, W., LIU, L., SU, H., LIU, Q., SHEN, J., DAI, H., ZHENG, W., LU, Y., ZHANG, W., BEI, Y. & SHEN, P. 2019. Chimeric antigen receptor macrophage therapy for breast tumours mediated by targeting the tumour extracellular matrix. *British Journal of Cancer,* 121**,** 837-845.
ZHAO, L. & CAO, Y. J. 2019. Engineered T Cell Therapy for Cancer in the Clinic. *Frontiers in Immunology,* 10.
ZHAO, Y., GE, X., XU, X., YU, S., WANG, J. & SUN, L. 2019. Prognostic value and clinicopathological roles of phenotypes of tumour-associated macrophages in colorectal cancer. *Journal of Cancer Research and Clinical Oncology,* 145**,** 3005-3019.

ZHENG, W.-P. & FLAVELL, R. A. 1997. The Transcription Factor GATA-3 Is Necessary and Sufficient for Th2 Cytokine Gene Expression in CD4 T Cells. *Cell,* 89**,** 587-596.

ZHENG, X., WEIGERT, A., REU, S., GUENTHER, S., MANSOURI, S., BASSALY, B., GATTENLÖHNER, S., GRIMMINGER, F., SAVAI PULLAMSETTI, S., SEEGER, W., WINTER, H. & SAVAI, R. 2020. Spatial Density and Distribution of Tumor-Associated Macrophages Predict Survival in Non-Small-Cell Lung Carcinoma. *Cancer Research***,** canres.0069.2020.

ZHONG, X.-S., MATSUSHITA, M., PLOTKIN, J., RIVIERE, I. & SADELAIN, M. 2010. Chimeric Antigen Receptors Combining 4-1BB and CD28 Signaling Domains Augment PI₃kinase/AKT/Bcl-X_L Activation and CD8⁺ T Cell–mediated Tumor Eradication. *Molecular Therapy,* 18**,** 413-420.

ZHOU, W., FONG, MIRANDA Y., MIN, Y., SOMLO, G., LIU, L., PALOMARES, MELANIE R., YU, Y., CHOW, A., O'CONNOR, SEAN TIMOTHY F., CHIN, ANDREW R., YEN, Y., WANG, Y., MARCUSSON, ERIC G., CHU, P., WU, J., WU, X., LI, ARTHUR X., LI, Z., GAO, H., REN, X., BOLDIN, MARK P., LIN, PENGNIAN C. & WANG, SHIZHEN E. 2014. Cancer-Secreted miR-105 Destroys Vascular Endothelial Barriers to Promote Metastasis. *Cancer Cell,* 25**,** 501-515.

ZHOU, W., KE, S. Q., HUANG, Z., FLAVAHAN, W., FANG, X., PAUL, J., WU, L., SLOAN, A. E., MCLENDON, R. E., LI, X., RICH, J. N. & BAO, S. 2015. Periostin secreted by glioblastoma stem cells recruits M2 tumour-associated macrophages and promotes malignant growth. *Nature Cell Biology,* 17**,** 170-182.

ZHU, J. & PAUL, W. E. 2010. Peripheral CD4+ T-cell differentiation regulated by networks of cytokines and transcription factors. *Immunological Reviews,* 238**,** 247-262.

ZHU, Y., KNOLHOFF, B. L., MEYER, M. A., NYWENING, T. M., WEST, B. L., LUO, J., WANG-GILLAM, A., GOEDEGEBUURE, S. P., LINEHAN, D. C. & DENARDO, D. G. 2014. CSF1/CSF1R blockade reprograms tumor-infiltrating macrophages and improves response to T-cell checkpoint immunotherapy in pancreatic cancer models. *Cancer Res,* 74**,** 5057-69.

ZINK, D., FISCHER, A. H. & NICKERSON, J. A. 2004. Nuclear structure in cancer cells. *Nat Rev Cancer,* 4**,** 677-87.

ZUKIEL, R., NOWAK, S., WYSZKO, E., ROLLE, K., GAWRONSKA, I., BARCISZEWSKA, M. Z. & BARCISZEWSKI, J. 2006. Suppression of human brain tumor with interference RNA specific for tenascin-C. *Cancer Biology & Therapy,* 5**,** 1002-1007.

ZULIANI-ALVAREZ, L., MARZEDA, A. M., DELIGNE, C., SCHWENZER, A., MCCANN, F. E., MARSDEN, B. D., PICCININI, A. M. & MIDWOOD, K. S. 2017. Mapping tenascin-C interaction with toll-like receptor 4 reveals a new subset of endogenous inflammatory triggers. *Nat Commun,* 8**,** 1595.